ALTERNATING SIDE-CHAIN LIQUID-CRYSTALLINE COPOLYMERS WITH POLAR MOIETIES IN THE BACKBONE - RENÉ P. NIEUWHOF

Promotor:

Dr. E.J.R. Sudhölter
Hoogleraar in de fysisch-organische chemie

Co-promotor:

Dr. A.T.M. Marcelis
Universitair docent in de fysisch-organische chemie

ALTERNATING SIDE-CHAIN LIQUID-CRYSTALLINE COPOLYMERS WITH POLAR MOIETIES IN THE BACKBONE

ALTERNERENDE ZIJKETEN VLOEIBAAR-KRISTALLIJNE COPOLYMEREN MET POLAIRE GROEPEN IN DE HOOFDKETEN

René P. Nieuwhof

Proefschrift

ter verkrijging van de graad van doctor op gezag van de rector magnificus van de Wageningen Universiteit, dr. C.M. Karssen, in het openbaar te verdedigen op vrijdag 8 oktober des namiddags te vier uur in de Aula.

Stellingen

1. Op grond van de reactiviteitsverhoudingen van maleïnezuuranhydride en stearyl-methacrylaat is het onwaarschijnlijk dat A. Leiva et al. alternerende copolymeren hebben verkregen.

   Leiva, A.; Gargallo, L.; Radic, D. L. *Macromol. Sci.-Phys.* **1998**, *B37*, 45.
   Dit proefschrift, hoofdstuk 6.

2. Het niet waarneembaar zijn van de glasovergang van een hooggeordend polymeer tijdens een DSC-experiment betekent niet automatisch dat dit polymeer geen glasovergang bezit.

   Molecular and cooperative dynamics of smectic B and smectic E phases of a side-chain liquid crystalline poly(maleic anhydride-*alt*-1-alkene) - a dielectric relaxation study – Wübbenhorst, M.; Nieuwhof, R. P.; Marcelis, A. T. M.; Sudhölter, E. J. R.; van Turnhout, J., to be submitted.

3. Het ontwikkelen van nieuwe kunststoffen is een artistieke bezigheid.

4. Het weergeven van de benzineprijzen in uitsluitend Euro's is een goedkope verkooptruc.

   Tankstation Oosterbeek.

5. Het injecteren van overheidsgeld in topinstituten is een verkapte vorm van subsidie aan de participerende bedrijven.

6. De huidige strenge wetgeving betreffende de verlaging van het oplosmiddelgehalte van verf voor professioneel gebruik zal de klant van de vakschilder naar de beunhaas lokken.

7. Deeltijdwerken is geen garantie voor minder stress.

8. Het uitblijven van positieve uitslagen bij de dopingcontroles tijdens de Tour de France van 1999 betekent niet vanzelfsprekend dat alle wielrenners zich negatief opstellen ten opzichte van doping.

9. In dit tijdperk van RSI is de keuze voor een kleine ronde computermuis door een bedrijf dat gebruikersvriendelijkheid hoog in het vaandel heeft op zijn minst opmerkelijk te noemen.

Stellingen behorende bij het proefschrift

Alternating Side-Chain Liquid-Crystalline Copolymers with Polar Moieties in the Backbone

Wageningen, 8 oktober 1999   René P. Nieuwhof

Abstract

Side-chain liquid-crystalline polymers (SCLCPs) obtained via the alternating copolymerization of maleic anhydride (MA) and mesogenic 1-alkenes are an interesting class of polymers that may show good adhesion towards metal surfaces and form ordered layered structures. If these polymers contain methoxybiphenyl mesogens, they have high glass transition temperatures and exhibit highly ordered mesophases. The mesogen density of these polymers has been increased by coupling mesogen-containing alcohols onto SCLCPs with MA moieties. Depending on the structure of the mesogens of the SCLCP and the alcohols, mesophases were obtained with different degrees of interdigitation of side chains and different degrees of order. Copolymerization of MA with swallow-tailed 1-alkenes having two mesogens yielded polymers with even a higher degree of order. These polymers exhibit isotropization temperatures that were lower and glass transitions that were higher than those of polymers with half the mesogen density. The amount of MA in SCLCPs was altered by copolymerization of MA with mesogenic methacrylates. For methoxybiphenyl mesogens, the isotropization temperature increases with MA content. The temperature window of the mesophase increases with increasing spacer length.

A completely new class of SCLCPs was obtained by the copolymerization of carbon monoxide and mesogenic 1-alkenes. For methoxybiphenyl mesogens, these copolymers exhibit highly ordered smectic E mesophases and high glass transition temperatures. The transition temperatures were tuned by altering the spacer length or by dilution of the mesogen content of the copolymer.

Rheology showed that the loss and storage moduli and the complex viscosity strongly decrease at phase transitions. In addition, a decrease in these properties was observed in the smectic A mesophase which can probably be ascribed to rotational diffusion of the mesogens. The Langmuir-Blodgett technique showed that SCLCPs with cyano groups form multilayers on the water subphase. Transfer of SCLCPs with methoxybiphenyl mesogens results in multilayer films with a double layer periodicity, which is different from that observed in the bulk. Annealing of these films results in a more uniform *d* spacing.

Contents

1

General introduction

1.1. Paint removal

The paint and coatings industry, which represents an € 50+ billion market,[1] is a mature industry that has been undergoing a continual change in technology. Over the past two decades, a transition has been observed from conventional solventborne coatings to new and novel coating technologies like high solids coatings,[2] waterborne coatings,[3] UV radiation curable coatings,[4] powder coatings,[5] and natural paints.[6] The main driving forces behind this process are the shift in consumer expectations for higher quality, performance at lower cost, and concerns related to energy consumption and environmental contamination.[1,7] These driving forces made the Netherlands Department of Economic Affairs start an innovative research program called IOP-Paint. The subjects of this program can be divided in four research area: (i) binding agents, (ii) dispersion, (iii) functional properties, and (iv) application and paint removal. The common research aim of the IOP-paint is "less-polluting coating systems".

Objects are painted for several reasons, e.g. to resist corrosion, increase its durability, guard against attack from chemicals, provide impact resistance, and protect it from the forces of nature.[8] Another very important reason to paint an object is for aesthetic reasons.[8] However, at some stage the paint has to be removed from the object e.g. to check for corrosion damage or to replace a weather-worn coating with a new coating. Finally, paint may also be stripped from a surface and repainted for aesthetic reasons.

Traditional paint removal techniques comprise abrasives or physical (mechanical) removal, chemical attack, and thermal destruction.[8] Like for coatings technologies, the more stringent environmental and occupational safety regulations resulted in the development of new paint removal techniques.[9] Some examples of these new techniques are ice-crystal blasting, salt-bath stripping, plastic media blasting, and sodium bicarbonate blasting, of which the pros and cons are summarized elsewhere.[8] Despite the variety of systems that are available, there is still a search for novel techniques.

1.2. Novel paint removal technique

Some new paint removal concepts have been patented making use of a primer layer between the object and the coating.[10,11] These primers have in common that they loose their mechanical properties under certain conditions, after which the paint can be removed. In one patent a surfactant is used as a primer.[10] Another patent reports the application of an ionic copolymer of an acrylic acid and a 1-alkene.[11] In both cases the paint is removed after treatment with hot water.

Within the framework of IOP-paint, a new concept has been introduced by us making use of a splittable primer layer. The concept is depicted schematically in Figure 1.1 and makes use of side-chain liquid-crystalline polymers (SCLCPs; see Chapter 2). The SCLCPs have to adhere well to metal surfaces and have to form lamellar structures. The coating, which is applied on top of the very thin primer layer, can be removed when the interactions between the lamellae in the primer layer decrease at elevated temperatures.
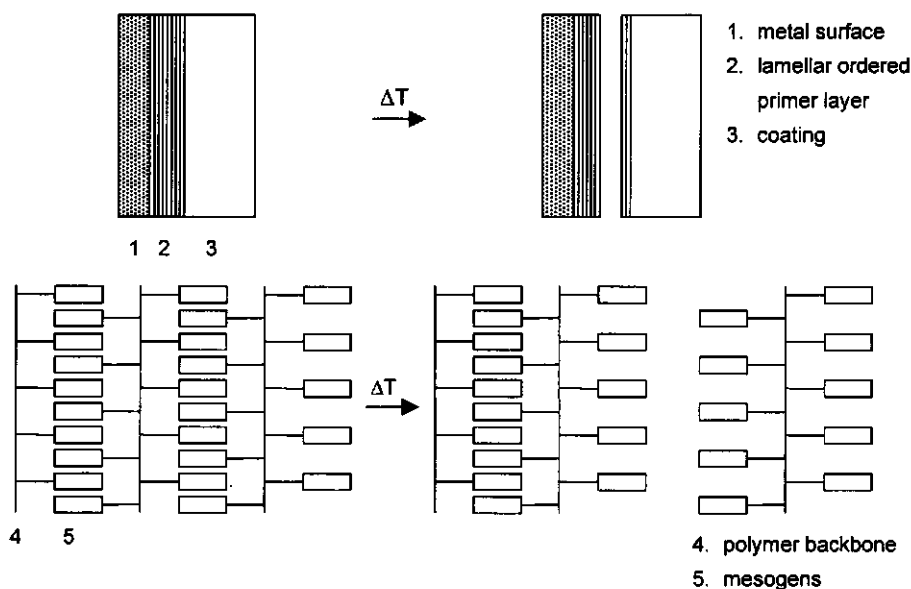
Figure 1.1. Schematic representation of coating removal: top, macroscopic view; bottom, nanoscopic view.

1.3. Contents of this thesis

The aim of the study presented in this thesis is to synthesize SCLCPs that may be applicable as a splittable primer, i.e. these polymers have to be able to form lamellar or

smectic structures and contain moieties that enhance adhesion. Therefore, novel SCLCPs are developed with polar moieties in the backbone that adhere well to metal or aluminum surfaces. These SCLCPs are obtained by copolymerization of monomers with rigid groups (mesogens) and monomers with polar moieties, like maleic anhydride and carbon monoxide. Special attention will be paid to the structure-property relations of these SCLCPs, in which the use of X-ray diffraction is indispensable. In addition, the polar moieties in the polymer backbone make these SCLCPs interesting for fundamental investigations in Langmuir and Langmuir-Blodgett films. These films may serve as a model system for the smectic structure in a primer film. Parallel to this study, the properties of some of these novel SCLCPs in spincoated films on silicium wafers were studied.[12] Special attention will be paid to the order in thin films, the development of order upon annealing, wetting behavior and the effect of surface roughness.

In *Chapter 2*, a literature review is given about SCLCPs. First, the principle of liquid crystallinity is explained, followed by a summary of the different types of liquid-crystalline phases. Special attention is paid to the research that has been focussed so far on SCLC polymers and SCLC copolymers. *Chapter 3* describes the synthesis and mesomorphic behavior of alternating SCLCPs from maleic anhydride and 1-alkenes. The influence of the molecular architecture of these copolymers on the mesomorphic properties will be studied. In *Chapter 4*, the effect of the mesogen density of these copolymers will be studied by grafting mesogen-containing alcohols onto these polymers. Three series will be described: a series in which methoxybiphenyl containing alcohols with variable spacer lengths are grafted, a series in which azobenzene-containing alcohols with different terminal subsituents are grafted and, finally, a series in which both methoxybiphenyl mesogens and cyanobiphenyl mesogens are combined. *Chapter 5* describes an alternative way to increase the mesogen density: copolymerization of maleic anhydride with swallow-tailed 1-alkenes. This approach may result in polymers that exhibit highly ordered mesophases. *Chapter 6* reports the copolymerization of mesogenic methacrylates with maleic anhydride. The advantage of methacrylates above 1-alkenes is that (i) the polymerization reaction proceeds more rapidly, (ii) the MA (or mesogen) fraction in the backbone can be altered. This chapter describes the effect of maleic anhydride content, spacer length and type of mesogen on the mesomorphic properties. *Chapter 7* deals with a completely new class of SCLCPs: SCLC poly(ketones). The effect of spacer length of methoxybiphenyl-containing side chains and mesogen density will be studied. In addition, this study reports the properties of SCLCPs obtained from the first-ever nitrogen-containing monomers used in this type of copolymerization reaction. *Chapter 8* describes the rheology of a selection of polymers from the preceding chapters. *Chapter 9* reports the behavior of a selection of polymers from the preceding chapters in Langmuir and Langmuir-Blodgett films.

1.4. References

1   Weiss, K. D. *Prog. Polym. Sci.* **1997**, *22*, 203.

2   Wicks, Z. W.; Jones, F. N.; Pappas, S. P. *Organic Coatings, Science and Technology, Volume 2: Applications, Properties and Performance*; John Wiley & Sons: New York, 1994, Chapter 28.

3   Wicks, Z. W.; Jones, F. N.; Pappas, S. P. *Organic Coatings, Science and Technology, Volume 2: Applications, Properties and Performance*; John Wiley & Sons: New York, 1994, Chapter 29.

4   Wicks, Z. W.; Jones, F. N.; Pappas, S. P. *Organic Coatings, Science and Technology, Volume 2: Applications, Properties and Performance*; John Wiley & Sons: New York, 1994, Chapter 32.

5   Wicks, Z. W.; Jones, F. N.; Pappas, S. P. *Organic Coatings, Science and Technology, Volume 2: Applications, Properties and Performance*; John Wiley & Sons: New York, 1994, Chapter 31.

6   van Opstal, M. *Chemisch Magazine* **1995**, 233.

7   Reisch, M. S. *Chem. Eng. News* **1995**, *September 25*, 30.

8   Springer Jr., J.; Stone, K. R. *Environmental Progress* **1995**, *14*, 266.

9   Kuipers, D. *Het verwijderen van verfsystemen van staal*, Thesis Hogeschool Enschede, Beschermingstechniek (1994).

10 Jentzsch, W.; Tecklenburg, H.; Daus, A.; Siegmann, L.; Jentzsch, G.; Musinski, H., German Patent DD 300 268 A7 (1992).

11 Maginnis, M. A., US Patent WO 93/01243 (1993).

12 van der Wielen, M. W. J. Dissertation Wageningen University and Research Center (1999).

2

Side-chain liquid-crystalline polymers

2.1. A new phase of matter

Between 1850 and 1888, researchers in different fields such as chemistry, biology, medicine and physics found that several materials behaved strangely at temperatures near their melting points. It was observed that the optical properties of these materials changed discontinuously with increasing temperature. One of the researchers was Friedrich Reinitzer, a botanist from Austria who was interested in the biological function of cholesterol in plants. In 1888, he observed that a cholesteryl derivative melted to a cloudy liquid at 145.5°C and became a clear liquid at 178.5°C.[1] He repeated an earlier experiment which showed that upon cooling the clear liquid, a brief appearance of a blue color could be seen at the transition to the cloudy liquid, and that a blue violet color appeared just before crystallization. At the time Reinitzer made these observations, he was unaware of the chemical structure of this compound which proved to be cholesteryl benzoate. However, this did not keep him from concluding that a parallel organization of molecules with an elongated structure must be responsible for this odd behavior. Together with Otto Lehmann, a German physicist, and others the new phase of mater was identified as the *liquid crystal (LC) phase*.

The LC phase, also known as mesophase, can be regarded as a phase with characteristics that are between a liquid or isotropic melt and a crystal, as is schematically depicted in Figure 2.1. The crystalline state is defined by a very low mobility and a periodic long-range order with respect to (i) the position of the molecules, (ii) their orientation and (iii) molecular
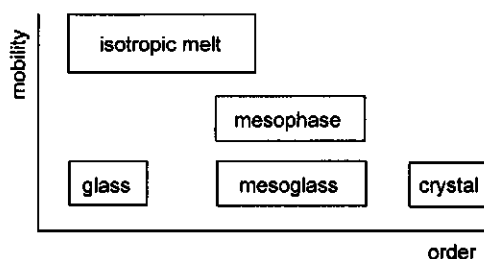
Figure 2.1. Classification of condensed phases in terms of order and mobility.

conformation. Maximum disorder and a high mobility are found in the isotropic melt. If the state of order of a condensed phase is less that that of a three dimensional regular crystal, but is still characterized by partial order with respect to the packing of the molecules, the phase can be classified as a mesophase or as its vitrified analogue, the mesoglass. Of these two phases the mesoglass lacks molecular mobility, whereas the molecules within the mesophase do possess a certain degree of mobility.

2.2. Liquid-crystalline phases

Traditionally, three types of LC phases are distinguished on the basis of positional order and orientation of rod-like molecules: nematic (N), smectic (S) and chiral nematic. More recently, it was found that disc-like shaped molecules have their own characteristic mesophases: columnar or discotic mesophases. Some examples of the different mesophases are given in Figure 2.2.

The *nematic* (N) mesophase has the lowest degree of order. The molecules have long-range orientational order but no long-range translational order. The molecules can move freely and rotate around their long axes as long as they remain more or less parallel to each other. A special class of nematic liquid crystals is called *chiral nematic*, also known as *cholesteric*. In this mesophase the director, the preferred direction the mesogens point along,

| nematic | smectic A | smectic C |

| smectic B | chiral nematic | columnar |
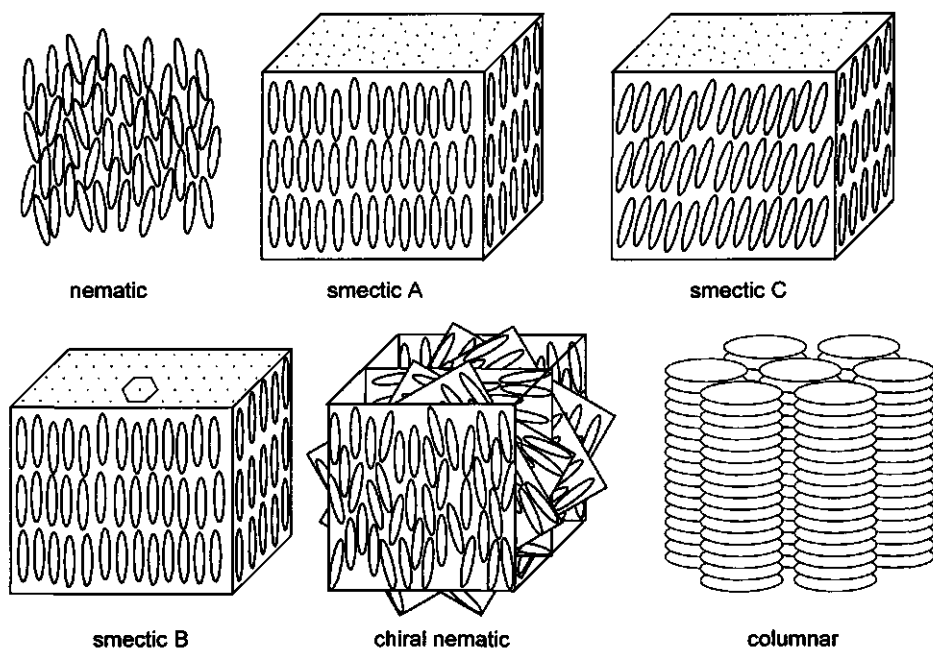
Figure 2.2. Schematic representation of molecular arrangements in several mesophases.

is turned at a constant angle around an axis perpendicular to the director. As a consequence, the mesophase has a helical structure. The helical structure results from chirality in the mesophase forming compound. A special feature of the cholesteric mesophase is that it reflects selectively one component of circularly polarized light of a certain wave length.

The *smectic* mesophase shows besides long-range orientational order also long-range translational order. In other words, the molecules tend to align themselves in layers or planes. Motion is partially restricted to within these layers, and separate layers are observed to flow past each other. Many smectic mesophases are known: so far, smectic A – smectic K mesophases have been observed.[2] Two common smectic mesophases are the *smectic A* (S_A) and the *smectic C* (S_C) mesophase. In the S_A mesophase the director is perpendicular to the smectic plane, and there is no particular positional order in the layer. The S_C mesophase is similar to the S_A, but the director is at a constant tilt angle with respect to the smectic layer. For these smectic layers, three different types of periodicity exist resulting in different layer thicknesses or *d* spacings. Firstly, if the *d* spacing equals the length of a molecule, the suffix *1* is added to the mesophase name, i.e. S_{A1}. Secondly, if the *d* spacing equals twice the length of a molecule, the suffix *2* is added. And finally, if the *d* spacing is between the length of a molecule and twice its length, the molecules interdigitate partially and the suffix *d* is added.

When the molecules within a layer with an S_A structure are arranged into a network of hexagons, two types of mesophases can be distinguished, i.e. hexatic smectics like *hexatic smectic B* (S_{Bhex}) or crystalline smectics like *crystalline smectic B* (S_{Bcryst}) and *smectic E* (S_E). These highly ordered smectics are characterized by long-range bond-orientational order. The main difference between S_{Bhex} and S_{Bcryst} mesophase is that in the S_{Bhex} mesophase there is only limited positional order, whereas in the S_{Bcryst} there is long-range positional order. On going from the S_{Bcryst} to the S_E mesophase, the degree of order within the layer increases. While in the S_{Bcryst} mesophase the herringbone packing (or chevron order, see Figure 2.3) is only local, in the S_E mesophase the herringbone packing is long-range. These phases are distinguished from ordinary crystals by a large amount of disorder and from the ability of the molecules to reorient.

The *columnar* or *discotic* mesophase can be found for molecules that are shaped like disks instead of long rods. For a columnar mesophase, the phase is characterized by columns of stacked molecules. The arrangement of the molecules within the columns and the
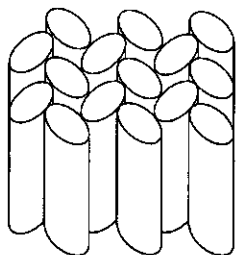

Figure 2.3. Schematic representation of a herringbone structure in the S_E mesophase.

intercolumnar arrangement lead to different mesophases. The columns can form orthogonal or tilted phases; the arrangement of the columns can be hexagonal or rectangular, and the organizations of the centers of mass of the molecules in the columns can be disordered or ordered.

2.3. Liquid-crystalline polymers

Liquid-crystallinity is not restricted to low molar-mass molecules, as described in Section 2.1, but can also occur in polymeric compounds. In comparison to low molar-mass materials, the relaxation processes in polymers are retarded. As a result, a large number of non-equilibrium states can be observed which can be falsely interpreted as equilibrium states. Equilibrium states can often be obtained only after prolonged annealing. Furthermore, the order of the mesogens can be frozen in upon cooling because polymers exhibit a glass transition temperature (T_g), whereas low-molecular-weight liquid crystals often undergo crystallization upon cooling. In comparison to low-molecular-weight liquid crystals, LC polymers (LCPs) often show an increase of temperature range of the mesophase. This has been illustrated for so-called side-chain (SC) LCPs (see Section 2.3.2.) by comparing the transition temperatures of alkoxycyanobiphenyls to those of SCLC poly(acrylate)s, poly(methacrylate)s and poly(siloxane)s containing cyanobiphenyl mesogens.[3]

2.3.1. Classification on the basis of conditions for liquid-crystallinity

With respect to the conditions for liquid-crystallinity, one can distinguish between lyotropic LCPs and thermotropic LCPs. Lyotropic LCPs have in common that they consist of very stiff chains of which the melting temperature of the crystalline phase is often far above the decomposition temperature of the polymer. However, after addition of a suitable solvent these polymers organize and form nematic LC phases. The critical concentration above which LC behavior can be observed decreases as the molecular weight increases. Commonly used solvents are concentrated sulfuric acid, chlorosulfonic acid and N,N-dimethylacetamide with dissolved LiCl.[4] Lyotropic liquid-crystallinity was demonstrated theoretically already in the 1950s by Onsager[5] and Flory[6] and then experimentally verified in studies with polypeptide solutions. However, it lasted till the 1970s before the experimental "explosion" occurred, when aromatic poly(amide)s were dissolved in very aggressive solvents and it was found that these solutions exhibit liquid-crystallinity.

The second class of LCPs is the thermotropic LCPs, which have been introduced in the mid-1970s. These polymers exhibit LC behavior in a certain temperature range, i.e. polymers exhibit LC behavior above the glass transition or melting point. This class of materials will be discussed in more detail in the following sections.

Since the introduction of LCPs, a lot of effort has been put in developing new materials and finding applications for these materials. Nowadays, liquid-crystalline polymers (LCPs) are applied in high-strength fibers (Twaron® and Kevlar®) and optical applications

like data storage, energy efficient liquid crystal displays (LCDs), foils to enhance the viewing angle of LCDs (Twistar®), optical amplifiers and nonlinear optics.

2.3.2. Classification on the basis of chemical structure

A general requirement for polymers to exhibit LC behavior is the presence of rod-like or disk-like moieties called mesogens. Figure 2.4 gives an overview the most common types of LCPs with mesogens. A detailed discussion and examples of these types of LCPs is given by Brostow.[7]

The mesogens may be attached to the polymer backbone as side groups (Figure 2.4 a-c) or be present in the polymer backbone (Figure 2.4 e-g), classified as Side-Chain (SC) LCPs and Main-Chain (MC) LCPs, respectively. Also combined LCPs have been developed that are hybrids between MCLCPs and SCLCPs (Figure 2.4 h,i).[8,9] More recently, elastomeric LCPs (Figure 2.4 d) have been developed[10] which are applied in LC displays in order to increase the efficiency or the viewing angle of these displays. These elastomeric networks are obtained by *in situ* polymerization of reactive molecules like mixtures of mesogenic diacrylates and acrylates. If these acrylates are photopolymerized in the mesophase, the order of the mesogenic monomers in the mesophase is preserved.

Some flexible polymers exhibit mesomorphic behavior and do not fit in the scheme of mesogen containing LCPs. Examples of these polymers are poly(ethylene),[11,12,13,14,15,16,17] trans-1,4-poly(butadiene),[18,19] poly(tetrafluorethylene)[12,20] and some organic-inorganic hybrid polymers like poly(di-n-alkylsiloxane)s,[21,22,23,24,25,26,27] poly(di-n-alkylsilylene)s[28,29,30] and poly(di-n-alkoxyphosphazene)s.[31,32] These polymers exhibit columnar phases in which the column consists of a polymer.
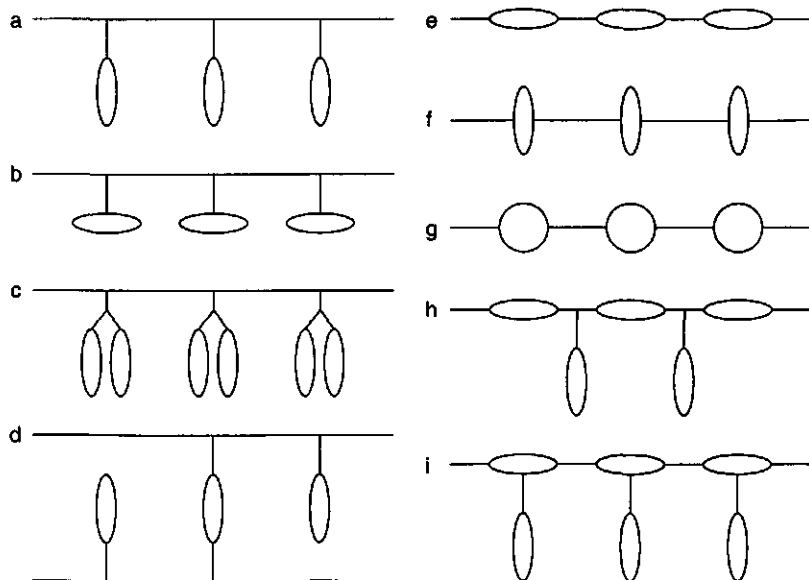

Figure 2.4. *Classification of LCPs on the basis of chemical structure.*

2.4. Molecular engineering of side-chain liquid-crystalline polymers

A SCLCP contains three primary structural variables each of which is significant in controlling the properties like mesomorphic behavior, mechanical behavior, processability and end-use. These primary variables are the polymer backbone, the spacer and the mesogen. Furthermore, the properties of a SCLCP are determined by polymer backbone variables like its nature, molecular weight, polydispersity, and tacticity. A summary of the effects of these structural variables on the polymer properties is given in the following sections.

2.4.1. Polymer backbone

Nature of the polymer backbone

The backbones that are used for SCLCPs are also present in commonly used industrial thermoplastics like poly(acrylate)s,[33,34,35,36] poly(methacrylate)s,[36,37,38] poly(styrene)s,[39,40,41] poly(siloxane)s,[42,43,44] poly(urethanes)[45,46,47] and poly(olefin)s.[48,49] More recently poly(thiirane)s,[50,51] poly(olefin sulfone)s,[52] poly(maleimide)s[53] and poly(norbornene)s[54,55,56] were used. The backbones of these polymers have different flexibilities, which again determine the phase behavior. The polymer flexibility also plays an important role in the decoupling of the motions of the mesogen and the polymer backbone. In general, the mesogen is more decoupled from the polymer backbone as the backbone flexibility increases. This is because the dynamics of ordering increase with increasing flexibility, which increases the ability of mesogens to form ordered mesophases and/or crystallize.[57] In addition, side-chain crystallization is observed at shorter spacer lengths as the polymer flexibility increases. As the flexibility of the polymer backbone increases, the glass transition temperature (T_g) of the SCLCP decreases, whereas the isotropization temperature (T_i) usually increases. However, exceptions to the last trend are known for e.g. cholesterol mesogens.[58,59] Because in this case the T_g shows a stronger decrease than T_i, the general trend is that the mesophase range increases with the flexibility of the backbone.

The glass transition of a polymer is not only determined by the polymer flexibility, but also by the free volume, interactions between chains and the chain length.[57] Therefore, it is difficult to assess the relative flexibility of two polymers from the glass transition alone.

The effect of backbone flexibility on the degree of order in the mesophases has been demonstrated for poly(norbornene)s and poly(butadiene)s with *p*-nitrostilbene mesogens.[56] For spacer lengths between six and twelve methylene units, it was found that the more flexible poly(butadiene)s exhibit smectic mesophases, whereas the relatively rigid poly(norbornene)s exhibit only nematic mesophases.

Molecular weight

A significant variable for the thermal and mechanical properties of a polymer is its molecular weight or degree of polymerization (DP). The effect of molecular weight on LC behavior has been studied by several authors.[36,55,56,60,61,62,63,64] An example is given in Figure

2.5 for poly(norbornene)s with methoxybiphenyl mesogens.[62] This figure shows that the phase transition temperatures rise with increasing DP. Above DP is twenty the dependence of phase transition temperatures on DP levels off. In contrast, the enthalpy changes are independent of DP.[55,57,62]
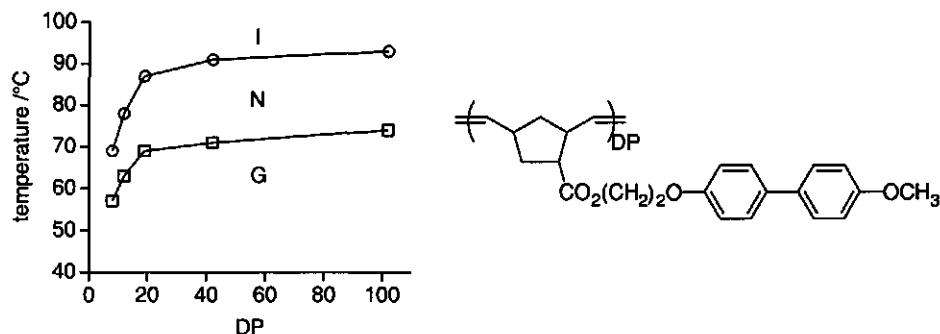
Figure 2.5. *Dependence of the glass (□) and N-I (○) transition temperatures on DP of poly(norbornene) with ethyl spacers and methoxybiphenyl mesogens.*[62]

For poly(vinyl ether)s with cyanobiphenyl mesogens it was found that the number and type of mesophase vary as a function of DP.[65] This is simply due to the fact that the phases have different dependencies on DP. The temperature range of at least the highest temperature mesophase increases with increasing DP due to the greater dependence of isotropization on DP compared to crystalline melting and the glass transition.[66]

Polydispersity

In contrast to low molar-mass liquid crystals, which undergo phase transitions over a few degrees, SCLCPs often exhibit extremely broad transitions. This wide biphasic region, in which two phases such as a mesophase and the isotropic melt coexist, is often attributed to the polydispersity of the polymers. The effect of polydispersity on phase behavior is one of the most fundamental questions still open regarding the structure-property relations of SCLCPs.

For poly(acrylate)s containing sulfoxide moieties in the mesogen, it has been found that smectic mesophases with different periodicities were found over a wide temperature range, which has been ascribed to the polydispersity of the sample.[67] In addition, from comparison of SCLC poly(styrene)s with a low and high polydispersity, it follows that polymers with a low polydispersity give the sharpest transitions.[64]

Komiya et al.[62] studied the effect of polydispersity on liquid crystalline behavior by blending well-defined poly(norbornene)s of varying molecular weights to create polydisperse samples. In this case, both monodisperse samples and multimodal blends underwent the nematic-isotropic transition over a narrow temperature range. Polydispersity also had no effect on the transition temperatures, which were only determined by DP.

11

Recently, it was shown that the width of the isotropization transition does not result from the polydispersity, but can be attributed to the limited miscibility of a mixture of polymers with different branching densities.[68] This was demonstrated by comparing the thermotropic behavior of linear and three-arm star poly(acrylate)s with cyanobiphenyl mesogens, and their binary blends and unmixed composites. As was found for poly(norbornene)s,[62] the biphasic region of linear polymers with polydispersities of 1.15-1.49 and mixtures of linear polymers with different DPs is extremely narrow. Although three-arm star polymers also exhibit extremely narrow isotropization transitions, binary mixtures of the star polymers with significant differences in branching density have limited miscibility and broad isotropization temperatures. For a radical-initiated SCLC poly(acrylate) it was demonstrated that the broad isotropization transition is a result of a mixture of branched structures. These branched structures can be attributed to chain transfer to polymer at high monomer conversion.[68]

Tacticity

Relatively little effort has been devoted to examine the effect of tacticity on well-defined SCLCPs prepared through living polymerization. However, Pugh et al.[69] have noted that the tacticity of poly(methacrylate)s mainly seems to affect melting points, which increase with stereoregularity. A high tacticity places the mesogenic side chains in the proper configuration to crystallize and/or form more ordered phases.[49] Because T_i remains more or less constant the mesophase range decreases. If the mesogens cannot form highly ordered mesophases, the primary effect of high tacticity is that it decreases the flexibility relative to the atactic polymer, which also results in a narrower mesophase range.[70] However, dielectric relaxation spectroscopy of poly(vinyl ether)s with cyanostilbene mesogens showed that tacticity plays a minor role for the relaxation behavior of this particular polymer.[71] The transition temperature, the activation energies and the relaxation strength were essentially the same for polymers with different tacticities. For poly(vinyl ether)s with 4-ethoxyphenylben-zoate mesogens X-ray diffraction has shown that the layer spacing is also unaffected by changes in tacticity.[72]

2.4.2. Spacer

Mesogens can be attached to the polymer backbone in two ways, i.e. (i) directly to the polymer backbone,[69,73] or (ii) via a flexible spacer. In order to obtain liquid-crystallinity, Finkelmann et al. predicted that the motion of the polymer backbone must be decoupled from that of the mesogens in the liquid state.[74,75] This concept is known as the *Spacer decoupling model* and assumes that a spacer should be inserted between the polymer backbone and a mesogen to ensure organization of mesogens. However, neutron scattering experiments have shown that the radius of gyration of a polymer backbone in the nematic phase has some anisotropy,[76] whereas it is highly anisotropic in a smectic phase.[77,78,79] These results indicate that the motions of the backbone and the mesogens are only partially decoupled. The most popular spacer is the oligomethylene spacer, but also spacers containing oxyethylene[80,81] and

siloxane[82,83] units are known. Introducing chirality in the spacer may yield polymers exhibiting chiral mesophases.[84]
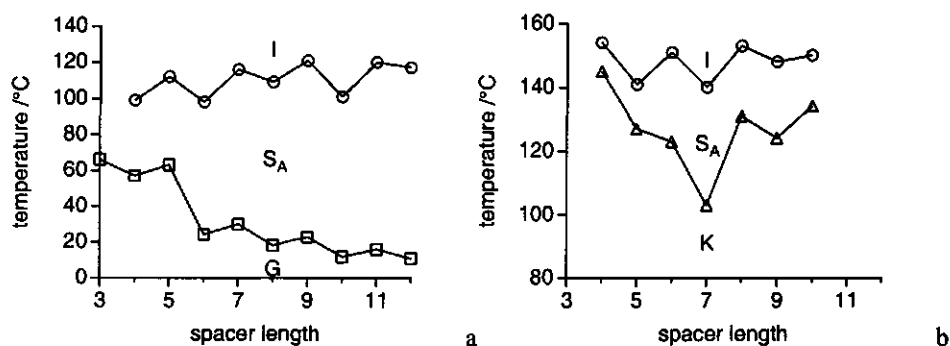

Figure 2.6. Dependence of transition temperatures from the glass (□), crystalline (△), and S_A (○) phases on the spacer length of cyanobiphenyl containing poly(methacrylate)s[85] (a) and methoxybiphenyl containing poly(norbornene)s[55] (b).

Figure 2.6 shows two examples of polymers in which the spacer length has been systematically varied. This figure shows that T_g decreases with increasing spacer length, which can be attributed to the decrease in packing density, also known as internal plasticization. Because the decrease in T_g is stronger than the decrease in T_i, the mesophase temperature range increases with spacer length.[57] Furthermore, an odd-even effect can be observed which sometimes attenuates with spacer length. Craig et al.[86] showed that the higher transition temperatures observed for the odd-membered spacers can be attributed to the higher amount of possible conformations for which the mesogens are coparallel. However, poly(norbornene)s show the opposite trend:[62] the highest transition temperatures are observed for the even-membered spacers. In this case the cyclopentane ring may be regarded as part of the spacer resulting in an odd-even effect comparable to that of poly(methacrylate)s. Other trends observed for spacer length are that (i) nematic mesophases normally arise at shorter spacer length, whereas longer spacers tend to encourage smectic phases; (ii) additional smectic phases may appear as spacer length increases; (iii) longer spacers may give rise to side-chain crystallization; and (iv) change in enthalpy and entropy at isotropization increase linearly with increasing spacer length.[87] This last trend can be explained by the constant increase in enthalpy or entropy change per methylene unit.[57] So far, no general trend for T_i has been observed.

2.4.3. Mesogen

The extensive literature on low molar-mass liquid crystals demonstrates that the chemical structure of a mesogen[88] and the spacer length of an SCLCP are the primary factors determining the mesophase type. The backbone should then be a secondary factor that governs the ordering of mesogens.

The mesogen consists of three significant components, e.g. (i) rigid segments (frequently phenyl rings), (ii) groups linking the rings, and (iii) substituents on the rings. An overview of different mesogens is given in Scheme 2.1. The main parameters in relation to LC behavior are type of mesogen, which will not be discussed here, the length of the mesogen and the type of substituents.

X = -   Y = CN
    -N=N-   O(CH₂)ₙCH₃
    -CH=CH-   NO₂
    -COO-   H
    -OCO-   F
    -CH=N-   (CH2)ₙCH₃
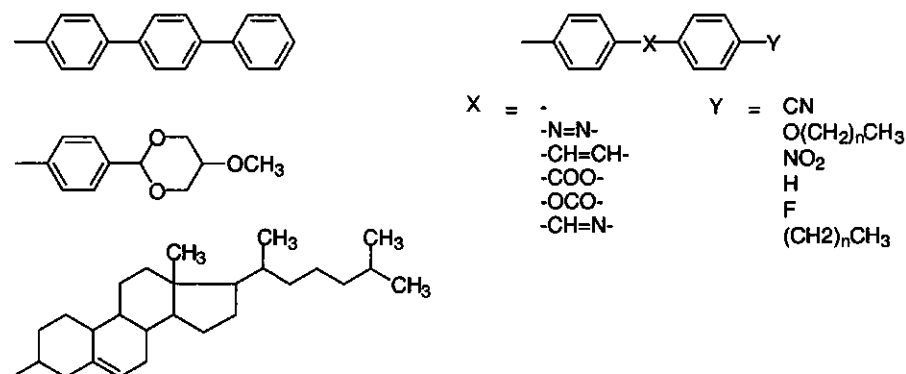
Scheme 2.1. *Overview of some different mesogens.*

Mesogen length

The general trend is that an increase in mesogen length, i.e. number of phenyl rings, leads to a broader mesophase range and better ordered phases.[89,90]
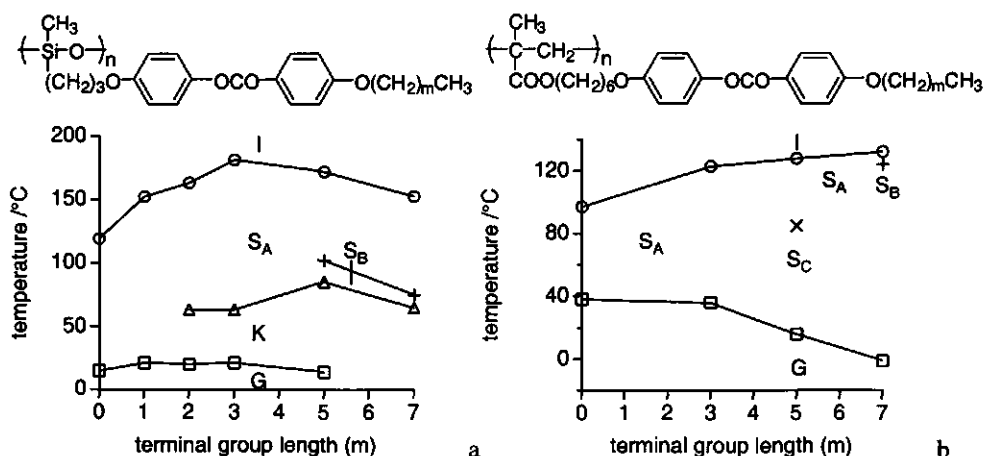
Figure 2.7. *Dependence of transition temperatures from the glass (□), crystalline (△), S_B (+), S_C (x) and S_A (o) phases on the terminal group length of poly(siloxane)s[91] (a) and poly(methacrylate)s[92] (b).*

An alternative way to increase the mesogen length is by increasing the terminal group length, which is shown for poly(siloxane)s[91] and poly(methacrylate)s[92] in Figure 2.7. This figure shows that T_g decreases with increasing terminal group length. This can be attributed to the decrease in packing density. In addition, the width of the mesophase tends to increase, although no general trend has been observed for T_i. T_i increases with terminal group length for a highly inflexible SCLC poly(olefin)s with a helical backbone,[49] whereas only slight variations for T_i as a function of terminal group length were observed for poly(oxetane)s[93] (m > 0) and polythiiranes.[51] Figure 2.7. shows that better ordered mesophases are obtained at higher terminal group lengths.

Substituents

Substituents can be attached to the mesogen laterally and terminally. The effect of terminal substituent has been studied by Richard et al.[43] for a series of poly(siloxane)s with phenylbenzoate mesogens. They observed the following trends: (i) without terminal substituent (Y = H, Scheme 2.1) no liquid crystalline behavior was observed; (ii) strongly polar substituents like cyano and nitro groups induce smectic mesophases and both mesogens induce similar T_is; (iii) less polar substituents like methoxy and methyl groups induce nematic mesophases; (iv) T_i increases with terminal group polarity.

Imrie et al.[94] studied the effect of terminal group of azobenzene mesogens for poly(styrene)s. The efficiency of the terminal group in stabilizing a mesophase is CN > NO$_2$ > OMe > F and this is in accord with the behavior found for poly(siloxane)s.[43] The transition entropy changes fall into two groups: SCLCPs with mesogens having F and OMe substituents exhibit significantly higher entropy changes than SCLCPs with mesogens having CN and NO$_2$ substituents. Wide-angle X-ray diffraction experiments showed that these two groups exhibit S_A mesophases with different degrees of interdigitation of the side chains. The side chains of SCLCPs with OMe and F terminal groups interdigitate completely, whereas the side chains in SCLCPs with CN or NO$_2$ terminal groups interdigitate partially. This partial interdigitation of side chains can be attributed to the tendency of CN and NO$_2$ containing mesogens to form antiparallel pairs, which serves to minimize the dipolar energy.

If a lateral substituent is attached to a mesogen, several effects can be observed for poly(siloxane)s with phenylbenzoate mesogens:[87] (i) mesophase formation is suppressed at low spacer length; (ii) crystalline and smectic mesophases are suppressed and nematics are obtained at spacer lengths of five to six methylene units; (iii) suppression of crystallinity beyond this spacer length can be observed. In addition, lateral substituents hinder rotational motions of mesogens around the long axis.[95]

2.5 Side-chain liquid-crystalline copolymers

By copolymerization of two or more monomeric species in varying ratios, polymeric products with an almost limitless variety of properties can be obtained. Scheme 2.2 shows the

```
AABBABBBAABAAAABBA      random

AAAAAAAAABBBBBBBB       block

ABABABABABABABABA       alternating

AAAAAAAAAAAAAAAAA       graft
    B       B       B
    B       B       B
    B       B       B
    B       B       B
    B       B       B
    B       B       B
    B       B       B
    B       B       B
    B       B       B
```

Scheme 2.2. *Different distributions of monomers A and B in a copolymer that can be obtained by chain polymerization.*

four different distributions of monomers in a polymer that can be obtained by chain polymerization of two different monomers. The properties of a random polymer are intermediate between those of the two homopolymers, whereas block and graft copolymers exhibit properties of both homopolymers. The properties of alternating polymers are unique.

The first three types of copolymers in Scheme 2.2 can be obtained by simultaneously copolymerizing two different monomers. The sequence of two monomers depends on r_1 and r_2, which are the monomer reactivity ratios of both monomers. The tendency of two monomers to copolymerize is noted by r values between zero and unity. An r_1 value greater than unity means that a polymer chain with a monomer 1 radical as propagating species ($M_1^\bullet$) preferentially adds monomer 1 (M_1) instead of monomer 2 (M_2), while an r_1 value less than unity means that $M_1^\bullet$ preferentially adds M_2. An r_1 value of zero would mean that M_1 is incapable of undergoing homopolymerization.

Random copolymers are formed in ideal copolymerizations where $r_1 \cdot r_2 = 1$. However, a truly random distribution of monomers requires $r_1 = r_2 = 1$, i.e. both monomers have equal probability of reacting with the propagating species. Alternating copolymers result if both reactivity ratios are close to zero due to little tendency of either monomer to homopolymerize ($r_1 = r_2 = 0$). Block copolymers can be formed in radical polymerization if $r_1 \gg 1$ and $r_2 \gg 1$. However, block copolymers are more effectively prepared by either sequential monomer addition in living polymerizations, or by coupling two or more telechelic homopolymers after their homopolymerization. Graft copolymers can be obtained by polymerization of macromonomers, which are obtained by ionic polymerization followed by end-capping with a functionalized end group that is capable to polymerize, e.g. a methacrylate.

By using one or two monomers with mesogenic moieties in a copolymerization, SCLCPs are obtained with monomer distributions as described above. The next sections will focus on two of these copolymers, e.g. random and alternating SCLC copolymers. In addition, a few examples of alternating SCLC copolymers obtained by step-growth polymerization will be described. The block and graft SCLC copolymers are described in more detail elsewhere[57,96,97,98,99] and are beyond the scope of this thesis.

2.5.1. Random SCLC copolymers

Random SCLC copolymers have several parameters than can be varied, i.e. the mesogen density, the combination of mesogens and the combination of spacers. The mesogen density can be altered by copolymerization of a mesogenic monomer with a non-mesogen-containing monomer. Different mesogen and spacer combinations can be obtained by copolymerization of two monomers containing different mesogens or spacers, respectively. An important aspect in these copolymerizations is the reactivity of the different monomers, which determines the randomness of the copolymers. The reactivity of a monomer is independent of a second functional group if they are separated by at least three methylene units.[100]
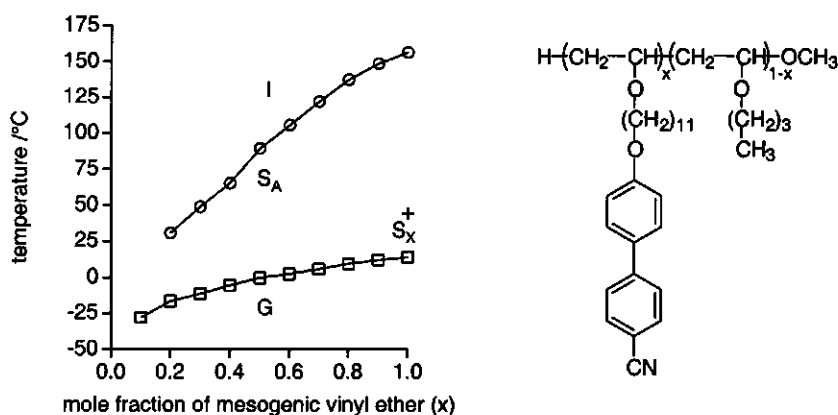
Figure 2.8. Dependence of T_g (□), S_X-S_A transition (+) and T_i (○) on the mole fraction of 11-(4'-cyanobiphenyl-4-yloxy)undecanyl vinyl ether in copolymers from 11-(4'-cyanobiphenyl-4-yloxy)undecanyl vinyl ether and butyl vinyl ether.

Mesogen density

Several authors[61,101,102,103,104,105,106,107] have studied the effect of mesogen density in SCLCPs that were obtained from copolymerizing mesogenic and non-mesogenic monomers. Changing the mesogen density showed to be a powerful tool to vary the mesophase range. The general trend is that T_g changes gradually between the T_gs of the respective homopolymers as the polymer composition is changed. In most cases, a non-mesogenic monomer is chosen that lowers the T_g of the SCLC copolymer relative to the parent SCLC homopolymer (Figure 2.8). Copolymerization of a mesogenic and a non-mesogenic monomer dilutes the mesogen concentration of the copolymer and below a minimum concentration the copolymer loses its LC behavior. This concentration is determined by the nature of both monomers. As a result, both T_g and T_i are affected by the mesogen concentration. For some polymers an almost linear relation between T_i and mesogen density has been found (Figure 2.8).[104,106] In addition, a linear relation has been observed between the enthalpy change at isotropization and the mesogen concentration.[104] From extrapolating this line to zero enthalpy

change the limiting mesogen fraction was determined at which liquid-crystallinity can be observed. This limiting mesogen fraction was calculated to be slightly smaller than 0.2 for the polymer shown in Figure 2.8, which agrees well with the experimental data.

Behavior deviating from the trends shown in Figure 2.8 has been observed for copolymers from mesogenic acrylates and acrylic acid.[107] Dilution with acrylic acid resulted first in an increase in order (N $\rightarrow$ S_A) and an increase in T_i and T_g, followed by a decrease in transition temperatures and disappearance of LC behavior. From comparison of this behavior with the mesomorphic behavior of copolymers from mesogenic acrylates and methyl acrylate, it was concluded that the odd behavior observed for acrylic acid copolymers can be attributed to the presence of hydrogen bonds. These hydrogen bonds increase the rigidity of the polymer backbone resulting in a more stretched conformation of the backbone. Therefore, the translational motion of mesogens is restricted and smectic layers are formed.

X-ray diffraction measurements of the polymer depicted in Figure 2.8 showed that the intermesogenic distance was independent on mesogen density.[105] However, the *d* spacing increased with decreasing mesogen concentration, which was partially ascribed to the formation of a disordered polymer layer between smectic layers. In addition, a change in side-chain interdigitation was observed, i.e. the S_{Ad} mesophase transformed into an S_{A2} mesophase upon decreasing the mesogen density.

A disordered backbone phase between mesogen layers, i.e. a microphase separated system, has been observed for poly(siloxane)s with paired mesogens (Figure 2.9).[101,102,103] One layer consists of the irregularly arranged backbone that can easily fold back because of its high flexibility, while the other layer consists of the mesogenic side chains. As a result, the *d* spacing increases linearly with decreasing mesogen density. The transition temperatures show only a small dependence on the mesogen concentration, which is typical of a microphase-separated system. Simultaneously, nonmicrophase-separated SCLCPs, in which the backbone is not present between mesogen layers but crosses these layers, show a strong dependence of transition temperatures on mesogen concentration.[101]

For some SCLC copolymers it has been observed that the width of the transitions, i.e. the biphasic region, increases with decreasing mesogen concentration.[104,105] A possible

$\bullet$ = S i

$\circ$ = O

Figure 2.9. Schematic model of the layer of a poly(siloxane) with paired mesogens with an assumed arrangement of the dimethylsiloxane segments between the Si-atoms linked to the dimesogenic side chains.

explanation for this behavior may be that a lower concentration of mesogenic side chains gives a larger percentage of mesogenic side chains being dissolved into the polymer backbone phase, which is present between mesogen layers.

Different mesogens

Several studies report the combination of different mesogens in SCLCPs.[33,37,108-110,112-118] The majority of these SCLCPs are obtained by copolymerizing monomers with different mesogens but similar polymerizable moieties, e.g. poly(methacrylate)s,[37,109,112,115,116,118] poly(acrylate)s[33,110] or poly(styrene)s.[113,114,117] Therefore, the two different mesogens are present in a random sequence. The majority of the studies focused on specific interactions between two different mesogens,[33,37,112-118] however, some studies focus on tuning the mesomorphic behavior without making use of these specific interactions[108-110].

Reesink et al.[108] studied the effect of copolymerizing epoxy monomers with biphenyl mesogens having different terminal alkoxy group lengths. In case of methoxy and octyloxy terminal groups, the mesomorphic behavior was an intermediate of the mesomorphic behavior of the two homopolymers. However, at equimolar amounts of both mesogens a reentrant S_A mesophase was observed. Combining butoxy and pentoxy terminal groups yielded both reentrant N and S_A mesophases over a broad composition range.

Two other studies report chiral mesophases that can be adjusted by copolymerizing different mesogens.[109,110] For poly(methacrylate)s, a cholesteric mesophase was observed upon copolymerization of monomers with a methoxybiphenyl and a cholesteryl mesogen, whereas the homopolymers of both monomers did not exhibit a cholesteric but an S_A mesophase.[109] In this case, the width of the cholesteric mesophase depends on the mole fraction of the chiral monomer. For poly(acrylate)s, it has been shown that the inverse pitch of the chiral nematic phase, i.e. the wavelength of reflected light, is proportional to the mole fraction of chiral monomer in the copolymer.[110]

The effect of combining mesogens with electron-withdrawing and electron-donating substituents on mesomorphic behavior has been investigated by several authors.[33,37,112-118] The combination of electron-poor and electron-rich mesogens gives rise to specific interactions. The precise nature of these interactions is unclear, although it is generally assumed that charge transfer complexes are involved.[111]

Some studies[112,113,114,115,116] describe a systematic investigation of the effect of copolymer composition on mesomorphic behavior, as is shown in Figure 2.10. The general trend is that T_i and the corresponding entropy change deviate significantly from the transition temperatures based on the composition-weighted average of both homopolymers, whereas T_g does not exhibit this deviation (Figure 2.11).[112-115] Furthermore, the strongest deviation is observed around a 1 : 1 ratio of both mesogens, although it is slightly shifted towards the component exhibiting the higher transition temperatures.[112] Also examples are known in which an S_A mesophase was found over a wide composition range, whereas both homopolymers prepared from the individual monomers are nematic. These trends agree with those observed for mixtures of low molar-mass liquid crystals.[112]
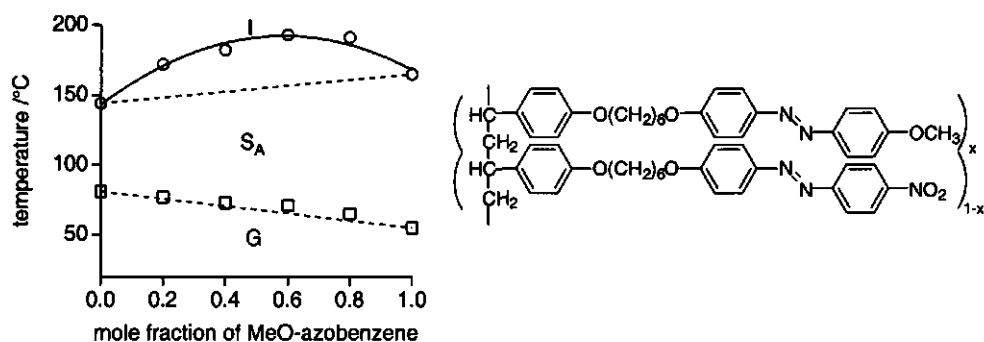
Figure 2.10. *Dependence of T_g(□) and T_i(o) on the mole fraction of methoxyazobenzene in a copoly(styrene) with both methoxyazobenzene and nitroazobenzene mesogens.[112] The dashed line represents the transition temperatures based on the weighted average of both homopolymers.*
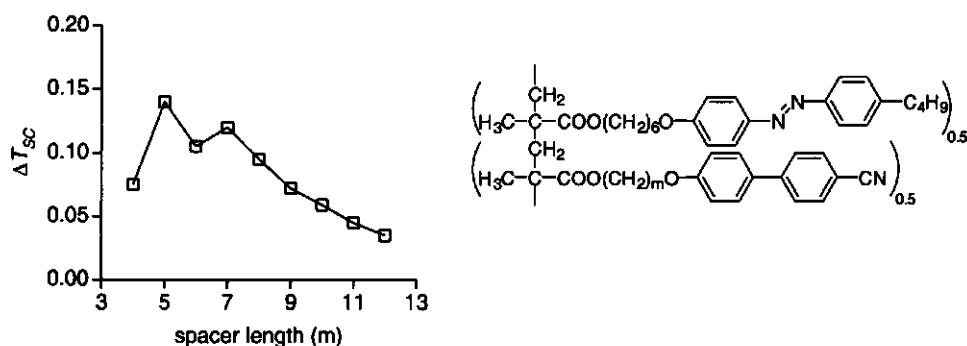
Figure 2.11. *Dependence of the scaled deviation (ΔT_{SC}) on spacer length m in the cyanobiphenyl terminated side chain for a random poly(methacrylate) containing butylazobenzene and cyanobiphenyl mesogens.*

Another way to control the mesomorphic behavior of SCLCPs while making use of specific interactions is varying the spacer length of one of the mesogenic mono-mers.[33,37,117,118] In order to compare the relative magnitudes of the deviations of T_i from ideal behavior, Imrie et al.[37,41,117] introduced a scaled deviation, ΔT_{SC}, as

$$\Delta T_{SC} = \frac{2T_{AB} - (T_A + T_B)}{(T_A + T_B)} \tag{2.1}$$

where T_{AB} is the T_i for the copolymer, and T_A and T_B are those of the homopolymers. If the copolymer has a lower T_i than predicted by ideal mixing, ΔT_{SC} will be negative, whereas a positive value of ΔT_{SC} indicates a higher T_i than predicted by ideal mixing. An example is given in Figure 2.11 for a random poly(methacrylate) with cyanobiphenyl and butylazobenzene mesogens.[37] In general, the spacer lengths of both mesogens do not

necessarily have to be of the same length in order to obtain the highest value of ΔT_{SC}. However, if the disparity in spacer length becomes too large, the overlap of mesogens decreases, resulting in a decrease of specific interactions, which is demonstrated by the decrease in ΔT_{SC}. Due to specific interactions the copolymer may exhibit smectic mesophases if the disparity in spacer length is small, whereas the homopolymers prepared from the individual monomers only exhibit nematic mesophases.[118]

Different spacer lengths

The last method to tune the mesomorphic properties of SCLC copolymers that will be discussed is the copolymerization of monomers with similar mesogens but different spacer lengths. Percec et al.[119,120,121] extensively studied the effect of copolymerizing cyanobiphenyl containing vinyl ethers with different spacer lengths on LC behavior. If copolymers are prepared from two different monomers that yield homopolymers that exhibit no LC behavior and an S_A mesophase, respectively, the resulting copolymers display a nematic mesophase over quite a broad range of copolymer compositions. In addition, if one of the monomers yields homopolymers with a nematic mesophase and the other one yields homopolymers with an S_A mesophase, the temperature range of the nematic mesophase of the resulting coppolymers is increased considerably. The transition temperatures of the copolymers show an almost linear dependence of copolymer composition.

Imrie et al. used the same approach to tune the LC properties of poly(styrene)s with methoxyazobenzene mesogens[122] and nitroazobenzene mesogens.[41] For methoxyazobenzene mesogens, no deviations from ideal behavior were observed ($\Delta T_{SC} = 0$). However, for nitroazobenzene mesogens ΔT_{SC} was slightly negative for different spacers. The deviation from ideal behavior increases with the disparity in spacer length. The difference in behavior of copolymers with methoxyazobenzene and copolymers with nitroazobenzene mesogens can be attributed to specific destabilizing dipolar interactions between nitroazobenzene mesogens, which do not play a role for methoxyazobenzene mesogens.

2.5.2. Alternating SCLC copolymers obtained by chain copolymerization

So far, relatively little attention has been paid to alternating SCLC copolymers. Alternating SCLC copolymers have unique properties due to the combination of two different monomers in an alternating fashion. Two kinds of alternating SCLC copolymers have been described that have been obtained by chain polymerization, i.e. poly(alkene-*alt*-sulfones)[52,127-129] and copolymers containing units derived from maleic anhydride (MA).[77,80,123,124,125,126]

Poly(olefin sulfones)

The first examples of SCLC poly(alkene-*alt*-sulfones) were reported in 1987 by Braun et al.[127] and were obtained by the alternating copolymerization of mesogenic olefins and sulfur dioxide. They used several mesogenic alkenes in the copolymerization reaction, but only obtained stable copolymers for 1-alkenes with methoxy or ethoxy terminated mesogens. The other polymers underwent thermal degradation in the mesophase.

21

Fawcett et al.[128] studied the effect of terpolymerization of cholesterol or cholestanol containing 1-alkenes with sulfur dioxide and 1-hexene. In this way alternating copolymers with a random distribution of 1-hexene units were obtained with different mesogen densities. The effect of mesogen density on T_i and T_m is shown in Figure 2.12. It can be seen that both transitions are significantly lowered as the mesogen fraction decreases. Furthermore, T_m and T_i of the cholestanyl series of polymers are more sensitive to mesogen dilution than those of the cholesteryl series of polymers. This has been ascribed to the fact that the cholesteric mesogen has a double bond at the 5-position that serves as an extra factor stabilizing the mesophase.

More recently Date et al. studied the properties of novel poly(1-alkene-*alt*-sulfones) in spincoated films.[52,129] The polymers contained cyanobiphenyl mesogens and exhibited S_A and S_B mesophases. Furthermore, it was stated that the backbone has a helical conformation and therefore provides a self-ordering system in the bulk where one chain may influence its neighbors in one or two extra dimensions. Spincoated films of these polymers became ordered on cooling from the melt or just on annealing.
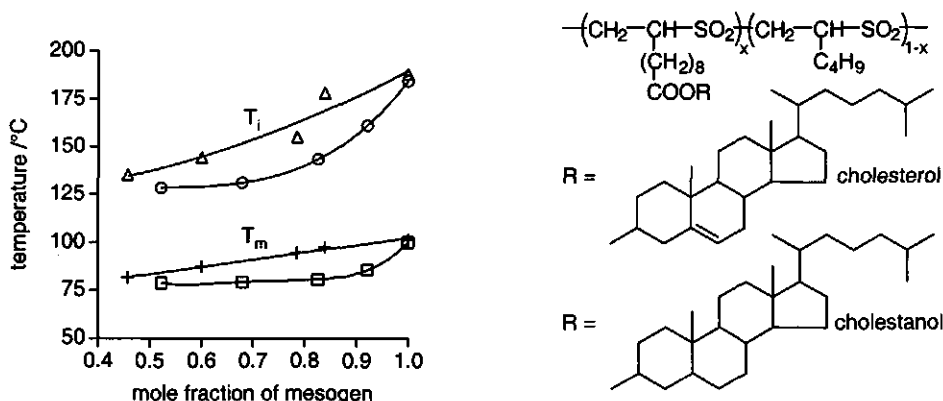
Figure 2.12. *Dependence of T_i and T_m on the mole fraction of mesogens for the cholesteryl (Δ, +) and cholestanyl (□, o) ester terpolymers.*
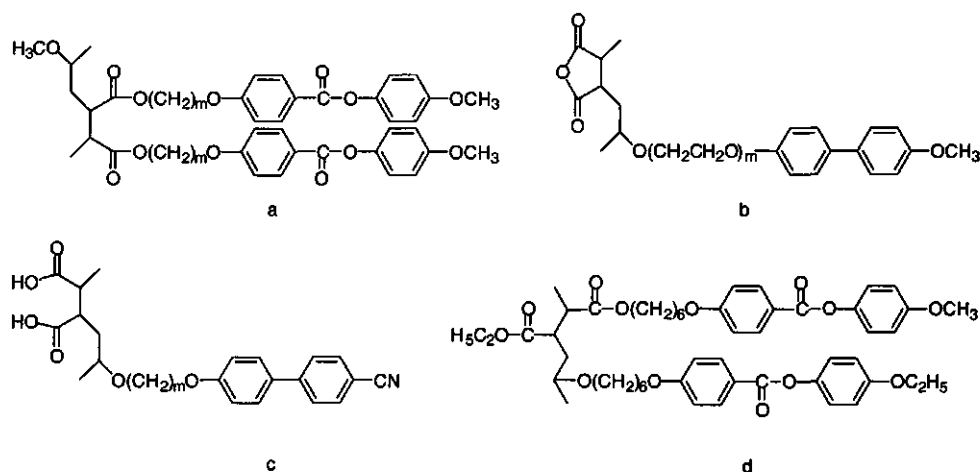
Copolymers containing MA or its derivatives

The majority of alternating SCLC copolymers obtained by chain polymerization contains MA moieties or MA derivatives.[77,80,123-126] These electron-poor monomers show an extremely low tendency to homopolymerize[130,131] and are known to copolymerize with a variety of monomers in an alternating fashion, e.g. alkenes,[131,132,133] styrenes,[134,135,136,137,138] vinyl ethers,[139] and vinyl acetate.[140] Recently, UV-spectroscopy and Monte-Carlo simulations have shown that the alternating copolymerization arises from the strong interactions between electron-poor and electron-rich monomers which result in donor-acceptor combinations that subsequently homopolymerize.[141]

Due to the presence of ring structures in the backbone, copolymers with MA moieties usually have rigid backbones that result in high T_gs. This high rigidity may prevent polymers

with MA moieties and mesogens to display liquid crystallinity, which has been demonstrated for poly(maleimide-*alt*-vinylpyridine)s[142] and poly(maleimide-*alt*-styrene)s.[143] These polymers do not exhibit LC behavior because the motion of the backbone cannot be decoupled from that of the mesogens.

The delicacy of the influence of molecular structure of polymers on LC behavior becomes clear when copolymers of styrenes and fumarates are considered. Copolymers from monomesogenic fumarates and styrenes exhibit (crystalline and) a N mesophase,[123] whereas copolymers from dimesogenic fumarates and styrene exhibit S_A mesophases.[124] These polymers also contain bulky phenyl side-groups and have mesogen densities that are comparable to those of poly(maleimide-*alt*-vinylpyridine)s[143] and poly(maleimide-*alt*-styrene)s.[143] The LC behavior of copolymers from styrenes and fumarates can probably be attributed to the absence of a ring-closed moiety like maleimide.

Scheme 2.3. *Overview of SCLCPs obtained from copolymerizing MA or its derivatives and vinyl ethers.*[77,80,125,126]

Some other SCLCPs with MA-like moieties are depicted in Scheme 2.3. These SCLCPs have in common that they are obtained by copolymerization of vinyl ethers and MA-like monomers. Keller[77] obtained SCLCPs from coupling ω-bromoalkyl mesogens to poly(methyl vinyl ether-*alt*-disodium maleate) under phase transfer conditions (Scheme 2.3a). These polymers exhibited N mesophases for methoxy terminal groups and smectic and N mesophases for longer terminal groups, e.g. -OC₃H₇, -OC₄H₉, -C₆H₅. S_E mesophases were observed for alternating copolymers from MA with vinyl ethers having oxyethylene spacers and cyanobiphenyl mesogens (Scheme 2.3b).[80] Comparable polymers, but with cyanobiphenyl mesogens and oligomethylene spacers were prepared by Nieuwkerk et al. (Scheme 2.3c) and exhibited smectic mesophases.[126] This study showed that the backbone flexibility decreased upon ring closure of the maleic acid moieties to MA moieties, which was demonstrated by a decrease in T_i and the corresponding enthalpy change.

Laus et al.[125] synthesized almost alternating SCLCPs from mesogenic fumarates and mesogenic vinyl ethers (Scheme 2.3d) by using an excess of vinyl ether. These polymers have mesogen densities that are comparable to those of the modified polymers depicted in Scheme 2.3a and also exhibit N mesophases or a combination of smectic and N mesophases. It was observed that the transition temperatures of these mesophases increase with increasing mole fraction of mesogenic vinyl ether in the copolymer. This can be attributed to the increase in backbone flexibility with increasing vinyl ether content.

### 2.5.3. Alternating SCLC copolymers obtained by step-growth copolymerization

In contrast to MCLCPs, which are usually obtained via step-growth polymerization,[144] the majority of SCLCPs are obtained via chain polymerization. Some SCLCPs are, however, obtained via step-growth polymerization. Because two different monomers are used containing one type of reactive group, alternating copolymers are obtained.

In 1992, Han et al.[145] reported the synthesis and behavior of poly(malonic ester)s, which are obtained via the polycondenstation of 1,6-dibromohexane and malonic esters with methoxyazobenzene mesogens and oxyethylene spacers. These polymers have low molecular weights and exhibit monotropic N mesophases. SCLCPs with high molecular weights can be obtained via the polycondensation of diphosgene and diol monomers carrying nitrostilbene mesogens.[146] These polymers exhibit N and/or S_{Ad} mesophases, where the partial interdigitation comes from the antiparallel organization of nitrostilbene mesogens. These polymers exhibit the same trends as observed for chain polymerized liquid crystals (see Section 2.4.2.): T_g decreases and the mesophase range increases with increasing spacer length.

Scheme 2.4 shows some SCLCPs that were obtained from the alternating copolymerization of mesogenic diethyl malonates and diols.[147,148,149] By varying the length of the diol, SCLCPs can be obtained with various mesogen densities (scheme 2.4a and 2.4b). Figures 2.13a and b show the dependence of transition temperatures on diol length m for polymers depicted in Scheme 3a and b, respectively. The general trend is that the transition temperatures decrease with increasing diol length, i.e. decreasing mesogen density,[147,148] which is in agreement with previous studies on the effect of mesogen density of the thermotropic behavior.[61,101-107]

Furthermore, terpolymers with a structure comparable to that depicted in Scheme 2.4b have been synthesized containing mesogens with electron-donating and electron-withdrawing substituents, i.e. nitroazobenzene and methoxybiphenyl mesogens.[148] These mesogens are incorporated in the SCLC copolymer in a random fashion. The random copolymers display a N mesophase over a much wider temperature range than the respective homopolymers, which has been ascribed to electron donor-acceptor interactions between the two mesogens in the monomer pair. However, induction of a smectic mesophase could not be achieved in these systems. A smectic mesophase has been observed for alternating SCLCPs containing mesogens with electron-donating and electron-withdrawing substituents as depicted in

Scheme 2.4c.[149] However, polymers with a comparable molecular structure but a random sequence of electron-rich and electron-poor mesogens displayed a larger temperature range of the mesophase.
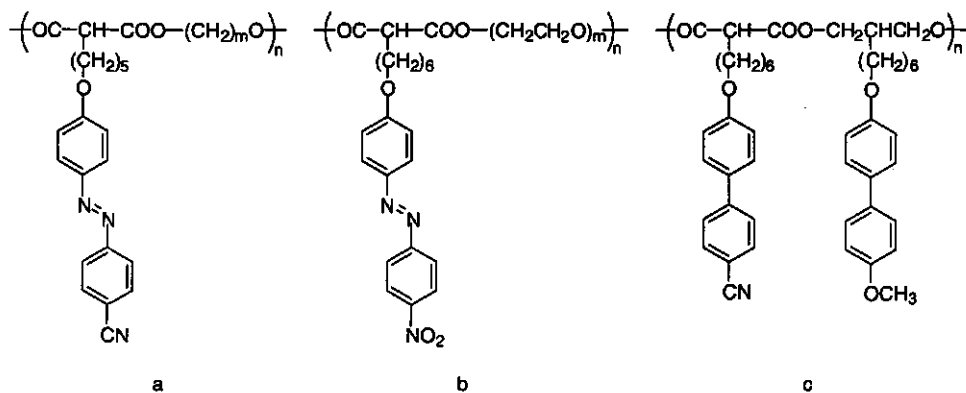
Scheme 2.4. SCLCPs from the alternating copolymerization of mesogenic diethyl malonates and diols.
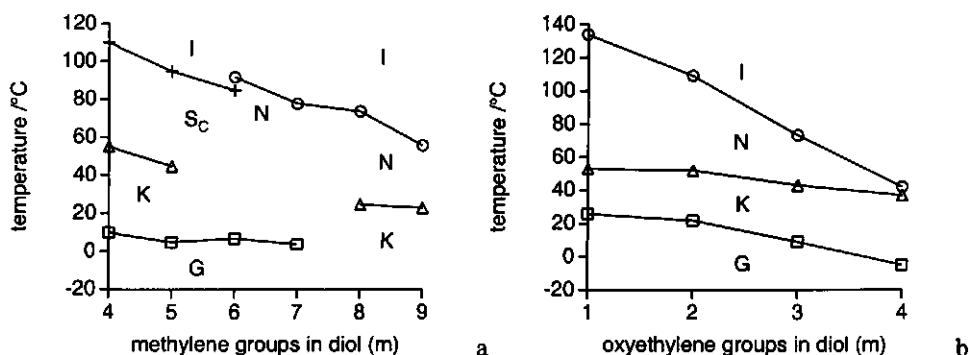
Figure 2.13. Dependence of T_g (□), T_m (Δ), S_C-N/S_C-I (+)and N-I transitions (o) on diol length (m) for polymers depicted in Scheme 4a (a)[147] and 4b (b).[148]

2.6. References

1   Reinitzer, F. *Monatsh. Chem.* **1888**, *9*, 421.

2   Noël, C. *Liquid Crystal Polymers: from Structures to Applications*; Collyer, A. A., Ed.; Elsevier Applied Science: London and New York, 1992.

3   Shibaev, V. P. *Liquid Crystalline Polymers*; Platé, N. A., Ed.; Plenum: New York, 1993.

4   Northolt, M. G.; Sikkema, D. J. *Liquid Crystal Polymers: From Structures to Applications*; Collyer, A. A., Ed.; Elsevier Applied Science: London and New York, 1992.

5   Onsager, L. *Ann. N.Y. Acad. Sci.* **1949**, *5*, 627.

6   Flory, P. *Proc. Roy. Soc. London* **1956**, *A234, No. 1*, 73.
7   Brostow, W. In *Liquid Crystal Polymers: From Structures to Applications*; Collyer, A. A., Ed.; Elsevier Applied Science: London and New York, 1992.
8   Reck, B.; Ringsdorf, H. *Makromol. Chem. Rapid Commun.* **1985**, *6*, 291.
9   Reck, B.; Ringsdorf, H. *Makromol. Chem. Rapid Commun.* **1986**, *7*, 389.
10   Hikmet, R. A. M.; Lub, J. *Prog. Polym. Sci.* **1996**, *21*, 1165.
11   Yamamoto, T.; Miyaji, H.; Asai, K. *Jpn. J. Appl. Phys.* **1977**, *16*, 1891.
12   Tanaka, H.; Takemura, T. *Polym. J.* **1980**, *12*, 355.
13   Ungar, G. *Macromolecules* **1986**, *19*, 1317.
14   Hikosaka, M.; Rastogi, S.; Keller, A.; Kawabata, H. *J. Macromol. Sci. – Phys.* **1992**, *B31*, 87.
15   Shulgin, A.; Godovsky, Y. *J. Thermal. Anal.* **1992**, *38*, 1243.
16   Annis, B.; Reffner, J.; Wunderlich, B. *J. Polym. Sci., Polym. Phys. Ed.* **1993**, *31*, 93.
17   Tsubakihara, S.; Nakamura, A.; Yasuniwa, M. *Polym. J.* **1996**, *28*, 489.
18   Möller, M. *Makromol. Chem., Rapid Commun.* **1988**, *9*, 107.
19   Rastogi, S.; Ungar, G. *Macromolecules* **1992**, *25*, 1445.
20   Weeks, J.; Eby, R.; Clark, E. *Polymer* **1981**, *22*, 1496.
21   Lee, C.; Johannson, O.; Flanigam, O.; Hahn, P. *Polym. Prepr.* **1967**, *10*, 1311.
22   White, M. In *Siloxane Polymers* ; Clarson, S., Semlyen, J., Eds.; PTR Prentice Hall: Englewood Cliffs, 1993.
23   Out, G.; Turetskii, A.; Möller, M., Oelfin, D. *Macromolecules* **1994**, *27*, 3310.
24   Out, G.; Turetskii, A.; Möller, M. *Macromol. Rapid Commun.* **1995**, *16*, 107.
25   Out, G.; Schlössels, F.; Turetskii, A.; Möller, M. *Macromol. Chem. Phys.* **1995**, *196*, 2035.
26   Zavin, B.; Rabkina, A.; Kuteinikova, L.; Blagodatskikh, I.; Dubovik, I.; Gerasimov, M.; Papkov, V. *Polym. Sci.* **1995**, *A37*, 355.
27   Molenberg, A.; Siffrin, S. Möller, M.; Boileau, S.; Teyssié, D. *Macromol. Symp.* **1996**, *102*, 199.
28   Schilling, F.; Bovey, F.; Lovinger, A.; Zeigler, J. *Macromolecules* **1986**, *19*, 2660.
29   Varma-Nair, M.; Cheng, J.; Jin, Y.; Wunderlich, B. *Macromolecules* **1991**, *24*, 5442.
30   Frey, H.; Out, G.; Möller, M.; Greszta, D.; Matyjaszewski, K. *Macromolecules* **1993**, *26*, 6231.
31   Desper, C.; Schneider, N. *Macromolecules* **1976**, *9*, 424.
32   Kulichikhin, V.; Antipov, E.; Borisenkova, E.; Tur, D. In *Liquid Crystalline and Mesomorphic Polymers*; Shibaev, V., Lam, L., Eds.; Springer: New York, 1994.
33   Portugall, M.; Ringsdorf, H.; Zentel, R. *Makromol. Chem.* **1982**, *183*, 2311.
34   Keller, P. *Macromolecules* **1984**, *17*, 937.
35   Kawakami, T.; Kato, T. *Macromolecules* **1998**, *31*, 4475.
36   Kostromin, S. G.; Talroze, R. V.; Shibaev, V. P.; Platé, N. A. *Makromol. Chem., Rapid Commun.* **1982**, *3*, 803.
37   Craig, A. A.; Imrie, C. T. *Polymer* **1997**, *38*, 4951.
38   Chovino, C.; Guillon, D.; Gramain, P. *Polymer* **1998**, *39*, 6385.
39   Crivello, J. V.; Deptolla, M.; Ringsdorf, H. *Liquid Crystals* **1988**, *3*, 235.
40   Attard, G. S.; Dave, J. S.; Wallington, A. *Makromol. Chem.* **1991**, *192*, 1495.
41   Imrie, C. T.; Karasz, F. E.; Attard, G. S. *Macromolecules* **1994**, *27*, 1578.
42   Finkelmann, H.; Rehage, G. *Makromol. Chem., Rapid Commun.* **1980**, *1*, 31.

43 Richard, H.; Mauzac, M., Nguyen, H. T.; Sigaud, G.; Achard, M. F.; Hardouin, F.; Gasparoux, H. *Mol. Cryst. Liq. Cryst.* **1988**, *155*, 141.

44 Hempenius, M. A.; Lammertink, R. G. H.; Vancso, G. J. *Macromolecules* **1997**, *30*, 266.

45 Tanaka, M.; Nakaya, T. *Makromol. Chem.* **1988**, *189*, 771.

46 Mirceva, A.; Oman, N.; Zigon, M. *Polym.Bull.* **1998**, *40*, 469.

47 Brecl, M.; Zigon, M.; Malavasic, T. *J. Polym. Sci.: Part A: Polym. Chem* **1998**, *36*, 2135.

48 Robert, P.; Villenave, J.-J.; Fontanille, M.; Gilli, J.-M.; Sixou, P. *Mol. Cryst. Liq. Cryst.* **1988**, *155*, 161.

49 Mallon, J. J.; Kantor, S. W. *Macromolecules* **1990**, *23*, 1249.

50 Bonnans-Plaisance, C.; Rétif, P.; Levesque, G. *Polym. Bull.* **1995**, *34*, 141.

51 Bonnans-Plaisance, C.; Corvazier, L.; Zhao, Y. *Polym. Bull.* **1998**, *40*, 569.

52 Haferkorn, J.; Geue, T.; Date, R. W.; Fawcett, A. H.; Stumpe, J. *Thin Solid Films* **1998**, *327-329*, 214.

53 Gangadhara; Noël, C.; Thomas, M.; Reyx, D. *J. Polym. Sci.: Part A: Polym. Chem.* **1998**, *36*, 2531.

54 Ungerank, M.; Winkler, B.; Eder, E.; Stelzer, F. *Macromol. Chem. Phys.* **1995**, *196*, 3623.

55 Winkler, B.; Ungerank, M.; Stelzer, F. *Macromol. Chem. Phys.* **1996**, *197*, 2343.

56 Maughon, B. R.; Weck, M.; Mohr, B.; Grubbs, R. H. *Macromolecules* **1997**, *30*, 257.

57 Pugh, C.; Kiste, A. L. *Prog. Polym. Sci.* **1997**, *22*, 601.

58 Shibaev, V. P.; Freidzon, Y. S.; Kostromin, S. G. *Liquid Crystalline and Mesomorphic Polymers*; Shibaev, V. P., Lam, L., Eds.; Springer: New York, 1994.

59 Freidzon, Y. S.; Shibaev, V. P. *Liquid Crystalline Polymers*; Platé, N. A., Ed.; Plenum: New York, 1993.

60 Stevens, H.; Rehage, G.; Finkelmann, H. *Macromolecules* **1984**, *17*, 851.

61 Percec, V.; Hahn, B. *Macromolecules* **1989**, *22*, 1588.

62 Komiya, Z.; Pugh, C.; Schrock, R. R. *Macromolecules* **1992**, *25*, 3609.

63 Rubin, S. F.; Kannan, R. M.; Kornfield, J. A.; Boeffel, C. *Macromolecules* **1995**, *28*, 3521.

64 Kawakami, Y.; Inoue, H.; Kishimoto, N.; Mori, A. *Polym. Bull.* **1996**, *36*, 653.

65 Percec, V.; Lee, M. *Macromolecules* **1991**, *24*, 1017.

66 Percec, V.; Keller, A. *Macromolecules* **1990**, *23*, 4347.

67 Galli, G.; Chiellini, E.; Laus, M.; Angeloni, A. S.; Francescangeli, O.; Yang, B. *Macromolecules* **1994**, *27*, 303.

68 Kasko, A. M.; Heintz, A. M.; Pugh, C. *Macromolecules* **1998**, *31*, 256.

69 Percec, V.; Pugh, C. *Side Chain Liquid Crystal Polymers*; McArdle, C. B., Ed.; Blackie: Glasgow and London, 1989.

70 Finkelmann, H. *Polymer Liquid Crystals*; Ciferri, A., Krigbaum, W. R., Meyer, R. B., Eds.; Academic Press: New York and London, 1982.

71 Gedde, U. W.; Liu, F.; Hellermark, C.; Hult, A.; Sahlén, F.; Boyd, R. H. *J. Macromol. Sci. – Pure Appl. Chem.* **1996**, *A33*, 1555.

72 Hellermark, C.; Gedde, U. W.; Hult, A. *Polymer* **1996**, *37*, 3191

73 Akiyama, E.; Ohtomo, M.; Nagase, Y.; Koide, N. *Macromol. Chem. Phys.* **1995**, *196*, 3391.

74 Finkelmann, H.; Ringsdorf, H.; Wendorff, J. H. *Makromol. Chem.* **1978**, *179*, 273.

75 Finkelmann, H.; Happ, M.; Portugall, M.; Ringsdorf, H. *Makromol. Chem.* **1978**, *179*, 2541.

76 Kirste, R. G.; Ohm, H. G. *Makromol. Chem., Rapid Commun.* **1985**, *6*, 179.

77 Keller, P. *Makromol. Chem., Rapid Commun.* **1985**, *6*, 707.

78 Keller, P. *Mol. Cryst. Liq. Cryst. Lett.* **1985**, *2*, 101.

79 Keller, P. *Macromolecules* **1985**, *18*, 2337.

80 Frère, Y.; Yang, F.; Gramain, P.; Guillon, D.; Skoulios, A. *Makromol. Chem.* **1988**, *189* 419.

81 Hsiue, G.-H.; Chen, Jr-H. *Macromolecules* **1995**, *28*, 4366.

82 Kawakami, Y.; Inoue, H.; Kishimoto, N.; Mori, A. *Polym. Bull.* **1996**, *36*, 653.

83 Hempenius, M. A.; Lammertink, R. G. H.; Vancso, G. J. *Macromol. Rapid Commun.* **1996**, *17*, 299.

84 Dubois, J. C.; Le Barny, P.; Mauzac, M.; Noël, C. *Acta Polymer.* **1997**, *48*, 47.

85 Craig, A. A.; Imrie, C. T. *Macromolecules* **1995**, *28*, 3617.

86 Craig, A. A.; Imrie, C. T. *J. Mater. Chem.* **1994**, *4*, 1705.

87 Simmonds, D. J. *Liquid Crystal Polymers: From Structures to Applications*; Collyer, A. A., Ed.; Elsevier Applied Science: London and New York, 1992.

88 Vertogen, G.; de Jeu, W. H. *Thermotropic Liquid Crystals, Fundamentals*; Schäfer, F. P., Ed.; Springer-Verlag: Berlin and Heidelberg, 1988.

89 Apfel, M. A.; Finkelmann, H.; Janini, G. M.; Laub, R. J.; Lühmann, B.-H.; Price, A.; Roberts, W. L.; Shaw, T. J.; Smith, C. A. *Anal. Chem.* **1985**, *57*, 651.

90 Hsiue, G.-H.; Chen, Jr.-H. *Macromolecules* **1995**, *28*, 4366.

91 Mauzac, M.; Hardouin, F.; Richard, H.; Achard, M. F.; Sigaud, G.; Gasparoux, H. *Eur. Polym. J.* **1986**, *22*, 137.

92 Rodekirch, G.; Rübner, J.; Zschuppe, V.; Wollf, D.; Springer, J. *Makromol. Chem.* **1993**, *194*, 1125.

93 Kawakami, Y.; Takahashi, K.; Hibino, H. *Macromolecules* **1991**, *24*, 4531.

94 Imrie, C. T.; Schleeh, T.; Karasz, F. E.; Attard, G. S. *Macromolecules* **1993**, *26*, 539.

95 Geßner, U.; Rübner, J.; Springer, J. *J. Prakt. Chem.* **1995**, *337*, 582.

96 Fischer, H.; Poser, S.; Arnold, M. *Macromolecules* **1995**, *28*, 6957.

97 van de Velde, K.; van Beylen, M.; Ottenburg, R.; Samyn, C. *Macromol. Chem. Phys.* **1995**, *196*, 679.

98 Libiszowski, J.; Goethals, E. J.; Mijs, W. J. *Polym. Bull.* **1996**, *37*, 7.

99 Walther, M.; Finkelmann, H. *Prog. Polym. Sci.* **1996**, *21*, 951.

100 Flory, P. J. *Principles of Polymer Chemistry*; Cornell University Press: Ithaca, New York (1953).

101 Engel, M.; Hisgen, B.; Keller, R.; Kreuder, W.; Reck, B.; Ringsdorf, H.; Schmidt, H.-W.; Tschirner, P. *Pure Appl. Chem.* **1985**, *57*, 1009.

102 Diele, S.; Hisgen, B.; Reck, B.; Ringsdorf, H. *Makromol. Chem., Rapid Commun.* **1986**, *7*, 267.

103 Diele, S.; Oelsner, S.; Kuschel, F.; Hisgen, B.; Ringsdorf, H.; Zentel, R. *Makromol. Chem.* **1987**, *188*, 1993.

104 Percec, V.; Lee, M. *J. Mater. Chem.* **1992**, *2*, 617.

105 Sahlén, F.; Peterson, M.-C.; Percec, V.; Hult, A.; Gedde, U. W. *Polym. Bull.* **1995**, *35*, 629.

106 Sänger, J.; Gronski, W. *Macromol. Rapid Commun.* **1997**, *18*, 59.

107 Shibaev, V. P.; Barmatov, E. B.; Barmatova, M. V. *Colloid Polym. Sci.* **1998**, *276*, 662.

108 Reesink, J. B.; Picken, S. J.; Witteveen, A. J.; Mijs, W. J. *Macromol. Chem. Phys.* **1996**, *197*, 1031.

109 Weidner, S.; Wollf, D.; Springer, J. *Liq. Cryst.* **1996**, *20*, 587.

110 Cowie, J. M. G.; Hinchcliffe, T. *Polymer* **1996**, *37*, 4937.

111 Blatch, A. E.; Fletcher, I. D.; Luckhurst, G. R. *Liq. Cryst.* **1995**, *18*, 801.

112 Imrie, C. T.; Karasz, F. E.; Attard, G. S. *Liq. Cryst.* **1991**, *9*, 47.

113 Schleeh, T.; Imrie, C. T.; Rice, D. M.; Karasz, F. E.; Attard, G. S. *J. Polym. Sci.: Part A: Polym. Sci.* **1993**, *31*, 1859.

114 Imrie, C. T.; Paterson, B. J. A. *Macromolecules* **1994**, *27*, 6673.

115 Kosaka, Y.; Kato, T.; Uryu, T. *Macromolecules* **1994**, *27*, 2658.

116 Choi, W. S.; Kim, J. L.; Hong, S. I. *Macromol. Chem. Phys.* **1998**, *199*, 2095.

117 Imrie, C. T.; Attard, G. S.; Karasz, F. E. *Macromolecules* **1996**, *29*, 1031.

118 Kosaka, Y.; Uryu, T. *Macromolecules* **1995**, *28*, 870.

119 Percec, V.; Lee, M. *Macromolecules* **1991**, *24*, 4963.

120 Percec, V.; Lee; M. *Polymer* **1991**, *32*, 2862.

121 Percec, V.; Lee; M. *Polym. Bull.* **1991**, *25*, 131.

122 Imrie, C. T.; Karasz, F. E.; Attard, G. S. *Macromolecules* **1992**, *25*, 1278.

123 Shiraishi, K.; Sugiyama, K. *Chem. Lett.* **1990**, 1697.

124 Jähnichen, K.; Voigt, D.; Jehnichen, D.; Rätzsch, M. *Macromol. Chem. Phys.* **1995**, *196*, 3323.

125 Laus, M.; Bignozzi, M. C.; Angeloni, A. S.; Galli, G.; Chiellini, E. *Macromolecules* **1993**, *26*, 3999.

126 Nieuwkerk, A. C.; Marcelis, A. T. M.; Sudhölter, E. J. R. *Macromolecules* **1995**, *28*, 4986.

127 Braun, D.; Herr, R.-P.; Arnold, N. *Makromol. Chem., Rapid Commun.* **1987**, *8*, 359.

128 Fawcett, A. H.; Szeto, D. Y. S. *Polym. Commun.* **1991**, *32*, 77.

129 Date, R. W.; Fawcett, A. H.; Geue, T.; Haferkorn, J.; Malcolm, R. K.; Stumpe, J. *Macromolecules* **1998**, *31*, 4935.

130 Trivedi, B. C.; Culbertson, B. M. *Maleic Anhydride*; Trivedi, B. C., Ed.; Plenum: New York, 1982.

131 Komber, H. *Macromol. Chem. Phys.* **1995**, *196*, 669.

132 Rätzsch, M.; Zschoche, S.; Steinert, V.; Schlothauer, K. *Makromol. Chem.* **1986**, *187*, 1669.

133 Arnold, M.; Rätzsch, M. *Makromol. Chem.* **1986**, *187*, 1593.

134 Sato, T.; Abe, M.; Otsu, T. *Makromol. Chem.* **1977**, *178*, 1061.

135 Hill, D. J. T.; O'Donnel, J. H., O'Sullivan, P. W. *Macromolecules* **1985**, *18*, 9.

136 Brown, P. G.; Fujimori, K. *Macromol. Rapid Commun.* **1994**, *15*, 61.

137 Brown, P. G.; Fujimori, K. *Polymer* **1995**, *36*, 1053.

138 Lin, Q.; Talukder, M.; Pittman Jr., C. U. *J. Polym. Sci.: Part A: Polym. Chem.* **1995**, *33*, 2375.

139 Bortel, E.; Kochanowski, A.; Witek, E. *J. Macromol. Sci.-Pure Appl. Chem.* **1995**, *A32*, 73.

140 Caze, C.; Loucheux, C. *J. Macromol. Sci.-Chem.* **1975**, *A9*, 29.

141 Schmidt-Naake, G.; Drache, M.; Leonhardt, K. *Macromol. Chem. Phys.* **1998**, *199*, 353.

142 Noordegraaf, M. A.; Kuiper, G. J.; Marcelis, A. T. M.; Sudhölter, E. J. R. *Macromol. Chem. Phys.* **1997**, *198*, 3681.

143 Ahlheim, M.; Lehr, F. *Macromol. Chem. Phys.* **1995**, *196*, 243.

144 MacDonald, W. A. *Liquid Crystal Polymers: From Structures to Applications*; Collyer, A. A., Ed.; Elsevier Applied Science: London and New York, 1992.

145 Han, Y.-K.; Kim, D.-Y.; Kim, Y. H. *J. Polym. Sci.: Part A: Polym. Chem.* **1992**, *30*, 1177.

146 Jansen, J.; den Ridder, P.; Addink, R.; Mijs, W. *Macromol. Chem. Phys.* **1995**, *196*, 2517.
147 Canessa, G. S.; Aguilera, C.; Serrano, J. L.; Oriol, L. *J. Polym. Sci.: Part A: Polym. Chem.* **1996**, *34*, 1465.
148 Kodaira, T.; Endo, M.; Kurachi, M. *Macromol. Chem. Phys.* **1998**, *199*, 2329.
149 Ogawa, K.; Mihara, T.; Koide, N. *Polym. J.* **1997**, *29*, 142.

3

Side-chain liquid-crystalline polymers from the alternating copolymerization of maleic anhydride and 1-alkenes carrying biphenyl mesogens

Side-chain liquid-crystalline copolymers (SCLCPs) were synthesized from the alternating copolymerization of maleic anhydride with mesogenic 1-alkenes. These SCLCPs showed high glass transition temperatures and highly ordered smectic mesophases. The mesophase width increased with spacer length. The terminal alkyl group length determined the degree of order in the hexatic mesophase that was present just above the glass transition temperature. A terminal methoxy group induced a hexatic smectic B mesophase, intermediate terminal alkyl groups induced a smectic E mesophase, and long terminal alkyl groups induced a crystal smectic B mesophase. If the spacer was shorter than the terminal alkyl group, an interdigitated smectic A mesophase was found in which the terminal alkyl groups overlap. A strong correlation was found between the glass transition temperature and the temperature at which the hexagonal or orthorhombic ordered mesophase disappears. Introduction of an ester linkage between the spacer and biphenyl mesogen or replacing the terminal alkoxy group by a cyano terminal group induced a lowering of transition temperatures and a lower degree of order in the mesophase.

3.1. Introduction

Since the introduction of side-chain liquid-crystalline polymers (SCLCPs) much effort has been put in studying the effect of molecular architecture on their liquid-crystalline properties.[1,2,3,4] The most common structural variables are spacer length, type of mesogen and length and type of the mesogenic terminal group. The properties of SCLCPs are also strongly influenced by the nature of the polymer backbone.[2,3,5,6] In the past, attention has been mainly

focussed on homopolymers like poly(acrylate)s,[4] poly(siloxane)s,[7] poly(phosphazene)s,[8] and poly(styrene)s.[9]

By copolymerization of two different monomers, polymers can be obtained in which the phase transitions and properties can be tuned to desired levels. A well-defined type of copolymerization is the alternating copolymerization in which the two monomers enter into the copolymer in equimolar amounts and in an alternating arrangement along the copolymer chain. Only few examples of alternating SCLCPs are known: (i) polymers consisting of mesogenic vinyl ethers and mesogenic fumarates,[10] and (ii) polymers consisting of mesogenic vinyl ethers and maleic anhydride (MA).[11,12]

Because of the extremely low tendency of MA to homopolymerize, MA forms alternating polymers with alkenes that also have a low tendency to homopolymerize.[13,14] Furthermore, a recent study describes the alternating polymerization of maleic acid derivatives with a variety of donor monomers.[15] UV-spectroscopy and Monte-Carlo simulations showed that the alternating copolymerization arises from the strong interactions between electron-poor and electron-rich monomers which result in donor-acceptor combinations that subsequently homopolymerize.

Thery et al.[21] found that anhydride moieties in polymers are chemically reactive towards oxidized surfaces and form strong bonds of the carboxylate type. During heat treatment, the anhydride moieties of the polymers migrate to the metal oxide surface. Van der Wielen et al.[16,17] found that heat treatment of spincoated films of some of the described SCLCPs on silica surfaces results in structures with an almost perfect smectic periodicity.

The presence of anhydride moieties results in low backbone flexibility and consequently a high glass transition temperature (T_g). This high T_g combined with the adhesive properties of MA moieties to metals[18,19,20,21] may be beneficial to application of the present SCLCPs in coatings and corrosion protection[19,22,23] in which SCLCPs should retain their mechanical stability up to high temperatures.

In this study we describe the synthesis and phase behavior of alternating copolymers of MA with 1-alkenes containing alkoxybiphenyl mesogens. The influence of spacer length and terminal alkyl group length on the transition temperatures is studied. Alkoxybiphenyl mesogens were used because they are easily available and their terminal alkyl group length can easily be changed. For comparison a compound with a cyanobiphenyl mesogen was also included in this study. The SCLCPs have been characterized by gel permeation chromatography, ^{1}H NMR, ^{13}C NMR, polarizing optical microscopy, differential scanning calorimetry and wide angle X-ray diffraction.

3.2. Experimental part

3.2.1. Materials

The tetrahydrofuran (THF) which was used for the polymerization reactions was purified by distillation over sodium under nitrogen atmosphere. Maleic anhydride was

sublimated before use and azoisobutyronitrile (AIBN) was recrystallized twice from methanol. Other reagents used for syntheses were commercially available and used without further purification. 1-Alkylene-ω-tosylate,[24] 4-hydroxy-4'-methoxybiphenyl[25] (2-0), 4-methoxy-4'-undec-10-enoylbiphenyl[26] (4), and 4-cyano-4'-undec-10-enyloxybiphenyl[27] (5) were synthesized according to literature procedures.

3.2.2. Equipment

Gel permeation chromatography (GPC) measurements were carried out using a series of four microstyragel columns with pore sizes of respectively 10^5, 10^4, 10^3, and 10^6 Å (Waters) with THF containing 5 wt% acetic acid as eluent. A dual detection system consisting of a differential refractometer (Waters model 410) and a differential viscometer (Viscotek model H502) was used. A calibration line was made with this setup, using narrow polystyrene reference standards in THF, and the molar mass (g/mol) of the synthesized polymers was determined referring to this calibration line. Thermal transitions were monitored with a Perkin-Elmer DSC-7. Scan rates of 10 K/min were used in the differential scanning calorimetry (DSC) experiments with sample masses of 5-15 mg. Transition temperatures were taken from the second heating cycle. Polarizing optical microscopy (POM) was performed on an Olympus BH-2 microscope equipped with a Mettler FP82HT hot stage and an FP80HT temperature controller. X-ray diffraction measurements were performed on a Siemens D5000 reflection diffractometer with a HTK oven and Cu Kα radiation. ^{1}H NMR spectra were recorded on a Bruker AC200 spectrometer at 200 MHz. FTIR spectra were recorded on a BioRad FTS-7 spectrometer.

3.2.3. Synthesis

4-Hydroxy-4'-alkoxybiphenyl (2-p)

All compounds were synthesized according to the same procedure, an example is given for $p = 7$:

1-Bromooctane (3.75 g, 19.4 mmol) was added to a stirred suspension of compound 1 (10.0 g, 54.0 mmol), potassium hydroxide (1.15 g, 20.5 mmol), and a catalytic amount of potassium iodide in ethanol (105 mL) and water (6.5 mL). After stirring at reflux temperature under nitrogen atmosphere for 24 h, the reaction mixture was concentrated by evaporation of the solvent, the residue was dissolved in ethyl acetate and washed with water. After being dried with magnesium sulfate, the solution was evaporated to dryness. The product was purified by silica gel chromatography with a mixture of 1.8 vol.% methanol in dichloromethane as eluent. Recrystallization from ethanol yielded colorless crystals (4.26 g, 14.3 mmol, 74%).

^{1}H NMR (acetone-d$_6$): δ = 7.45 (2d, biphenyl, 4H); 6.91 (2d, biphenyl, 4H); 4.00 (t, -CH$_2$O, 2H); 1.77 (quintet, -CH_2CH$_2$O, 2H); 1.18 - 1.51 (m, -CH$_2$-, 10H); 0.87 (t, -CH$_3$, 3H)

Yields and melting temperatures for the homologous compounds are given in Table 3.1.

Table 3.1. *Yields (%) and melting temperatures (°C) of 4-hydroxy-4'-alkoxybiphenyl (2-p).*

p	yields	melting temp
0	65	182
2	67	174
3	43	169
5	63	156
7	74	153
8	47	150

4-Alkoxy-4'-alk-ω-enyloxybiphenyl (3-m,p)

All compounds were synthesized according to the same procedure, an example is given for $m = 9$ and $p = 0$:

1-Undecene-11-tosylate (or the corresponding 11-bromo-1-undecene) (7.5 g, 23.1 mmol) was added to a stirred suspension of 4-hydroxy-4'-methoxybiphenyl (4.4 g, 22.0 mmol), potassium carbonate (4.76 g, 33.0 mmol) and a catalytic amount of potassium iodide in 2-butanone (105 mL). After stirring at reflux temperature under nitrogen atmosphere for 24 h, the reaction mixture was concentrated by evaporation of the solvent, dissolved in dichloromethane and washed subsequently with water, 10 % NaOH and water. After being dried with magnesium sulfate, the solution was evaporated to dryness. Recrystallization from petroleum ether 60/80 yielded colorless crystals (7.25 g, 20.6 mmol, 94 %).

^{1}H NMR (CDCl$_3$): δ = 7.45 (2d, biphenyl, 4H); 6.93 (2d, biphenyl, 4H); 5.81 (m, =CH-, 1H); 4.91 (2d, CH$_2$=, 2H) ; 3.97 (t, -CH$_2$O, 2H); 3.83 (s, CH$_3$OAr-, 3H); 2.03 (q, =CHC*H*$_2$, 2H); 1.79 (quintet, -C*H*$_2$CH$_2$O, 2H); 1.21 - 1.54 (m, -CH$_2$-, 12H)

Yields and transition temperatures for the homologous compounds are given in Table 3.2. The yield of monomer **3-2,0** was 20%, because in that case elimination of HBr during etherification is an important side reaction.

Polymerization of maleic anhydride and 3-m,p, 4, or 5 (6-m,p; 7 and 8)

All copolymers were synthesized according to a modified literature procedure,[28] an example is given for $m = 9$ and $p = 0$:

Maleic anhydride (0.73 g, 7.4 mmol), 4-methoxy-4'-undec-10-enyloxybiphenyl (2.5 g, 7.1 mmol), and AIBN (12.8 mg, 0.075 mmol) were dissolved in freshly distilled THF (3 mL), and the mixture was placed in a sealable glass pressure vessel. A vacuum line capable of < 2 kPa was used to degas the mixture by three or four freeze-thaw cycles, and the vessel was put under argon at $1.1 \cdot 10^5$ Pa and placed in an oil bath of 60°C. After 14 days the vessel was cooled, the pressure was released and THF was added. The solution was added to cold methanol (10 volumes) to precipitate the polymer. The latter was collected and repeatedly precipitated from THF into petroleum ether 40/60 (10 volumes) to remove unreacted monomer (in some cases diethyl ether was used to precipate the polymer). A white powder (2.35 g, 74%) was obtained after filtration.

^{13}C NMR signals (solution in aceton-d$_6$) of the polymer backbone were in excellent agreement with that reported for a highly alternating propene-maleic anhydride copolymer.[29] Anal. Calcd for polymer **8** (1 : 1 copolymer): C, 75.5; H, 7.01; N, 3.14. Found: C, 75.3; H, 7.28; N, 2.99.

*Table 3.2. Yields (%) and phase transition temperatures (°C) of monomers 3-m,p, 4 and 5.^{a}*

monomer	yield	phase behavior
3-2,0	20	K 121 I
3-3,0	86	K 122 I
3-4,0	89	K 113 I
3-6,0	72	K 106 I
3-8,0	79	K 105 I
3-9,0	94	K 107 I
3-9,2	90	K 107 I
3-9,3	88	K 108 I
3-9,5	91	K 101 (40) S$_A$ 104 (27) I
3-9,7	92	K 98.9 (29) S$_X$ 99.4 (10) S$_C$ 101 (0.25) S$_A$ 104 (30) I
3-9,8	56	K 98.2 (89) S$_A$ 99.0 (17) I
3-3,8	93	K 115 (18) S$_A$ 116 (39) I
3-4,7	89	K 110 I
3-6,5	82	K 111 I
3-8,3	93	K 109 I
4	79	K 74.8 (358) N 78.1 (2.2) I
5[27]	86	K 57.6 (106) S$_A$ 74.1 (1.5) N 75.1 (3.3) I

^{a} *In case of liquid crystalline behavior the entropy changes (J/mol K) at phase transitions and the mesophase types are given. K = crystalline, S$_{A,C}$ = different smectic phases, S$_X$ = not identified, N = nematic, I = isotropic phase.*
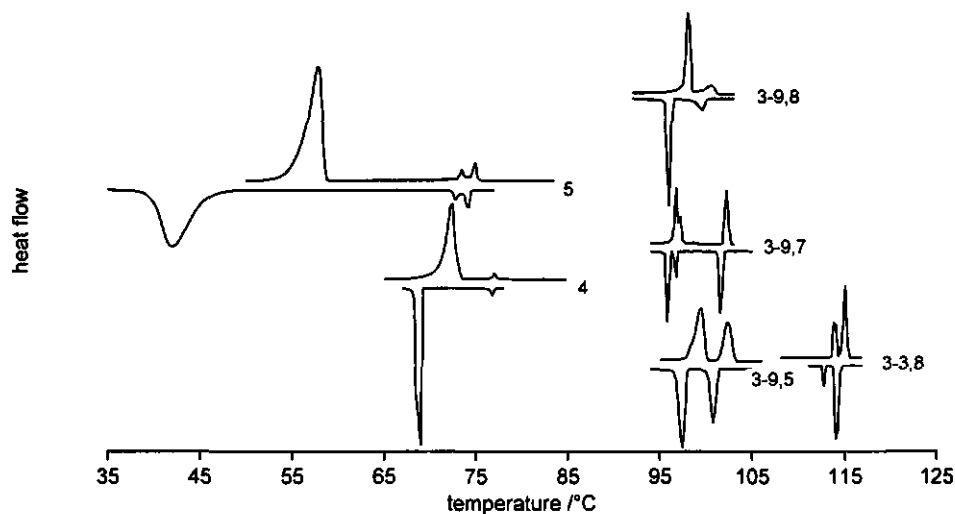
3.3. Results and discussion

3.3.1. Monomers

The synthesis of monomers **3-m,p** and the structure of monomers **4** and **5** are depicted in Scheme 3.1. All monomers were obtained in satisfactory yields and high purity. The observed ^{1}H-NMR signals agree well with the chemical structure.
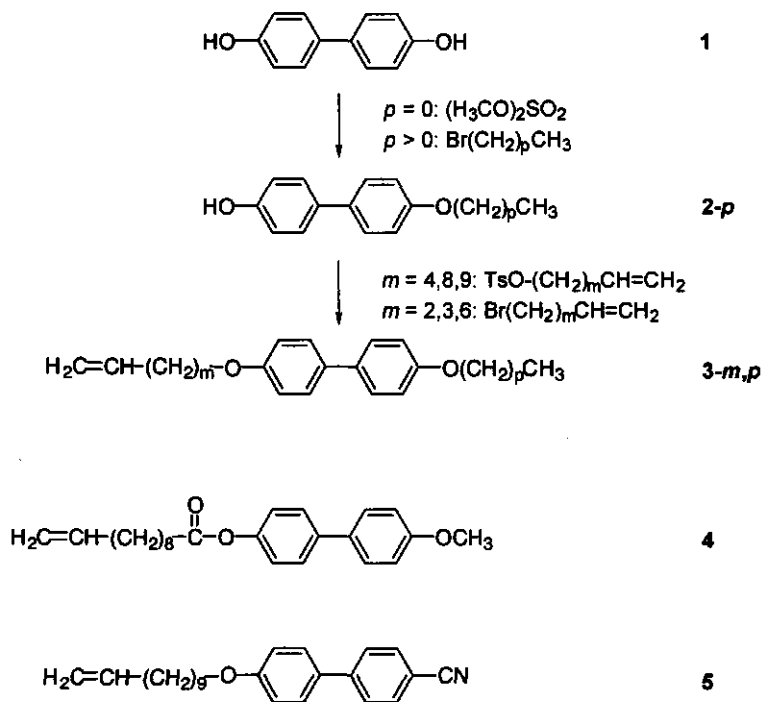
**Scheme 3.1.** *Synthesis and structures of monomers 3-m,p, 4, and 5.*

Figure 3.1. *DSC thermograms of monomers 3-3,8, 3-9,5, 3-9,7, 3-9,8, 4, and 5. For all compounds the second heating and cooling traces are given.*

The DSC thermograms in Figure 3.1 show that monomers **3-3,8**, **3-9,5**, **3-9,7**, **3-9,8**, **4**, and **5** exhibit liquid-crystalline behavior and that their phase transitions are reversible. The transition temperatures and corresponding entropy changes, which were determined from DSC traces, are summarized in Table 3.2. The mesophases were characterized based on the textures observed with polarizing optical microscopy (POM). Transition temperatures observed with POM were in good agreement with those found with DSC.

All liquid-crystalline monomers showed common smectic and/or nematic mesophases, however, monomer **3-9,7** exhibited an additional mesophase (S_X) after melting at 98.9°C. The X-ray diffraction pattern of this mesophase displayed reflections up to the fifth order corresponding to d spacings of 31.1, 16.2, 10.0, 7.5 and 6.0Å. The length of the molecule, which is 34 Å, and the amount of reflections indicate that a regularly layered smectic mesophase was formed without interdigitation. However, from the absence of a sharp reflection corresponding to a d spacing of about 4.4 Å, it can be concluded that no order was present within these layers. The S_X mesophase transformed into a smectic C (S_C) mesophase at 99.4°C and a smectic A (S_A) mesophase at 101.3°C. In the DSC thermogram, the S_C - S_A transition is not represented by an endothermic peak but an exothermic shift in baseline upon heating. Monomer **5** has been described before[27] and the transition temperatures were in good agreement with those found in literature.

3.3.2. Polymer synthesis

Polymers **6-*m,p***, **7**, and **8** were synthesized according to Scheme 3.2. Before further characterization was performed, polymers were dried in vacuo over P_2O_5 at 100°C until FTIR showed that the carboxylic acid groups, which were formed to a small degree due to hydrolysis during work-up and storage, were ring closed again to anhydride moieties by a dehydration reaction.[12] This process was characterized by the disappearance of the C=O stretching band characteristic for a carboxyl group at 1733 cm^{-1} and the appearance of the
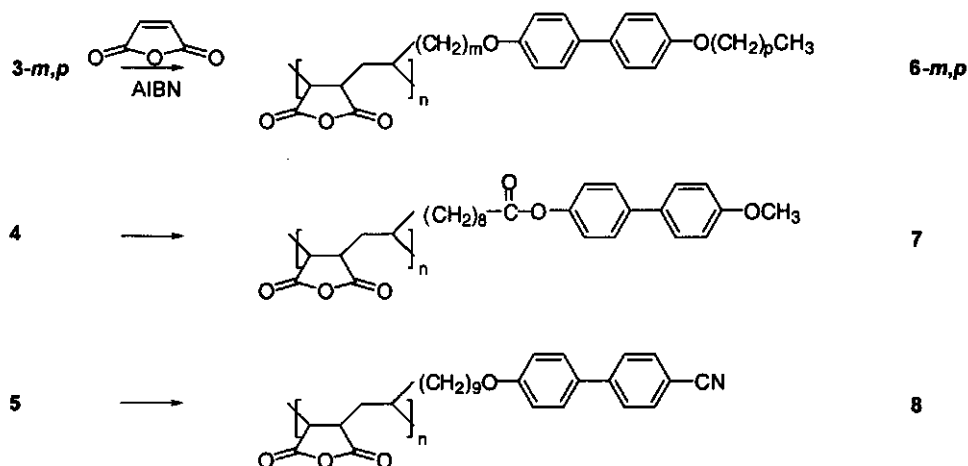
***Scheme 3.2.** Synthesis of polymers **6-m,p**, 7, and 8.*

symmetric and antisymmetric stretching bands at 1861 and 1780 cm^{-1} typical for an anhydride. ^{1}H-NMR signals corresponded to the expected chemical structures. Broadening of the signals and disappearance of the vinyl signals indicated polymer formation.

It is well-known that (i) MA has an extremely low tendency, if any, to homopolymerize in a radical polymerization[13] and (ii) MA copolymerizes with unactivated 1-alkenes to give highly alternating 1 : 1 copolymers.[14] Elemental analysis of polymer **8** was consistent with this. Furthermore, the ^{13}C NMR signals of the polymer backbone of polymer **6-9,0** were in excellent agreement with that reported for a highly alternating propene-MA copolymer.[29]

The molecular weights of the polymers were determined by GPC and are listed in Table 3.3. Interactions between the polymer and the packing material of the GPC column were avoided using THF with 5% acetic acid as an eluent.[30] The molecular weights are low if the amount of initiator applied (1.05 mol% based on monomer) is considered. Low degrees of polymerization (DP) are probably caused by chain-transfer reactions. The polydispersity indices are low if compared to some other radical polymerizations, which may be caused by fractionation during precipitation. After precipitation, polymer yields varied between 20 and 90%.

Table 3.3. *Number-average molecular weights (M_n), weight-average molecular weights (M_w), polydispersity indices (PDI), degrees of polymerization (DP) as determined by GPC, and yields (%) of polymers 6-m,p, 7, and 8.*

polymer	10^{-3} M_n	10^{-3} M_w	PDI	DP	Yield
6-2,0	2.01	2.67	1.32	11	20
6-3,0	2.81	5.26	1.87	15	54
6-4,0	3.99	6.54	1.64	21	90
6-6,0	3.27	5.66	1.73	16	76
6-8,0	3.74	5.98	1.60	17	57
6-9,0[a]	3.37	5.32	1.58	15	74
6-9,0[b]	4.05	5.43	1.34	18	65
6-9,2	4.44	6.51	1.47	19	59
6-9,3	4.48	6.34	1.42	18	57
6-9,5	3.43	4.86	1.42	13	60
6-9,7	4.11	5.89	1.43	15	43
6-9,8	3.17	4.49	1.42	11	49
6-3,8	3.02	4.48	1.48	13	63
6-4,7	3.34	4.81	1.44	14	62
6-6,5	4.29	6.96	1.62	18	58
6-8,3	5.55	8.10	1.46	23	61
7	5.09	7.82	1.54	22	59
8	5.89	8.42	1.43	26	60

[a] *First batch.* [b] *Second batch.*

3.3.3. Transition temperatures and mesophases of SCLCPs

Table 3.4 summarizes the mesophases of the polymers, their phase transition temperatures and the corresponding entropy changes. The reproducibility of the polymer synthesis was checked by synthesizing two batches of polymer **6-9,0**. Both polymers showed similar molecular weights and transition temperatures (Table 3.3 and 3.4). Because the molecular weights and polydispersity indices of the various polymers are similar direct comparison of transition temperatures appears reasonable. The mesophases in Table 3.4 were assigned based on the X-ray diffraction patterns of the mesoglass and textures observed with POM. The assignment of mesophases will be discussed later on.

Table 3.4. *Phase transition temperatures in °C (corresponding heat capacity or entropy changes in J/mol K) as determined by DSC and phase types of polymers **6-m,p**, 7, and 8.[a]*

polymer	phase behavior				
6-2,0	G 112 (117)				I
6-3,0	G_{Bhex} 146 (123)		S_{Ad} 170 (7.4)		I
6-4,0	G_{Bhex} 120 (-)	S_{Bhex} 128 (7.1)	S_{Ad} 136 (10)		I
6-6,0	G_{Bhex} 129 (112)	S_{Bhex} 140 (5.6)	S_{Ad} 161 (8.1)		I
6-8,0	G_{Bhex} 103 (61)	S_{Bhex} 117 (5.7)	S_{Ad} 156 (13)		I
6-9,0[b]	G_{Bhex} 99 (81)	S_{Bhex} 112 (3.7)	S_{Ad} 164 (13)		I
6-9,0[c]	G_{Bhex} 101 (104)	S_{Bhex} 111 (3.3)	S_{Ad} 165 (16)		I
6-9,2	G_E 142 (99)	S_E 156 (14)	S_{Ad} 177 (9.0)		I
6-9,3	G_E 143 (124)	S_E 158 (19)	S_{Ad} 181 (17)		I
6-9,5	G_E 133 (266)	S_E 146 (21)	S_{Ad} 165 (14)		I
6-9,7	G_{Bcryst} 129 (119)	S_{Bcryst} 139 (12)	S_{Ad} 160 (21)		I
6-9,8	G_{Bcryst} 118 (113)	S_{Bcryst} 127 (11)	S_{Ad} 144 (12)	S_{Adt} 151 (7.7)	I
6-3,8	G 129 (115)			S_{Adt} 208 (3.7)	I
6-4,7	G 117 (87)			S_{Adt} 187 (5.2)	I
6-6,5	G_{Bhex} 118 (91)			$S_{Ad/Adt}$ 163 (7.8)	I
6-8,3	G_E 147 (158)	S_E 159 (17)	S_{Ad} 181 (16)		I
7	G 86 (57)		S_{Ad} 122 (7.3)		I
8	G 70 (26)			N 99 (3.9)	I

[a] *I = isotropic phase; $S_{Ad,Adt}$ = different smectic A phases; S_{Bhex} = hexatic smectic B; S_{Bcryst} = crystal smectic B; S_E = smectic E; G_X= glass phase, in which X is the hexagonally ordered mesophase.*
[b] *First batch.*
[c] *Second batch.*

Table 3.5. *Experimental d spacings, calculated d spacings, mesophase and corresponding correlation length ζ obtained from wide-angle X-ray diffraction experiments of polymers 6-m,p, 7 and 8 in the glassy state (at room temperature).*

polymer	d spacings /Å	calcd d spacing /Å		mesophase	ζ /Å
		$S_A{}^a$	$S_{Ad}{}^b$		
6-2,0	-				
6-3,0	22.0; 11.1	19.5	24.1	S_{Bhex}	6.8
6-4,0	23.9; 11.9	20.9	26.6	S_{Bhex}	6.7
6-6,0	26.1; 13.1; 8.75 4.43	23.3	31.8	S_{Bhex}	10.5
6-8,0	30.2; 15.0 4.47	25.7	36.8	S_{Bhex}	9.5
6-9,0	31.8; 15.6 4.44	26.8	39.4	S_{Bhex}	12.5
6-9,2	32.1; 18.0; 16.4; 10.9; 8.17 4.49; 4.08; 3.23	29.5	39.4	S_E	32.0
6-9,3	32.6; 18.4; 16.5; 11.1; 8.34 4.48; 4.09; 3.23	30.5	39.4	S_E	20.0
6-9,5	34.6; 19.0; 17.1; 11.5; 8.61; 5.76 4.42; 4.09; 3.23	33.0	39.4	S_E	15.4
6-9,7	37.2; 20.8; 19.0; 12.7 4.43	35.4	39.4	S_{Bcryst}	42.6
6-9,8	51.9^c; 38.7; 22.3; 19.8; 13.3 4.43	36.7	61.6^d 39.4	S_{Bcryst}	86.2
6-3,8	45.3; 23.5; 15.8	29.1	46.3^d 24.1		4.6
6-4,7	45.0; 23.4; 15.8	29.1	47.5^d 26.6		4.5
6-6,5	43.0; 32.7; 17.8; 16.5 4.35	29.2	50.1^d 31.8	S_{Bhex}	11.1
6-8,3	32.7; 17.8; 16.0; 10.8 4.46; 4.12; 3.25	29.3	36.8	S_E	31.6
7	34.4; 17.6;	27.0	39.1		5.8
8	-				

^{a} *Calculated based on a smectic layer without interdigitation.*

^{b} *Calculated based on an interdigitated mesophase with maximum overlap of the biphenyl moieties (Figure 3.4).*

^{c} *Determined in the S_{Ad} mesophase.*

^{d} *Calculated based on an interdigitated mesophase with terminal alkyl group overlap (Figure 3.8).*

Table 3.5 represents the X-ray diffraction data, comprising experimental d spacings, calculated d spacings, the type of the hexagonally ordered mesophase and its correlation length ζ. d Spacings were determined in the glassy state at room temperature, after the polymer was cooled down from the isotropic state to the glassy state at a cooling rate of 5°C/s. The degree of interdigitation was determined from comparison of experimental d spacings in the mesoglass and calculated smectic d spacings.

Spacer length

Figure 3.2 shows the DSC thermograms of polymers **6-*m*,0**. On heating, the T_g is represented by an endothermic shift in baseline, which can clearly be seen for polymer **6-2,0**. For the other polymers the endothermic peak just after T_g complicates the determination of T_g.

On cooling from the isotropic melt, a sandlike texture was observed with POM that transformed into small domains of bandlike colored textures after annealing for several hours. These bandlike textures, corresponding to an S_A mesophase, became clearer when the cover slip was moved by applying mechanical stress before annealing. Most polymers exhibit an additional transition just above T_g in the DSC thermogram (Figure 3.2). However, as a result
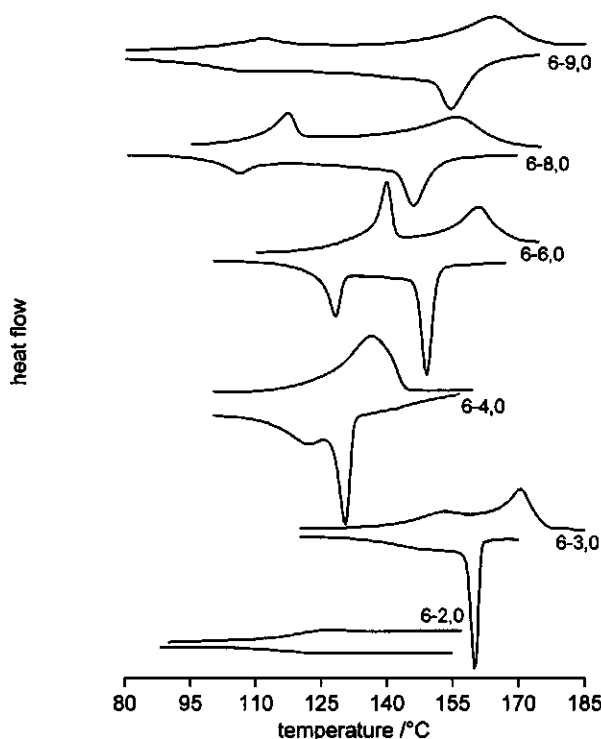
Figure 3.2. DSC thermograms of polymers 6-m,0. For all compounds the second heating and cooling traces are given.

41

of the high viscosity just above T_g, no change in texture could be observed on passing this transition.

The X-ray data in Table 3.5 show that polymers **6-*m*,0** exhibit S_{Ad} mesophases. The difference between experimental and calculated d spacings increases up to 20% for a spacer length of nine carbon atoms. This increase is comparable to the increase found before for polymers with acrylic backbones.[31] The deviations are ascribed to deviations in the all-trans conformation of the spacer while for the calculated d spacings the presence of an all-trans conformation is assumed.

In the wide-angle region of the X-ray diffraction pattern, a sharpening of the reflection corresponding to a d spacing of 4.4 Å can be observed; however, this reflection is not resolution limited. This reflection results from hexagonal order within the smectic layers, which disappears just above T_g (Table 3.4 and Figure 3.2). Because this reflection is not resolution limited, the correlation length can be calculated from the width at half-height of the reflection (Table 3.5).

The low values of the correlation length in Table 3.5 may result from (1) a hexatic smectic B (S_{Bhex}) mesophase (limited positional order and long-range bond-orientational order) or (2) a crystal smectic B (S_{Bcryst}) mesophase (long-range positional and bond-orientational order) in which the correlation length is limited by a finite domain structure. The finite domain structure in the S_{Bcryst} mesophase arises from fluctuations of the hexagonal lattice vector.[32] These fluctuations result in a correlation length of 30-100 Å for SCLCPs with a S_{Bcryst} mesophase.[33] A correlation length of 4-8 Å is found for smectics with liquid packing of the mesogenic groups.[33] According to this description the present polymers do not show a S_{Bhex} mesophase. However, on the basis of the presence of enthalpic effects observed with DSC (Figure 3.2) we denote the mesophase just above T_g as S_{Bhex}. The significance of the different correlation lengths is difficult to estimate because of the high cooling rates from the isotropic melt that were used.

Figure 3.3 shows the X-ray diffraction patterns of polymers **6-3,0** and **6-6,0**. The first
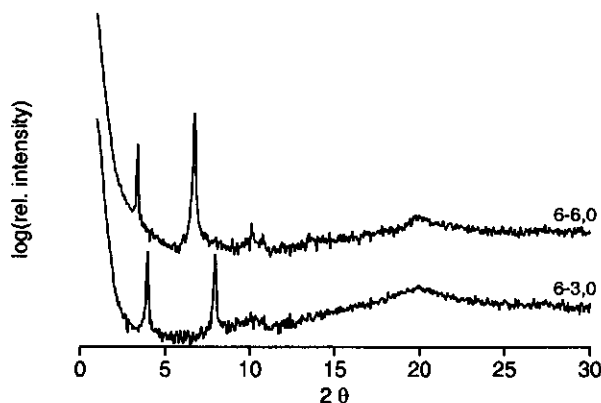
Figure 3.3. *Wide-angle X-ray diffraction patterns of polymer **6-3,0** and **6-6,0** in the glassy state.*

order reflection in the X-ray diffraction pattern of **6-6,0** exhibits a lower intensity than the second order reflection. This results from an additional plane of symmetry in the electron density profile. A model of the probable layer structure (Figure 3.4) shows that the electron densities are almost equal in both the polymer backbone layer and the mesogen layer. The electron density in the alkyl layer is significantly lower. This additional plane of symmetry induces an apparent *d* spacing (the strongest small angle reflection) which is half the smectic *d* spacing. Because the electron density in the polymer backbone and the mesogen layer are not exactly equal, the first order reflection can still be observed.
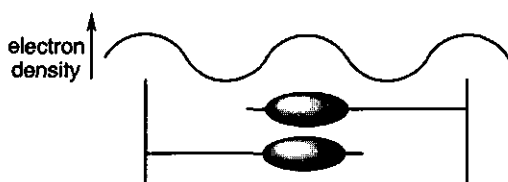
Figure 3.4. *Schematic representation of the ordering of the mesogens and the corresponding electron density profile in an S_{Ad} mesophase.*

In Figure 3.3 it can also be seen that the intensity of the second-order reflection as compared to the first-order reflection increases with spacer length. This is thought to result from a more distinct plane of symmetry in the electron density profile for longer spacers: the differences between the maxima in the electron densities of the polymer backbone and the mesogen layer decrease. Furthermore, the electron density fluctuates more strongly in a smectic layer.

The effect of spacer length on the transition temperatures is illustrated in Figure 3.5. This figure shows that longer spacers broaden the temperature window of the mesophase.[34]
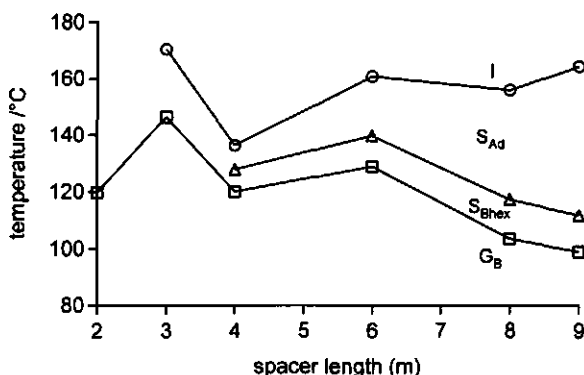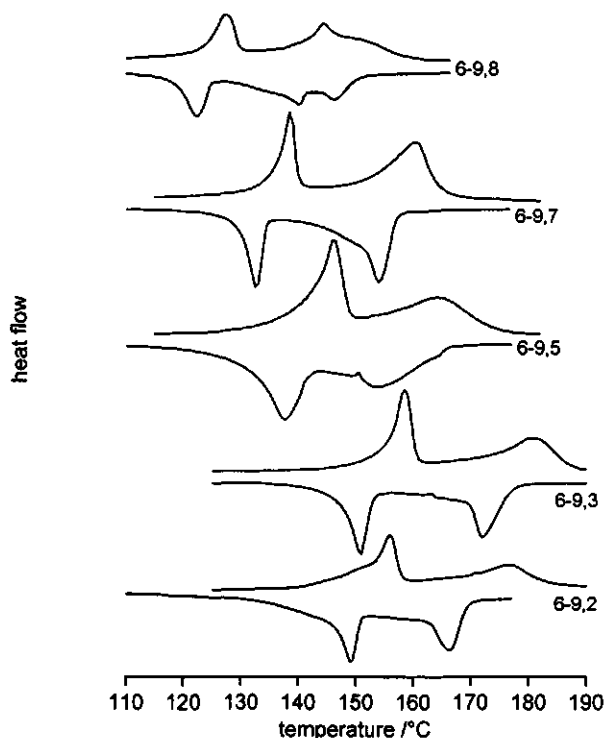

Figure 3.5. *Dependence of the transition temperatures as found with DSC on spacer length m for polymers 6-m,0: (□) glass transitions; (Δ) hexatic smectic B-smectic A_d transitions; (o) isotropic transitions.*

43

Figure 3.6. *DSC thermograms of polymers **6-9,p**. For all compounds the second heating and cooling traces are given.*

The broadening results from both a decrease of T_g and an increase in T_i. The decrease in T_g originates from an increase in distance between backbones which increases the backbone flexibility. The increase in T_i originates from a higher degree of decoupling between the motions of the mesogen and the polymer backbone. On going from a spacer length of three to a spacer length of four carbon atoms, T_g and T_i decreased. This odd behavior has been observed before for SCLCPs with a poly(acrylate) backbone, however, no explanation was given.[35]

Figure 3.5 also shows a coupling of T_g and the S_{Bhex}-S_{Ad} transition. On cooling, the S_{Ad} mesophase transforms into the more ordered S_{Bhex} mesophase. The hexagonally ordered mesogens restrict the degree of freedom of the polymer backbone to some extent and induce a glass transition temperature. This will be described in more detail in a forthcoming paper.[36]

Terminal alkyl group length

Figure 3.6 shows the DSC thermograms of polymers **6-9,p**. From the number of peaks it can be concluded that all polymers except polymer **6-9,8** show two distinct mesophases. On cooling polymer **6-9,8** shows three peaks which correspond to three distinct mesophases. As for polymers **6-m,0**, a hexagonally ordered mesophase is found just above T_g. The peak

corresponding to the transition from this mesophase to an S_{Ad} mesophase complicates the exact determination of T_g.

On cooling from the isotropic melt, POM showed that the textures of polymers **6-9,p** are comparable to those of polymers **6-m,0**. However, polymer **6-9,8** revealed an additional texture. On cooling below 147°C, small domains with a bandlike texture developed which were surrounded by homeotropic regions. This texture transformed into a sandlike texture upon cooling below 140°C. The transition temperatures found with POM agreed well with those observed with DSC.

An increase in ordering in smectic layers on going from a methoxy group to longer terminal alkoxy groups results in a higher number of reflections in the X-ray diffraction pattern (Table 3.5). The experimental *d* spacings agree well with the calculated *d* spacings for an S_{Ad} mesophase, although they are slightly smaller. This difference decreases with increasing terminal alkyl group length because the cavities between mesogens and the neighboring polymer backbones are better filled. As a result the difference in electron density between alkyl layers and biphenyl and backbone layers decreases. This effect is represented by a decrease in the intensity of the second-order reflection as compared to the first order reflection.

From the DSC thermograms in Figure 3.6 and POM, it can be seen that polymer **6-9,8** exhibits three mesophases. This phenomenon was studied in more detail by temperature-dependent X-ray diffraction experiments (see Figure 3.7). Between 130°C and 144°C, three reflections can be observed corresponding to an S_{Ad} mesophase. Above 136°C, a reflection develops corresponding to an interdigitated smectic A mesophase with terminal alkyl group overlap (S_{Adt}), as depicted schematically in Figure 3.8. A similar mesophase has been reported before.[37] It is assumed that due to interactions between the long terminal alkyl groups and the neighboring polymer backbone the S_{Ad} mesophase is destabilized and transforms into an S_{Adt} mesophase at a certain temperature.
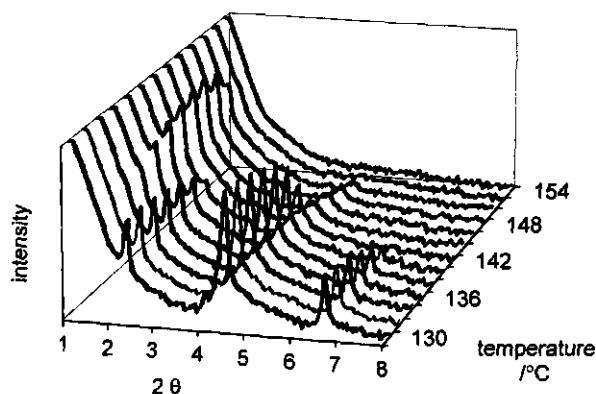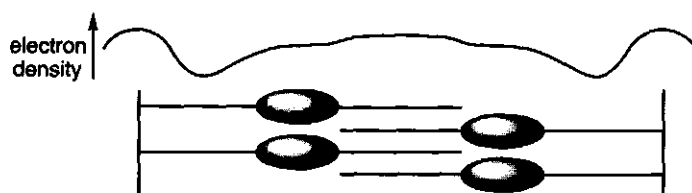

Figure 3.7. *Temperature-dependent wide-angle X-ray diffraction patterns of polymer **6-9,8**.*

Figure 3.8. *Schematic representation of the ordering of the mesogens and the corresponding electron density profile in an S_{Adt} mesophase.*

The terminal alkyl group length strongly affects the type and degree of hexagonal packing just above T_g. The hexagonally ordered mesophase with the lowest degree of order is observed for polymer **6-9,0**. From the small correlation length and the presence of one reflection in the wide-angle region it can be concluded that the mesophase is an S_{Bhex} mesophase. Increasing the terminal alkyl group length results in three reflections in the wide-angle region which correspond to (110), (200) and (210) reflections. This means that polymers **6-9,2**, **6-9,3** and **6-9,5** exhibit a smectic E (S_E) mesophase. The corresponding orthorhombic cell parameters are given in Table 3.6. From this table it is clear that terminal alkyl group length does not affect the a and b dimensions of the orthorhombic cell. For longer terminal alkyl groups (polymers **6-9,7** and **6-9,8**) the (110) and (200) reflections coincide as a result of hexagonal symmetry. The high correlation lengths indicate that the hexagonally ordered mesophase now is a crystal smectic B (S_{Bcryst}) mesophase.[33] The transition from an orthorhombic ordered S_E into a hexagonally ordered S_{Bcryst} mesophase is caused by the long terminal alkyl groups which loosen the mesogen packing.

Table 3.6. *Dimensions of the orthorhombic cell^a and the calculated d spacings of polymers 6-8,3, 6-9,2, 6-9,3, and 6-9,5 in the glassy state (G_E).*

Polymer	a /Å	b /Å	c /Å
6-8,3	8.24	5.30	32.7
6-9,2	8.15	5.37	32.1
6-9,3	8.17	5.35	32.7
6-9,5	8.18	5.25	34.2

^{a} *Derived from the experimental d spacings according to least-square analysis.*

Figure 3.9 displays the X-ray diffraction pattern of polymer **6-9,5** in the glassy state. The second-order reflection of polymers **6-9,p** has a higher intensity than the first order reflection, which can be ascribed to an additional plane of symmetry in the electron density profile as was found polymers **6-m,0**. If m > p, polymers **6-9,p** exhibit an additional peak at the low angle side of the second order reflection ($2\theta \sim 5°$) in the X-ray diffraction pattern. The intensity of this additional peak decreases with terminal alkyl group length. We can not explain the presence of this additional peak but we assume that a superstructure is superposed on the S_{Ad} mesophase.
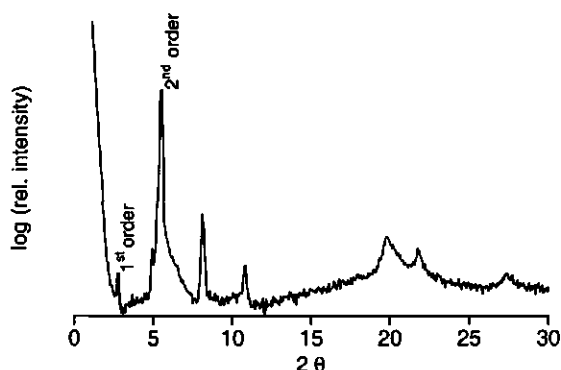
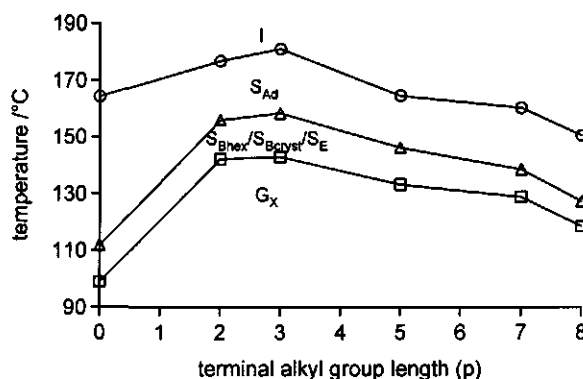**Figure 3.9.** *Wide-angle X-ray diffraction pattern of polymer* **6-9,2.**

Figure 3.10. *Dependence of the transition temperatures as found with DSC on terminal alkyl group length p for polymers* **6-9,p**: *(□) glass transitions; (Δ) hexagonally ordered mesophase-smectic Ad transitions; (o) isotropic transitions. Hexagonally ordered mesophases are: hexatic smectic B, crystal smectic B or smectic E.*

The effect of terminal alkyl group length on the transition temperatures is illustrated in Figure 3.10. The mesophase width remains almost constant as a function of terminal alkyl group length but the transition temperatures exhibit a maximum for the polymers with an S_E mesophase ($p = 2, 3, 5$). Transition temperatures decrease if the terminal alkyl group increases from six to nine carbon atoms. A similar trend has been observed before for other LCPs with rigid backbones like poly(styrene)s[38] and poly(methacrylate)s.[39] In these cases, the backbone restricts the mobility of the mesogens to some extent by preventing them to orient in an appropriate fashion. Long terminal alkyl groups have a plasticizing effect by loosening the mesogen packing. Polymers with flexible backbones, including poly(ethylene oxide)s[40] and poly(carbonate)s,[41] show opposite behavior: longer terminal alkyl groups tend to stabilize the mesogen packing. The observed coupling between T_g and the S_{Bhex} /S_E/S_{Bcryst}-S_{Ad} transition is comparable to the behavior of polymers **6-m,p**.
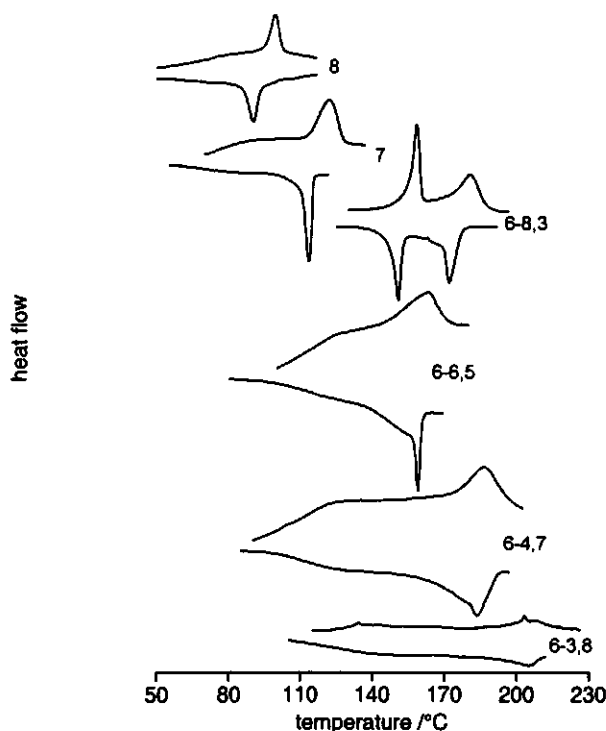
Figure 3.11. *DSC thermograms of polymers **6-m,p** (m + p = 11), 7, and 8. For all compounds the second heating and cooling traces are given.*

Table 3.4 shows that for polymers **6-9,p** the entropy change at T_i slightly increases with increasing terminal alkyl group length. The entropy change at the $H_B/S_E/S_B-S_{Ad}$ transition passes through a maximum for polymers with an S_E mesophase.

Location of the mesogen in the side chain

Figure 3.11 shows the DSC thermograms of polymers in which the location of the mesogen in the side chain is varied. Polymer **6-8,3** exhibits an S_E and an S_{Ad} mesophase (Table 3.5). Table 3.6 shows that the dimensions of the orthorhombic cell are comparable to those of polymers **6-9,p**.

Polymer **6-6,5** shows only one mesophase (Figure 3.11); however, from the observed *d* spacings in the X-ray diffraction pattern (Table 3.5) it can be concluded that this polymer exhibits both an S_{Ad} and an S_{Adt} mesophase. This suggest that the S_{Ad} and S_{Adt} mesophases coexist in the temperature range between T_g and T_i and reflects the polydisperse nature of the polymeric material.[42]

The DSC results (Figure 3.11) and the X-ray reflection results (Table 3.5) of polymers **6-4,7** and **6-3,8** show that these polymers exhibit an S_{Adt} mesophase; i.e. the terminal alkyl

groups overlap. The transition temperatures of these two polymers are the highest in this series which indicates that the presence of an additional layer of alkyl chains between two layers of mesogens stabilizes the mesophase. The long terminal alkyl groups fill up the smectic mesophase, especially in the case of short spacer lengths. The short spacers give rise to a low degree of order in the mesophase, which is represented by the low isotropization entropy (Table 3.4).

Other structural variations

From the combination of the DSC results (Figure 3.11) and the X-ray diffraction results (Table 3.5) of polymer **7** it follows that this polymer only exhibits an S_{Ad} mesophase. The larger *d* spacing of this S_{Ad} mesophase in comparison to polymer **6-9,0**, the absence of a hexagonally ordered mesophase and the low T_i indicate that the ester linkage partially disturbs the order.

The DSC thermogram of polymer **8** (Figure 3.11) shows a T_g at 70°C and a T_i at 99°C. Between these temperatures POM revealed a vague yellowish texture with bright yellow Maltese crosses around air bubbles. In combination with the absence of reflections in the X-ray diffraction pattern it is concluded that the mesophase is nematic.

3.4. Conclusions

The alternating copolymerization of maleic anhydride with 1-alkenes carrying biphenyl mesogens yields SCLCPs with a low degree of polymerization and high glass transition temperatures. Most of the parent mesogenic 1-alkenes did not show liquid-crystalline behavior.

The transition temperatures and degree of order can be altered by molecular structure variations of the SCLCP. Spacer length determines the width of the mesophase: the isotropization temperature increases and the glass transition temperature decreases with increasing spacer length. For long spacers, the terminal alkyl group length has little effect on the mesophase width, however, transition temperatures pass through a maximum for a butoxy terminal group. On cooling from the S_{Ad} into the hexagonally ordered mesophase, the highly ordered mesogens restrict the polymer backbone mobility and induce a glass transition. Different hexagonally ordered mesophases can be observed just above the glass transition temperature depending on the terminal alkyl group length. A methoxy terminal group induces an S_{Bhex} mesophase, intermediate terminal alkyl groups induce an S_E mesophase, and long terminal alkyl groups induce an S_{Bcryst} mesophase.

X-ray diffraction experiments indicate the presence of two different interdigitated smectic A mesophases. If the spacer is longer than the terminal alkyl group, an S_{Ad} mesophase is observed in which the mesogens overlap. If the terminal alkyl group is longer than the spacer, an S_{Adt} mesophase is observed in which the terminal alkyl groups overlap. If

spacer and terminal alkyl group length are equal, both mesophases can be observed either in coexistence (polymer **6-6,5**) or in succession (polymer **6-9,8**).

For polymers in which the location of the mesogen in the side chain is altered, it is found that lengthening of the terminal alkyl group and shortening of the spacer leads to the disappearance of the hexagonal order and the appearance of the S_{Adt} mesophase.

Introduction of an ester linkage between the spacer and methoxybiphenyl mesogen lowers the transition temperatures, and no hexagonally ordered mesophase is obtained, however, the S_{Ad} mesophase is still observed. Replacing a methoxy terminal group by a cyano terminal group also lowers transition temperatures, and now only a nematic mesophase is found.

3.5. References

1   Shibaev, V. P.; Freidzon, Ya. S.; Kostromin, S. G. *Liquid Crystalline and Mesomorphic Polymers*; Shibaev, V. P. Lam, L., Eds.; Springer-Verlag: New York, 1994.

2   Finkelmann, H. *Polymer Liquid Crystals*; Ciferri, A., Krigbaum, W. R., Meyer, R. B., Eds.; Academic Press: New York and London, 1982.

3   Simmonds, D. J. *Liquid Crystal Polymers, From Structures to Applications*; Collyer, A. A., Ed.; Elsevier Applied Science: London and New York, 1992.

4   Percec, V.; Pugh, C. *Side Chain Liquid Crystal Polymers*; McArdle, C. B., Ed.; Blackie: Glasgow, UK, 1989.

5   Percec, V.; Tomazos, D.; Willingham, R. A. *Polym. Bull.* **1989**, *22*, 199.

6   Maughon, B. R.; Weck, M.; Mohr, B.; Grubbs, R. H. *Macromolecules* **1997**, *30*, 257.

7   Stevens, H.; Rehage, G.; Finkelmann, H. *Macromolecules* **1984**, *17*, 851.

8   Allcock, H. R.; Kim, C. *Macromolecules* **1989**, *22*, 2596.

9   Percec, V.; Rodriguez-Parada, J. M.; Ericsson, C. *Polym. Bull.* **1987**, *17*, 347.

10 Laus, M.; Bignozzi, M. C.; Angeloni, A. S.; Galli, G.; Chiellini, E. *Macromolecules* **1993**, *26*, 3999.

11 Frère, Y.;Yang, F.; Gramain, P.; Guillon, D.; Skoulios, A. *Makromol. Chem.* **1988**, *189*, 419.

12 Nieuwkerk, A. C.; Marcelis, A. T. M.; Sudhölter, E. J. R. *Macromolecules* **1995**, *28*, 4986.

13 Komber, H. *Macromol. Chem. Phys.* **1995**, *196*, 669.

14 Trivedi, B. C.; Culbertson, B. M. *Maleic Anhydride*; Trivedi, B. C., Ed.; Plenum: New York, 1982.

15 Schmidt-Naake, G.; Drache, M.; Leonhardt, K. *Macromol. Chem. Phys.* **1998**, *199*, 353.

16 van der Wielen, M. W. J.; Cohen Stuart, M. A.; Fleer, G. J.; de Boer, D. K. G.; Leenaers, A. J. G.; Nieuwhof, R. P.; Marcelis, A. T. M.; Sudhölter, E. J. R. *Langmuir* **1997**, *13*, 4762.

17 de Boer, D. K. G.; Leenaers, A. J. G.; van der Wielen, M. W. J.; Cohen Stuart, M. A.; Fleer, G. J.; Nieuwhof, R. P.; Marcelis, A. T. M.; Sudhölter, E. J. R. *Physica B* **1998**, *248*, 274.

18 Frost, A. M.; Kolosentseva, I. A.; Razumovskii, V. V. *Zh. Prikl. Khim.* **1974**, *47(4)*, 731.

19 Kurbanova, R. A.; Mirzaoglu, R.; Kurbanov, S.; Karatas, I.; Pamuk, V.; Ozcan, E.; Okudan, A.; Güler, E. *J. Adhesion Sci. Technol.* **1997**, *11*, 105.

20 Bistac, S.; Vallat, M. F.; Schultz, J. *J. Adhesion* **1996**, *56*, 205.

21   Thery, S.; Jacquet, D.; Mantel, M. *J. Adhesion* **1996**, *56*, 15.

22   Kolosentseva, I. A.; Frost, A. M.; Razumovskii, V.V. *Zakakras. Mater. Ikh. Primen* **1975**, *2*, 10.

23   Müller, B.; Mebarek, D. *Angew. Makromol. Chem.* **1994**, *221*, 177.

24   Vogel, A. I. *Textbook of Practical Organic Chemistry* 5th ed; Longman Scientific & Technical: Essex, 1989, p. 886.

25   Rodriguez-Parada, J. M.; Percec, V. *J. Polym. Sci., Part A: Polym. Chem.* **1986**, *24*, 1363.

26   Marcelis, A. T. M.; Koudijs, A.; Sudhölter, E. J. R. *Liq. Cryst.* **1995**, *18*, 843.

27   Hsu, C. S.; Rodriguez-Parada, J. M.; Percec, V. *J. Polym. Sci. Part A: Polym. Chem.* **1987**, *25*, 2425.

28   Davis, F.; Hodge, P.; Towns, C. R.; Ali-Adib, A. *Macromolecules* **1991**, *24*, 5695.

29   Rätzsch, M.; Zschoche, S.; Steinert, V.; Schlothauer, K. *Makromol. Chem.* **1986**, *187*, 1669.

30   Tacx, J. C. J. F.; Meijerink, N. L. J.; Suen, K. *Polymer* **1996**, *37*, 4307.

31   Ebbut, J.; Richardson, R. M.; Blackmore, J.; McDonnel, D. G.; Verral, M. *Mol. Cryst. Liq. Cryst.* **1995**, *261*, 549.

32   Davidson, P.; Levelut, A. M. *Liq. Crystals* **1992**, *11*, 469.

33   Shibaev, V. P. *Liquid-Crystal Polymers* (Ed. N. A. Platé); Plenum Press: New York, 1993.

34   Nieuwhof, R. P.; Marcelis, A. T. M.; Sudhölter, E. J. R.; van der Wielen, M. W. J.; Cohen Stuart, M. A.; Fleer, G. J. *Macromol. Symp.* **1998**, *127*, 115.

35   Gemmel, P. A.; Gray, G. W.; Lacey, D.; Alimoglu, A. K.; Ledwith, A. *Polymer* **1985**, *26*, 615.

36   Wübbenhorst, M.; Nieuwhof, R. P.; Marcelis, A. T. M.; Sudhölter, E. J. R.; van Turnhout, J., to be published.

37   Shibaev, V. P.; Platé, N. A. *Pure & Appl. Chem.* **1985**, *57*, 1589.

38   Niemelä, S.; Selkälä, R.; Sundholm, F.; Taivainen, J. *J. Macromol. Sci.-Pure Appl. Chem.* **1992**, *A29(11)*, 1071.

39   Kossmehl, G.; Pithart, C. *Acta Polym.* **1991**, *42*, 438.

40   Reesink, J. B.; Picken, S. J.; Witteveen, A. J.; Mijs, W.J. *Macromol. Chem. Phys.* **1996**, *197*, 1031.

41   Jansen, J. C. *Side-chain liquid crystalline polycarbonates, synthesis, mesomorphic properties and dielectric and mechanical analysis*; Thesis Delft University of Technology, The Netherlands, 1996.

42   Galli, G.; Chiellini, E.; Laus, M.; Caretti, D.; Angeloni, A.S. *Makromol. Chem., Rapid Commun.* **1991**, *12*, 43.

4

Modification of side-chain liquid-crystalline poly(maleic anhydride-alt-1-alkene)s with mesogen-containing alcohols

Side-chain liquid-crystalline copolymers from maleic anhydride and 1-alkenes carrying biphenyl mesogens were modified by reaction of the anhydride moieties with different mesogenic alcohols to give maleic acid monoesters. FTIR and ^1H NMR showed high degrees of modification. Grafting methoxybiphenyl-containing alcohols having different spacer lengths onto methoxybiphenyl-containing polymers yielded polymers exhibiting smectic A mesophases with a variable degree of interdigitation. The glass transition temperature decreased with spacer length, whereas the isotropization temperature remained almost constant. Grafting azobenzene-containing alcohols onto methoxybiphenyl-containing copolymers yielded side-chain liquid-crystalline polymers exhibiting nematic mesophases. The effect of the 4'-azobenzene terminal group on the temperature window of the mesophase was CN > OMe > F > H. Grafting a cyanostilbene-containing alcohol onto a methoxybiphenyl-containing copolymer resulted in a polymer that exhibited a smectic E mesophase with complete interdigitation of side chains. Introducing methoxybiphenyl mesogens into cyanobiphenyl-containing copolymers or vice versa resulted in polymers with smectic A mesophases. Furthermore, an increase in isotropization temperatures was observed in comparison with polymers carrying only one type of mesogen. This indicates specific favorable interactions between unlike mesogens.

4.1. Introduction

In a previous study, the synthesis and phase behavior of side-chain liquid-crystalline polymers (SCLCP) from maleic anhydride (MA) and 1-alkenes have been reported.[1,2] The backbone of these SCLCPs has a well-defined structure because of the alternating sequence

53

of 1-alkene and MA moieties. The polymers show high glass transition temperatures and highly ordered smectic mesophases. Because of its reactivity toward amines and alcohols, the anhydride moiety constitutes a nice handle to modify the polymers. These modifications may for example alter the liquid-crystalline properties or enhance the aqueous solubility of the polymers.[3]

Modification may also be used to increase the mesogen density of the polymers in order to tune the liquid-crystalline properties. So far, two approaches have been described that increase mesogen density: (i) coupling compounds with paired mesogens to a preformed polymer,[4,5] and (ii) polymerization of monomers carrying two mesogens.[6,7,8] In comparison to polymers carrying only one mesogen per repeating unit, these polymers show more stable smectic phases with high degrees of order. In this chapter a new method to increase mesogen density by grafting a mesogen-containing alcohol onto an MA-containing SCLC copolymer is described. This approach enables the combination of different spacer lengths and different mesogenic units in an almost alternating sequence in one polymer, which may lead to interesting properties.

The effect of different spacer lengths in one polymer on the phase behavior of SCLCPs has been studied before for poly(vinyl ether)s with cyanobiphenyl mesogens,[9,10,11] and poly(styrene)s with methoxyazobenzene[12] or nitroazobenzene[13] mesogens. Depending on spacer length, poly(vinyl ether)s with cyanobiphenyl mesogens give homopolymers that exhibit nematic (N), smectic A or no liquid-crystalline phases. When two monomers with different spacer lengths are used of which the corresponding homopolymers give no liquid-crystalline and smectic A phases, respectively, the resulting copolymers display a nematic mesophase over a quite broad range of copolymer compositions.[9-11] In addition, if one of the monomers yields homopolymers that exhibit nematic mesophases, the temperature range of this nematic mesophase can be increased considerably by copolymerization with a monomer of which the corresponding homopolymer exhibits an S_A mesophase. The combination of ethyl and undecyl spacers results in polymers with isotropization temperatures that are significantly lower than the weighted averages of the isotropization temperatures of the corresponding homopolymers. If the disparity in spacer length is smaller than eight carbon atoms, the isotropization temperatures of the copolymers deviate only slightly from ideal behavior. A small deviation from ideal behavior was observed for poly(styrene)s with methoxyazobenzene[12] or nitroazobenzene mesogens and small disparities in spacer length.[13]

Liquid-crystalline behavior can also be influenced by combining mesogens with electron-withdrawing and electron-donating substituents in the same polymer. The combination of electron-poor and electron-rich mesogens gives rise to specific interactions.[14,15,16,17,18,19,20,21] The precise nature of these interactions is unclear, although it is generally assumed that charge transfer complexes are involved.[22] In general, the transition temperatures of polymers with different mesogens are higher than those of either polymers with one type of mesogen.

In this chapter polymers are described that are prepared by grafting mesogen-containing alcohols onto SCLC poly(MA-*alt*-1-alkenes), described in a previous chapter.[1] The effect of different spacer lengths and different mesogens in these almost perfectly alter-

nating copolymers on the liquid-crystalline properties are investigated and compared with the properties of the unmodified parent polymers. Three different series will be described: a series in which methoxybiphenyl-containing alcohols with variable spacer lengths are grafted to investigate the disparity in spacer length; another series in which azobenzene-containing alcohols with different terminal substituents or cyanostilbene mesogens are grafted; and finally a series in which electron-rich methoxybiphenyl mesogens are combined with electron-poor cyanobiphenyl mesogens in different ways in the same copolymer. The SCLCPs have been characterized by gel permeation chromatography, ^{1}H NMR, polarizing optical microscopy, differential scanning calorimetry, FTIR and wide angle X-ray diffraction.

4.2. Experimental part

4.2.1. Materials

The benzene used for polymer modifications was dried over sodium. 4-Hydroxy-4'-methoxyazobenzene, 4-cyano-4'-hydroxyazobenzene, 4-hydroxyazobenzene, and 4-fluoro-4'-hydroxyazobenzene were prepared by reaction of the diazonium salt of 4-methoxyaniline, 4-cyanoaniline, aniline, and 4-fluoroaniline respectively with phenol[23]. 4-Hydroxy-4'-methoxybiphenyl,[24] mesogenic alcohols[25] **2-*m*, 2-3OBu, 3, 4, 5** (Scheme 4.1), and copolymers **6, 7,** and **8**[1,2] (Scheme 4.2) were synthesized as described before. Other reagents used for syntheses were commercially available and used without further purification.

4.2.2. Equipment

Gel permeation chromatography (GPC) measurements were carried out using a series of four microstyragel columns with pore sizes of 10^5, 10^4, 10^3 and 10^6 Å (Waters) respectively, with THF containing 5 wt% acetic acid as eluent.[26] A dual detection system consisting of a differential refractometer (Waters model 410) and a differential viscometer (Viscotek model H502) was used. A calibration line was made with this setup, using narrow polystyrene reference standards in THF, and the molar mass (g/mol) of the synthesized polymers was determined referring to this calibration line. Thermal transitions were monitored with a Perkin-Elmer DSC-7. Scan rates of 10 K/min were used in the differential scanning calorimetry (DSC) experiments with sample masses of 5-10 mg. Transition temperatures were taken from the second heating cycle. Polarizing optical microscopy (POM) was performed on an Olympus BH-2 microscope equipped with a Mettler FP82HT hot stage and an FP80HT temperature controller. X-ray diffraction measurements were performed on a Siemens D5000 reflection diffractometer with a HTK oven and Cu Kα radiation. ^{1}H NMR spectra were recorded on a Bruker AC200 spectrometer at 200 MHz. FTIR spectra were recorded on a BioRad FTS-7 spectrometer.

The degree of modification of SCLCPs was determined from FTIR absorption spectra of modified SCLCPs in THF referring to a calibration line. This calibration line was obtained by

determining the peak intensities at 1730 and 1780 cm^{-1} of mixtures of succinic anhydride and the monomethylester of succinic acid in different ratios in THF. The peaks at 1730 and 1780 cm^{-1} correspond to the C=O stretching band of the carbonyl and the antisymmetric C=O stretching band of the anhydride, respectively.

4.2.3. Synthesis

Modification of SCLCPs

All compounds were synthesized according to a modified literature procedure,[27] as an example is given for polymer **9-3**:

6 (0.45 g, 1.19 mmol MA-units) was dissolved in benzene (7 mL) at 80°C under nitrogen atmosphere. The solution was cooled to 60°C and **2-3** (0.57 g, 2.20 mmol) and 4-dimethylaminopyridine (0.023 g, 0.19 mmol) were added. The reaction mixture was stirred for 8 h under a nitrogen atmosphere at 60°C, cooled to 50°C and stirred for another 2 h. The mixture was added to hexane (10 volumes) to precipitate the polymer and the mesogenic alcohol. The precipitate was collected and repeatedly precipitated from THF into 2-propanol (10 volumes) until TLC showed complete removal of any unreacted mesogenic alcohol. A white powder (0.38 g) was obtained after filtration.

4.3. Results and discussion

4.3.1. Synthesis

An overview of the employed mesogenic alcohols **2-m**, **2-3OBu**, **3**, **4**, and **5** is given in Scheme 4.1. These monomers were obtained via the etherification of bromo- or chloro


2-m   m = 2,3,6,8,11
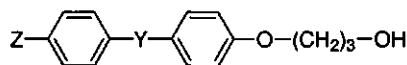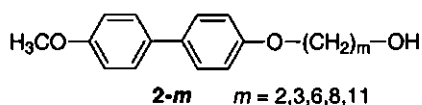
alcohol	Y	Z
2-3OBu	-	OC$_4$H$_9$
3	-	CN
4-OMe	N=N	OCH$_3$
4-CN	N=N	CN
4-H	N=N	H
4-F	N=N	F
5	C=C	CN

Scheme 4.1. Structure of alcohols 2 - 5.

Table 4.1. Yields (%) and phase transition temperatures (°C) of compounds **2, 3, 4,** and **5**.[a]

mesogenic alcohol	yield	transition temperature
2-2	40	K 174 I
2-3	55	K 170 I
2-6	65	K 149 I
2-8	67	K 145 I
2-11	62	K 143 I
2-3OBu	81	K 166 I
3	64	K 144 I
4-OMe	56	K 145 I
4-CN	70	K (N 161) 170 I
4-H	63	K 97 I
4-F	63	K 116 I
5	75	K 144 N 176 I

[a] K = crystalline, N = nematic, I = isotropic phase.
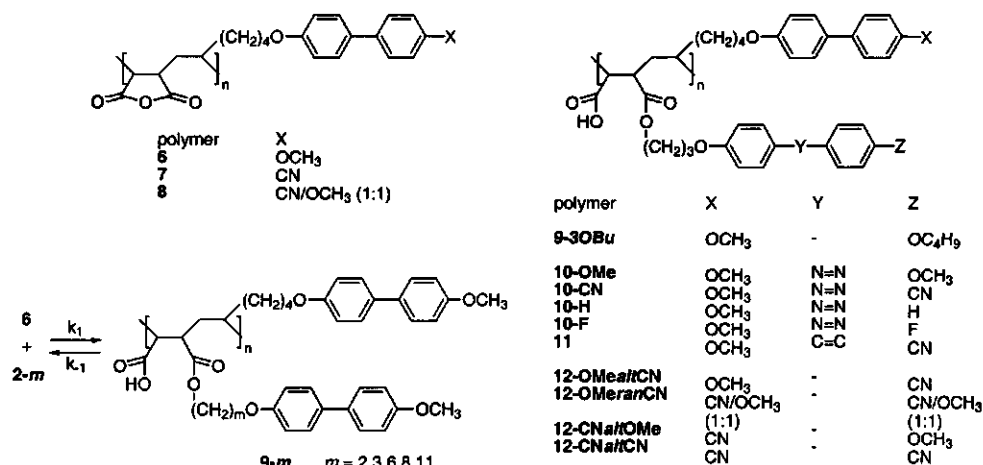
Scheme 4.2. Synthesis and structures of polymers **6 - 12**.

alcohols with the phenols.[25] All monomers were obtained in satisfactory yields and high purity. The observed ^{1}H NMR signals agree well with the chemical structure.

The yields and transition temperatures, which were determined from polarizing optical microscopy (POM), are summarized in Table 4.1. Only compounds **4-CN** and **5** exhibit liquid-crystalline behavior. For both compounds Schlieren textures were observed with POM indicating a nematic mesophase. The transition temperatures observed with POM agree well with those found with DSC.

Polymers **6, 7,** and **8** (see Scheme 4.2) were synthesized by copolymerization of the mesogenic 1-alkenes with MA.[1] Before further characterization or modification reactions

Table 4.2. *Number-average molecular weights (M$_n$), weight-average molecular weights (M$_w$), polydispersity indices (PDI), degrees of polymerization (DP) as determined by GPC and yields (%) of polymers 6, 7, and 8.*

polymer	10^{-3} M$_n$	10^{-3} M$_w$	PDI	DP	yield
6	3.99	6.54	1.64	21	90
7	2.46	3.70	1.50	13	45
8	2.89	4.04	1.39	15	39

were performed, the polymers were dried in vacuo over P$_2$O$_5$ at 100°C until FTIR showed that all carboxylic acid groups were ring closed to anhydride moieties.[1] The molecular weights of the unmodified polymers were determined by GPC and are listed in Table 4.2.

Scheme 4.2 displays the modification reaction of the SCLCPs and gives an overview of the synthesized polymers. Normally, the reaction of anhydride moieties with alcohols results in monoesterification that proceeds very slowly without an efficient catalyst. Classical catalysts such as 2-dimethylaminopyridine, tributylamine and pyridine showed a low activity.[27] However, 4-dimethylaminopyridine is an efficient catalyst[27] and was therefore used to obtain polymers with a high degree of modification. For this catalyst it was found that the reaction is reversible and that the equilibrium constant of the reaction decreases significantly with increasing temperature.[27] Therefore, the reaction was started at 60°C, followed by further reaction at 50°C. According to FTIR measurements using a calibration line, modification degrees between 94% and 98% were obtained with an experimental error of 5%. An example is given for polymer 9-3 in Figure 4.1. This Figure shows that the absorptions at 1780 and 1858 cm^{-1} from the anhydride moiety are almost completely converted into the absorption at 1730 cm^{-1}, which is representative for the acid/ester moiety.
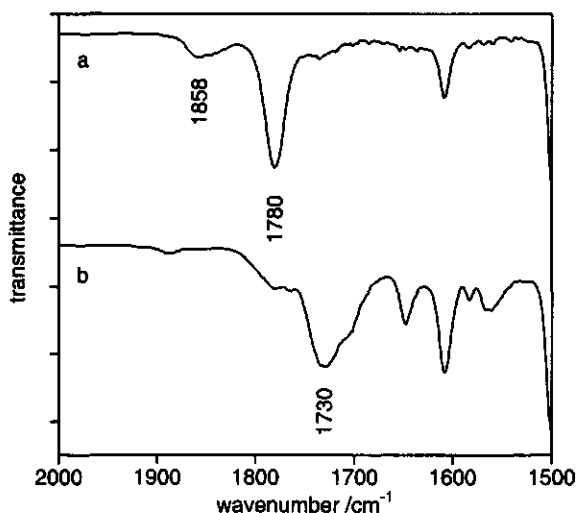
Figure 4.1. *FTIR absorption spectra of polymer 6 (a) and polymer 9-3 (b).*

^{1}H NMR signals of the modified polymers correspond to the expected chemical structures and the peak integrals for polymers with different mesogens also confirmed the high degrees of modification. For example, integration of the methoxybiphenyl and cyanobiphenyl signals of polymers **12-OMealtCN**, **12-OMeranCN**, and **12-CNaltOMe** confirm that these polymers contain about equal amounts of methoxybiphenyl and cyanobiphenyl mesogens.

Due to the similar degrees of polymerization of the unmodified polymers and the high degrees of modification, comparison of transition temperatures of different polymers is justified.

4.3.2. Transition temperatures and mesophases of SCLCPs

Table 4.3 summarizes the mesophases of the polymers, their phase transition temperatures, and the corresponding entropy changes. The mesophases in Table 4.3 were assigned on the basis of X-ray diffraction patterns of the mesoglass and textures observed with POM. The assignment of mesophases will be discussed later.

Table 4.4 represents the X-ray diffraction data, comprising experimental d spacings and calculated d spacings. d Spacings were determined in the glassy state at room

Table 4.3. *Phase transition temperatures (°C), corresponding heat capacity or entropy changes (J/mol K) in parenthesis as determined by DSC, and phase types[a] of the polymers.*

polymer	phase behavior				
6	G_{Bhex} 120 (-)	S_{Bhex} 128 (7.1)	S_{Ad} 136 (10)		I
7	G 114 (103)				I
8	G 137 (137)		S_{Ad} 177 (5.3)		I
9-2	G_{Bcryst} 132 (178)	S_{Bcryst} 138 (15.8)	$S_{A1,inc}$ 147 (7.3)		I
9-3	G_E 134(-)	S_E 144 (24.9)	S_{A1} 150 (9.0)		I
9-6	G_{Bcryst} -	S_{Bcryst} 136 (19.9)	S_{A1} 148 (13.4)		I
9-8	G_{Bcryst} 98 (137)	S_{Bcryst} 108 (7.9)	S_{A1} 145 (5.3)	S_{A2} 147 (4.9)	I
9-11	G 93 (74)		S_{Ad} 141 (13.9)		I
9-3OBu	G_E -	S_E 139 (8.9)	S_{A1+A2} 147 (3.1)	S_{A2} 159 (4.9)	I
10-OMe	G 96 (101)			N 148 (5.0)	I
10-CN	G 108 (99)			N 164 (7.5)	I
10-H	G 95 (58)			N 123 (7.8)	I
10-F	G 97 (83)			N 143 (4.8)	I
11	G -	S_E 154 (15.0)			I
12-OMealtCN	G_{Bcryst} -	S_{Bcryst} 154 (6.6)	S_{A1} 170 (9.0)		I
12-OMeranCN	G_{Bhex} -	S_{Bhex} 129 (3.7)	S_{Ad} 157 (8.1)		I
12-CNaltOMe	G 109 (115)		S_{Ad} 150 (7.0)		I
12-CNaltCN	G -		S_{Ad} 134 (-)	S_{AX} 137 (-)	I

[a] *I = isotropic phase; S_{Ad}, S_{A1}, S_{A2} = different smectic A phases; S_{AX} = unidentified smectic A phase ; S_{Bhex} = hexatic smectic B; S_{Bcryst} = crystal smectic B; S_E = smectic E; G_X= glass phase, in which X is the frozen in hexagonally or orthorhombically ordered mesophase.*

Table 4.4. *Experimental d spacings (Å) at different temperatures obtained from wide-angle X-ray diffraction experiments and calculated d spacings (Å) of the polymers.*

| polymer	T	d spacings		calcd d spacings	
	°C			S_{Al}	S_{Ad}
6	25	23.9; 11.9		20.9	26.6
7	25	-		-	-
8	25	23.3; 11.5		20.9	26.6
9-2	25	26.3; 22.3; 11.0	4.48	20.6	26.1
9-3	25	21.8; 10.7; 7.25	4.47; 3.94; 3.21	21.8	28.5
9-6	25	22.9; 11.5	4.45	25.4	36.3
9-8	25	23.7; 11.9	4.46	26.9	39.3
9-11	25	32.1; 16.3; 10.8		30.7	46.7
9-3OBu	25	39.6; 21.8; 19.6; 13.2; 11.0	4.49; 3.99; 3.22	25.8	28.5
	142	40.1; 21.8; 20.3; 13.5; 11.0			
	155	39.2; 20.1; 13.3			
10-OMe	25	21.5; 10.8		24.2	30.3
10-CN	25	21.6; 10.8		23.4	30.3
10-H	25	22.1; 10.9		21.9	30.3
10-F	25	21.3; 10.7		22.3	30.3
11	25	11.2; 7.5	4.39; 3.99; 3.17	23.7	30.7
10-OMe*alt***CN**	25	21.5; 10.8; 7.22	4.47	21.3	26.6
10-OMe*ran***CN**	25	23.5; 11.7	4.44	21.8	28.5
10-CN*alt***OMe**	25	24.1; 12.0	4.38	21.8	28.5
10-CN*alt***CN**	25	27.2		21.8	28.5

temperature, after the polymer was cooled from the isotropic state via the liquid-crystalline state to the glassy state at a cooling rate of 5°C/s.

Unmodified SCLCPs

Figure 4.2 shows the DSC thermograms of the parent polymers **6**, **7**, and **8**. Polymer **7**, containing cyanobiphenyl mesogens, shows a T_g and does not exhibit any liquid-crystalline behavior. Polymer **6**, containing methoxybiphenyl mesogens, exhibits both a hexatic smectic B (S_{Bhex}) and an interdigitated smectic A (S_{Ad}) mesophase.[1] Because the T_g is almost immediately followed by the S_{Bhex}-S_{Ad} transition, determination of T_g was difficult. For polymer **8**, which has a random distribution of equimolar amounts of methoxy- and cyanobiphenyl mesogens along the polymer backbone, a higher isotropization temperature (T_i) is found than can be expected from the mesomorphic behavior of polymers **6** and **7**. This behavior has been observed before and has been ascribed to specific favorable interactions between electron-rich and electron-poor groups.[19,20,21]

If 50% of the methoxybiphenyl mesogens in polymer **6** are replaced by cyanobiphenyl mesogens, like in polymer **8**, the S_{Bhex} mesophase disappears (Figure 4.2 and
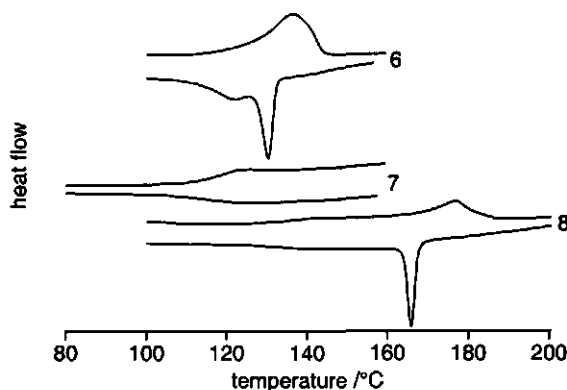
Figure 4.2. *DSC thermograms of polymers 6, 7 and 8. For all compounds the second heating and cooling traces are given.*

Table 4.3). Introduction of cyanobiphenyl mesogens in a methoxybiphenyl matrix disturbs the efficient packing of mesogens and only an S_{Ad} mesophase is found. Consequently, a distinct T_g is found.

Alkoxybiphenyl mesogens

Figure 4.3 shows the DSC thermograms of polymers that were obtained by modifying polymer **6** with methoxybiphenyl-containing alcohols having different spacer lengths. In addition, an alkoxybiphenyl mesogen with a butoxy terminal group and a propyl spacer has been grafted onto polymer **6**. From Figure 4.3, it is clear that these polymers undergo two or even three phase transitions. Polymers **9-2**, **9-3** and **9-11** exhibit distinct glass transitions in the second heating and cooling scans. Due to the presence of a highly ordered mesophase, polymer **9-8** only exhibits a distinct glass transition in the first heating scan. This can be attributed to absence of hexagonal order in the freshly precipitated polymer. For polymers **9-6** and **9-3OBu** no glass transition was found with DSC.

On cooling from the isotropic melt, polymers **9** show textures with POM that were similar to those of polymer **6**,[1] although they seem to develop faster during annealing and the domains were slightly bigger. When polymer **9-8** is cooled from the isotropic melt, a different texture developed with small bandlike domains that are surrounded by homeotropic regions. After additional cooling, this texture transformed into a more sandlike texture similar to that observed for the other polymers that exhibit an S_{A1} mesophase. These observations agree well with DSC-results that showed two peaks in a narrow temperature interval. DSC also showed an additional transition for polymer **9-3OBu**. However, no change in texture was observed with POM at the transition temperature of 147°C.

The X-ray diffraction pattern of polymer **9-2** shows peaks from two first order reflections that correspond to a mesophase with partially interdigitated side chains (S_{Ad}) and one with fully interdigitated side chains (S_{A1}) (Table 4.4). This combination of mesophases is

61
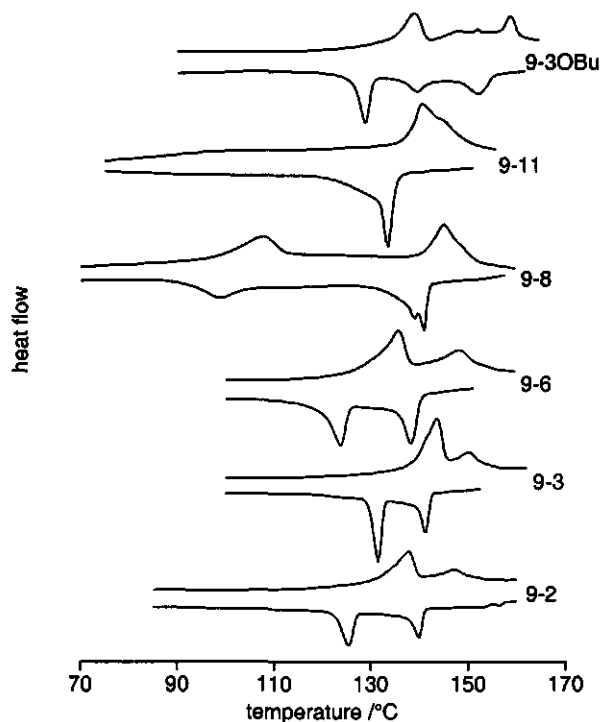
Figure 4.3. *DSC thermograms of polymers **9-m** and **9-3OBu**. For all compounds the second heating and cooling traces are given.*

also known as $S_{A1,inc}$. The experimental d spacing of the S_{A1} periodicity is slightly higher than the calculated d spacing, which can be attributed to the presence of an S_{Ad} mesophase that partially disturbs the S_{A1} periodicity. The sharpened reflection in the wide-angle region results from a regular lateral distance between mesogens of 4.48 Å. From the width at half-height of this peak the correlation length of the lateral order was calculated. The magnitude of both the correlation length (14.0 Å) and the entropy change associated with the S_B-$S_{A1,inc}$ transition (see Table 4.3) are indicative of an S_{Bcryst} mesophase; i.e. besides long-range bond-orientational order there is also long-range positional order.

Polymer **9-3** (Table 4.4) exhibits an S_{A1} mesophase between 144°C and 150°C. For the mesoglass, the (110), (200) and (210) reflections emerged in the wide-angle region. These reflections result from deviations from hexagonal symmetry which means that polymer **9-3** exhibits a smectic E (S_E) mesophase. In this S_E mesophase the mesogens are densely packed in an orthorhombic cell with the following dimensions: a = 7.89 Å; b = 5.43 Å and c = 21.8 Å. The surface area (a · b) of the orthorhombic cell has a value of 42.8 Å^2, which is considerably smaller than the 43.7 Å^2 of unmodified polymers with an S_E mesophase and S_{Ad}

62
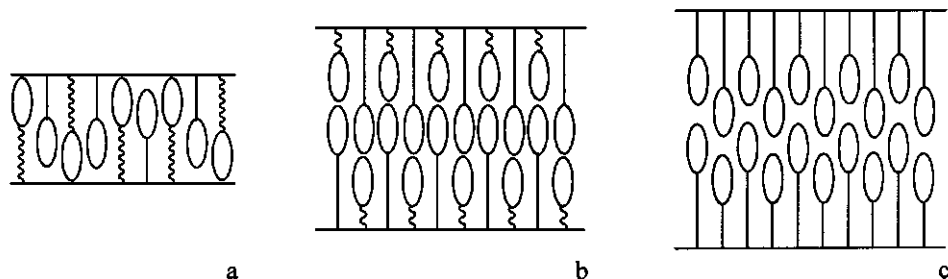
Figure 4.4. *Schematic representation of different smectic mesophases for polymers with different spacer lengths: a. S_{A1} mesophase; b. S_{Ad} mesophase; and c. S_{A2} mesophase.*

periodicity.[1] The difference can be attributed to a denser packing of mesogens in the S_{E1} mesophase than in the S_{Ed} mesophase.

The d spacing of polymer **9-6** is 22.9 Å which is 1.1 Å longer than the d spacing of **9-3**. However, on going from a propyl to a hexyl spacer an all-trans conformation of the hexyl spacer would lead to an increase of 3.9 Å. This difference is found because this system strives for a maximum of mesogenic interactions and a minimum of free volume. Therefore, the longest spacer (i.e. hexyl spacer) has to adjust its conformation; i.e. the longest spacer has an increased number of gauche conformations. The result is a kind of distorted layer with S_{A1} periodicity (Figure 4.4a). In addition, polymer **9-6** exhibits an S_{Bcryst} mesophase with a correlation length of 13.3 Å. The disparity in spacer lengths prevents the mesogens from attaining the better ordered S_E phase as found for polymer **9-3**.

Below 145°C polymer **9-8** exhibits an S_{A1} mesophase with a d spacing of 23.7 Å (Table 4.4, Figure 4.5). As found for polymer **9-6**, the d spacing is smaller than expected for an S_{A1} mesophase with an all-trans conformation of the octyl spacer. Due to steric hindrance in the smectic layers, the S_{A1} mesophase transforms into an S_{A2} mesophase with a d spacing
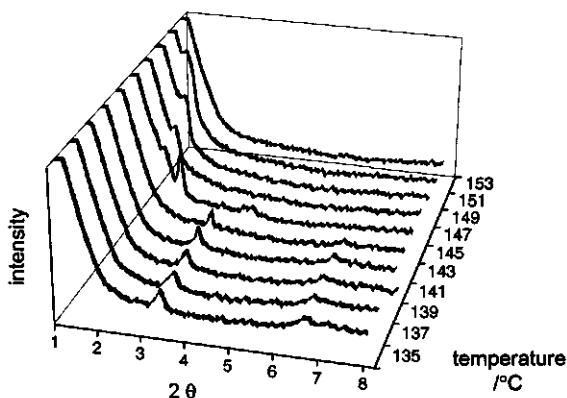
Figure 4.5. *Temperature dependent wide-angle X-ray diffraction patterns of polymer 9-8.*
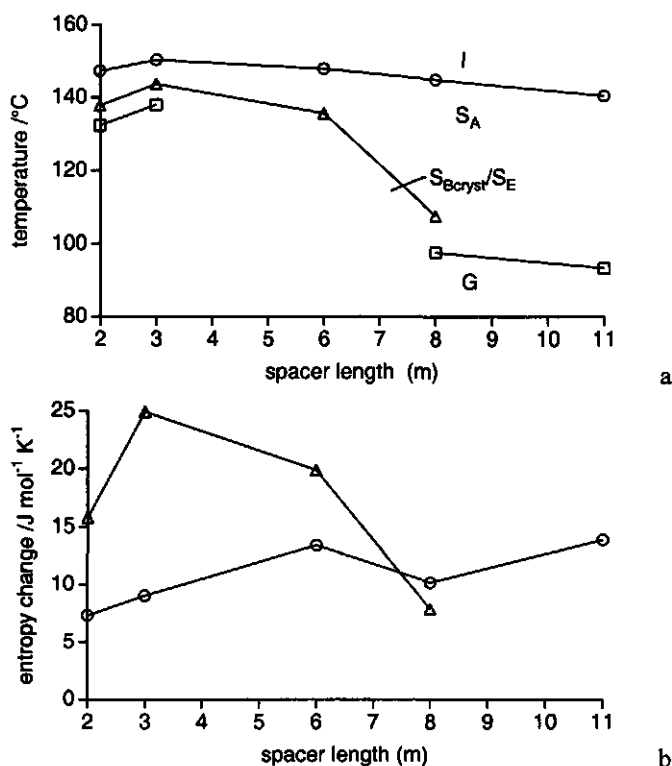
Figure 4.6. *Dependence of the transition temperatures as found with DSC on spacer length m for polymers 9-m: (□) glass transitions; (Δ) S$_B$/S$_E$-S$_A$ transitions; (o) isotropization transitions; b. Dependence of the entropy change as found with DSC on spacer length m for polymers 9-m: (Δ) S$_B$/S$_E$-S$_A$ transitions; (o) isotropization transitions.*

of 49.0 Å at 145°C (Figure 4.4c). In the S$_{A2}$ mesophase there is no overlap of side chains and the *d* spacing is twice the length of a side chain. In addition, a reflection corresponding to a *d* spacing of 39.2 Å can be observed at 145°C, which corresponds to an S$_{Ad}$ mesophase with overlap of biphenyl mesogens with octyl spacers (Figure 4.4b). However, this mesophase is constrained because of the low disparity in spacer length and it transforms almost immediately in the S$_{A2}$ mesophase (Figure 4.4c). Below 108°C, polymer **9-8** exhibits an S$_{Bcryst}$ mesophase with a correlation length of 15.4 Å.

The *d* spacing of 32.1 Å of polymer **9-11** (Table 4.4) indicates that the side chains interdigitate partially. The strong disparity in spacer length prevents the mesogens from ordering hexagonally.

In the X-ray diffraction pattern of polymer **9-3OBu**, five weak reflections can be seen that arise from a smectic structure with *d* spacings of 21.8 Å and 39.6 Å. These *d* spacings correspond to S$_{A1}$ and an S$_{A2}$ periodicity, respectively. Up to 147°C these two periodicities coexist, but between 147 and 159°C only the S$_{A2}$ periodicity remains. Besides the S$_A$ mesophases, polymer **9-3OBu** also exhibits an S$_E$ mesophase of which the orthorhombic cell

dimensions are a = 9.00 Å and b = 4.48 Å. Comparison of these values to those of polymer **9-3** shows that the presence of a terminal butoxy tail group hardly affects the mesogen packing.

Figure 4.6a illustrates the effect of the spacer length *m* of mesogenic alcohols on the transition temperatures of polymers **9-*m***. In comparison to the unmodified polymer **6**, it is clear that for low *m* modification results in (i) higher transition temperatures, and (ii) more ordered mesophases. Increasing spacer length *m* hardly affects T_i. The T_g and S_E-S_A or S_B-S_A transition are strongly affected by spacer length: T_g decreases as a consequence of the increase in free volume.

In Figure 4.6b the entropy changes at the S_{Bcryst}-S_{A1} and isotropization transition are plotted against spacer length *m*. For comparison the total enthalpy change of the S_{A1}-S_{A2} and S_{A2}-I transitions for polymer **9-8** is given. It can be seen that the isotropization entropy tends to increase with spacer length. The entropy change at the S_E-S_A or S_B-S_A transition increases on going from *m* = 2 to *m* = 3 and decreases for longer spacers, which agrees with the X-ray diffraction results that showed the highest degree of order for polymer **9-3**. A large disparity in spacer length prevents the mesogens from attaining a mesophase with order within smectic layers.

Stilbene and azobenzene mesogens

The effect of terminal substituent on the liquid-crystalline behavior has been studied by grafting azobenzene-containing alcohols with different terminal substituents onto methoxybiphenyl-containing polymer **6**. In addition, a cyanostilbene-containing alcohol has been grafted onto polymer **6**.

DSC showed that the resulting azobenzene-containing polymers **10** all exhibit a clear glass transition followed by an isotropization transition (Figure 4.7). In addition, POM revealed Schlieren textures which indicate a nematic mesophase. This was confirmed by X-ray diffraction, although some reflections with a very low intensity were observed in the low-angle region. These reflections result from smectic fluctuations with S_{A1} periodicity (Table 4.4).

The effect of the terminal group of the azobenzene mesogen on the temperature range of the mesophase is CN > OMe > F > H (Table 4.3). This is in complete agreement with the behavior of low-molar-mass mesogens[28] and SCLCPs with a poly(styrene) backbone.[29] This trend has been explained by the polarizability of the terminal group and its capability to give different conjugative interactions.[28]

Polymer **11**, which contains cyanostilbene mesogens, exhibits only an S_E mesophase which is obvious from the one transition observed with DSC (Figure 4.7) and the X-ray diffraction pattern (Table 4.4). In the small-angle area, the X-ray diffraction pattern only shows the second and third order reflections. The absence of a first order reflection results from an additional maximum in the electron density profile, which induces an apparent *d* spacing (the strongest small angle reflection) that is half the smectic *d* spacing. The smectic *d* spacing of 22.4 Å (Table 4.4) corresponds to a mesophase with S_{A1} periodicity. The orthorhombic cell dimensions of polymer **11** in the S_E mesophase are: a = 7.98 Å; b = 5.25 Å. The a-dimension of the orthorhombic cell is slightly bigger and the b-dimension is 0.18 Å

smaller than the values found for polymer **9-3**. The presence of cyanostilbene mesogens results in a slightly different packing of mesogens than found for biphenyl mesogens. Because of the presence of a highly ordered S_E mesophase, the change in specific heat capacity at T_g was too low to be detected by DSC.[30]

If we compare the mesomorphic behavior of polymers **10** and **11**, it is remarkable that polymers **10** exhibit nematic mesophases, whereas polymer **11** exhibits an S_E mesophase. The only difference between these mesogens is the polarity of the central linkage in the mesogen, which is an azo or a vinyl moiety, respectively. An explanation for this behavior could be that in case of the apolar stilbene mesogens, the polar backbone is strictly phase separated from the apolar mesogen layer, whereas in the case of azobenzene mesogens the polar polymer backbone can mix with the polar azobenzene moieties and phase separation is not so strict. This results in less ordered mesophases for polymers **10**.

Specific interactions

The effect of combining electron-rich and electron-poor mesogens on liquid-crystalline behavior has been studied by grafting cyanobiphenyl mesogens and methoxybiphenyl mesogens onto polymers **6** and **7**, respectively. These reactions yield polymers in which mesogens are attached to the polymer backbone in an almost alternating sequence. A random arrangement of mesogens was obtained by grafting a 1 : 1 mixture of
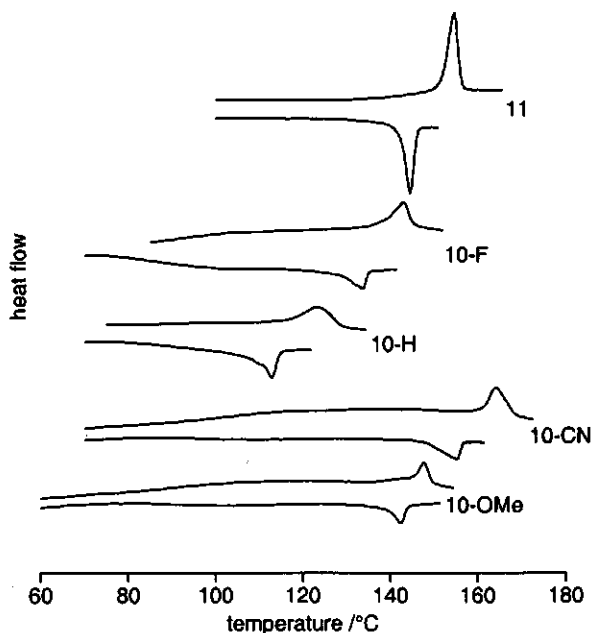
Figure 4.7. *DSC thermograms of polymers 10 and 11. For all compounds the second heating and cooling traces are given.*
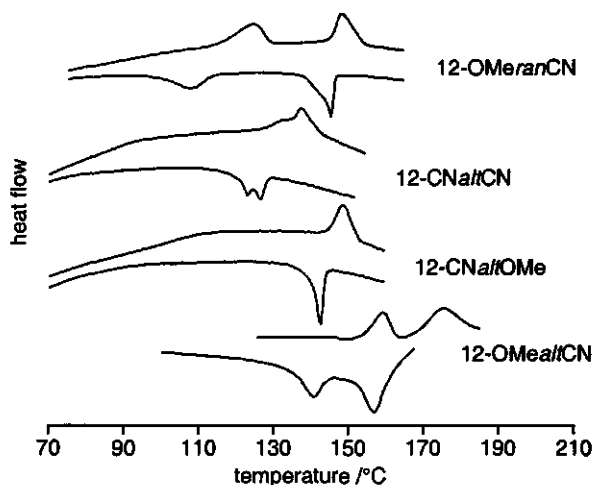
Figure 4.8. *DSC thermograms of polymers 12. For all compounds the second heating and cooling traces are given.*

cyanobiphenyl and methoxybiphenyl mesogens onto polymer **8**. The properties of these polymers will be described below and compared to those of polymers with only one type of mesogen, i.e. polymers **9-3** and **12-CN***alt***CN**.

Polymer **12-OMe***alt***CN** undergoes two phase transitions; however, no glass transition was observed by DSC (Figure 4.8). This polymer exhibits mesophases with S_{A1} periodicity and a *d* spacing of 21.5 Å. Below 154°C the mesogens are hexagonally ordered with a lateral distance of 4.47 Å. The correlation length of 13.3 Å indicates that the hexagonally ordered mesophase is of the S_{Bcryst} type.

Polymer **12-OMe***ran***CN** undergoes two phase transitions, but no glass transition was observed with DSC (Figure 4.8). POM and X-ray diffraction showed that this polymer exhibits an S_{Ad} mesophase with a *d* spacing of 23.5 Å and below 129°C the mesogens order hexagonally. The magnitude of both the correlation length (8.6 Å) and the entropy change associated with the S_B-S_{Ad} transition are indicative of an S_{Bhex} mesophase, i.e. there is only long-range bond-orientational order but no long-range positional order.

In contrast to polymer **12-OMe***alt***CN**, polymer **12-CN** *alt***OMe** exhibits a distinct glass transition and an S_{Ad} mesophase (Figure 4.8) with a *d* spacing of 24.1 Å. No hexagonal order was found. Polymer **12-CN***alt***CN** exhibits a distinct glass transition and two other transitions at 134 and 137°C (Figure 4.8). However, POM only showed the isotropization transition at 137°C. Furthermore, temperature dependent X-ray diffraction did not reveal any change at 134°C: below and above 134°C this polymer probably exhibits an S_{Ad} mesophase with a *d* spacing of 27.2 Å. This kind of mesophase is common for cyanobiphenyl mesogens because of the tendency to form antiparallel pairs.[31]

67

The degree of interdigitation of side chains increases on going from **12-CN*alt*OMe** to **12-OMe*ran*CN** to **12-OMe *alt*CN**. The concentration of methoxybiphenyl mesogens is not exactly equal for these polymers due to the fact that the grafting reaction does not proceed completely. This could mean that the degree of interdigitation of the side chains increases with increasing concentration of methoxybiphenyl mesogens. The observed trend in degree of interdigitation can then be explained by the tendency of cyanobiphenyl mesogens to form antiparallel pairs and the tendency of methoxybiphenyl containing side chains to interdigitate completely.[31]

Since the transition temperatures of both polymers with one type of mesogen (**9-3** and **12-CN*alt*CN**) and polymers with different types of mesogens (**12-OMe*alt*CN**, **12-OMe*ran*CN**, and **12-CN *alt*OMe**) are known (Table 4.3), the relative magnitude of deviations from ideal behavior can be calculated. Therefore, a scaled deviation temperature, ΔT_{SC}, has been introduced defined as:[20]

$$\Delta T_{SC} = \frac{2T_{AB} - (T_A + T_B)}{(T_A + T_B)} \tag{4.1}$$

where T_{AB} is the T_i for the copolymer, and T_A and T_B are those of the homopolymers. If the copolymer has a lower T_i than predicted by ideal mixing, ΔT_{SC} will be negative, whereas a positive value of ΔT_{SC} indicates a higher T_i than predicted by ideal mixing. The values of ΔT_{SC} for polymers **12-OMe *alt*CN**, **12-OMe*ran*CN** and **12-CN*alt*OMe** are 0.18, 0.09 and 0.04, respectively, and runs parallel to the trend observed for the degree of interdigitation. For comparison, for poly(styrene)s with nitroazobenzene and methoxyazobenzene mesogens the maximum value of ΔT_{SC} is 0.08,[19] whereas for poly(methacrylate)s with cyanobiphenyl and butylazobenzene mesogens a value of 0.14 has been found.[20]

The positive values of ΔT_{SC} for polymer **12-OMe *alt*CN**, **12-OMe*ran*CN** and **12-CN*alt*OMe** mean that the interactions between unlike mesogens are stronger than the interactions between like mesogens; i.e. specific favorable interactions exist between unlike mesogens. In addition, ΔT_{SC} increases with increasing degree of interdigitation. This can probably be ascribed to the increase in packing density of mesogens with increasing degree of interdigitation.[31]

Because of small variations in polymer composition and the influence of these variations on ΔT_{SC}, it was not possible to determine whether two different mesogens should be attached to the backbone in an alternating or a random sequence in order to obtain SCLCPs with a maximum ΔT_{SC}.

4.4. Conclusions

This study showed that SCLCPs with high mesogen densities can be obtained by reaction of mesogen-containing alcohols with maleic anhydride-containing SCLCPs in the presence of 4-dimethylaminopyridine as a catalyst. Grafting of methoxybiphenyl-containing

alcohols with different spacer lengths onto maleic anhydride-containing SCLCPs induces an increase in the degree of order in the mesophase and broadens the temperature window of the mesophase. The best ordered modified polymers were obtained from alcohols with a spacer length comparable to the spacer length in the parent polymer. In this case, an S_E mesophase is obtained. For slightly smaller or larger spacer lengths S_B mesophases are obtained and if the disparity in spacer length is high, the tendency to form an S_{Ad} mesophase increases. The isotropization temperature was hardly affected by the spacer length of the grafted mesogenic alcohol. However, for octyl and undecyl spacers the increase in free volume in their S_A mesophases resulted in strongly decreased glass transition temperatures.

In contrast, grafting azobenzene-containing alcohols onto methoxybiphenyl-containing polymer **6** yielded polymers that exhibit only nematic mesophases. This is ascribed to the absence of microphase separation between mesogen and polymer layers. Therefore, no lamellar structure is obtained. The effect of the terminal group on the temperature range of the mesophase is CN > OMe > F > H. The coupling of a cyanostilbene mesogen to polymer **6** resulted in a SCLCP with a smectic E mesophase with smectic A1 periodicity.

Combining methoxybiphenyl and cyanobiphenyl mesogens in both unmodified and modified polymers resulted in smectic A mesophases with higher isotropization temperatures than can be expected on the basis of the weighted average of the isotropization temperatures of both polymers with only one type of mesogen. This can be attributed to specific favorable interactions between electron-rich methoxybiphenyl mesogens and electron-poor cyanobiphenyl mesogens.

Summarizing, increasing the mesogen density by grafting mesogen-containing alcohols with spacers and mesogens differing from those of the parent SCLCP is a powerful tool to tune the transition temperatures and to alter the mesophase types.

4.5. References

1   Nieuwhof, R. P.; Marcelis, A. T. M.; Sudhölter, E. J. R.; Picken, S. J.; de Jeu, W. H. *Macromolecules* **1999**, *32*, 1398 (Chapter 3).
2   Nieuwhof, R. P.; Marcelis, A. T. M.; Sudhölter, E. J. R.; van der Wielen, M. W. J.; Cohen Stuart, M. A.; Fleer, G. J. *Macromol. Symp.* **1998**, *127*, 115.
3   Nieuwkerk, A. C.; van Kan, E. J. M.; Koudijs, A.; Sudhölter, E. J. R. *Langmuir* **1998**, *14*, 5702.
4   Diele, S.; Hisgen, B.; Reck, B.; Ringsdorf, H. *Makromol. Chem., Rapid Commun.* **1986**, *7*, 267.
5   Diele, S.; Oelsner, S.; Kuschel, F.; Hisgen, B.; Reck, B.; Ringsdorf, H. *Makromol. Chem.* **1987**, *188*, 1993.
6   Sugiyama, K.; Shiraishi, K. *Bull. Chem. Soc. Jpn.* **1991**, *64*, 1715.
7   Ungerank, M.; Winkler, B.; Eder, E.; Stelzer, F. *Macromol. Chem. Phys.* **1995**, *196*, 3623.
8   Winkler, B.; Ungerank, M.; Stelzer, F. *Macromol. Chem. Phys.* **1996**, *197*, 2343.
9   Percec, V.; Lee, M. *Polymer* **1991**, *32*, 2862.
10 Percec, V.; Lee, M. *Polym. Bull.* **1991**, *25*, 131.

11 Percec, V.; Lee, M. *Macromolecules* **1991**, *24*, 4963.

12 Imrie, C. T.; Karasz, F. E.; Attard, G. S. *Macromolecules* **1992**, *25*, 1278.

13 Imrie, C. T.; Karasz, F. E.; Attard, G. S. *Macromolecules* **1994**, *27*, 1578.

14 Portugall, M.; Ringsdorf, H.; Zentel, R. *Makromol. Chem.* **1982**, *183*, 2311.

15 Schleeh, T.; Imrie, C. T.; Rice, D. M.; Karasz, F. E.; Attard, G. S. *J. Pol. Sci.:Part A: Polym. Chem.* **1993**, *31*, 1859.

16 Kosaka, Y.; Kato, T.; Uryu, T. *Macromolecules* **1994**, *27*, 2658.

17 Imrie, C. T.; Paterson, B. J. A. *Macromolecules* **1994**, *27*, 6673.

18 Kosaka, Y.; Uryu, T. *Macromolecules* **1995**, *28*, 870.

19 Imrie, C. T.; Attard, G. S.; Karasz, F. E. *Macromolecules* **1996**, *29*, 1031.

20 Craig, A. A.; Imrie, C. T. *Polymer* **1997**, *38*, 4951.

21 Ogawa, K.; Mihara, T.; Koide, N. *Polym. J.* **1997**, *29*, 142.

22 Blatch, A. E.; Fletcher, I. D.; Luckhurst, G. R. *Liq. Cryst.* **1995**, *18*, 801.

23 Vogel, A. I. *Textbook of Practical Organic Chemistry* 5th ed; Longman Scientific & Technical: Essex, 1989, p. 949.

24 Rodriguez-Parada, J. M.; Percec, V. *J. Polym. Sci., Part A: Polym. Chem.* **1986**, *24*, 1363.

25 Komiya, Z.; Pugh, C.; Schrock, R. R. *Macromolecules* **1992**, *25*, 3609.

26 Tacx, J. C. J. F.; Meijerink, N. L. J.; Suen, K. *Polymer* **1996**, *37*, 4307.

27 Hu, G. H.; Lindt, J. T. *J. Pol. Sci.: Part A: Pol. Chem.* **1993**, *31*, 691.

28 Gray, G. W. *The Molecular Physics of Liquid Crystals*; Luckhurst, G. R.; Gray, G. W., Eds.; Academic Press: New York, 1979.

29 Imrie, C. T.; Schleeh, T.; Karasz, F. E.; Attard, G. S. *Macromolecules* **1993**, *26*, 539.

30 Mirceva, A.; Oman, N.; Zigon, M. *Polym. Bull.* **1998**, *40*, 469.

31 Craig, A. A.; Imrie, C. T. *Macromolecules* **1995**, *28*, 3617.

5

Highly ordered side-chain liquid-crystalline polymers from maleic anhydride and swallow-tailed 1-alkenes having two mesogens

Side-chain liquid-crystalline polymers (SCLCPs) were synthesized from the alternating copolymerization of maleic anhydride with swallow-tailed 1-alkenes having two mesogens. In contrast to similar polymers from 1-alkenes with one mesogen per repeating unit, these novel polymers exhibited lower isotropization temperatures and higher glass transition temperatures. The degree of order in the mesophase strongly increased: these SCLCPs exhibited a highly ordered smectic H phase. The polymers with a hexyl spacer between the malonate junction and the mesogen exhibited a uniaxially limited-correlation-length smectic E mesophase (S_{E_u}) which has, according to our knowledge, not been observed before. The highest transition temperatures and entropy changes were observed for polymers with completely interdigitated side chains.

5.1. Introduction

In a previous study the synthesis and phase behavior of side-chain liquid-crystalline polymers (SCLCPs) from maleic anhydride (MA) and 1-alkenes (Scheme 5.1) have been reported.[1,2] These polymers contain methoxybiphenyl mesogens and exhibit smectic mesophases over a temperature range up to 66°C. SCLCPs with hexyl or longer spacers exhibit a hexatic smectic B and an interdigitated smectic A mesophase. These polymers, however, only contain one mesogen per four carbon atoms in the polymer backbone, whereas common SCLCPs like poly(siloxane)s, poly(methacrylate)s, and poly(vinyl ether)s contain one mesogen per two atoms in the polymer backbone. Therefore, it is interesting to study the effect of doubling the mesogen density on the mesomorphic behavior of poly(MA-*alt*-1-alkenes).
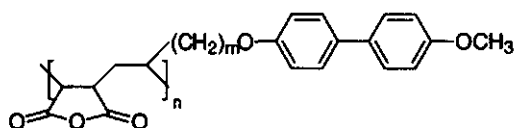
Scheme 5.1. *General structure of poly(MA-alt-1-alkene)s.*

From literature several approaches are known that can be applied in order to increase the mesogen density.[3,4,5,6,7,8] One approach is the coupling of swallow-tailed 1-alkenes with two mesogens to poly(siloxane)s by hydrosilylation.[3,4] These studies have shown that the width of the mesophase is retained down to low mesogen contents. In contrast, for polymers with only one mesogen per repeating unit mesophase formation is hampered by dilution of mesogens with non-mesogenic units. In other approaches monomers with two mesogens, e.g. itaconates,[5] norbornenes[6,7] and fumarates,[8] have been homopolymerized. The general trend was that both the temperature window of the mesophase and the degree of order in the mesophase increased in comparison to polymers from monomers with one mesogen.

In the present chapter the effect of doubling the mesogen density with respect to polymers depicted in Scheme 5.1 is described. The SCLC poly(MA-*alt*-1-alkene)s with doubled mesogen density are obtained by the alternating copolymerization[1,9,10] of MA with swallow-tailed 1-alkenes bearing two mesogens. Previous studies have already shown that SCLCPs with MA moieties exhibit very interesting physical behavior.[2,11,12] Spincoated films of these polymers on silicon oxide show lamellar ordering upon annealing above the glass transition temperature (T_g).[2,11] In addition, these polymers adhere well on silicon oxide surfaces and exhibit autophobicity.[12]

The mesophases of the SCLC poly(MA-*alt*-1-alkenes) with doubled mesogen density are identified by wide-angle X-ray diffraction combined with polarizing optical microscopy. The influence of the molecular architecture of these polymers on the transition temperatures and the mesophase types has been studied. The SCLCPs are characterized by gel permeation chromatography, ^{1}H NMR, polarizing optical microscopy, differential scanning calorimetry and wide-angle X-ray diffraction.

5.2. Experimental Part

5.2.1. Materials

The tetrahydrofuran (THF) that was used for the polymerization reactions was purified by distillation over sodium under a nitrogen atmosphere. Other reagents used for syntheses were commercially available and used without further purification. 4-Hydroxy-4'-methoxybiphenyl[13] (**1**), 4-methoxy-4'-(ω-hydroxyalk-1-oxy)biphenyl[14] (**2-** *p*), dimethyl alkenemalonate[15] (**3-***m*) and alkenemalonic acid[15] (**4-** *m*) were synthesized according to literature procedures (Scheme 5.2). Copolymerization of **5-***m,p* with MA was performed by a method described previously.[1]

5.2.2. Equipment

Gel permeation chromatography (GPC) measurements were carried out using a series of four microstyragel columns with pore sizes of 10^5, 10^4, 10^3 and 10^6 Å (Waters), respectively with THF containing 5 wt% acetic acid as eluent.[16] A dual detection system consisting of a differential refractometer (Waters model 410) and a differential viscometer (Viscotek model H502) was used. A calibration line was made with this setup, using narrow polystyrene reference standards in THF, and the molar mass (g/mol) of the synthesized polymers was determined referring to this calibration line. Thermal transitions were monitored with a Perkin-Elmer DSC-7. Scan rates of 10 K/min. were used in the differential scanning calorimetry (DSC) experiments with sample masses of 5 - 10 mg. Transition temperatures were taken from the second heating cycle. Polarizing optical microscopy (POM) was performed on an Olympus BH-2 microscope equipped with a Mettler FP82HT hot stage and an FP80HT temperature controller. X-ray diffraction measurements were performed on a Siemens D5000 reflection diffractometer with a HTK oven and Cu Kα radiation. ^{1}H NMR spectra were recorded on a Bruker AC200 spectrometer at 200 MHz. FTIR spectra were recorded on a BioRad FTS-7 spectrometer.

5.2.3. Synthesis

Monomers **5-*m,p***. All compounds were synthesized according to the same procedure, an example is given for monomer **5-2,6**:

4-2 (1.51 g, 9.6 mmol) was dissolved in thionyl chloride (15 mL) and refluxed under a nitrogen atmosphere for 2 hours. Benzene (15 mL) was added and the mixture was concentrated by evaporation in order to remove the remaining thionyl chloride. The product was dissolved in chloroform (10 mL) and a solution of **2-6** (6.31 g, 21.0 mmol) in chloroform (40 mL) and pyridine (4.3 g, 54.4 mmol) was added at 0°C during 30 minutes followed by stirring at room temperature for 48 hours. Dichloromethane was added and the reaction mixture was washed with 1 M HCl and water. After drying with magnesium sulfate, the solution was evaporated to dryness. The crude product was purified by silica gel chromatography with a mixture of 2 vol% petroleum ether (40/60) in dichloromethane as eluent followed by 2 vol% methanol in dichloromethane. After recrystallization from hexane white crystals were obtained (2.35 g, 3.26 mmol, 34 %). Melting point (T_m) = 109 °C.

^{1}H NMR (CDCl$_3$): δ = 7.43 (2 biphenyl, 8H); 6.92 (2 biphenyl, 8H); 5.82 (m, =CH-, 1H); 4.98 (dd, CH$_2$=, 2H); 4.12 (t, 2 -COOCH$_2$-, 4H); 3.94 (t, 2 -CH$_2$OAr, 4H); 3.81 (s, 2 -OCH$_3$, 6H); 3.35 (t, -CH-, 1H); 2.05 (q, =CH-C$\underline{H}_2$, 2H); 1.89-1.61 (m, 2 -C$\underline{H}_2$CH$_2$OAr + 2 –COOCH$_2$C$\underline{H}_2$- + -C$\underline{H}_2$CH- , 10H); 1.60 - 1.36 (m, 4 -CH$_2$-, 8H)

Yields and melting points of homologous compounds **5-*m,p***:

5-3,3: Yield = 37%, T_m = 111 °C
5-3,6: Yield = 30%, T_m = 107 °C
**5-4,6**: Yield = 40%, T_m = 110 °C

5.3. Results and discussion

5.3.1. Synthesis

The synthesis of polymers **6-*m,p*** is depicted in Scheme 5.2. Polymers **6-*m,p*** were obtained by a radical-initiated (AIBN) copolymerization of **5-*m,p*** and MA in THF. In a previous study[1] it has been shown that copolymerization of mesogenic 1-alkenes and MA results in alternating copolymers. All compounds were obtained in satisfactory yields and high purity. The observed ^{1}H NMR signals agreed well with the expected chemical structure and the disappearance of vinyl signals and broadening of the other signals in the ^{1}H NMR spectra indicated the formation of polymer. After precipitation, polymer yields varied between 59 and 70 % (Table 5.1).

The molecular weights of the polymers were determined by GPC and are listed in Table 5.1. The molecular weights of these polymers are low if the amount of initiator applied is considered, which can be attributed to chain transfer reactions. Although the molecular weights are in the regime where the transition temperatures depend on molecular weight, the transition temperatures can be compared meaningfully because polymers **6-*m,p*** have similar degrees of polymerization and polydispersity indices.
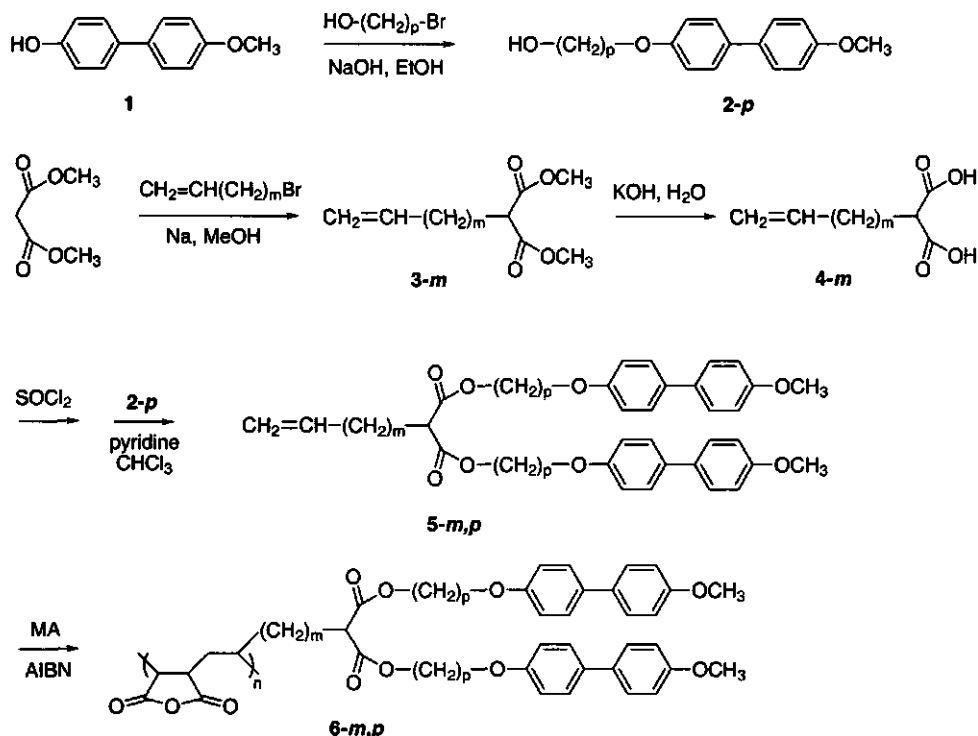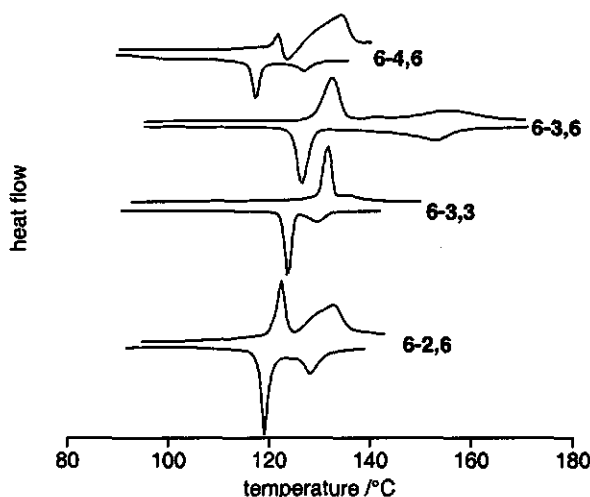

Scheme 5.2. Synthesis of polymers 6-m,p.

Table 5.1. *Number-average molecular weights (M_n), weight-average molecular weights (M_w), polydispersity indices (PDI), degrees of polymerization (DP) as determined by GPC and yields (%) of polymers 6-m,p.*

polymer	10^{-3} M_n	10^{-3} M_w	PDI	DP	yield
6-2,6	3.90	6.17	1.58	10	60
6-3,6	4.46	7.41	1.66	11	64
6-4,6	3.18	4.87	1.53	8	59
6-3,3	3.78	6.43	1.70	10	70

Figure 5.1. *DSC thermograms of polymers 6-m,p.*

5.3.2. Mesomorphic behavior

Polymers **6-m,p** all exhibit mesomorphic behavior. DSC showed that all compounds exhibit two first order transitions, except polymer **6-3,6** that shows three transitions (Figure 5.1). For all compounds T_g could also be observed, except for polymer **6-3,6**. The observed transition temperatures and corresponding entropy changes are given in Table 5.2. The mesophases were identified with X-ray diffraction and POM. The identification of the mesophases of polymer **6-3,6** will be given in detail.

On cooling from the isotropic melt, POM revealed the development of a homeotropic sample with "oily streaks" for polymer **6-3,6**, as is depicted in Figure 5.2a. These "oily-streaks" and homeotropic ordering correspond to a mesophase with an S_A structure. Additional cooling resulted in Schlieren-textures (Figure 5.2b), which may indicate that a mesophase with tilted mesogens has developed. The transition temperatures observed with POM agree well with those observed with DSC.

Table 5.2. *Phase transition temperatures (°C) and corresponding heat capacity or entropy changes (J/mol K) in parentheses as determined by DSC, and phase types[a] of polymers 6-m,p.*

polymer	phase behavior							
6-2,6	$G_{H2,inc}$	114 (80)	$S_{H2,inc}$	122 (14.5)	S_{E2,inc_u}	133 (22.0)		I
	I	128 (7.8)	$S_{A2,inc}$	-	S_{E2,inc_u}	119 (20.4)	$S_{H2,inc}$ -	$G_{H2,inc}$
6-3,6	G_{HI}	-	S_{HI}	132 (26.5)	S_{E1_u}	141 (0.5)	S_{A1} 156 (15.2)	I
6-4,6	G_{Hd}	115 (338)	S_{Hd}	119 (-)	S_{Ed_u}	133 (43.4)		I
	I	125 (4.8)	S_{Ad}	-	S_{Ed_u}	117 (14.8)	S_{Hd} -	G_{Hd}
6-3,3	G_{HI}	104 (65)	S_{HI}	131 (25.9)			S_{A1} 136 (1.3)	I

[a] *I = isotropic phase; S_{A1} = smectic A with fully interdigitated side chains; S_{E1_u} = uniaxially-limited-correlation-length smectic E (S_{E_u}) with S_{A1} periodicity; S_{Ed_u} = S_{E_u} with partially interdigitated side chains (S_{Ad}) ; S_{E2,inc_u} = S_{E_u} with partially interdigitated side chains in coexistance with non-interdigitated side chains ($S_{A2,inc}$ periodicity); S_H = smectic H, G_H = mesoglass H.*
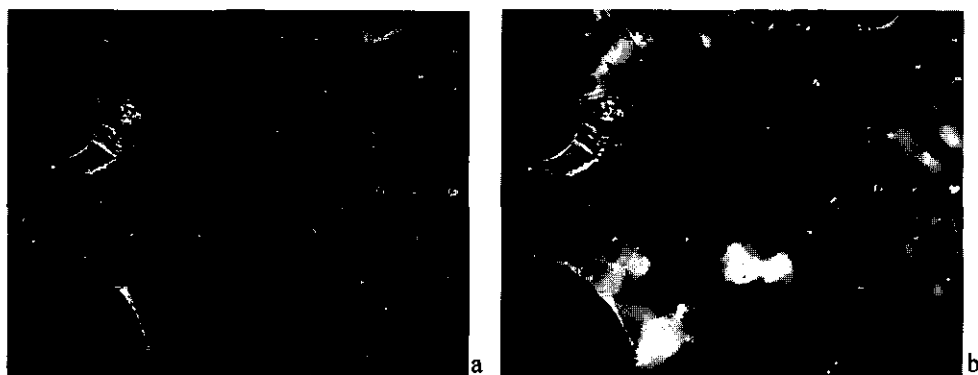
Figure 5.2. *Polarizing optical micrographs of polymer 6-3,6: a. S_{E_u} mesophase, and b. S_H phase.*

The DSC thermograms in Figure 5.1 show that this polymer exhibits two strong endothermic transitions upon heating. These two transitions were observed with POM by a change in texture. In addition, a small enthalpic effect was observed with DSC at 141°C that was not discernible upon cooling, probably because this transition is very broad. The absence of a distinct glass transition is probably due to the presence of a highly ordered mesophase.

Figure 5.3 shows the temperature dependent X-ray diffraction pattern of polymer 6-3,6 that was used to obtain more detailed information about the mesophase types. Three different temperature regions can be distinguished in this figure. Firstly, between 140°C and the isotropization temperature (T_i), the first and second-order reflections of smectic layers are observed at 2θ is 2.75° and 5.45°, respectively. These reflections correspond to a *d* spacing of 31.1 Å (Table 5.3), indicating that this polymer exhibits an S_{A1} mesophase in which the *d* spacing equals the length of a side chain.
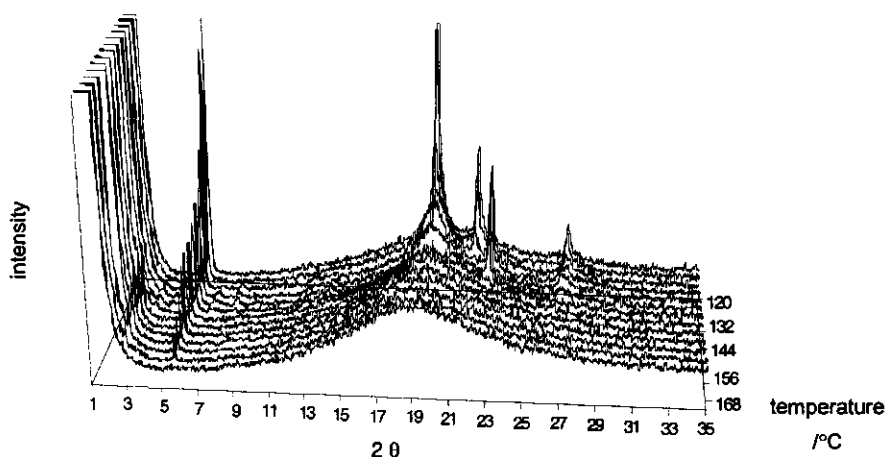
Figure 5.3. Temperature dependent wide-angle X-ray diffraction patterns of polymer 6-3,6.
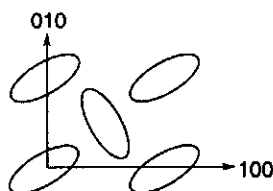

Figure 5.4. Schematic representation of mesogens in an orthorhombic cell.

Secondly, the first-order reflection corresponding to a d spacing of 31.1 Å disappears below 140°C, whereas the second-order reflection remains visible (Figure 5.3). This indicates that there is an additional plane of symmetry in the electron density profile, which results from microphase separation between the polymer backbone and the mesogen layer. The additional maximum in the electron density profile induces an apparent d spacing (strongest small-angle reflection) which is half the smectic d spacing. Furthermore, (110), (200) and (210) reflections appear in the wide-angle area indicating the presence of hexagonal asymmetry. The mesogens within a smectic layer are ordered orthorhombically (Figure 5.4), i.e. polymer 6-3,6 exhibits an S_E mesophase. Figure 5.5 shows the X-ray diffraction pattern at 134°C in which the (110) and (210) reflections are broad, whereas the (200) reflection is very sharp. This indicates that the S_E mesophase has a low correlation length in the (010) direction, which has according to our knowledge not been observed before. We propose to denote such a partially disordered S_E phase as S_{E_u}.

Thirdly, the (200) reflection shifts to a smaller angle and the (110) and (210) reflections sharpen upon cooling below 130°C (Figure 5.5). The shift of the (200) reflection to a smaller angle during cooling from the S_{E_u} to the low-temperature mesophase (Figure 5.5) indicates that the mesogens rearrange in the (100) direction. This rearrangement corresponds

77
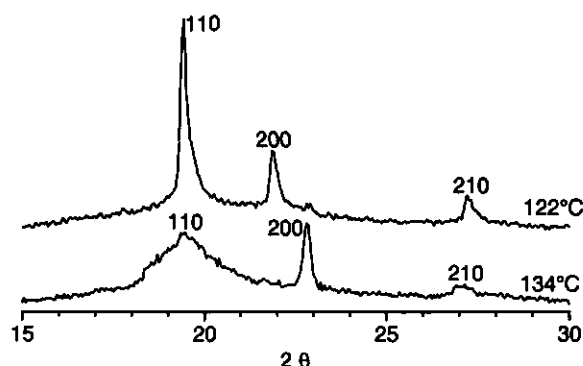
Figure 5.5. X-ray diffraction patterns of polymer **6-3,6** at 122 °C (S_H) and 134 °C (S_E_a).

Table 5.3. Experimental d spacings (Å) obtained from wide-angle X-ray diffraction experiments at 110 °C and calculated d spacings of polymers **6-m,p**.

polymer	d spacings	calcd d spacing S_{A1}
6-2,6	34.6; 22.1; 17.0; 14,7; 11.1; 4.56; 4.04; 3.20	29.6
6-3,6	31.1; 15.5; 4.56; 4.07; 3.31	30.6
6-4,6	17.7; 11.5; 4.56; 4.04; 3.20	32.1
6-3,3	28.0; 14.1; 4.56; 4.05; 3.26	28.5

probably to tilting of mesogens, which also explains the Schlieren textures observed with POM. This kind of mesophase, in which the mesogens are monoclinically ordered, is known as an S_H mesophase.[17] Like a common S_E mesophase, this mesophase has long-range positional and orientational order.

The other polymers were also investigated by POM, DSC and X-ray diffraction. The observed d spacings of the mesophases in the glassy state are given in Table 5.3. Comparison with the calculated d spacings leads to the assignments of the mesophases as given in Table 5.2.

The mesomorphic behavior of polymer **6-3,3** was comparable to that of polymer **6-3,6**, with the exception that no S_{E_a} was observed (Table 5.2). In contrast, polymers **6-2,6** and **6-4,6** do exhibit an S_{E_a} mesophase, however, for these polymers the S_{E_a} mesophase was not succeeded by an S_A mesophase but transformed into the isotropic melt upon heating. The mesophases of these polymers also have a different smectic periodicities (Table 5.2).

The DSC thermograms of polymers **6-2,6** and **6-4,6** (Figure 5.1) show anomalous behavior: the transition enthalpies during cooling and heating are different. However, for polymer **6-2,6** the overall change in enthalpy from the isotropic state to the glass are the same during both cooling and heating. The small exothermic effect at T_i observed upon cooling probably indicates the formation of a monotropic $S_{A2,inc}$ mesophase, because an I-S_E transition would result in a higher entropy change. The enthalpy change of the second transition upon cooling is larger than was observed upon heating. Furthermore, the

thermogram does not reach to the same level of heat flow as in the melt or in the mesoglass, which may indicate a broad transition. Because of these two features we propose that the I-$S_{A2,inc}$ transition is succeeded by a broad $S_{A2,inc}$-S_{E2,inc_u} transition, that partially overlaps with the S_{E2,inc_u}-$S_{H2,inc}$ transition.

For polymer **6-4,6** the glass transition is succeeded upon heating by an endothermic transition, an exothermic transition, and the isotropization transition. From the presence of (110), (200), and (210) reflections during heating it can be concluded that this polymer does not exhibit an enantiotropic S_{Ad} mesophase. On cooling, the mesomorphic behavior is comparable to that of polymer **6-2,6** (Table 5.2): the polymer exhibits a monotropic S_{Ad} mesophase.

5.3.3. Structure-property relations

Figures 5.6a and 5.6b display the phase transition temperatures and the corresponding
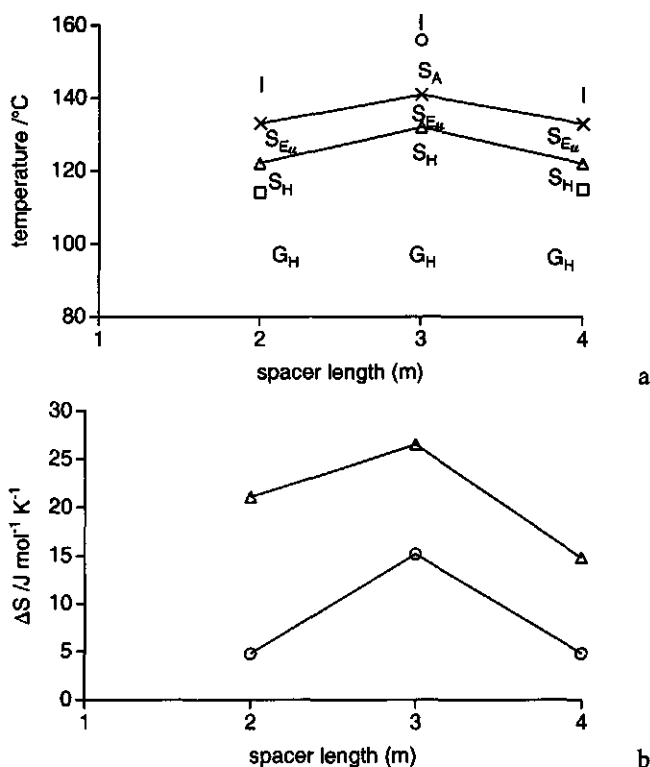
Figure 5.6. Dependence of the transition temperatures on spacer length m for polymers 6-m,6 (as found with DSC): (□) glass transition; (Δ) S_H-S_{E_u} transition; (x) S_{E_u}-S_{A1}/I transition; (o) S_{A1}-I transition; b. Dependence of the entropy change (ΔS) on spacer length m for polymers 6-m,6 (as found with DSC upon cooling): (Δ) S_H-S_{E_u} transition; (o) isotropization transition.

79

entropy changes of polymers **6-*m*,6**, respectively. The transition temperatures and entropy changes of polymer **6-3,6** are higher than those of polymers **6-2,6** and **6-4,6**. Polymers **6-2,6** and **6-4,6** exhibit a mesophase with partially interdigitated side-chains (S_{Ad} structure, Table 5.2), whereas polymer **6-3,6** exhibits a mesophase with fully interdigitated side-chains (S_{A1} structure, Table 5.2). The degree of interdigitation of side chains influences the values of the transition temperatures and entropy changes, as has been shown in a previous study:[18] polymers exhibiting S_{A1} mesophases have higher transition temperatures and entropy changes than comparable polymers exhibiting S_{Ad} mesophases. This can be ascribed to the higher amount of free volume in the S_{Ad} mesophase than in the S_{A1} mesophase. Polymer **6-3,3** also exhibits mesophases with fully interdigitated side-chains, but the lower degree of decoupling between the motions of the mesogens and those of the polymer backbone (due to the shorter spacer) yields lower transition temperatures and entropy changes than observed for polymer **6-3,6** (Table 5.2).

An enantiotropic S_A mesophase is observed only for polymers **6-3,3** and **6-3,6**, in which the side chains interdigitate completely. Polymers **6-2,6** and **6-4,6** only exhibit monotropic S_A mesophases.

An interesting feature of all polymers **6-*m*,6** is the presence of an S_E mesophase with a limited correlation length in the (010) direction (S_{E_a}). The cell parameters a and b of the orthorhombic cell in the S_{E_a} mesophase of polymers **6-*m*,6** are 7.81 Å and 5.66 Å, respectively, resulting in a cross-section of 44.2 Å^2. The product of the a and b parameter of a modified poly(MA-*alt*-1-alkene)s (Scheme 5.3) that have comparable mesogen densities is slightly smaller, i.e. 42.9 Å^2.[19] This reflects the lower packing density of mesogens for polymers **6-*m*,p** in the uniaxially liquid-like S_{E_a} mesophase.

Table 5.4 shows the mesomorphic properties of unmodified SCLC poly(MA-*alt*-1-alkenes) (Scheme 5.1) with an octyl or a nonyl spacer and methoxybiphenyl mesogens.[1] The polymer backbone of these polymers is comparable to that of polymers **6-*m*,p**. The main difference between these different types of polymers is the mesogen density: the SCLC poly(MA-*alt*-1-alkenes) contain one mesogen per four atoms in the backbone, whereas polymers **6-*m*,p** contain one mesogen per two atoms in the backbone. The glass transition temperatures (T_g) of SCLC poly(MA-*alt*-1-alkenes) from Scheme 5.1 are slightly lower than those of polymers **6-*m*,p**. This can be attributed to the higher mesogen density of polymers **6-*m*,p** that decreases the amount of free volume. The higher mesogen density, however, does not result in a higher T_i. This probably results from the low degree of polymerization of
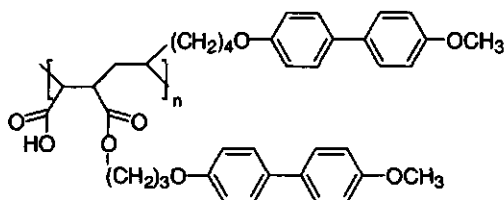
Scheme 5.3. *Molecular structure of modified poly(MA-alt-1-alkene)s.*

polymers **6-m,p**, which is a factor two lower than for the SCLC poly(MA-*alt*-1-alkenes) in Scheme 5.1. Previous studies have shown that especially for low molecular weights the transition temperatures increase drastically with molecular weight.[20,21,22] As a result of the decrease in T_i and the increase of T_g for polymers **6-m,p** the temperature range of the mesophase decreases.

Table 5.4. *Phase transition temperatures (°C) and corresponding heat capacity or entropy changes (J/mol K) in parentheses as determined by DSC, and phase types[a] of SCLC poly(MA-alt-1-alkenes) (Scheme 5.1).*[1,2]

m	phase behavior
8	G_{Bhex} 103 (61) S_{Bhex} 117 (5.7) S_{Ad} 156 (13) I
9	G_{Bhex} 101 (104) S_{Bhex} 111 (3.3) S_{Ad} 165 (16) I

[a] *I = isotropic phase; S_{Ad} = smectic A with partially interdigitated side chains; S_{Bhex} = hexatic smectic B; G_{Bhex} = mesoglass B_{hex}.*

Doubling the mesogen density results in a higher degree of order in the mesophase: polymers **6-m,p** exhibit S_H, S_E and S_A mesophases, whereas SCLC poly(MA-*alt*-1-alkenes) exhibit hexatic smectic B (S_{Bhex}) and S_A mesophases.[1,2] The tilting of mesogens that results in an S_H mesophase can probably be attributed to the combination of a malonate junction with a rigid backbone. In contrast, modified SCLC poly(MA-*alt*-1-alkenes) with similar mesogen densities (Scheme 5.3) do not exhibit mesophases with tilted mesogens but exhibit S_A and crystalline phases.[19] Furthermore, flexible SCLC poly(siloxane)s[3,4] containing similar swallow-tailed side chains also do not exhibit mesophases with tilted mesogens.

The trend observed for the degree of order in the mesophase of polymers **6-m,p** is comparable to that of SCLCPs as depicted in Scheme 5.3, which were obtained by grafting mesogen-containing alcohols onto poly(MA-*alt*-1-alkene)s from Scheme 5.1.[19] Both types of polymers have the same mesogen density and for both polymers the increase in mesogen density with respect to that of the polymers from Scheme 5.1 results in highly ordered mesophases. The polymers depicted in Scheme 5.3 exhibit a highly ordered smectic E mesophase.

Polymers **6-m,p** differ from other polymers with increased mesogen density described in literature[3-8] because they do not contain 1 mesogen per atom in the polymer backbone but one mesogen per two atoms in the polymer backbone. Therefore, the properties of these polymers cannot be compared meaningfully. However, the properties of polymers **6-m,p** can be compared to those of poly(fumarates)s,[8] poly(itaconate)s[5] and poly(siloxane)s[3,4] in which the mesogen density has been lowered by copolymerization with styrene, dioctyl itaconate and dimethyl siloxane, respectively. These copolymers, that have mesogen densities comparable to those of polymers **6-m,p**, displayed nematic mesophases or smectic mesophases which have a substantially lower degree of order than polymers **6-m,p**. Polymers with a backbone comparable to that of polymers **6-m,p** have been obtained from the alternating copolymerization of mesogenic vinyl ethers and mesogenic fumarates.[23] The

resulting copolymers also exhibit smectic and nematic mesophases with a lower degree of order than polymers **6-*m,p***. This emphasizes that copolymerization of swallow-tailed 1-alkenes bearing two mesogens with MA is a successful method to obtain highly ordered SCLCPs.

5.4. Conclusions

The alternating copolymerization of maleic anhydride with swallow-tailed 1-alkenes having two mesogens yielded low-molecular-weight polymers that exhibit liquid-crystalline behavior. At low temperatures the polymers exhibit a smectic H mesophase, in which the mesogens are tilted, that transforms for polymers **6-*m*,6** into a smectic E mesophase with a limited correlation length in one direction ($S_{E_{u}}$). In these mesophases, the polymer backbones are phase separated from the mesogen layers. In comparison to SCLC poly(MA-*alt*-1-alkene)s with half the mesogen density, the present polymers exhibit a higher glass transition temperature and a lower isotropization temperature. The degree of order in the mesophase, is however significantly higher.

Molecular architecture strongly influences the type of mesophases exhibited by the present polymers. Polymers **6-3,3** and **6-3,6** exhibit mesophases with complete interdigitation of side chains, whereas polymers **6-2,6** and **6-4,6** exhibit mesophases in which the side chains interdigitate partially. An enantiotropic smectic A mesophase is only observed for polymers **6-3,3** and **6-3,6**, in which the side chains interdigitate completely. The S_A mesophases of polymers **6-2,6** and **6-4,6** are monotropic. In the series of polymers **6-*m*,6**, the polymer with the smectic A_1 structure showed the highest transition temperatures and entropy changes.

Concluding, the approach of copolymerizing MA with swallow-tailed 1-alkenes bearing two mesogens is a powerful tool to obtain highly ordered SCLCPs.

5.5. References

1   Nieuwhof, R. P.; Marcelis, A. T. M.; Sudhölter, E. J. R.; Picken, S. J.; de Jeu, W. H. *Macromolecules* **1999**, *32*, 1398 (Chapter 3).
2   Nieuwhof, R. P.; Marcelis, A. T. M.; Sudhölter, E. J. R.; van der Wielen, M. W. J.; Cohen Stuart, M. A.; Fleer, G. J. *Macromol. Symp.* **1998**, *127*, 115.
3   Diele, S.; Oelsner, S.; Kuschel, F.; Hisgen, B.; Ringsdorf, H.; Zentel, R. *Makromol. Chem.* **1987**, *188*, 1993.
4   Diele, S.; Hisgen, B.; Reck, B.; Ringsdorf, H. *Makromol. Chem., Rapid. Commun.* **1986**, *7*, 267.
5   Sugiyama, K.; Shiraishi, K. *Bull. Chem. Soc. Jpn.* **1991**, *64*, 1715.
6   Ungerank, M.; Winkler, B.; Eder, E.; Stelzer, F. *Macromol. Chem. Phys.* **1995**, *196*, 3623.
7   Winkler, B.; Ungerank, M.; Stelzer, F. *Macromol. Chem. Phys.* **1996**, *197*, 2343.
8   Jähnichen, K.; Voigt, D.; Jehnichen, D.; Rätzsch, M. *Macromol. Chem. Phys.* **1995**, *196*, 3323.
9   Komber, H. *Macromol. Chem. Phys.* **1995**, *196*, 669.

10   Trivedi, B. C.; Culbertson, B. M. *Maleic Anhydride*; Trivedi, B. C., Ed.; Plenum: New York, 1982.

11   van der Wielen, M. W. J.; Cohen Stuart, M. A.; Fleer, G. J.; de Boer, D. K. G.; Leenaers, A. J. G.; Nieuwhof, R. P.; Marcelis, A. T. M.; Sudhölter, E. J. R. *Langmuir* **1997**, *13*, 4762.

12   van der Wielen, M. W. J.; Cohen Stuart, M. A.; Fleer, G. J. *Langmuir* **1998**, *14*, 7065.

13   Rodriguez-Parada, J. M.; Percec, V. *J. Polym. Sci., Part A: Polym. Chem.* **1986**, *24*, 1363.

14   Komiya, Z.; Pugh, C. Schrock, R. R. *Macromolecules* **1992**, *25*, 3609.

15   Vogel, A. I. *Textbook of Practical Organic Chemistry* 5th ed.: Longman Scientific & Technical: Essex, U.K., 1989

16   Tacx, J. C. J. F.; Meijerink, N. L. J.; Suen, K. *Polymer* **1996**, *37*, 4307.

17   Demus, D. *Liquid Crystals*; Stegemeyer, H., Ed.; Steinkopff Verlag, Darmstadt, Germany, 1994.

18   Craig, A. A.; Imrie, C. T. *Macromolecules* **1995**, *28*, 3617.

19   Nieuwhof, R. P.; Marcelis, A. T. M.; Sudhölter, E. J. R. *Macromolecules* in press (Chapter 4).

20   Percec, V.; Pugh, C. *Side Chain Liquid Crystal Polymers*; McArdle, C. B., Ed.; Blackie: Glasgow, UK, 1989.

21   Simmonds, D. J. *Liquid Crystal Polymers, From Structures to Applications*; Collyer, A. A., Ed.; Elsevier Applied Science: London and New York, 1992.

22   Pugh, C.; Kiste, A. L., *Prog. Polym. Sci.* **1997**, *22*, 601.

23   Laus, M.; Bignozzi, M. C.; Angeloni, A. S.; Galli, G.; Chiellini, E. *Macromolecules* **1993**, *26*, 3999.

6

Thermotropic behavior of side-chain liquid-crystal-line copolymers from maleic anhydride and mesogen-containing methacrylates

Side-chain liquid-crystalline copolymers (SCLCPs) were synthesized by copolymerization of maleic anhydride (MA) and mesogenic methacrylates. For copolymers with a hexyl spacer and methoxybiphenyl mesogens, smectic A1 and smectic E1 mesophases were observed. Furthermore, it was found that the isotropization temperature increased and the width of the monotropic smectic A1 mesophase decreased with increasing MA content. For methoxybiphenyl-containing copolymers with about 25% MA, the glass transition temperature decreased with increasing spacer length, whereas the isotropization temperature shows little dependence on spacer length, although a small odd-even effect was observed. For octyl or shorter spacers, these polymers exhibited a smectic E mesophase, whereas for longer spacers these polymers exhibited smectic B mesophases. These mesophases were succeeded by a smectic A1 mesophase for SCLCPs with heptyl or longer spacers. SCLCPs with cyanoazobenzene mesogens exhibited only a smectic Ad mesophase, whereas SCLCPs with cyanobiphenyl mesogens were not liquid crystalline.

6.1. Introduction

Since the introduction of side-chain liquid-crystalline polymers (SCLCPs), much effort has been put in studying the effect of molecular architecture on the liquid-crystalline properties.[1,2,3,4] Structural variables that received a lot of attention are spacer length, type of mesogen and the nature of the mesogenic substituent. The properties of SCLCPs are also strongly influenced by the nature of the polymer backbone.[1,3,5,6] Much attention has been paid to SCLCPs with a poly(methacrylate) backbone.[6,7,8,9,10,11,12,13,14] For these SCLCPs, it has

been found that (i) backbone tacticity hardly affects the liquid-crystalline order,[7] (ii) the polymer backbone is not strictly confined between mesogen layers and shows layer hopping between smectic layers,[9,15] and (iii) SCLCPs with cyanobiphenyl mesogens exhibit lower transition temperatures than SCLCPs with methoxybiphenyl mesogens.[13,14] The low-temperature mesophases of these poly(methacrylate)s with methoxybiphenyl mesogens were characterized correctly only recently by using X-ray diffraction,[8] which shows the importance of this technique in characterizing highly ordered mesophases.

By copolymerization of two different monomers in varying ratios, copolymers with an almost limitless variety of properties can be obtained. In a previous study, it was shown that maleic anhydride (MA) copolymerizes with mesogenic 1-alkenes yielding SCLCPs with adhesive properties.[16,17] On polar substrates, thin films may be obtained from SCLCPs with MA moieties that form lamellar structures upon annealing[18] and show autophobicity.[19] The same strategy may be applied to obtain SCLC poly(methacrylate)s with adhesive properties. Contrary to the copolymerization of MA with 1-alkenes, which yields perfectly alternating copolymers,[16,20,21] copolymerization of MA with methacrylates is not strictly alternating due to the tendency of methacrylates to homopolymerize. MA does not homopolymerize under the applied conditions.[20,21] Therefore, the MA content of the MA-methacrylate copolymer can be influenced by changing the amount of MA in the monomer feed and, consequently, both backbone flexibility and mesogen density can be altered. The presence of polar MA moieties makes these SCLCPs also suitable for Langmuir and Langmuir-Blodgett films.[22]

In this chapter the effect of introducing MA moieties in a SCLC poly(methacrylate) by copolymerizing mesogenic methacrylates with MA is described. The synthesis and phase behavior of copolymers containing methoxybiphenyl mesogens will be described. The mesomorphic properties are compared to those of previously described poly(MA-*alt*-1-alkene)s[16,17] and those of poly(methacrylate)s containing similar mesogens.[8,13] The influence of spacer length and MA content on transition temperatures is studied. For comparison, compounds with cyanobiphenyl and cyanoazobenzene mesogens are also included in this study. The SCLCPs are characterized by gel permeation chromatography, ^{1}H NMR, and differential scanning calorimetry. The mesophases of these copolymers are identified with wide-angle X-ray diffraction and polarizing optical microscopy.
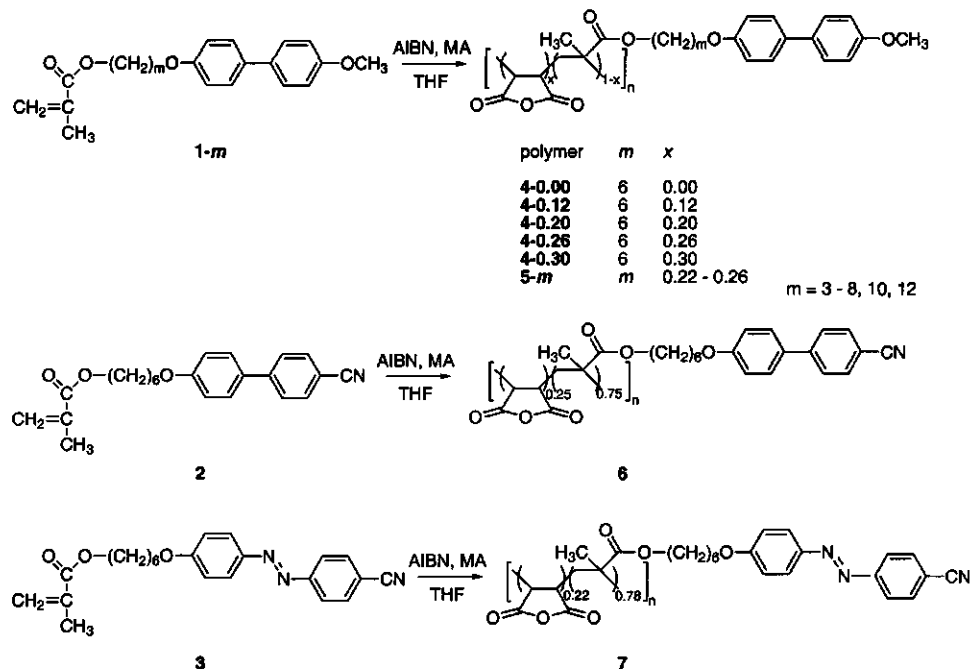
6.2. Experimental part

6.2.1. Materials

The tetrahydrofuran (THF) which was used for the polymerization reactions was purified by distillation over sodium under nitrogen atmosphere. MA was sublimated before use and azoisobutyronitrile (AIBN) was recrystallized twice from methanol. Other reagents used for syntheses were commercially available and used without further purification. Monomers **1-*m*, 2**, and **3**,[13,14] and polymers **4-*x*, 5-*m*, 6**, and **7**[16] were synthesized according to literature procedures. However, the polymerization time was reduced to 48 h.

6.2.2. Equipment

Gel permeation chromatography (GPC) measurements were carried out using a series of four microstyragel columns with pore sizes of 10^5, 10^4, 10^3, and 10^6 Å (Waters), respectively with THF containing 5 wt% acetic acid as eluent.[23] A dual detection system consisting of a differential refractometer (Waters model 410) and a differential viscometer (Viscotek model H502) was used. A calibration line was made with this setup, using narrow polystyrene reference standards in THF, and the molar mass (g/mol) of the synthesized polymers was determined referring to this calibration line. Thermal transitions were monitored with a Perkin-Elmer DSC-7. Scan rates of 10 K/min were used in the differential scanning calorimetry (DSC) experiments with sample masses of 5-15 mg. Transition temperatures were taken from the second heating cycle. Polarizing optical microscopy (POM) was performed on an Olympus BH-2 microscope equipped with a Mettler FP82HT hot stage and an FP80HT temperature controller. X-ray diffraction measurements were performed on a Siemens D5000 reflection diffractometer with a HTK oven and Cu Kα radiation. ^{1}H NMR spectra were recorded on a Bruker AC200 spectrometer at 200 MHz. FTIR spectra were recorded on a BioRad FTS-7 spectrometer. The maleic anhydride content in the copolymers was determined from FTIR absorption spectra of the SCLCPs in THF referring to a calibration line. This calibration line was made by determining the peak intensities at 1850 cm^{-1} and 1780 cm^{-1} of mixtures of succinic anhydride and methylisobutyrate in different ratios in THF.

polymer	m	x
4-0.00	6	0.00
4-0.12	6	0.12
4-0.20	6	0.20
4-0.26	6	0.26
4-0.30	6	0.30
5-m	m	0.22 - 0.26

m = 3 - 8, 10, 12

Scheme 6.1. Synthesis of polymers 4-x, 5-m, 6 and 7.

6.3. Results and discussion

6.3.1. Polymer synthesis

The synthesis of polymers **4-*x*, 5-*m*, 6** and **7** is depicted in Scheme 6.1. During work-up, some anhydride moieties are hydrolyzed. Therefore, the polymers were dried in vacuo prior to characterization. Under these conditions ring closure of maleic acid moieties to anhydride moieties occurs.[16] Thin layer chromatography (TLC) showed that only maleic acid moieties were ring-closed and the ester bond of the methacrylate moiety did not participate in ring-closure. Ring-closure of the methacrylate moiety would yield a mesogen-containing alcohol that was not observed with TLC. ^{1}H NMR signals correspond to the expected chemical structures. Broadening of the signals and disappearance of the vinyl signals indicate polymer formation.

The molecular weights as determined by GPC, the MA content in the polymers as determined by FTIR, and the yields are listed in Table 6.1. The molecular weights are low if the amount of initiator (1.05 mol% based on monomer) is considered. This has also been observed for SCLC poly(MA-*alt*-1-alkene)s and can be ascribed to chain-transfer reactions.[16] The polydispersity indices for SCLC poly(MA-methacrylate)s are considerably higher than for poly(MA-*alt*-1-alkene)s. For polymers **5-*m***, the degree of polymerization and the MA content varies only slightly (Table 6.1), which means that the mesomorphic behavior of polymers **5-*m*** can be compared meaningfully. In contrast to the copolymerization of 1-

Table 6.1. *Number-average molecular weights (M_n), weight-average molecular weights (M_w), polydispersity indices (PDI), and degrees of polymerization (DP) as determined by GPC, MA content (x) as determined by FTIR, and yields (%) of polymers **4-x**, **5-m**, **6** and **7**.*

polymer	$10^{-3} M_n$	$10^{-3} M_w$	PDI	DP	x	yield
4-0.00	43.8	275	6.28	119	0	74
4-0.12	9.70	32.3	3.34	29	0.12	61
4-0.20	12.6	50.6	4.02	40	0.20	61
4-0.26	7.32	19.9	2.72	25	0.26	45
4-0.30	6.30	18.8	2.98	26	0.30	65
5-3	4.95	16.3	3.30	19	0.26	69
5-4	8.84	31.5	3.56	32	0.25	53
5-5	5.73	19.8	3.45	19	0.22	65
5-6^a	7.32	19.9	2.72	25	0.26	45
5-7	6.42	16.2	2.53	20	0.22	31
5-8	7.52	25.2	3.35	23	0.23	65
5-10	6.32	26.4	4.20	18	0.24	87
5-12	8.67	29.7	3.43	23	0.22	71
6	8.21	24.5	2.99	28	0.25	47
7	11.3	22.2	1.98	35	0.22	52

^{a} *polymers **4-0.26** and **5-6** are identical.*

alkenes with MA, the copolymerization of methacrylates with MA proceeds rapidly and gives already high yields after 48 h.
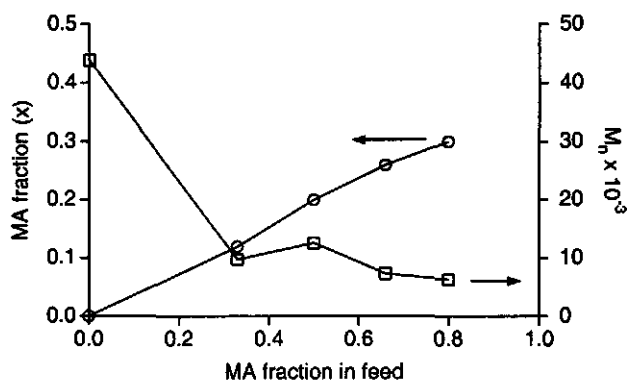

Figure 6.1. *Dependence of the built-in MA fraction x (o) and M_n (□) of the copolymer on the MA fraction in the feed.*

Table 6.2. *Phase transition temperatures (°C), corresponding heat capacity or entropy changes (J/mol K) in parentheses, and the phase types[a] of polymers **4-x**, **5-m**, **6** and **7**.*

polymer	phase behavior				
4-0.00	G_E 80 (37)	S_{EI} 119 (11.7)	S_{AI} 135 (1.5)	N 137 (3.9)	I
4-0.12	G_E -	S_{EI} 138 (27.7)			I
4-0.20	G_E -	S_{EI} 146 (16.8)	S_{AI} 148 (6.3)		I
4-0.26	G_E 137 (92)	S_{EI} 146.5 (17.8)			I
4-0.30	G_E -	S_{EI} 146 (13.4)			I
5-3	G_E -	S_{EI} 152 (10.1)			I
5-4	G_E -	S_{EI} 150 (17.3)			I
5-5	G_E 131 (57)	S_{EI} 168 (16.6)			I
5-6[b]	G_E 137 (92)	S_{EI} 146.5 (17.8)			I
5-7	G_E -	S_{EI} 139 (13.4)	S_{AI} 151 (9.7)		I
5-8	G_E 112 (62)[c]	S_{EI} 119 (7.4)	S_{AI} 140 (10.7)		I
5-10	G_{Bcryst} 88 (108)[c]	$S_{Bcryst1}$ 100 (2.2)	S_{AI} 140 (11.6)		I
5-12	G_{Bcryst} 91 (141)[c]	$S_{Bcryst1}$ 99 (3.6)	S_{AI} 142 (12.9)		I
6	G 73 (54)				I
7	G_A 81 (108)		S_{Ad} 148 (3.0)		I

[a] *I = isotropic phase; N = nematic; S_{AI} = smectic A mesophase with fully interdigitated side chains; $S_{Bcryst1}$ = crystalline smectic B with S_{AI} periodicity; S_{EI} = smectic E with an S_{AI} structure; G_X = mesoglass, in which X is the vitrified mesophase.*
[b] *polymers **4-0.26** and **5-6** are identical.*
[c] *determined during the first heating scan.*

Figure 6.1 shows that the MA fraction x of the polymer increases almost linearly with the MA content of the feed. It is seen that all copolymers have a lower MA content than perfectly alternating copolymers which would have an MA content of 0.5. Copolymerizations of methacrylates and MA have been studied before and it has been found that the reactivity ratios of methyl methacrylate and MA were 3.10 - 3.85 and 0.01 - 0.02, respectively.[24] In agreement with these reactivity ratios, other studies have shown that MA does not homopolymerize under radical polymerization conditions.[20,21] Therefore, it is expected that the copolymerization of MA and methacrylates has a tendency towards alternation, which has already been observed before for the radical initiated copolymerization of MA and stearyl methacrylate.[25]

Figure 6.1 also shows that the number-average molecular weight (M_n) decreases after copolymerization with MA and does not change significantly with the MA fraction in the feed. This may indicate that the relatively low degrees of polymerization of the copolymers may be attributed to chain transfer to MA.

6.3.2. Transition temperatures and mesophases of SCLCPs

Table 6.2 summarizes the mesophases of the polymers, their phase transition temperatures, and the corresponding entropy changes. The mesophases were assigned based on X-ray diffraction patterns and textures observed with POM.

Table 6.3 shows the X-ray diffraction data, comprising experimental and calculated d spacings. d Spacings were determined in the mesoglass at room temperature, after the polymer was cooled down from the isotropic state to the mesoglass at a cooling rate of 5°C/s.

Table 6.3. *Experimental d spacings (Å) obtained from wide-angle X-ray diffraction and calculated d spacings (Å) of polymers **4-x**, **5-m**, **6**, and **7**.*

polymer	d spacings			calcd d spacings	
				S_{Al}	S_{Ad}
4-0.00	26.4; 12.9; 8.53;	4.49; 4.01; 3.21		26.6	38.7
4-0.12	13.1; 8.67;	4.51; 4.02; 3.23		26.6	38.7
4-0.20	13.2; 8.79;	4.51; 4.03; 3.23		26.6	38.7
4-0.26	13.5; 9.97;	4.53; 4.02; 3.24		26.6	38.7
4-0.30	28.4; 13.8;	4.53; 4.04; 3.23		26.6	38.7
5-3	23.2; 11.5;	4.50; 4.01; 3.21		23.3	31.0
5-4	24.3; 12.1;	4.52; 4.01; 3.22		24.1	33.7
5-5	25.6; 12.7; 8.38;	4.53; 4.02; 3.25		25.8	36.2
5-6	13.5; 9.97;	4.53; 4.02; 3.24		26.6	38.7
5-7	14.1; 9.35;	4.51; 4.05; 3.25		28.3	41.2
5-8	30.4; 15.0; 9.87;	4.48; 4.04; 3.23		29.1	43.8
5-10	32.7; 16.1; 10.7;	4.34		31.4	48.9
5-12	34.0; 17.3; 11.4;	4.32		34.1	54.0
7	16.0			27.4	40.1
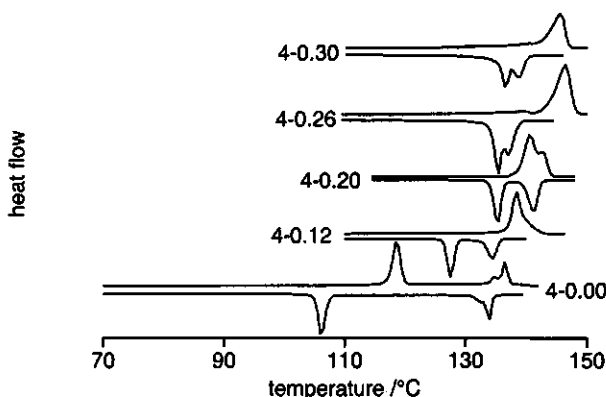
Figure 6.2. *DSC thermograms of polymers 4-x. For all compounds the second heating and cooling traces are given.*

Influence of MA content

Polymer **4-0.00** has been synthesized before and showed phase behavior that was similar to that reported in a previous study (G_E 88 S_E 117 S_A - N 134 I).[13] Below 134°C, POM showed that polymer **4-0.00** exhibits a poorly defined focal-conic fan texture.[10]

Upon cooling, the other polymers **4-x** show textures with POM that were observed before for poly(MA-*alt*-1-alkenes), i.e. sandlike textures that transformed into small domains of a bandlike texture after annealing for several hours.[16] For poly(MA-*alt*-1-alkene)s, it was already concluded that these textures correspond to an S_A mesophase. After copolymerization of monomer **1-6** with MA the S_A and N mesophases observed for polymer **4-0.00** disappear in the heating curves of the DSC-thermogram (Figure 6.2). Upon cooling, a monotropic S_A mesophase was observed and its width decreased with increasing MA content. The isotropization temperature (T_i) increases until the MA fraction x reaches a value of 0.26, which means that T_i increases with backbone flexibility. For poly(MA-stearyl methacrylate) it has been found that the copolymer has a higher flexibility than the homopolymer of stearyl methacrylate.[25] Above an MA fraction of 0.26 the decreasing mesogen density becomes significant and T_i decreases slightly.

From the X-ray diffraction data in Table 6.3, it follows that polymers **4-x** exhibit mesophases with a periodicity corresponding to S_{A1}. Furthermore, the presence of (110), (200) and (210) reflections in the wide-angle region of the X-ray diffraction pattern indicate that the mesogens within the smectic layers are ordered orthorhombically i.e. these polymers exhibit S_E mesophases. The corresponding orthorhombic cell parameters a and b are 8.01 – 8.07 Å and 5.41 – 5.48 Å, respectively. The a-parameter is larger than the a-values of S_E mesophases of modified poly(MA-*alt*-1-alkene)s with one mesogen per two atoms in the backbone (a = 7.90 Å), which were obtained by grafting mesogen-containing alcohols onto SCLC poly(MA-*alt*-1-alkenes).[26] Because the b-parameters of the S_E phase of polymers **4-x** differ only slightly from b-values of the S_E phases of modified poly(MA-*alt*-1-alkene)s (b =
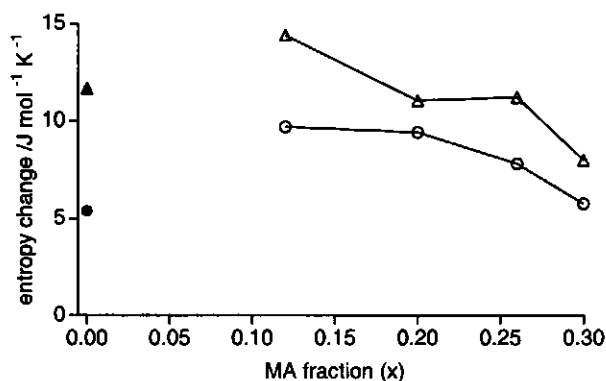
Figure 6.3. *Dependence of the entropy change at the* S_E-S_A *transition* (△) *and the isotropization transition* (○) *as found with DSC on MA fraction x for polymers 4-x. The entropy changes have been determined from the second cooling scan.*

5.43 Å), it can be concluded that the mesogens are packed less densely for the poly(MA-methacrylate)s.

The d spacings slightly increase with MA content, which can be attributed to a decrease in mesogen density, whereas the lateral distance (wide-angle X-ray reflections) is independent on mesogen density (Table 6.3). If the mesogen density decreases, the polymer backbone has to reorient in order to retain the same organization of mesogens as for polymers with a high mesogen density. For a polymer backbone that is confined between two orthorhombic smectic layers, the reorientation results in an increase in d spacing. As was already observed for poly(MA-*alt*-1-alkene)s,[16] the second-order reflection in the X-ray diffraction pattern of copolymers **4-x** (x ≠ 0) was stronger than the first-order reflection (*vide infra*).

Figure 6.3 shows that the entropy changes at isotropization and the S_E-S_A transition decrease with increasing MA fraction. This can be attributed to the decrease in mesogen density with increasing MA fraction, which results in a lower degree of order in the mesophase.[27]

Influence of spacer length

For copolymers with an MA fraction of about 0.24 the effect of spacer length on the thermotropic behavior is studied. The DSC thermograms of polymers **5-m** are depicted in Figure 6.4. If the spacer length is shorter than six methylene units, only one transition can be observed. Upon cooling, this transition shows a high degree of supercooling, which indicates the formation of a highly ordered phase. Above a spacer length of six methylene units the thermograms show two transitions. For polymers **5-m** with $m \geq 5$, no change in texture was observed on cooling from the S_A mesophase to the higher ordered mesophases.
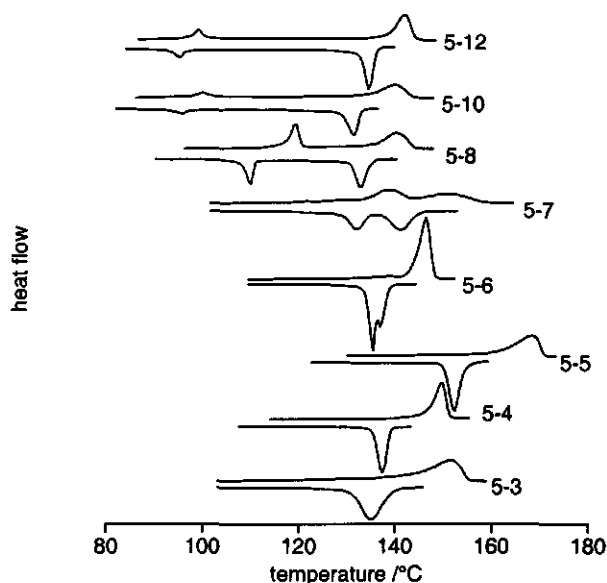
Figure 6.4. DSC thermograms of polymers 5-m. For all compounds the second heating and cooling traces are given.

X-ray experiments (Table 6.3) showed that polymers **5-m** all exhibit mesophases with a periodicity corresponding to S_{A1}. The corresponding *d* spacings increase linearly with spacer length. Like polymers **4-x**, polymers **5-3 - 5-8** exhibit S_E mesophases, as can be seen from the (110), (200) and (210) reflections in the X-ray diffraction pattern. For polymers **5-10** and **5-12**, only one reflection was observed in the wide-angle area, indicating that these polymers exhibit an S_B mesophase. From the rather large correlation lengths of 32 Å and 35 Å, respectively, calculated from the width at half-height of the wide-angle peak, it can be concluded that this is an S_{Bcryst} mesophase.

The intensity of the first-order reflection in the X-ray diffraction patterns is smaller than of the second-order reflection, which can probably be ascribed to an additional plane of symmetry in the electron density profile. This additional plane of symmetry induces an apparent *d* spacing (the strongest small angle reflection) that is half the smectic *d* spacing. The intensity of the second-order reflection as compared to that of the first-order reflection increases with spacer length. This is thought to result from a more distinct plane of symmetry in the electron density profile for longer spacers: the differences between the maxima in the electron densities for the different smectic sublayers increase. Davidson and Levelut[28] have pointed out that it is possible to determine the localization of the backbone in smectic phases from the relative intensities of the Bragg reflections from the layers. Relative intensities of the Bragg reflections as found for polymers **5-m** are typical for microphase separated SCLCP systems like poly(acrylate)s and poly(siloxane)s, in which the polymer backbones are confined in sublayers between mesogen layers.[15] In contrast, for poly(methacrylate)s with
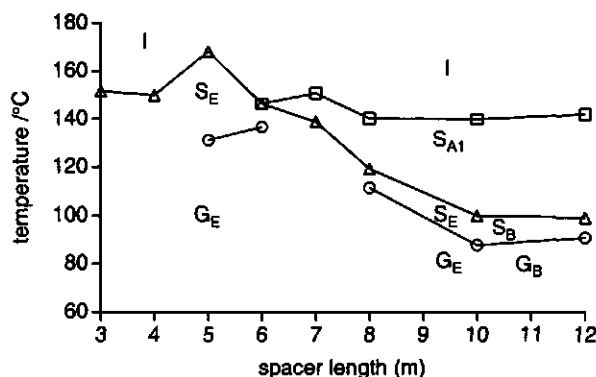
Figure 6.5. *Dependence of the transition temperatures on spacer length m for polymers 5-m:*
(○) glass transition; (△) S_E-I/S_E-S_{A1}/S_B-S_{A1} transition; (□) S_A-I transition.

methoxybiphenyl mesogens the backbones are not microphase separated and cross the layers of mesogens and, consequently, the first order reflection was clearly observed, whereas the second order reflection was barely detectable.[15] This indicates that the microphase separation for poly(MA-methacrylate)s can be ascribed to the polarity of the polymer backbone, which prevents mixing of the backbone with mesogens.

Figure 6.5 displays the transition temperatures and different mesophases as a function of spacer length *m*. The glass transition temperature decreased with increasing spacer length, which can be attributed to the plasticizing effect of the spacers. The isotropization temperature showed little dependence on spacer length, although a small odd-even effect was observed. However, this odd-even effect was not clearly observed for the change in entropy. As found for other SCLCPs,[1] the S_{A1} mesophase broadens when the spacer length increases. From the high degree of order in the mesophase for short spacers, it follows that the mesogenic interactions govern the structural phase behavior of these SCLCPs.

The mesomorphic behavior of poly(MA-methacrylate)s is different from that of poly(methacrylate)s[8,13] and poly(MA-*alt*-1-alkene)s.[16,17] Although all polymers show a decrease of T_g with spacer length, only the poly(MA-*alt*-1-alkene)s show an increase in T_i with spacer length. Both the poly(methacrylate)s and the poly(MA-methacrylate)s show little dependence of T_i on spacer length, although both types of polymers show an odd-even effect for T_i. This odd-even effect was the strongest for the poly(methacrylate)s.

The three types of polymers have in common that the width of the mesophase increases with spacer length. For poly(MA-*alt*-1-alkenes) and poly(methacrylate)s, the S_A mesophase is very narrow for short spacers. For short even-membered spacers, the poly(methacrylate)s even exhibit an N mesophase instead of an S_A mesophase. For poly(MA-methacrylate)s, no S_A mesophase was found for short spacers: these polymers exhibit only an S_E mesophase.

The side-chains of poly(MA-*alt*-1-alkenes) are partially interdigitated in the mesophase, whereas the side-chains are completely interdigitated for poly(MA-
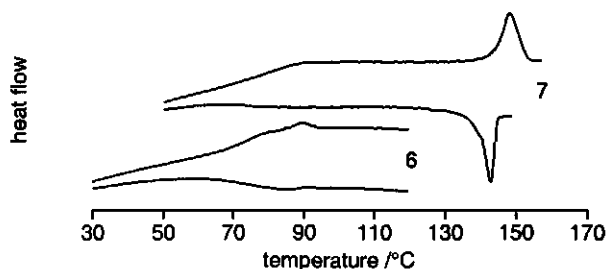
Figure 6.6. *DSC thermograms of polymers 6 and 7. For both polymers the second heating and cooling traces are given.*

methacrylate)s and poly(methacrylate)s. This can probably be ascribed to differences in mesogen density: due to the alternating sequence of 1-alkene and MA units, the poly(MA-*alt*-1-alkenes) have the lowest mesogen density. These differences in mesogen density also result in different degrees of order within smectic layers. Poly(methacrylate)s and poly(MA-methacrylate)s exhibit a S_E mesophase that, as a result of the higher mobility of mesogens, transforms into an S_{Bcryst} mesophase for longer spacers. In contrast, poly(MA-*alt*-1-alkene)s, exhibit the less ordered hexatic smectic B (S_{Bhex}) mesophase.

Influence of mesogen

In contrast to polymers **4-x** and **5-m** that contain methoxybiphenyl mesogens, polymer **6** with cyanobiphenyl mesogens does not show liquid-crystallinity. In the DSC thermograms shown in Figure 6.6 only a glass transition at 73°C is visible. As found for poly(methacrylate)s,[14] the presence of cyanobiphenyl mesogens results in less ordered mesophases than the presence of methoxybiphenyl mesogens. However, poly(methacrylate)s with cyanobiphenyl mesogens do exhibit liquid-crystallinity, which can probably be ascribed to the higher mesogen density in comparison to that of polymer **6**. Poly(MA-*alt*-1-alkenes) with cyanobiphenyl mesogens also exhibit liquid-crystallinity, i.e. an N mesophase;[16] however, this type of polymer has a more flexible backbone than poly(MA-methacrylates) and, hence, there is a higher degree of decoupling between the motions of the backbone and those of the mesogens.

Polymer **7** was the only polymer in this series that exhibited clear bandlike textures immediately after cooling from the isotropic melt, which indicates that this polymer exhibits an S_A mesophase. DSC (Figure 6.6) shows distinct glass and isotropization transitions. X-ray measurements (Table 6.3) reveal that polymer 7 exhibits an S_{Ad} mesophase. The formation of an S_{Ad} mesophase can probably be ascribed to the tendency of mesogens with cyano terminal groups to form antiparallel pairs.[14,29] The difference in mesomorphic behavior between cyanobiphenyl and cyanoazobenzene mesogens has been observed before for low-molecular-weight liquid crystals[30] and SCLC poly(styrene)s[29] and has been ascribed to differences in polarizability and conjugative interactions of the mesogen, which are stronger for azobenzene mesogens.[30]

95

6.4. Conclusions

The copolymerization of maleic anhydride (MA) with mesogenic methacrylates yields copolymers with low degrees of polymerization, which can probably be ascribed to chain transfer to monomer. The MA fraction in these copolymers can be varied by adjusting the MA content in the feed and the polymerization rate is higher than for poly(MA-*alt*-1-alkenes).

For methoxybiphenyl mesogens and hexyl spacers, it is found that besides an S_{EI} mesophase these copolymers exhibit a monotropic S_{A1} mesophase. The width of this mesophase decreases and the isotropization temperature increases with increasing MA fraction. X-ray diffraction measurements indicate that the polymer backbone of these SCLCPs is confined between mesogen layers. This microphase separation can probably be ascribed to differences in polarity of the polymer backbone and mesogens.

An increase of the spacer length results in an increase of the temperature range of the mesophase: T_g decreases with spacer length, whereas T_i remains almost constant, although a small odd-even effect for T_i is observed. Spacer length hardly affects the type of mesophase. SCLCPs with short spacers exhibit a highly ordered S_{E1} mesophase. For spacer length $m \geq 7$, the S_{E1} mesophase is succeeded by an S_{A1} mesophase. For $m \geq 10$, the S_{E1} mesophase observed for SCLCPs with shorter spacers is replaced by an $S_{Bcrystl}$ mesophase. The mesogenic interactions govern the structural phase behavior of these SCLCPs.

The copolymer of MA and a cyanobiphenyl-containing methacrylate does not exhibit liquid crystallinity. In contrast, a comparable polymer containing cyanoazobenzene mesogens exhibits an S_{Ad} mesophase.

6.5. References

1   Pugh, C.; Kiste, A. L. *Prog. Polym. Sci.* **1997**, *22*, 601.
2   Shibaev, V. P.; Freidzon, Y. S.; Kostromin, S. G. *Liquid Crystalline and Mesomorphic Polymers*, Shibaev, V. P., Lam, L., Eds.; Springer-Verlag, New York, 1994.
3   Simmonds, D. J. *Liquid Crystal Polymers, From Structures to Applications*, Collyer, A. A., Ed.; Elsevier Applied Science, London and New York, 1992.
4   Percec, V.; Pugh, C. *Side Chain Liquid Crystal Polymers*, McArdle, C. B., Ed;, Blackie, Glasgow, UK, 1989.
5   Maughon, B. R.; Weck, M.; Mohr, B.; Grubbs, R. H. *Macromolecules* **1997**, *30*, 257.
6   Percec, V.; Tomazos, D.; Willingham, R. A. *Polym. Bull.* **1989**, *22*, 199.
7   Chovino, C.; Guillon, D.; Gramain, P. *Polymer* **1998**, *39*, 6385.
8   Koltzenburg, S.; Wolff, D.; Springer, J.; Nuyken, O. *J. Polym. Sci.: Part A: Polym. Chem.* **1998**, *36*, 2669.
9   Noirez, L.; Boeffel, C.; Daoud-Aladine, A. *Phys. Rev. Lett.* **1998**, *80*, 1453.
10   Rodekirch, G.; Rübner, J.; Zschuppe, V.; Wolff, D.; Springer, J. *Makromol. Chem.* **1993**, *194*, 1125.

11 Âlimoglu, A. K.; Ledwith, A.; Gemmell, P. A.; Gray, G. W.; Lacy, F. R. S. and D. *Polymer* **1984**, *25*, 1342.

12 Percec, V.; Tomazos, D. *Polymer* **1990**, *31*, 1658.

13 Craig, A. A.; Imrie, C. T. *J. Mater. Chem.* **1994**, *4*, 1705.

14 Craig, A. A.; Imrie, C. T. *Macromolecules* **1995**, *28*, 3617.

15 Davidson, P. *Prog. Polym. Sci.* **1996**, *21*, 893.

16 Nieuwhof, R. P.; Marcelis, A. T. M.; Sudhölter, E. J. R.; Picken, S. J. de Jeu, W. H. *Macromolecules* **1999**, *32*, 1398 (Chapter 3).

17 Nieuwhof, R. P.; Marcelis, A. T. M.; Sudhölter, E. J. R.; van der Wielen, M. W. J.; Cohen Stuart, M. A.; Fleer, G. J. *Macromol. Symp.* **1998**, *127*, 115.

18 van der Wielen, M. W. J.; Cohen Stuart, M. A.; Fleer, G. J.; de Boer, D. K. G.; Leenaers, A. J. G.; Nieuwhof, R. P.; Marcelis, A. T. M.; Sudhölter, E. J. R. *Langmuir* **1997**, *13*, 4762.

19 van der Wielen, M. W. J.; Cohen Stuart, M. A.; Fleer, G. J. *Langmuir* **1998**, *14*, 7065.

20 Komber, H. *Macromol. Chem. Phys.* **1995**, *196*, 669.

21 Trivedi, B. C.; Culbertson, B. M. *Maleic Anhydride*, Trivedi, B. C., Ed.; Plenum, New York, 1982.

22 Davis, F.; Hodge, P.; Towns, C. R.; Ali-Adib, Z. *Macromolecules* **1991**, *24*, 5695.

23 Tacx, J. C. J. F.; Meijerink, N. L. J.; Suen, K. *Polymer* **1996**, *37*, 4307.

24 Tsuchida, E.; Shimomura, T.; Fujimori, K.; Ohtani, Y.; Shinohara, I. *Kobunshi Kagaku* **1966**, *69*, 1230 (1966).

25 Leiva, A.; Gargallo, L.; Radic, D. *J. Macromol. Sci.-Phys.* **1998**, *B37*, 45.

26 Nieuwhof, R. P.; Marcelis, A. T. M.; Sudhölter, E. J. R. *Macromolecules* in press (Chapter 4).

27 Percec, V.; Lee, M. *J. Mater. Chem.* **1992**, *2*, 617.

28 Davidson, P.; Levelut, A. *Liq. Cryst.* **1992**, *11*, 469.

29 Imrie, C. T.; Schleeh, T.; Karasz, F. E.; Attard, G. S. *Macromolecules* **1993**, *26*, 539.

30 Gray, G. W. *The Molecular Physics of Liquid Crystals*, Luckhurst, G. R., Gray, G. W., Eds.; Academic Press: New York, 1979.

7

Side-chain liquid-crystalline poly(ketone)s: effect of spacer length, mesogen type and mesogen density on mesomorphic behavior

Novel side-chain liquid-crystalline copolymers (SCLCPs) were synthesized via the Pd(II) catalyzed alternating copolymerization of mesogenic 1-alkenes and carbon monoxide. For methoxybiphenyl mesogens, these copolymers exhibited highly ordered smectic E mesophases and high glass transition temperatures. The transition temperatures of these polymers were tuned by altering the spacer length or by dilution of mesogen-containing alkenes with 1-hexene. Polymers with cyanobiphenyl or methoxyazobenzene mesogens exhibited nematic mesophases. These polymers were the first ever nitrogen containing copolymers of this type. Increase of the spacer length or the 1-hexene content of methoxybiphenyl-containing copolymers resulted in a decrease of the surface polarity of spincoated films. The decomposition temperature of these SCLCPs started far above the isotropization temperature of the polymers.

7.1. Introduction

Polymeric materials with anisotropic properties are of great interest for commercial applications. One way to introduce anisotropy in polymers is by using stiff moieties, for example mesogens. These mesogens may be present in the backbone (main-chain liquid-crystalline polymers) or attached to the backbone via flexible spacers (side-chain liquid-crystalline polymers, SCLCPs). A great variety of polymer backbones has been used for SCLCPs, like poly(acrylate)s,[1] poly(siloxane)s,[2] poly(phosphazene)s,[3] poly(styrene)s,[4] and poly(maleic anhydride-*alt*-1-alkene)s.[5]

A completely new type of polymer backbone for SCLCPs may be poly(1,4-ketone)s. Throughout the past few years, poly(1,4-ketone)s have attracted a growing attention by academic as well as industrial research groups.[6,7] Evidently, this is related to the fact that

carbon monoxide (CO) is a low price monomer. Furthermore, copolymerization with 1-alkenes affords a class of polymeric materials which in their spectrum of properties differ from the widespread poly(olefin) commodities like poly(ethylene), poly(propylene) and poly(styrene). This results from the presence of polar carbonyl moieties in the polymer backbone, which strictly alternate with the apolar olefin fragments.[8] It has been demonstrated that these carbonyl functionalities are suitable handles for chemical modification, yielding polymers that may show an improved adhesive behavior. Some time ago, a method for the control of the molecular weight of poly(propene-*alt*-CO)s has been introduced by using methanol or water as chain transfer agent.[9,10] This resulted in novel poly(ketone) materials exhibiting the mechanical properties of thermoplastic elastomers.[9,10,11] By adding higher 1-alkenes as termonomers both the surface polarity as well as the glass transition temperature can be tuned.[8]

This chapter reports the first example of poly(ketone)-based SCLCPs, synthesized via Pd(II) catalyzed copolymerization of CO and 1-alkenes carrying methoxybiphenyl mesogens. In these polymers the effect of spacer length and mesogen density is studied. The latter was achieved by terpolymerizing CO with a mesogenic 1-olefin and 1-hexene, in different molar ratios. For comparison, poly(1,4-ketone)s with cyanobiphenyl and methoxyazobenzene mesogens are synthesized, which are the first ever nitrogen-containing monomers used in this type of copolymerization reaction.

The combination of liquid crystallinity and the physical properties depicted above, i.e. good adhesion and interesting mechanical behavior, can be expected to establish a new type of versatile polymeric materials.

7.2. Experimental part

7.2.1. Materials

4-hydroxy-4'-methoxyazobenzene was prepared by reaction of the diazonium salt of 4-methoxyaniline with phenol.[12] Monomers 1-*m*[5] and monomers 2 and 3[13] were synthesized as described previously. [Pd(NCCH$_3$)$_4$](BF$_4$)$_2$ was purchased from Aldrich and 1,3-bis(diphenylphosphino)propane (dppp) from Strem Chemicals. [Pd(dppp)(NCCH$_3$)$_2$](BF$_4$)$_2$ was prepared according to a literature procedure.[14] CH$_2$Cl$_2$ was distilled from CaH$_2$ and methanol was treated with sodium methoxide/dimethylterephthalate and subsequently distilled. All other chemicals were of commercial grade and were used as received.

7.2.3. Equipment

Gel permeation chromatography (GPC) measurements were carried out using a series of four microstyragel columns with pore sizes of 10^5, 10^4, 10^3 and 10^6 Å (Waters), respectively with THF as eluent. A dual detection system consisting of a differential refractometer (Waters model 410) and a differential viscometer (Viscotek model H502) was

used. A calibration line was made with this setup, using narrow polystyrene reference standards in THF, and the molar mass (g/mol) of the synthesized polymers was determined referring to this calibration line. Thermal transitions were monitored with a Perkin-Elmer DSC-7. Scan rates of 10 K/min were used in the differential scanning calorimetry (DSC) experiments with sample masses of 5-10 mg. Transition temperatures were taken from the second heating cycle. Polarizing optical microscopy (POM) was performed on an Olympus BH-2 microscope equipped with a Mettler FP82HT hot stage and an FP80HT temperature controller. X-ray diffraction measurements were performed on a Siemens D5000 reflection diffractometer with a HTK oven and Cu Kα radiation. ^{1}H NMR spectra were recorded on a Bruker AC200 spectrometer at 200 MHz. FTIR spectra were recorded on a BioRad FTS-7 spectrometer. Measurement of equilibrium contact angles was conducted by the sessile drop method using a G 40 (Krüss GmbH) set-up at ambient temperature. Bidistilled water was employed as the wetting liquid. Samples of polymer films were prepared from 1 wt.% solutions in CH_2Cl_2 by spincoating on precleaned glass platelets at 3000 rpm for 20 s. The coated glass platelets were dried under vacuum at ambient temperature for 24 h. Thermogravimetric analysis (TGA) was performed by means of a TG system from Perkin Elmer using a scan speed of 20 K/min under a nitrogen atmosphere.

7.2.3. Synthesis

Copolymerization of mesogenic 1-alkenes with CO[9]

All polymerization experiments were carried out in a 100 mL steel autoclave. For methoxybiphenyl-containing monomers (**1-m**), the autoclave was charged with a solution of 46 mg (4.92 x 10^{-5} mol) [Pd(dppp)(NCCH$_3$)$_2$](BF$_4$)$_2$, 0.4 mL (2 mL in case of polymer **4-4a**) of MeOH, and the mesogenic 1-alkene (28.5 mmol) in 45 mL of CH_2Cl_2 and CO (5.0 x 10^6 Pa). In terpolymerization experiments we used 25 mmol of the mesogen together with 1-hexene. Monomer **2** (14.7 mmol) or **3** (17.2 mol) and 35 mg (3.74 · 10^{-5} mol) of the catalyst precursor were dissolved in 25 mL of CH_2Cl_2 and 0.3 mmol of MeOH was added. The reaction mixtures were stirred at 35 °C (50 °C in case of monomer **2**) for 16 hours. After that, the unreacted carbon monoxide was vented off and the reaction mixture was precipitated into an excess of methanol in order to quench the polymerization. The precipitate was collected and repeatedly precipitated from THF into petroleum ether 40/60 (10 volumes) until TLC showed that the unreacted monomer was removed completely. Catalyst residues were removed by filtering the polymer dissolved in THF over a small column of silica into methanol. The white powder that was obtained after filtration was subsequently dried under high vacuum.

Anal. calcd for polymer **5**, calculated for a 1:1 copolymer: C, 78.66; H, 6.27; N, 3.14. Found: C, 78.50; H, 6.32; N, 4.49. Anal calcd for polymer **6**, calculated for a 1:1 copolymer: C, 70.98; H, 6.55; N, 8.28. Found: C, 70.90; H, 6.60; N, 8.39.
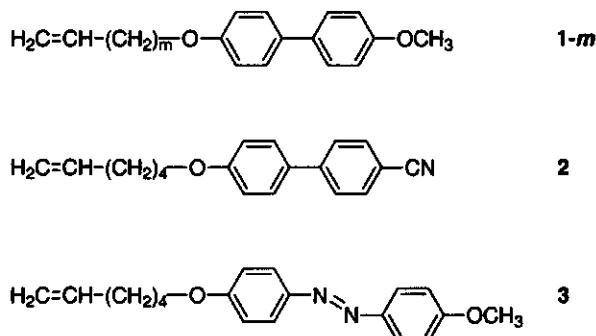
Scheme 7.1. *Structures of monomers 1-m, 2 and 3.*

7.3. Results and discussion

7.3.1. Monomers

The structures of monomers **1-m**, **2** and **3** are depicted in Scheme 7.1. All monomers were obtained in satisfactory yields and high purity. The observed ^{1}H NMR signals agreed well with the chemical structure.

The DSC thermograms showed that monomers **2** and **3** exhibit liquid-crystalline behavior and that their phase transitions are reversible, whereas monomers **1-m** are only crystalline. For monomer **2**, the melting temperature at 32 °C was preceded by several crystal-crystal transitions. The transition temperatures which were determined from DSC traces, are:

monomer **2**: K 32 N 55 I;
monomer **3**: K 90 N 94 I.

For monomers **2** and **3**, POM revealed Schlieren textures which correspond to a nematic mesophase. Transition temperatures observed with POM were in good agreement with those found with DSC.

7.3.2. Polymer synthesis

Polymers **4-m**, **5**, **6** and **7-x** were synthesized according to Scheme 7.2. The co- and terpolymerizations were carried out in CH_2Cl_2 at elevated temperature (usually 35 °C) using the dicationic palladium(II) complex [Pd(dppp)(NCCH$_3$)$_2$](BF$_4$)$_2$ as a catalyst precursor. Activation of the catalyst was performed by addition of a defined amount of methanol. Pd(0) formation was not observed under these reaction conditions. In most cases, the reaction mixture remained colorless. However, for polymers **4-2** and **4-6** it was observed that the reaction mixture had a red color before the polymerization was quenched. This may be due to the formation of a chelate including coordination of one of the oxygen atoms. The FTIR-
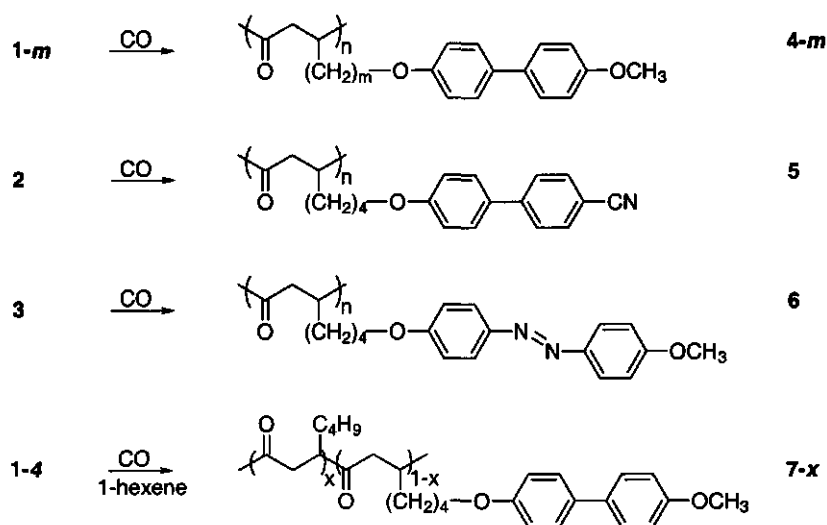
Scheme 7.2. *Synthesis of polymers 4-m, 5, 6, and 7-x.*

spectra of polymers **4-m**, **5**, **6** and **7-x** showed a strong absorption at 1707 cm^{-1} that can be ascribed to poly(1,4-ketone) carbonyl groups. No spectroscopic indication was found for the formation of spiroketal units,[15,16] which have been observed before for some other poly(ketone)s.[15,17] Jiang et al.[15] postulated a possible mechanism for spiroketal formation (Scheme 7.3) and found that the cyclization appears to be favored in a regio/stereo regular disposition of the carbonyl groups. Previous studies,[14] however, have shown that the copolymerization of carbon monoxide with propene using [Pd(dppp)(NCCH$_3$)$_2$](BF$_4$)$_2$ as a catalyst yields regiochemically random copolymers and therefore will not result in copolymers containing spiroketal units.

    The molecular weights of the polymers were determined by GPC and are listed in Table 7.1. The values are moderate compared to molecular weights obtained for
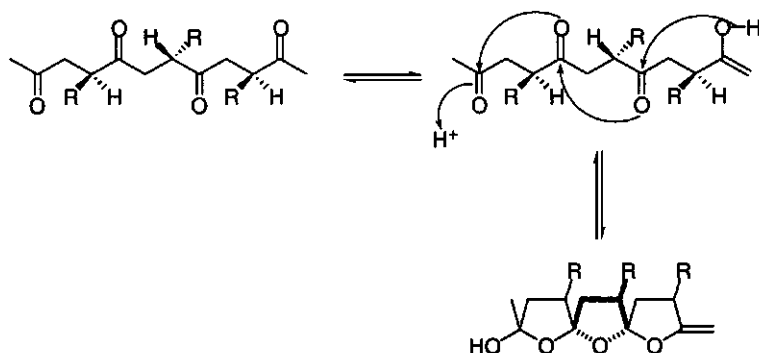
Scheme 7.3. *Possible mechanism for the interchange between the backbone 1,4-keto and the spiroketal units in isotactic alternating poly(CO-1-alkene).*

Table 7.1. *Number-average molecular weights (M_n), weight-average molecular weights (M_w), polydispersity indices (PDI), degrees of polymerization (DP) as determined by GPC and yields (%) of SCLC poly(ketone)s.*

polymer	$10^{-3} M_n$	$10^{-3} M_w$	PDI	DP	yield
4-2	3.33	4.53	1.36	24	11
4-4a	3.99	8.61	2.16	26	14
4-4b	7.70	19.2	2.50	50	21
4-6	-	-	-	-	3.0
4-9	3.62	7.56	2.09	19	21
5	1.76	2.69	1.54	12	6.9
6	9.46	15.0	1.54	56	15
7-0.016	4.95	9.20	1.86	33	40
7-0.028	4.25	8.14	1.92	28	17
7-0.033	4.73	7.95	1.68	32	23
7-0.138	3.99	7.65	1.96	30	20
7-0.235	4.50	9.15	2.03	34	22
7-0.244	7.34	11.9	1.63	56	14

polymerizations of CO with ethene or propene.[18] This can be ascribed to the higher steric hindrance of longer 1-alkenes, their ability to undergo isomerization reactions[18] and a reduction of the double bond concentration with increasing chain length. In addition, the mesogenic monomers may also coordinate via their functional mesogen moieties, leading to a blocking of free coordination sites of the catalyst.

For polymer **4-4**, two batches with different molecular weights (**4-4a** and **4-4b**) were synthesized by variation of the methanol concentration. The higher molecular weight was obtained at the lower activator to catalyst ratio, indicating that methanol acts as a chain transfer reagent. Polymer **4-6** was obtained in a poor yield, which can probably be ascribed to the previously mentioned chelate-like coordination including coordination of one of the oxygen atoms of the mesogen. For polymer **4-6**, this coordination may be strong enough to suppress polymerization yielding polymers with low molecular weights and low yields.

Polymer **5** has a degree of polymerization of 12. This low degree of polymerization can be explained by coordination of the cyano group to the catalyst complex, which results in a lower propagation rate. Therefore, termination reactions become more competitive with propagation and a polymer with a lower molecular weight is obtained.

Polymers with different mesogen densities were obtained by terpolymerization of carbon monoxide and monomer **1-4** with different quantities of 1-hexene. The amount of 1-hexene in the terpolymer was determined from ^{1}H NMR spectroscopy. These measurements showed that the fraction of 1-hexene in the terpolymer was about the same as in the feed, which indicates that both monomers have equal reactivities and are incorporated in the polymer backbone in a random fashion.

Table 7.2. *Phase transition temperatures (°C), corresponding heat capacity or entropy changes (J/mol) as determined by DSC in parenthesis, and phase types[a] of SCLC poly(ketone)s.*

polymer	phase behavior			
4-2	G_{EI} -	S_{EI} 155 (23)		I
4-4a	G_{EI} -	S_{EI} 145 (28)		I
4-4b	G_{EI} -	S_{EI} 151 (28)		I
4-6	G_{EI} 76 (63)	S_{EI} 108 (25)		I
4-9	G_{EI} 81 (56)	S_{EI} 126 (41)		I
	I 115 (9.3)	S_{AI} 102 (34)	S_{EI} -	G_{EI}
5	G_N 48 (111)		N 124 (2.0)	I
6	G_N 54 (120)		N 137 (2.1)	I
7-0.016	G_{EI} -	S_{EI} 142 (27)		I
7-0.028	G_{EI} -	S_{EI} 140 (26)		I
7-0.033	G_{EI} -	S_{EI} 140 (26)		I
7-0.138	G_{EI} 111 (-)	S_{EI} 131 (19)		I
7-0.235	G_{EI} 108 (-)	S_{EI} 130 (10)		I
7-0.244	G_{EI} 82 (91)	S_{EI} 114 (5.5)		I

[a] G_{EI} = glass phase, in which the S_{EI} mesophase is frozen in; S_{EI} = smectic E with a periodicity corresponding to S_{AI}; S_{AI} = smectic A with complete interdigitation of the side-chains; I = isotropic.

7.3.3. Transition temperatures.

Table 7.2 summarizes the mesophases of the polymers, their phase transition temperatures and corresponding entropy changes. The mesophases in Table 7.2 were assigned based on textures observed with POM and the X-ray diffraction patterns of the mesoglass. The assignment of mesophases will be discussed later.

The effect of the degree of polymerization on transition temperatures is demonstrated for polymer **4-4**. Increasing the degree of polymerization by a factor of 2 results in an increase of the isotropization temperature (T_i) of 6 °C. This means that the thermal behavior of different polymers can be compared meaningfully because (i) the molecular weights of the polymers differ only slightly and (ii) transition temperatures do not vary significantly if the molecular weight is increased by a factor of 2.

Influence of spacer length.

On cooling from the isotropic melt, POM revealed a sandlike texture that transformed into a texture with small bandlike colored domains after annealing just below T_i for several hours. These textures, corresponding to mesophases with an S_A structure, became more clear when the cover slip was moved before annealing by applying mechanical stress.

The DSC thermograms of polymers **4-m** are depicted in Figure 7.1. On heating, polymers **4-2**, **4-4a** and **4-4b** showed a peak corresponding to isotropization but no glass
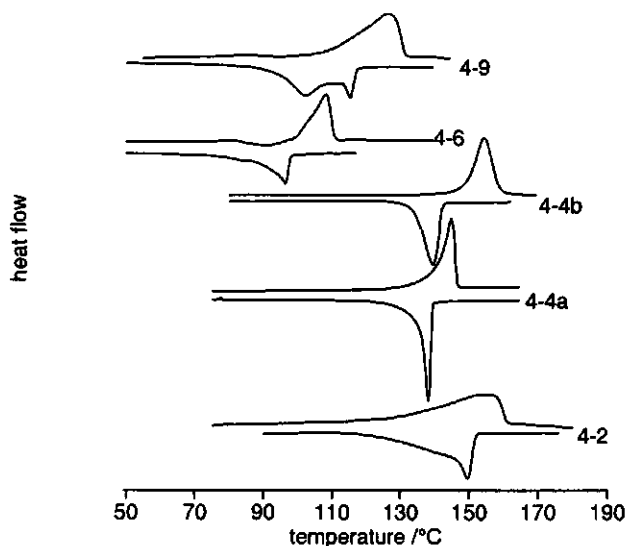
Figure 7.1. *DSC thermograms of polymers **4-m**. For all compounds the second heating and cooling traces are given.*

transition was observed. However, polymers **4-6** and **4-9** do exhibit a glass transition. For polymer **4-6**, glass transition was followed by an exothermic peak that can probably be attributed to crystallization. Polymer **4-9** undergoes one transition during heating while during cooling two transitions were observed, of which the total enthalpy change was comparable to that of the transition observed during heating. X-ray diffraction clarified that the high-temperature mesophase observed upon cooling is an S_{A1} mesophase and the low-temperature mesophase is an S_{E1} mesophase.

Figure 7.2a shows that T_i decreases with increasing spacer length. The observed decline is different from the trend in T_i for SCLC poly(maleic anhydride-*alt*-1-alkene)s,[5] for which an increase in T_i with spacer length was found. This can be attributed to the dualistic character of the spacer: higher molecular mobility and longer spacers enhance the shape anisotropy of the side chain resulting in better liquid-crystalline properties, whereas a higher molecular flexibility also serves to decrease T_i. As a consequence, no general relation exists between spacer length and T_i.[19] From the high degree of order for short spacers, it follows that the mesogenic interactions govern the structural phase behavior.

The effect of spacer length on entropy changes is presented in Figure 7.2b. In the series of polymers **4-m**, the entropy change at T_i increases with spacer length, which can be ascribed to a constant increase in entropy change per methylene unit. In concurrence with a previous study[20], an almost linear relation was found between spacer length and isotropization entropy.
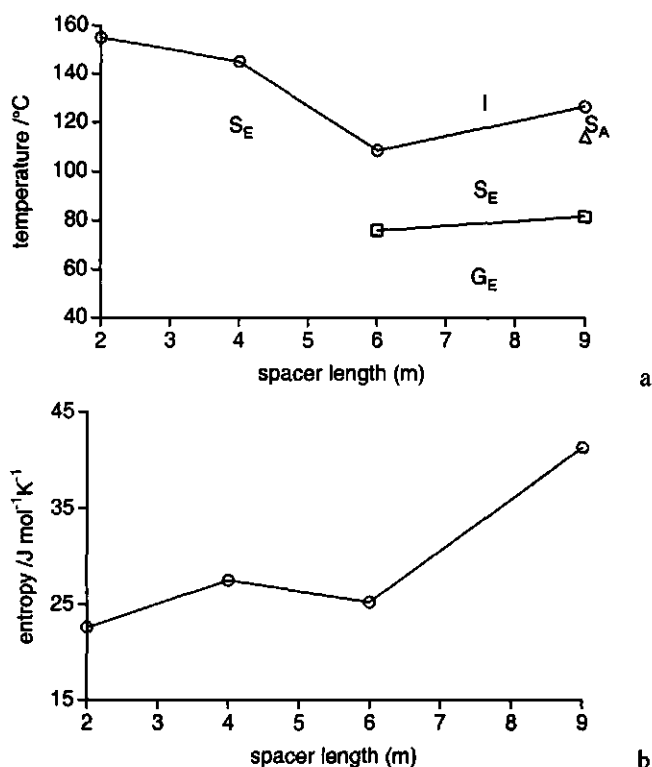
Figure 7.2. a. Dependence of the transition temperatures on spacer length m for polymers 4-m as found with DSC: (□) glass transitions; (△) smectic E-smectic A₁ transitions; (o) isotropization transitions; b. Dependence of the isotropization entropy on spacer length m for polymers 4-m as found with DSC.

Influence of mesogen.

The DSC thermograms of polymers 5 and 6 show a genuine T_g and T_i (Figure 7.3). Both polymers show Schlieren or threaded textures that develop upon cooling from the isotropic melt (Figure 7.4). These textures correspond to a nematic mesophase.

Introduction of a cyano group instead of a methoxy group at the mesogen lowers the transition temperatures and reduces the degree of order in the mesophase. This has been observed before for poly(maleic anhydride-*alt*-1-alkene)s that also have polar moieties in the polymer backbone.[5] Poly(methacrylate)s with methoxybiphenyl or cyanobiphenyl mesogens show similar differences in T_i and the degree of order in the smectic mesophase.[21] This has been ascribed to differences in the degree of interdigitation of side-chains, which is partial for cyanobiphenyl-containing polymers and complete for methoxybiphenyl-containing polymers. Furthermore, methoxybiphenyl mesogens have more packing possibilities than cyanobiphenyl mesogens. Due to the strong dipole moment in the cyanobiphenyl mesogen,

107
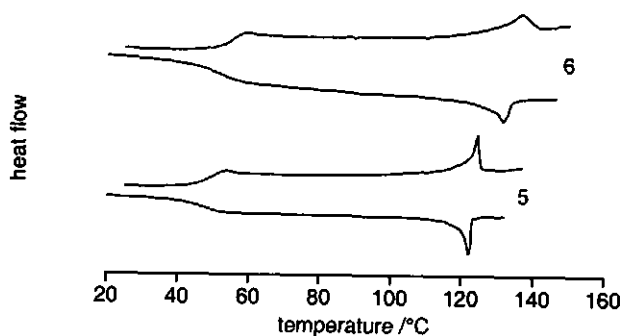
Figure 7.3. DSC thermograms of polymers 5 and 6. For both compounds the second heating and cooling traces are given.

these mesogens organize in antiparallel pairs, whereas methoxybiphenyl mesogens can order in both a antiparallel and a parallel fashion.

Polymer **6** with a methoxyazobenzene mesogen instead of a methoxybiphenyl mesogen showed similar behavior as polymer **5**. Like the cyanobiphenyl mesogen, the methoxyazobenzene mesogen is more polar than a methoxybiphenyl mesogen. Polymer **6**, which has methoxyazobenzene mesogens, has a higher T_i and isotropization entropy change than polymer **5**, which has cyanobenzene mesogens. This can probably be attributed to the larger conjugated system of azobenzenes and the higher molecular weight of polymer **6**. The degree of order in the mesophase for polymer **6** is, however, lower than for polymer **4-4** (nematic and S_E, respectively). This can probably be attributed to the presence of a polar azo moiety in the mesogen for polymer **6**. For poly(MA-*alt*-1-alkene)s with a combination of methoxybiphenyl and azobenzene mesogens, it has been found that the presence of an azo moiety in the mesogen resulted in suppression of the phase separation between the apolar mesogens and the polar polymer backbone.[22] This phase separation was observed only for polymers with apolar methoxybiphenyl mesogens.
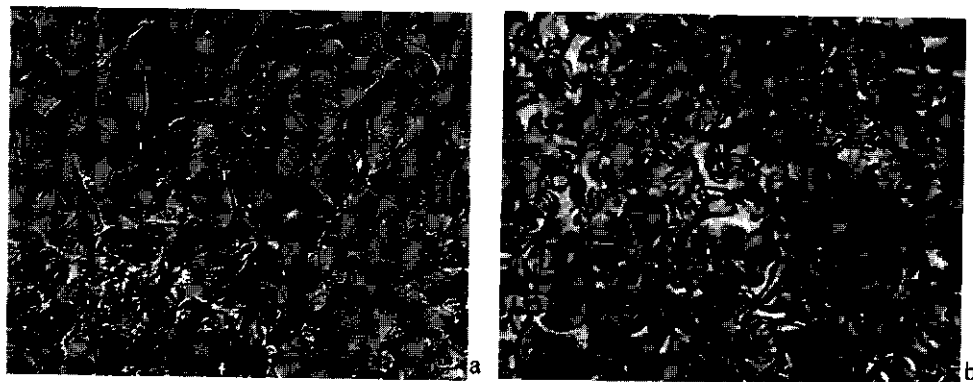
*Figure 7.4. Threaded texture for polymer 5 (a) and Schlieren-texture for polymer 6 (b) as observed with POM.*
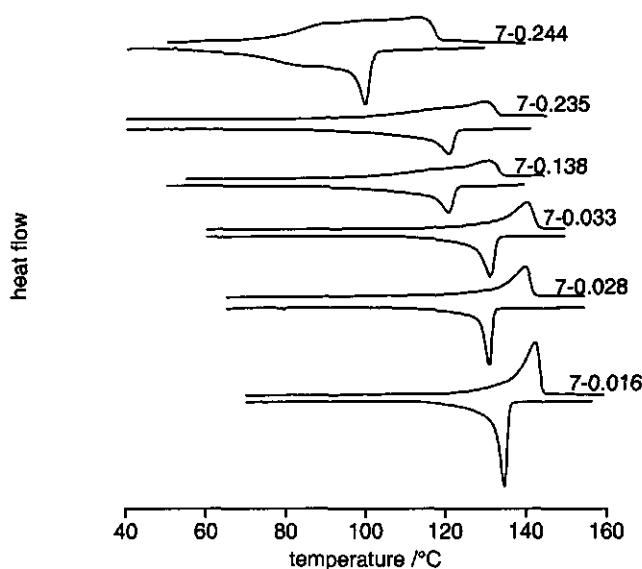
Figure 7.5. *DSC thermograms of polymers 7-x. For all compounds the second heating and cooling traces are given.*

Effect of mesogen density.

POM indicates that polymers 7-x exhibit mesophases that are similar to those of polymers **4-m**, i.e. polymers 7-x exhibit mesophases with a smectic A structure. For the polymers with a low 1-hexene content only T_i and no T_g was observed by DSC (Figure 7.5) similar to polymer **4-4** (Figure 7.1). For polymers **7-0.138, 7-0.235** and **7-0.244** the isotropization was preceded by a genuine transition from glass to S_E. In addition, it can be seen that the width of the isotropization transition increases with decreasing mesogen density. Percec et al. ascribed this widening of the isotropization transition with decreasing mesogen content to dissolution of a fraction of the mesogenic side-chains into the polymer backbone layer.[23] Upon increasing the 1-hexene content not only the mesomorphic behavior is modified, but also the structural and miscibility properties of the copolymer are strongly modified.

T_i decreases with increasing 1-hexene fraction (Figure 7.6a), which can be attributed to dilution of mesogens. In comparison to polymer 4-4, low 1-hexene fractions result in a strong decrease in T_i. T_i levels off above a 1-hexene fraction of 0.033. For poly(olefin-sulfone)s, dilution of mesogens via terpolymerization had a similar effect on melting and isotropization transitions.[24] Above a 1-hexene fraction of 0.235, T_i drops strongly for the poly(ketone)s. Probably, the limiting concentration is approached where the polymer is no longer liquid-crystalline.

The T_g of polymers 7-x also decreases with increasing 1-hexene content (Figure 7.6a). This behavior can be attributed to (i) lower interfering effects of the mesogens on the
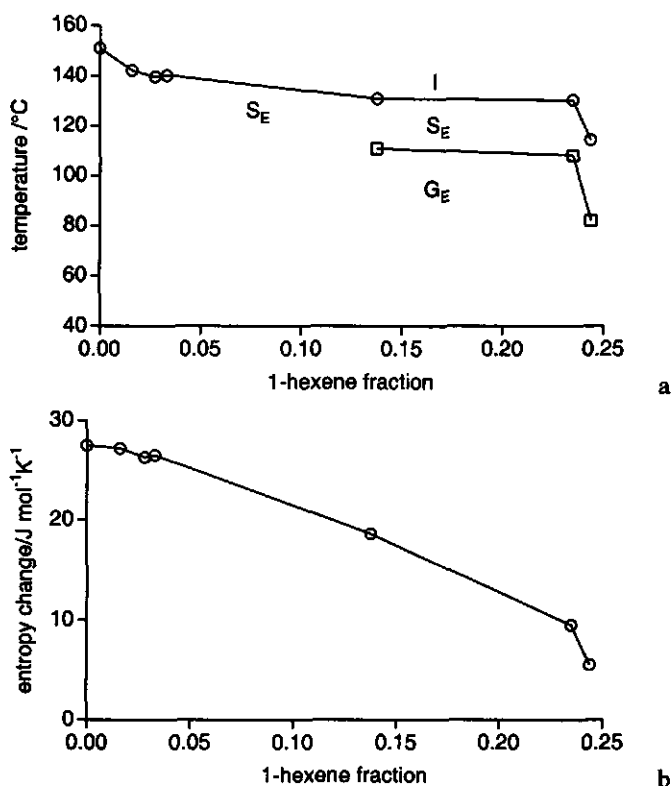
Figure 7.6. *a. Dependence of the transition temperatures as found with DSC of polymers 7-x on 1-hexene fraction (x):* (□) *glass transitions;* (o) *isotropic transitions; b. Dependence of the isotropization entropy as found with DSC of polymers 7-x on 1-hexene fraction.*

polymer backbone at high 1-hexene contents and (ii) the T_g (20°C) of poly(CO-*alt*-1-hexene),[8] which is lower than the T_g of polymer **4-4**.

The effect of 1-hexene content on entropy changes at T_i is presented in Figure 7.6b. The entropy change associated with isotropization shows a gradually decrease with 1-hexene content. The effect of nonmesogenic monomer content on the entropy change associated with isotropization in a SCLCP has been studied before[23] and it was found that the entropy change showed a linear dependence on the nonmesogenic monomer content in the copolymer. Above a 1-hexene fraction of 0.235, the entropy change decreases rapidly , which agrees with the decline observed for T_i.

7.3.4. Mesophase characterization by X-ray diffraction

The degree of interdigitation of side-chains and the type of order within smectic layers has been determined by X-ray diffraction. Table 7.3 shows the experimental *d* spacings and the calculated *d* spacings of smectic layers with completely interdigitated side chains.

Table 7.3. *Experimental d spacings (Å) obtained from wide-angle X-ray diffraction experiments in the mesoglass (at room temperature) and calculated d spacings (Å) for an S_{Al} mesophase of polymers 4-m and 7-x.*

polymer	d spacings		calcd d spacing
4-2	17.4	4.54; 4.00; 3.23	18.6
4-4a	20.5; 10.2; 6.76	4.52; 4.01; 3.23	20.9
4-4b	19.8; 9.92; 6.62	4.48; 3.99; 3.21	20.9
4-9	26.7; 13.5; 8.83	4.43; 3.94; 3.18	26.9
7-0.016	20.0; 10.1; 6.62	4.48; 3.96; 3.20	20.9
7-0.028	20.5; 10.2; 6.75	4.51; 3.99; 3.23	20.9
7-0.033	20.8; 10.3; 6.83	4.51; 3.99; 3.23	20.9
7-0.138	21.5; 10.7	4.51; 3.97; 3.23	20.9
7-0.235	22.3; 11.1	4.51; 3.94; 3.20	20.9
7-0.244	22.4; 11.2	4.49; 3.92; 3.19	20.9

The d spacings were determined in the glassy state at room temperature, after the polymer was cooled down from the isotropic state to the glassy state at a cooling rate of 5°C/s.

From comparison of the experimental and the calculated d spacings, it follows that polymers 4-m and 7-x exhibit smectic mesophases with complete interdigitation of side chains. In the wide-angle area, three peaks were observed that result from (110), (200) and (210) reflections. This means that the mesogens are ordered orthorhombically and the polymers exhibit S_E mesophases. The orthorhombic cell parameters calculated from these reflections are a = 7.94 Å and b = 5.46 Å.

The d spacing increases with 1-hexene content in polymer 7-x, whereas the lateral distance between mesogens does not change (Table 7.3). This has been observed before for poly(siloxane)s with paired mesogens;[25] however, these poly(siloxane)s show a more distinct increase in d spacing upon mesogen dillution. It has been found that the poly(siloxane) backbone is strictly phase separated from the mesogen layers and folds back within an amorphous layer in order to retain the same organization of mesogens as found for backbones with a higher mesogen density. For poly(ketone)s, the low dependence of d spacing on 1-hexene content illustrates that the polymer backbones and mesogens are not strictly phase separated. This is also confirmed by the intensity ratios of the first-order and second-order reflections in the X-ray diffraction pattern: the first-order reflection has a higher intensity than the second-order reflection. For a phase-separated system consisting of distinct polymer backbone layers and mesogen layers an additional maximum in the electron density profile is present. In such a system, the second-order reflection is strong and the first-order reflection vanishes.[26]

7.3.5. Surface polarity of SCLCPs

An important property of polymer films is the surface polarity. The surface polarity determines the adhesion and wetting behavior of other materials, like water or other coatings.
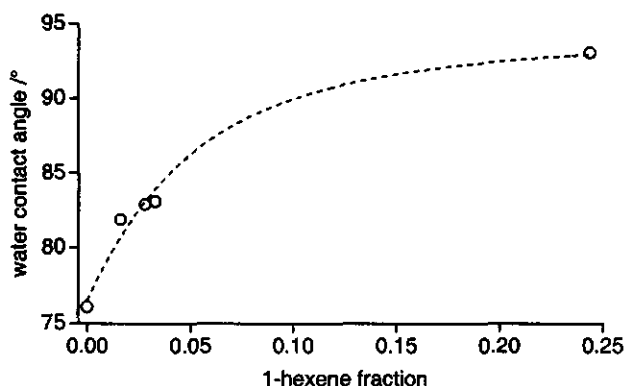
Figure 7.7. *Dependence of the sessile drop contact angle of water on 1-hexene fraction (x) for spincoated films of polymers 7-x.*

A measure for the surface polarity of spincoated films is the contact angle of water. The contact angles of water on spincoated polymer films on glass were determined by the sessile drop technique. For polymers **4-4** and **4-9** water contact angles of 76.1° and 84.8°, respectively were obtained, whereas for poly(propene-*alt*-CO) a value of 82.5° has been reported.[8] This indicates that both the type and length of the side chain govern the water contact angle, which is a measure for the surface polarity of spincoated films.

Although films of both poly(propene-*alt*-CO) and polymer **4-4** have similar water contact angles, these values arise from different structural elements. For poly(propene-*alt*-CO) the surface polarity of a film is presumably dominated by the polar carbonyl group in the polymer backbone. This carbonyl group can be shielded stepwise by increasing the length of the apolar side chain and finally the pendant side chain controls the surface polarity. This has been demonstrated for copolymers of CO with higher 1-alkenes.[8] For the present SCLCPs the side chains also shield the polar carbonyl group. However, depending on the spacer length, the presence of a polar ether linkage in the mesogens increases the surface polarity of the film again. Therefore, it may be concluded that for SCLCPs the side chains control the surface polarity. This was confirmed by increasing the apolar spacer part in the side chains: on going from a butyl to a nonyl spacer the water contact angle increases and the surface polarity decreases.

Surface polarity can also be tuned by incorporation of 1-hexene, which is demonstrated in Figure 7.7. Substitution of relatively polar mesogenic side chains by apolar alkyl side chains yields terpolymers that exhibit an enhanced water contact angle, indicating their reduced surface polarity.

7.3.6. Thermal stability of SCLCPs

With respect to possible applications and processing of these polymers a very important property is the thermal stability. Especially for SCLCPs is interesting to know whether these polymers are thermally stable in the mesophase. The thermal stability of

Table 7.4. *Temperatures (in °C) of 2 % weight loss ($T_{2\%}$) and 50 % weight loss ($T_{50\%}$) as determined by thermogravimetric analysis (TGA).*

polymer	$T_{2\%}$	$T_{50\%}$
4-4	320	440
4-9	250	400
7-0.033	270	380
7-0.138	260	390
7-0.244	260	390

SCLCPs was investigated by TGA measurements under an inert gas atmosphere (N_2). The thermal stability of methoxybiphenyl-containing SCLCPs (Table 7.4) was similar to that of poly(propene-*alt*-CO)s, for which the thermal decomposition starts at about 270°C (weight loss of 2 %), whereas at 400°C a weight loss of 50 % was observed. Only polymer **4-4** showed higher decomposition temperatures: $T_{2\%}$ is 320°C and $T_{50\%}$ is 440°C. In all cases the thermal decomposition of the SCLCPs starts far above T_i.

7.4. Conclusions

Novel SCLC poly(ketone)s were synthesized by Pd(II) catalyzed alternating copolymerization of carbon monoxide and various mesogenic monomers. The molecular weight of these polymers could be altered by changing the amount of methanol. The mesomorphic behavior was easily tuned by changing the molecular composition. The isotropization temperature decreased with increasing spacer length. Furthermore, the glass transition was only observed if the spacer length was longer than 6 methylene units. These polymers exhibited a smectic E mesophase with a periodicity corresponding to S_{A1}. A drastic change in mesophase was observed if cyanobiphenyl or methoxyazobenzene mesogens were used. These polymers exhibit nematic mesophases and, as a result, lower glass transition temperatures.

Another way of tuning the mesomorphic behavior was substitution of mesogens by alkyl side chains. Both the isotropization temperatures and the entropy changes associated with isotropization decreased with increasing 1-hexene content. However, all these terpolymers exhibited a smectic E mesophase. From the ratio of the intensities of the first and second-order reflections in the X-ray diffraction profile, it follows that the polymer backbone is not strictly confined between mesogen layers. The limiting 1-hexene content at which liquid-crystalline behavior may be observed is approximately 0.25.

Surface polarity of the co- and terpolymers based on methoxybiphenyl monomers was governed by the chemical nature of the pendant side chain. The surface polarity can be tuned by increasing the length of the alkyl spacer or by substitution of mesogenic side chains by alkyl side chains. In both cases a decrease of polarity was observed.

113

For the SCLC poly(ketone)s, thermal decomposition started far above the isotropization temperature. The relation between temperature and weight loss in per cent was comparable to poly(propene-*alt*-CO)s.

7.5. References

1   Percec, V.; Pugh, C. *Side Chain Liquid Crystal Polymers*; McArdle, C. B., Ed., Blackie: Glasgow, UK, 1989.

2   Stevens, H.; Rehage, G.; Finkelmann, H. *Macromolecules* **1984**, *17*, 851.

3   Allcock, H. R.; Kim, C. *Macromolecules* **1989**, *22*, 2596.

4   Percec, V.; Rodriguez-Parada, J. M. *Polym. Bull.* **1987**, *17*, 347.

5   Nieuwhof, R. P.; Marcelis, A. T. M.; Sudhölter, E. J. R.; Picken, S. J.; de Jeu, W. H. *Macromolecules* **1999**, *32*, 1398 (Chapter 3).

6   Drent, E.; Budzelaar, H. M. *Chem. Rev.* **1996**, *96*, 663.

7   Abu-Surrah, A. S.; Rieger, B. *Polymerization Catalysis*, in press.

8   Abu-Surrah, A. S.; Wursche, R.; Rieger, B. *Macromol. Chem. Phys.* **1997**, *198*, 1197.

9   Rieger, B.; Abu-Surrah, A. S.; Horn, H. Ch.; Spahl, R.; Müller, H.-J. DE-A patent application 19610358.4 (1996).

10   Abu-Surrah, A. S.; Wursche, R.; Rieger, B.; Eckert, G.; Pechhold, W. *Macromolecules* **1996**, *29*, 4806.

11   Abu-Surrah, A. S.; Eckert, G.; Pechhold, W.; Wilke, W.; Rieger, B. *Macromol. Chem. Rapid Commun.* **1996**, *17*, 559.

12   Vogel, A. I. *Textbook of Practical Organic Chemistry* 5th Ed.; Longman Scientific & Technical: Essex, UK, 1989; p. 949.

13   Hsu, C. S.; Rodriguez-Parada, J. M.; Percec, V. *J. Polym. Sci., Part A: Polym. Chem.* **1987**, *25*, 2425.

14   Xu, F. Y.; Zhao, A. X.; Chien, J. C. W. *Makromol. Chem.* **1993**, *194*, 2579.

15   Jiang, Z.; Sen, A. *J. Am. Chem. Soc.* **1995**, *117*, 4455.

16   Batistini, A.; Consiglio, G.; Sutter, U. W. *Organometallics* **1992**, *11*, 1766.

17   Kacker, S.; Jiang, Z.; Sen, A. *Macromolecules* **1996**, *29*, 5852.

18   Jiang, Z.; Dahlen, G. M.; Houseknecht, K.; Sen, A. *Macromolecules* **1992**, *25*, 2999.

19   Simmonds, D. J. *Liquid Crystal Polymers, From Structures to Applications*; Collyer, A. A., Ed.; Elsevier Applied Science: London and New York, 1992

20   Pugh, C.; Kiste, A. L. *Prog. Polym. Sci.* **1997**, *22*, 601.

21   Craig, A. A.; Imrie, C. T. *Macromolecules* **1995**, *28*, 3617.

22   Nieuwhof, R. P.; Koudijs, A.; Marcelis, A. T. M.; Sudhölter, E. J. R. *Macromolecules* in press (Chapter 4).

23   Percec, V.; Lee, M. *J. Mater. Chem.* **1992**, *2*, 617.

24   Fawcett, A. H.; Szeto, D. Y. S. *Polym. Commun.* **1987**, *8*, 359.

25   Diele, S.; Oelsner, S.; Kuschel, F.; Hisgen, B.; Ringsdorf, H.; Zentel, R. *Makromol. Chem.* **1987**, *188*, 1993.

26   Davidson, P. *Prog. Polym. Sci.* **1996**, *21*, 893.

8

Rheology of side-chain liquid-crystalline copolymers with maleic anhydride moieties in the backbone

Side-chain liquid-crystalline copolymers (SCLCPs) from maleic anhydride and mesogenic 1-alkenes or methacrylates were studied with rheology and temperature-dependent X-ray diffraction. Rheology revealed a transition in the smectic A mesophase that can probably be ascribed to the emergence of rotational diffusion of the mesogen. The viscoelastic behavior of the materials was mainly governed by the mesogenic interactions instead of the polymeric nature of the materials. Temperature-dependent X-ray diffraction revealed drastic changes in the smectic order just below the isotropization transition. For the poly(maleic anhydride-alt-1-alkene) based SCLCP it was found that the smectic Ad-smectic A2 transition was accompanied by a strong decrease in loss and storage modulus and the complex viscosity, whereas the smectic A2-isotropic transition was not accompanied by a significant change in these mechanical properties.

8.1. Introduction

In the previous chapters, the mesomorphic behavior of the side-chain liquid-crystalline polymers (SCLCPs) has been characterized with common techniques like polarizing optical microscopy, differential scanning calorimetry and X-ray diffraction. These techniques give information about whether mesophases can be formed, which type of mesophase is formed and in which temperature range they exist. However, these techniques provide no information about the dynamic behavior of the polymers. The dynamic behavior of polymers strongly changes at transitions that can be attributed to changes in local motions of the side chains or the backbone. Therefore, techniques that monitor the molecular dynamics may reveal transitions that remain indiscernible with other techniques. Three

techniques that provide information about the molecular dynamics are dynamic mechanical analysis (DMA), rheology and dielectric relaxation spectroscopy (DRS). DMA is used to study the mechanical properties around and below the glass transition, whereas rheology is used to study the flow-properties above the glass transition. DRS provides information about the dynamic behavior of dipolar moieties in the polymer over a wide frequency and temperature range.

Rheological experiments can be a powerful tool in characterizing SCLCPs above their glass transition or melting point. Because the viscoelastic properties are very sensitive to structural changes, transitions can be detected that are not characterized by strong changes in thermal properties. For SCLCPs this means that transitions may be observed that remain indiscernible with common techniques like DSC or polarizing optical microscopy. Furthermore, rheology can provide information about the effect of an applied shear force on the behavior of the polymer backbone and the mesogenic moieties. With respect to the applications of SCLCPs it is necessary to study their rheological behavior, not only for anticipating their flow during processing, but also for being able to manipulate their alignment through processing.

Although a considerable amount of work has been done on the rheological behavior of main-chain liquid-crystalline polymers,[1,2] relatively little research has been devoted to SCLCPs. Characteristic of this class of liquid-crystalline polymers is the presence of rigid mesogenic groups in the side chains. The decoupling between the motions of the mesogens and the polymer backbone leads to a complex flow behavior, and the final properties of processed liquid-crystalline polymers depend on the microstructure developed during processing. In order to understand the complex behavior of SCLCPs, an increasing amount of studies has been devoted to the viscoelastic properties of these polymers.[3-13]

This study concerns the rheological experiments of polymers that are representatives of two types of previously described polymers,[14,15] since we are especially interested in the mechanical behavior of these polymers in both the mesophase and the melt (see Chapter 1).

The majority of rheologic studies report viscoelastic properties which have been determined with oscillatory shear measurements. In these experiments the shear strain γ varies sinusoidally in time t

$$\gamma = \gamma_0 \sin(\omega t). \tag{8.1}$$

The measured shear stress σ is sinusoidal with the same frequency ω, but shifted in phase by phase angle δ that depends on the angular frequency ω

$$\sigma = \sigma_0 \sin(\omega t + \delta). \tag{8.2}$$

The work we report corresponds to the linear viscoelastic regime that is observed at sufficiently low strain amplitudes. In this linear viscoelastic regime, the stress amplitude σ_0 is proportional to γ_0 and, consequently, the material properties G' and G" are only dependent on the angular frequency ω. The stress σ in the linear viscoelastic regime is described by

$$\sigma = \gamma_0 (G' \sin(\omega t) + G'' \cos(\omega t)). \tag{8.3}$$

Herein G' and G'' are the storage and loss modulus, respectively. In the case of a purely elastic material $G'' = 0$, and in the case of a purely viscous material $G' = 0$.

8.2. Experimental part

The dynamic mechanical measurements were performed on a Rheometrics RMS800 mechanical spectrometer with a plate-plate geometry (diameter 25 mm, distance between plates 2 mm). The strain was adjusted during measurements because of phase transitions. The measurements were performed upon cooling. A frequency sweep was preceded by a pause of 5 min. in order to stabilize the temperature.

X-ray diffraction measurements were performed on a Siemens D5000 reflection diffractometer with a HTK oven and Cu Kα radiation.

8.3. Results and discussion

8.3.1. Synthesis and phase behavior

The rheological behavior was studied for two different types of polymers shown in Scheme 8.1. These polymers consist of a poly(maleic anhydride-*alt*-1-alkene) or a
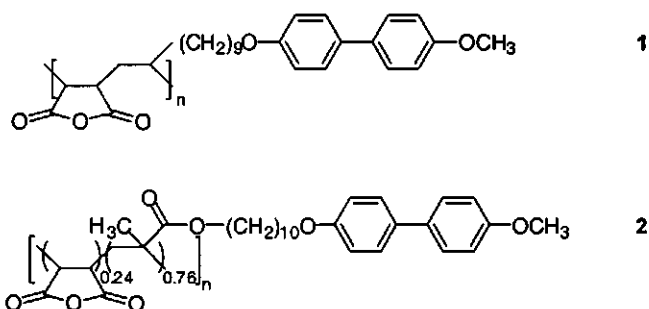
Scheme 8.1. Structure of polymers 1 and 2.

Table 8.1. Phase transition temperatures (°C) and the phase types[a] of polymers 1 and 2.

polymer	phase behavior						
1	G_{Bhex}	101	S_{Bhex}	111	S_{Ad}	165	I
2	G_{Bcryst}	88[b]	S_{Bcryst}	100	S_{Al}	140	I

[a] I = *isotropic phase;* S_{Ad} = *smectic A mesophase with partially interdigitated side chains;* S_{Al} = *smectic A mesophase with fully interdigitated side chains;* S_{Bhex} = *hexatic smectic B;* S_{Bcryst} = *crystalline smectic B;* G_X = *mesoglass, in which X is the vitrified mesophase.*
[b] *determined during the first heating scan.*

poly(maleic anhydride-methacrylate) backbone, respectively, with methoxybiphenyl-containing side chains. The synthesis and characterization of the polymers has been reported elsewhere.[14,15] The thermal properties of these polymers are collected in Table 8.1. The degree of polymerization of polymers 1 and 2 is rather low, i.e. 18. From Table 8.1 it can be seen that polymers 1 and 2 exhibit mesophases with different degrees of interdigitation of the side chains: for polymer 1 the side chains are partially interdigitated, whereas for polymer 2 the side chains are fully interdigitated. Both polymers 1 and 2 exhibit smectic B and smectic A mesophases.

8.3.2. Rheological measurements

Complex viscosity of polymers 1 and 2

In Figure 8.1a and b, the complex viscosity (η^*) and the storage (G') and loss (G") modulus at an angular frequency of 1 rad s^{-1} (so that $\eta^* = G^* = G' + iG"$) are shown as a function of temperature for polymers 1 and 2, respectively. The transitions observed with rheological measurements agree well with the transition temperatures observed with DSC (Table 8.1) except for the isotropization transition of polymer 1. Furthermore, for both polymers 1 and 2 rheological measurements reveal an additional transition in the S_A meso-
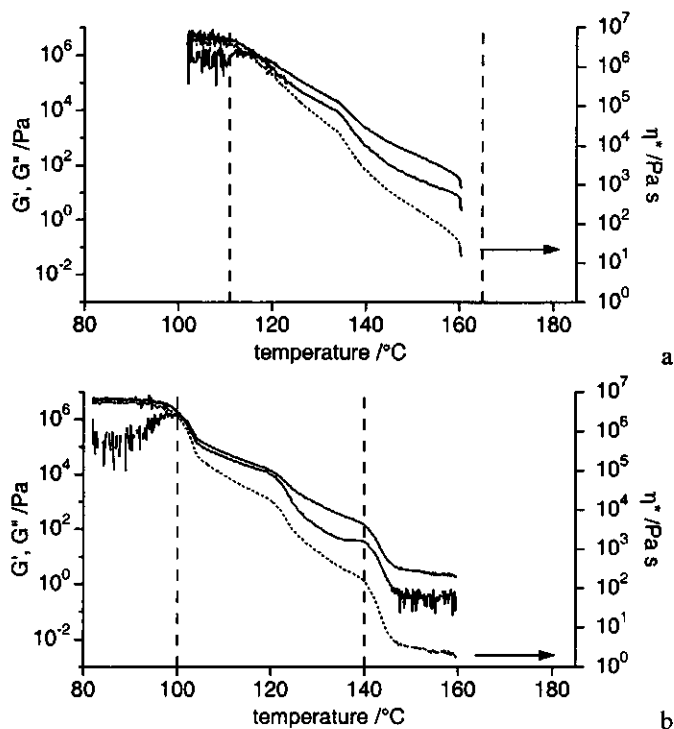
Figure 8.1. *The complex viscosity* η^* *(···), the storage G' (lower solid curve) and loss G" (upper solid curve) modulus (ω = 1 rad s^{-1}) versus temperature for polymers 1 (a) and 2 (b).*

phase that was not observed with DSC. Temperature-dependent X-ray diffraction experiments were performed to obtain additional information about this phase transition (Section 8.3.3.).

On going from the S_B to the S_A mesophase, polymers **1** and **2** show different changes in mechanical behavior. For polymer **2**, the S_B-S_A transition at 101°C is accompanied by a strong decrease in complex viscosity, whereas this transition is hardly visible for polymer **1**. This can probably be attributed to the difference in order in the S_B mesophases of both polymers. Polymer **1** exhibits an S_{Bhex} mesophase, in which there is long-range bond-orientational order but only short-range positional order. Polymer **2** exhibits a S_{Bcryst} mesophase with a higher degree of order than the S_{Bhex} mesophase. In the S_{Bcryst} mesophase there is both long-range orientational and positional order. Therefore, the S_{Bcryst}-S_A transition is accompanied by a stronger decrease in mechanical properties than the S_{Bhex}-S_A transition.

Polymer 1

The rheological results of polymer **1** are depicted in Figure 8.2, where the storage (G') and loss modulus (G") are plotted against the angular frequency at 5°C intervals. The transitions of the polymer are represented by clear gaps between the curves in these plots. Clear gaps in both moduli can be observed between 131°C and 136°C and 156°C and 161°C. The first transition was not observed with DSC, whereas the second transition corresponds to the isotropization transition (Table 8.1). It is obvious that the largest gap in modulus can be observed near the clearing point. Such a large gap in modulus is characteristic for S-I and S-N transitions.[3,4,11,12]

Polymer **1** does not exhibit the usual rubber plateau at approximately 10^5 Pa where the storage modulus is almost independent of frequency. For common thermoplastics, this
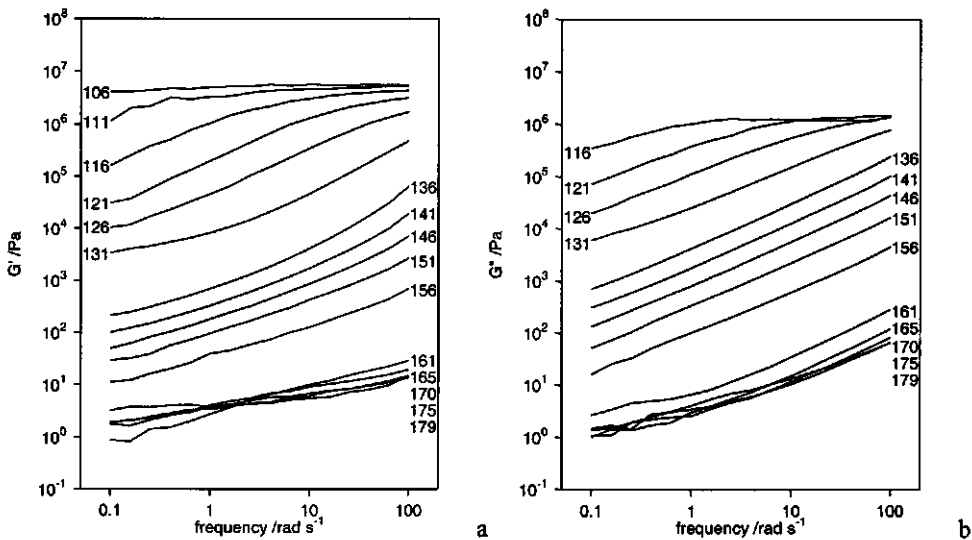
Figure 8.2. *Rheological spectra of polymer 1: storage modulus (a) and loss modulus (b).*

rubber plateau is a result of chain entanglements, which act as physical crosslinks between polymer chains. In a certain frequency range, these physical crosslinks will be disrupted by applying shear to the polymer sample. The absence of a rubber plateau at 10^5 Pa can probably be attributed to the molecular weight of polymer **1** ($M_n = 4.05 \cdot 10^3$, $M_w = 5.43 \cdot 10^3$),[14] which is too low for allowing chain entanglements. For comparison, SCLC poly(methacrylate)s have an entanglement molecular weight, i.e. the molecular weight of the polymer chain between two entanglements, of roughly $2 \cdot 10^5$.[16]

At 106°C, the storage modulus is constant at a value of $5 \cdot 10^6$ Pa over a frequency range of three decades (Figure 8.2a). This indicates the presence of a highly ordered phase, which agrees with the S_B mesophase observed with X-ray diffraction (Table 8.1). The highly ordered domains behave as physical crosslinks between polymer backbones and therefore result in a kind of rubber plateau with a very high value (Figure 8.2a). This high degree of order disappears above 111°C, which corresponds to the S_{Bhex}-S_{Ad} transition observed with DSC and X-ray diffraction (Table 8.1).

Between 136°C and 156°C and at low frequencies, the storage modulus levels off and becomes less dependent of frequency. The value of the resulting plateau is, however, significantly lower than the rubber plateau of common thermoplastics. This indicates the presence of physical crosslinks, i.e. interactions between mesogens of different polymer backbones.[13] In other words: the viscoelastic behavior of these materials is mainly governed by the mesogenic interactions instead of the polymeric nature of these materials.

The physical crosslinks even remain present in the melt, as can be seen from the frequency independence of the storage modulus at low frequencies above 161°C (Figure 8.2a). The level of the resulting plateau is considerably lower than in the mesophase, which indicates that the isotropic melt is a dynamic system in which the mesogens associate and
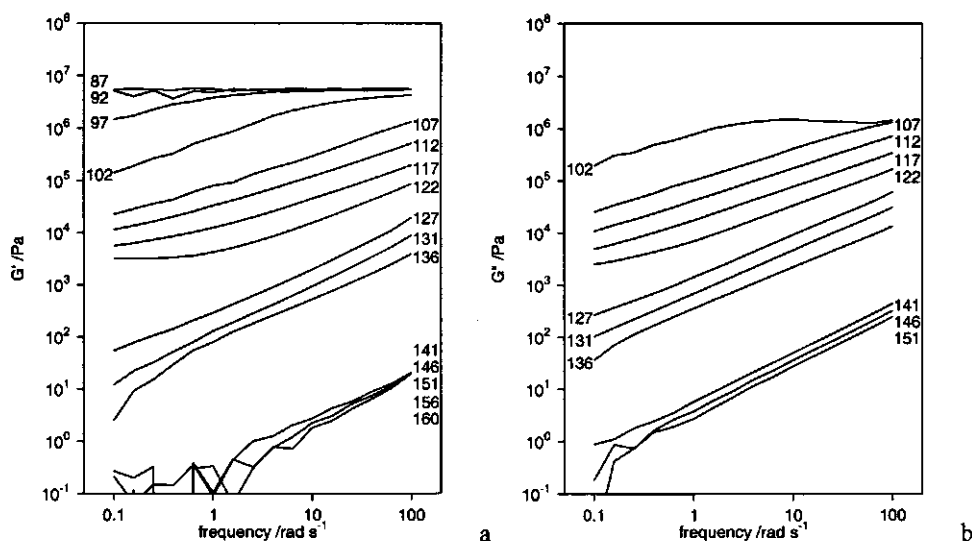

Figure 8.3. Rheological spectra of polymer 2: storage modulus (a) and loss modulus (b).

dissociate continuously. Although the values of the dynamic moduli are rather low at temperatures above 160°C, the polymer does not behave like a Newtonian liquid. The slopes of G' and G" deviate strongly (Figure 8.2) from those which are obtained for liquidlike behavior, in which case they are 2 and 1 for G' and G", respectively.

Polymer 2

The results of the rheologic measurements of polymer **2** are shown in Figure 8.3, where the storage (G') and loss modulus (G") are plotted against the angular frequency. Clear gaps in the moduli are present between 102°C and 107°C, 122°C and 127°C, and 136°C and 141°C. The first and last transitions correspond to the S_{Bcryst}-S_{A1} and isotropization transition respectively (Table 8.1). The second transition was not observed with DSC.

The behavior of polymer **2** is comparable to that of polymer **1**. At 87°C and 92°C polymer **2** exhibits a highly ordered mesophase. No evidence for a glass transition was observed. Between 107°C and 122°C, a rubber plateau can be observed at low frequencies, indicating interactions between mesogens that act as physical crosslinks. The strong drop in dynamic moduli between 136°C and 141°C suggest the transition from a smectic mesophase to the isotropic melt.

8.3.3. Temperature-dependent X-ray diffraction

The rheological measurements have shown that polymers **1** and **2** exhibit a transition that has not been observed with DSC. Furthermore, the highest temperature transition of polymer **1** occurs at a significantly lower temperature than the isotropization temperature. Therefore, temperature dependent X-ray diffraction measurements have been performed in order to determine whether these transitions are accompanied by structural changes in the smectic order.

Figures 8.4a and b display the temperature dependent X-ray diffraction profiles of polymers **1** and **2**. Previous studies[14,15] have shown that these profiles correspond to mesophases with a periodicity corresponding to S_{Ad} and S_{A1} for polymers **1** and **2**, respectively. For both polymers **1** and **2**, the first-order reflection in the X-ray diffraction pattern is of a lower intensity than the second-order reflection. This can be attributed to an additional plane of symmetry in the electron density profile, which means that the polymer backbones and the mesogens are phase separated. The additional plane of symmetry induces an apparent *d* spacing (the strongest small angle reflection) which is half the smectic *d* spacing. Because the electron densities in the polymer backbone and the mesogen layers are not exactly equal, the first-order reflection can still be observed.[14,15] Additionally, at low temperatures, a very weak third-order reflection is visible for both polymers.

X-ray diffraction (Figures 8.4a and b) shows an almost continuous decrease in intensity of the reflections with increasing temperature. Furthermore, no shift of the first-, second-, and third-order reflections was observed in the smectic mesophases. This indicates that the transitions at 131-136°C and 122-127°C observed with rheological measurements for polymers **1** and **2**, respectively, are not accompanied by changes in the smectic order.
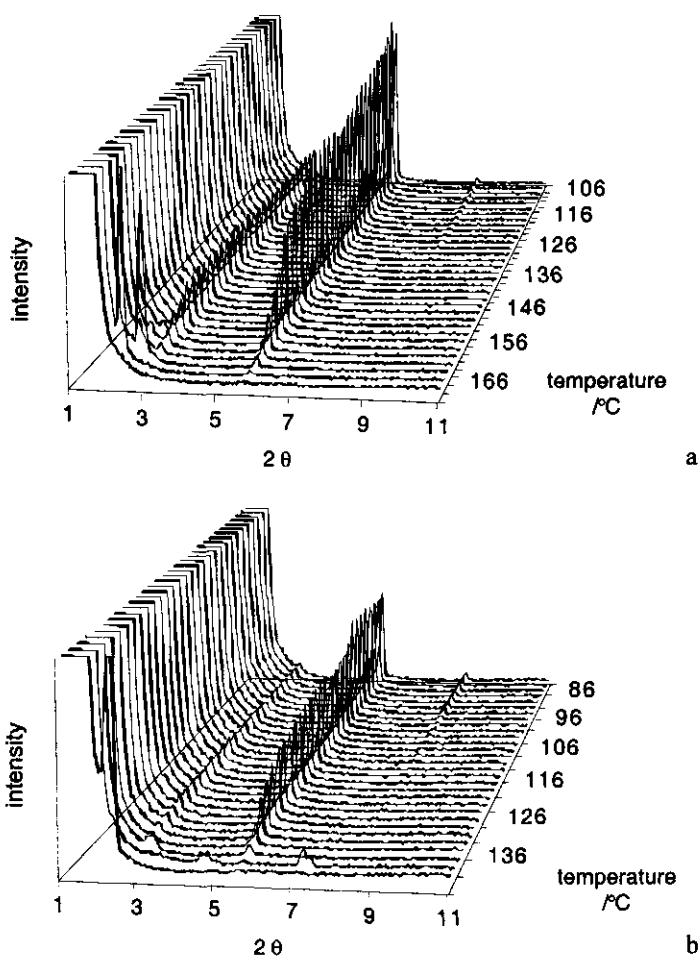
Figure 8.4. *Temperature dependent wide-angle X-ray diffraction patterns of polymer 1 (a) and polymer 2(b).*

Just below the isotropization transition, both polymers **1** and **2** exhibit drastic changes in the smectic structure. For polymer **1**, an additional reflection can be observed between 156°C and 168°C corresponding to a smectic structure with a *d* spacing larger than that of the original S_{Ad} mesophase. This *d* spacing increases with temperature and corresponds to a S_{A2} mesophase with a *d* spacing of 41 Å at 168°C. Rheological measurements at an angular frequency of 1 rad s^{-1} (Figure 8.1a) showed that the development of the S_{A2} mesophase is accompanied by a drastic decrease in complex viscosity and the storage and loss modulus (Figure 8.2). These material properties do not change significantly on going from the S_{A2} mesophase to the isotropic melt.
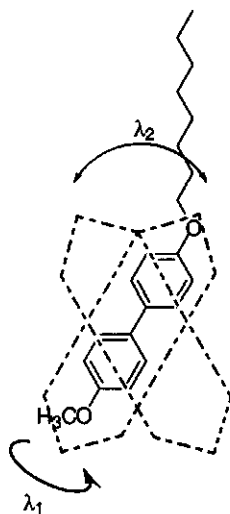
Scheme 8.2. *Schematic representation of the rotational diffusion of the mesogen around the short axis.*

For polymer **2**, the S_{A1} mesophase transforms into an S_{Ad} mesophase at 142°C with a *d* spacing of about 39 Å. This mesophase remains present for about 2°C before it transforms into the isotropic melt at 144°C. For this polymer, the S_{A1}-S_{Ad} and/or S_{Ad}-I transitions are accompanied by a large change in mobility. Because both transitions occur in a small temperature range it is not possible to assign the change in mechanical properties to a specific phase transition.

Since for both polymers **1** and **2** the transitions observed in the S_A mesophase are not accompanied by changes in the smectic order, the decrease in mechanical properties must have another origin. Because relaxations of the main-chain are active in the whole temperature area above the glass transition, a possible explanation for the observed transition may be a relaxation of the side-chain that shows up above 131°C and 122°C for polymers **1** and **2**, respectively. From dielectric spectroscopy it is known that two side-chain relaxations emerge in the S_A mesophase, i.e. rotational diffusion of the mesogen around the long axis (λ_1) and around the short axis (λ_2) of the mesogen (Scheme 8.2).[17,18,19] Of these two relaxations, the relaxation around the short axis of the mesogen can not be monitored with dielectric relaxation spectroscopy for the present polymers, due to the absence of a significant dipole moment in the symmetric bisalkoxybiphenyl. Therefore, the relaxation around the short axis, which is the slowest relaxation of the two mesogenic relaxations, is not dielectrically active. The change in dielectric properties as a function of the temperature and frequency are therefore attributed to rotational diffusion of the mesogen.

8.4. Conclusions

Rheology is very effective for studying the molecular dynamics of SCLCPs in the mesophase, since it reveals transitions that remain indiscernible with DSC and polarizing optical microscopy. The mesophase transition temperatures observed with rheology agree well with those observed with DSC and polarizing optical microscopy.

Since the additional transition in the S_A mesophase is not accompanied by changes in the smectic order, it can be concluded that this transition is due to the emergence of a relaxation that corresponds to rotational diffusion of the mesogen.

The viscoelastic behavior of these materials is mainly governed by the mesogenic interactions instead of the polymeric nature of these materials. Besides the interactions between mesogens in the smectic mesophases, which act as physical crosslinks, there are also interactions between mesogens in the melt albeit in a smaller amount. The polymer melt does not behave as a Newtonian liquid.

Temperature-dependent X-ray diffraction shows drastic changes in the smectic order just below T_i. For the poly(MA-*alt*-1-alkene) based SCLCP, the S_{Ad} mesophase transforms into an S_{A2} mesophase that is accompanied by a strong decrease in mechanical properties. In contrast, no significant change in mechanical properties is observed at the S_{A2}-I transition. For the poly(MA-methacrylate) based SCLCP the S_{A1} mesophase transforms into an S_{Ad} mesophase before becoming isotropic.

8.5. References

1   Kim, S. S.; Han, C. D. *J. Rheol.* **1993**, *37*, 847 and references cited therein.
2   Han, C. D.; Chang, S.; Kim, S. *Mol. Cryst. Liq. Cryst.* **1994**, *254*, 335 and references cited therein.
3   Pakula, T.; Zentel, R. *Makromol. Chem.* **1991**, *192*, 2401.
4   Colby, R. H.; Gillmor, J. R.; Galli, G.; Laus, M.; Ober, C. K.; Hall, E. *Liq. Cryst.* **1993**, *13*, 233.
5   Gallani, J. L.; Hilliou, L.; Martinoty, P.; Keller, P. *Phys. Rev. Lett.* **1994**, *72*, 2109.
6   Rubin, S. F.; Kannan, R. M.; Kornfield, J. A.; Boeffel, C. *Macromolecules* **1995**, *28*, 3521.
7   Laus, M.; Ferrie, D. *J. Polym. Sci.: Part B: Polym. Phys.* **1996**, *34*, 1085.
8   Chang, S.; Dae Han, C. *Macromolecules* **1997**, *30*, 2021.
9   Berghausen, J.; Fuchs, J.; Richtering, W. *Macromolecules* **1997**, *30*, 7581.
10 Craig, A. A.; Winchester, I.; Madden, P. C.; Larcey, P.; Hamley, I. W.; Imrie, C. T. *Polymer* **1998**, *39*, 1197.
11 Zentel, R.; Wu, J. *Makromol. Chem.* **1987**, *188*, 665.
12 Yamaguchi, T.; Iwamoto, Y.; Asada, T. *Polym. Bull.* **1991**, *192*, 611.
13 Rottink, J. B. H.; te Nijenhuis, K.; Addink, R.; Mijs, W. *J. Polym. Bull.* **1993**, *31*, 221.
14 Nieuwhof, R. P.; Marcelis, A. T. M.; Sudhölter, E. J. R.; Picken, S. J.; de Jeu, W. H. *Macromolecules* **1999**, *32*, 1398 (Chapter 3).

15 Nieuwhof, R. P.; Marcelis, A. T. M.; Sudhölter, E. J. R. *Macromol. Chem. Phys.* in press (Chapter 6).

16 Kannan, R. M.; Kornfield, J. A.; Schwenk, N.; Boeffel, C. *Macromolecules* **1993**, *26*, 2050.

17 Moscicki, J. K. *Liquid Crystal Polymers: From Structures to Applications*; Collyer, A. A., Ed.; Elsevier Applied Science: London and New York, 1992.

18 Haws, C. M.; Clark, M. G.; Attard, G. S. In *Side Chain Liquid Crystal Polymers*; McArdle, C. B., Ed.; Blackie: Glasgow, UK, 1989.

19 Simon, G. P. *Dielectric Spectroscopy of Polymeric Materials*; Runt, J. P.; Fitzgerald, J. J., Eds.; ACS: Washington, DC, 1997.

9

Langmuir and Langmuir-Blodgett films of side-chain liquid-crystalline poly(maleic acid-alt-1-alkene)s

The formation and transfer of Langmuir layers of side-chain liquid-crystalline (SCLC) poly(maleic acid-alt-1-alkene)s with biphenyl mesogens on aqueous subphases was studied by the use of the Langmuir-Blodgett technique. Brewster angle microscopy showed that the SCLCPs with methoxybiphenyl mesogens strongly aggregate on the water subphase and form islands. These islands merge upon compression. In contrast, SCLCPs with cyanobiphenyl mesogens spread nicely. Compression of these polymers resulted in the formation of triple layers. Langmuir monolayers of SCLCPs with methoxybiphenyl mesogens show Z-type transfer. AFM and X-ray reflectivity measurements of the resulting Langmuir-Blodgett mono- and/or multilayers indicate that the side chains of these polymers are possibly tilted. The multilayers have a double layer periodicity, which requires a reorientation of the side chains during or after transfer. Annealing of these Langmuir-Blodgett films resulted in an increase of the mean film thickness and a more uniform d spacing within the multilayer. With AFM droplets were observed on top of the multilayer indicating dewetting of the upper layer.

9.1. Introduction

The Langmuir-Blodgett (LB) technique consists of successive transfer of a Langmuir monolayer to a substrate and allows the fabrication of ultrathin films with controllable thickness[1]. This well-controlled transfer results in LB-films that are ordered at a molecular level. Therefore, these films have attracted considerable attention in the field of electro-optical and information storage devices.[2,3,4,5] The ordered structure of LB-films also makes these films interesting for model studies of thin films of side-chain liquid-crystalline copolymers.[6,7,8] To understand the built-up of this layered structure, detailed analysis of the Langmuir monolayer is necessary.[9,10]

127

A class of polymers that has been applied successfully in LB technology is polymers containing maleic anhydride moieties.[11,12,13,14,15,16,17,18,19,20,21,22] Although the majority of the studied polymers contains alkyl side chains,[12-15,19-22] some polymers have been reported having mesogen-containing side chains.[11,16-18] Recently, novel poly(maleic anhydride-*alt*-1-alkene)s were synthesized with methoxybiphenyl or cyanobiphenyl mesogens in the side chain.[23] Whereas the polymer with cyanobiphenyl mesogens exhibits a nematic mesophase, the polymers with methoxybiphenyl mesogens exhibit smectic A or higher ordered mesophases.[23] Van der Wielen et al. [24,25] studied the behavior of some of these polymers in spincoated films on silica. After annealing above the glass transition, he found that the spincoated film adopts a smectic structure with a *d* spacing comparable to that in the bulk. At the polymer-substrate interface the side chains lie flat on the surface.

The present study describes the monolayer behavior on water of several side-chain liquid-crystalline copolymers with maleic acid moieties in the backbone. The maleic acid moieties in the copolymer are expected to improve the adhesion.[26,27,28,29,30] The monolayer behavior has been studied by recording surface pressure-area isotherms and Brewster-Angle microscopy (BAM). In addition, the monolayer behavior of polymers with a doubled mesogen density[31,32] has been studied. Langmuir monolayers of a polymer with methoxybiphenyl mesogens have been transferred to glass and silica substrates. The properties of the resulting LB-films have been studied by X-ray reflection and atomic force microscopy. Finally, the properties of LB-films are compared to those of spincoated films as described by van der Wielen et al.[24,25]

9.2. Experimental

9.2.1. Materials

The water for the subphase was purified by filtration through a Seralpur Pro C90 purification system. The solvents that were used were commercially available and used without further purification. The synthesis and characterization of the polymers has been described elsewhere.[23,31,32]

9.2.2. Methods

The surface pressure-area isotherms were recorded on a Lauda FW2 Filmwaage, which was thermostated at 25°C. The polymers were spread from chloroform/DMSO solutions (98/2 v/v) (1 mg/mL) onto the aqueous subphase by use of a Hamilton syringe. After spreading, the monolayer was allowed to equilibrate for 10 min. before compression started. A compression rate of 2 $Å^2$/(repeating unit min.) was used.

Monolayers were transferred onto both hydrophobic and hydrophilic glass and silicon oxide substrates at a constant pressure of 15-20 mN/m for polymer **1-9,0**. The substrates were cleaned with chloroform, treated with 30% H_2O_2/25% NH_3-solution (caution) and ultrapure

water (1/1/5 v/v/v) at 50 - 80°C for 30 min., washed with ultrapure water, sonified in 5% HCl in water for 15 min., dipped into ultrapure water, sonified in methanol for 15 min., sonified in methanol/chloroform (3/1 v/v) for 15 min, and sonified in chloroform for 15 min. The substrates were stored in methanol. Before use the substrates were dried by purging with a stream of nitrogen. Some substrates were hydrophobized by standing in 1,1,1,3,3,3-hexamethyldisilazane for 24 h.

The Brewster angle microscope was home-built. Technical details on the assembly of this microscope are published elsewhere.[33]

The X-ray reflectivity measurements were performed with a 2-circle-diffractometer using the CuKα_1-radiation of a rotating anode. The collimation of the beam was effected by a primary graphite monochromator and the slit setting which led to a resolution in q_z direction of $4 \cdot 10^{-3}$. The data were scaled to unit incident intensity and corrected for the variance of the illuminated sample area at small incidence angles as well as for the background scattering. The data were analyzed according to a matrix-iterative formalism derived from Fresnels equations[34,35] by taking into account the deviation from the ideal decay of the reflectivity for a perfectly smooth surface due to the presence of roughness. AFM measurements were executed in the tapping mode with a commercial ND-MDT microscope in ambient air. Annealing of the LB film was done under nitrogen atmosphere at 135°C.

Hydrolysis of polymers

The maleic anhydride moieties in all polymers except polymers **5-*m*** were hydrolyzed by dissolving 0.2 g of polymer in a tetrahydrofuran/water mixture (95/5 v/v) followed by refluxing during 48 hrs. The reaction mixture was poured into hexane, which resulted in precipitation of the polymer. The polymer was obtained as a white powder by filtration. FTIR showed that all maleic anhydride moieties were ring-opened to maleic acid moieties. This process was characterized by the disappearance of the symmetric and antisymmetric stretching bands at 1861 and 1780 cm^{-1} typical for an anhydride and the appearance of the C=O stretching band at 1733 cm^{-1} characteristic for a carboxyl group.[23] TLC showed that the ester bonds in polymers **2** and **6** were not cleaved under these conditions.

9.3. Results and discussion

9.3.1. Langmuir films of alternating polymers with maleic anhydride moieties

Figures 9.1a and b show the π – A isotherms of polymers **1-*m,p*, 2, 3** and **4** (Scheme 9.1). The corresponding surface areas per repeating unit, i.e. per alternating pair of monomer units in the backbone, are summarized in Table 9.1. The surface areas per repeating unit of compounds **1-*m,p*** and **2** are smaller than the values of 0.39 and 0.37 nm^2 of poly(maleic acid-*alt*-hexadec-1-ene)[14] and poly(maleic acid-*alt*-octadec-1-ene), i.e. polymer **4**. This may result from the degree of polymerization: low molecular weight polymers are compressed more easily to relatively compact and ordered monolayers than high molecular weight polymers.
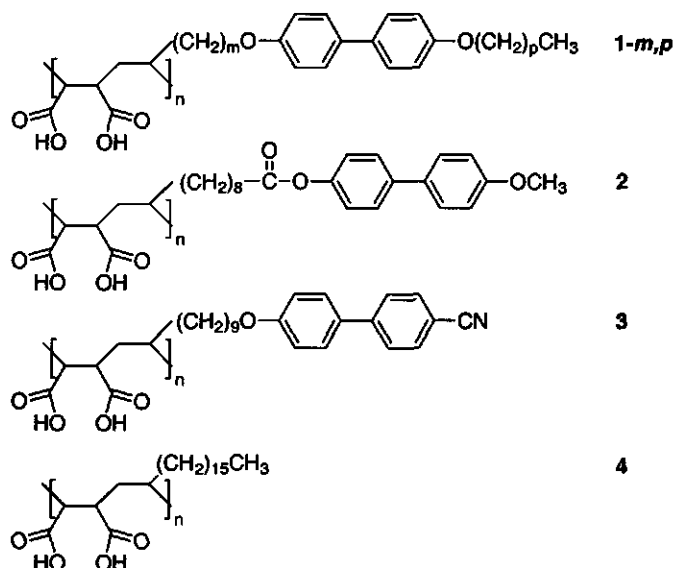
Scheme 9.1. *Molecular structure of polymers 1 - 4.*
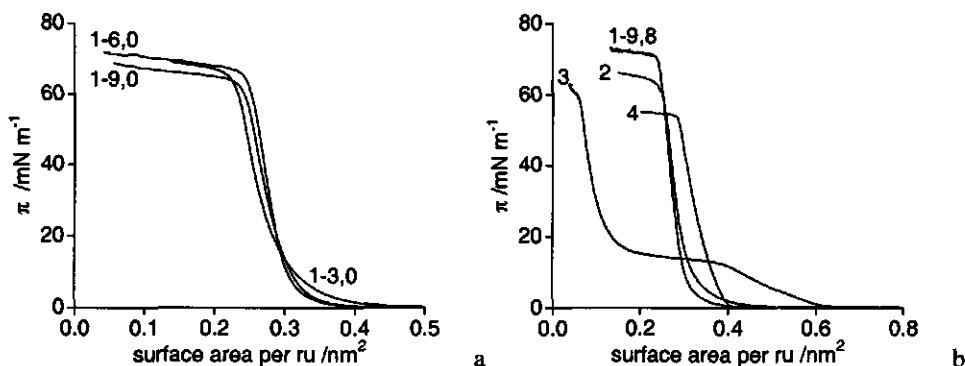
Figure 9.1. $\pi - A$ *Isotherms of polymers 1-m,0 (a) and 1-9,8; 2 - 4 (b).*

Furthermore, the mesogen-mesogen interactions of the SCLCPs may result in more compact aggregates. The degrees of polymerization of poly(maleic acid-*alt*-hexadec-1-ene) and poly(maleic acid-*alt*-octadec-1-ene) are 230 and 64 respectively, while the present polymers have degrees of polymerization of about 18.

The surface areas per repeating unit of compounds **1-m,p** - **4** (Table 9.1) are much larger than the cross-sectional area of a methylene chain combined with a biphenyl mesogen (approximately 26 Å^2). This means that the polymer backbone determines the minimal area necessary to accommodate the repeating units and the interactions between the mesogens do not influence this area. Probably, the hydrophilic head groups are large and therefore they

Table 9.1. *Properties of Langmuir films.*

| polymer | area per repeating unit | |
	0 mN/m, nm^{2} [a]	30 mN/m, nm^2
1-3,0	0.30	0.267
1-6,0	0.31	0.279
1-9,0	0.31	0.276
1-9,8	0.30	0.276
2	0.31	0.285
3	0.61	0.098
4	0.37	0.321
5-3	0.51	0.454
5-6	0.51	0.474
6	0.54	0.472

[a] *By extrapolation of the linear section of the isotherm to zero pressure.*

include both carboxylic acid groups; i.e. both these groups are in contact with the water surface.

The isotherms shown in Figure 9.1a are relatively steep with high collapse pressures, suggesting that the compressed films are well ordered. This was confirmed for polymer **1-9,0** by temperature dependent measurements, which showed that the surface area per repeating unit increased only by about 0.01 nm on going from 11 to 42°C. There is an interesting trend in the quality of the isotherms, and presumably the order in the monolayers, as the length of the spacer increases. For nonyl and hexyl spacers the shape of the isotherms does not differ significantly; the surface area per repeating unit for different surface pressures are similar (Table 9.1 and Figure 9.1a). For a propyl spacer, however, the isotherm is less steep and the pressure increases at a higher surface area than for polymers **1-9,0** and **1-6,0**. This indicates that, for short spacers, the arrangement of the polymer backbone determines the orientation of the mesogens, i.e. the motions of the mesogens are coupled to motions of the polymer backbone as has already been described in the spacer-decoupling effect for SCLCPs.[36]

Figure 9.1b shows that the isotherms of polymers **1-9,8** and **2** have shapes comparable to those of polymers **1-*m*,0**. However, the isotherm of polymer **1-9,8** is somewhat steeper and has a lower area per repeating unit at 0 mN/m (Table 1) indicating a higher degree of order in the monolayer. This behavior is comparable to that of the bulk, which showed that the degree of order in the mesophase increased with the length of the mesogenic tail.[23]

Polymer **3**, which contains cyanobiphenyl mesogens, has a surface area per repeating unit that is considerably larger than that of polymers with apolar mesogenic substituents. This can be ascribed to interactions between the polar mesogenic tails and the water surface. Everaars et al. observed that double-chained ammonium amphiphiles containing cyanobiphenyl mesogens can adopt a flat orientation of cyanobiphenyl mesogens on the water surface.[37] However, for the present polymers a completely flat orientation of cyanobiphenyl mesogens can be ruled out because this situation would require a surface area
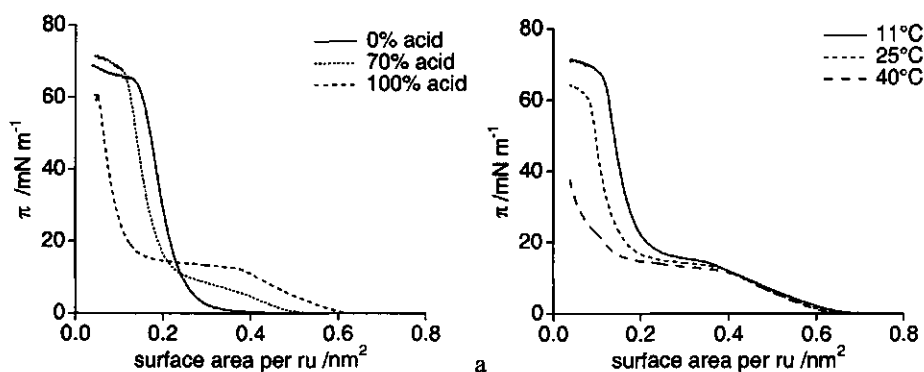
Figure 9.2. *π – A Isotherms of polymer 3, a: for different anhydride contents in the backbone; and b: at different temperatures.*

per repeating unit of more than 0.82 nm^2 instead of the observed 0.61 nm^2. Furthermore, this polymer shows a plateau in the $\pi - A$ isotherm. The molecular area at the low area side of this plateau, approximately 0.13 nm^2/repeating unit, is too small to accommodate a monolayer. This indicates that a multilayer is formed upon compression, probably a triple layer, as has been observed before for poly(maleic anhydride-*alt*-vinyl ethers) with cyanobiphenyl mesogens.[11]

To study the effect of the backbone flexibility on the interactions between the mesogenic cyano substituents and the water subphase the isotherms of polymers with different acid contents were recorded (see Figure 9.2a). When the maleic anhydride moieties are converted into maleic acid moieties the flexibility of the polymer backbone increases. Figure 9.2a shows that for low acid contents the shape of the isotherms resembles that of polymers **1-*m,p***. This may indicate that a stiff polymer backbone prevents the cyano groups from interactions with the water subphase.

Figure 9.2b shows that with increasing temperature the surface area per repeating unit at 0 mN/m remains constant, but the length of the plateau increases and the collapse pressure decreases. At 25°C, the molecular area at the low area side equals about one-third of the molecular area at the start of the plateau. This suggests the formation of a triple layer, which has been observed before for some low molecular weight fatty acids[38] and compounds with cyanobiphenyl moieties.[11,39,40] At 11°C, the monolayer is very rigid and the applied compression speed is probably too high to result in a well-defined triple layer. At 40°C, the flexibility of the triple layer is high enough so that another small plateau can be observed at the low area side. The surface area at the low area side of this plateau is about one-fifth of the molecular area at the start of the plateau.

The multilayer formation can be attributed to the tendency of cyanobiphenyl mesogens to form antiparallel pairs.[41,42] At low surface pressure, the interactions of cyanobiphenyl mesogens with water are strong enough to suppress the antiparallel orientation and the polymer is present as a monolayer on the water subphase.[11] With an increase of surface pressure the antiparallel orientation is obtained in the multilayer by the cooperative
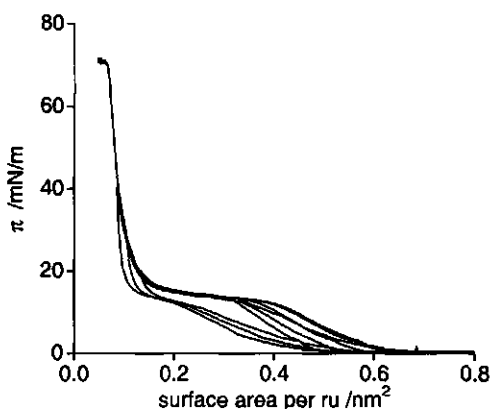
*Figure 9.3. Consecutive compression-expansion cycles for polymer 3 at 25°C.*

sliding of a bilayer on top of the original monolayer. Polymers with methoxybiphenyl mesogens do not show this behavior because these mesogens do not tend to form antiparallel pairs.[41]

Consecutive compression-expansion cycles (Figure 9.3) show that the π - A isotherms are completely reversible after compression before or into the plateau. After compression beyond the plateau, the lift-off area of the following compression cycle shifts to a lower value. Compression beyond the plateau results in a highly condensed and stiff multilayer that does not rapidly return into the monolayer after expansion. Because the surface area of a compressed multilayer does not change for hysteresis cycles above the plateau pressure, it can be concluded that the formation of a triple layer is completely reversible and no additional layers on top of this triple layer are formed at 25°C.

The monolayer stability of polymers 1-*m,p*, 2 and 3 was investigated on pure water at 25°C and different surface pressures. Polymers 1-*m,p* and 2 showed stable monolayers at surface pressures of 25 and 15 mN/m after 30-45 min. Polymer 3 showed a stable monolayer below the plateau pressure, i.e. at 5 and 8 mN/m, within 45 min. Thus the initial area reduction can be attributed to the reorganization of the monolayer and is not due to collapse or dissolution into the subphase. At 30 mN/m, an almost stable multilayer was obtained after 90 minutes, however, during the following 2 h the area kept reducing slightly. This indicates the formation of a stable triple layer.

Brewster angle microscopy is used to visualize the morphology and domain structures of the monolayers of polymers 1-9,0 and 3 on water at 25°C. Figure 9.4 shows the micrographs for polymer 1-9,0 at 0 and at 50 mN/m. Immediately after spreading, the film consists of polymer islands which merge upon compression (Figure 9.4a). This behavior has been observed before for poly(siloxane)s with benzoylbiphenyl mesogens,[9] poly(glutamate)s with decyloxybiphenyl mesogens[7] and poly(maleimide-*alt*-vinyl)pyridine)s with cyanoazobenzene mesogens.[43] At 50 mN/m, the monolayer collapses as can be seen from the horizontal lines with increased intensity (Figure 9.4b). Polymer 3 shows similar behavior if all acid moieties are converted into anhydride moieties.
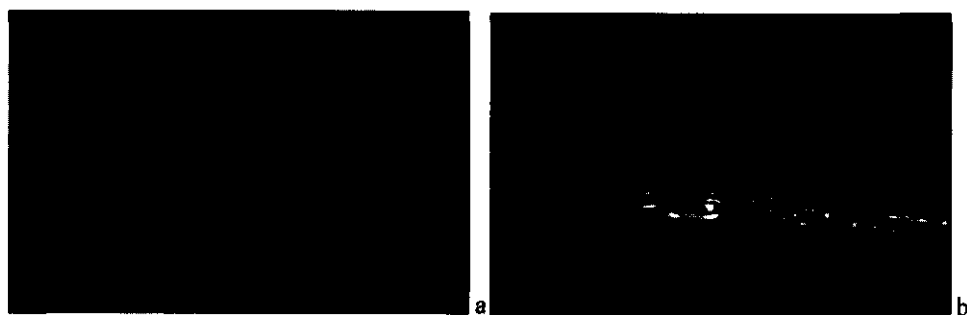
Figure 9.4. *Brewster angle micrographs of polymer 1-9,0 at 0 mN/m (a) and 50 (b) mN/m. Image size approximately 500 · 500 μm.*
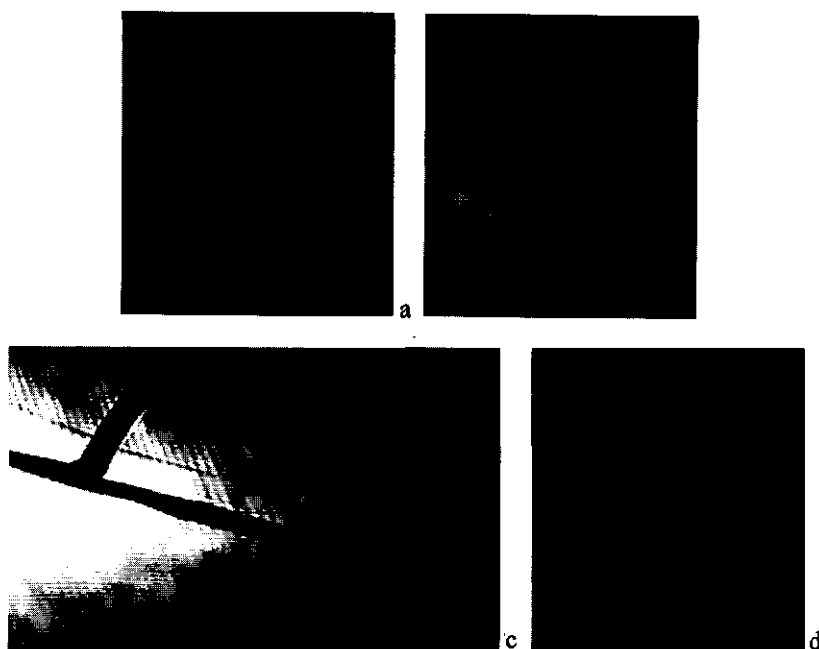
Figure 9.5. *Brewster angle micrographs of polymer 3 at plateau pressure (a and b), 40 mN/m (c) and after expansion of a condensed film (d). Image size approximately 500 · 300 μm (a, b and d) or 500 · 500 μm (c).*

Figure 9.5 shows the micrographs of polymer **3** at different surface pressures. Immediately after spreading the film is homogeneous. Upon compression in the plateau, straight white and black lines are observed parallel to the barrier (Figure 9.5a and b), probably resulting from the formation of a triple layer. At the point where the layer folds the differences in refractive indices result in lighter and darker regions in the micrograph. Further compression of the layer resulted in a lighter color of the Langmuir layer, but no other

changes were observed. Above 40 mN/m cracks develop in the triple layer and collapse of the triple layer is observed (Figure 9.5c). After expansion of a condensed multilayer, small holes are observed in an otherwise homogeneous film (Figure 9.5d), which confirm the observations of the consecutive hysteresis experiments. Relaxation of this film for several hours yields a homogeneous film without holes.

9.3.2. Langmuir films of SCLCPs with doubled mesogen density

So far, the polymers we have discussed contain one mesogen per four atoms in the backbone. The surface area per repeating unit of these polymers is mainly governed by the size of the hydrophilic head groups. Doubling the mesogen density may result in different monolayer behavior, because the surface area per repeating unit may now be governed by the mesogens. Figure 9.6 shows the $\pi - A$ isotherms of polymers **5-*m*** and **6** (Scheme 9.2) that have twice the mesogen density of polymers **1 - 3**. The corresponding surface areas per repeating unit are summarized in Table 1.

The surface areas per repeating unit for polymers **5-3** and **5-6** are similar (Figure 9.6). However, polymer **5-6** exhibits a slightly steeper isotherm. From the high surface areas per repeating unit in comparison to that of unmodified polymers, it can be seen that for polymers **5-*m*** the minimal area necessary to accommodate the repeating units is governed by the mesogenic side groups. In a non-crystalline packing of mesogens the cross-sectional area for two mesogens is approximately 53Å^2 (calculated from reference 23) which is comparable to the observed surface area per repeating unit for polymers **5-*m***.

Increasing the mesogen density by copolymerizing MA and swallow-tailed 1-alkenes with two mesogens yields polymers that show a pressure-area isotherm (Figure 9.6) that is very similar to that of polymers **5-*m***, although the rise in surface pressure is slightly less steep.
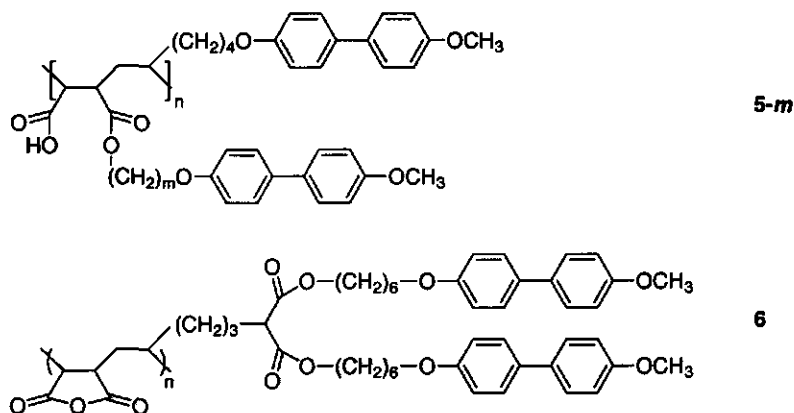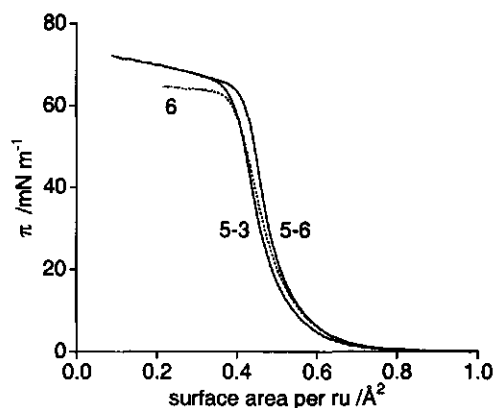

Scheme 9.2. Molecular structure of polymers 5-m and 6.

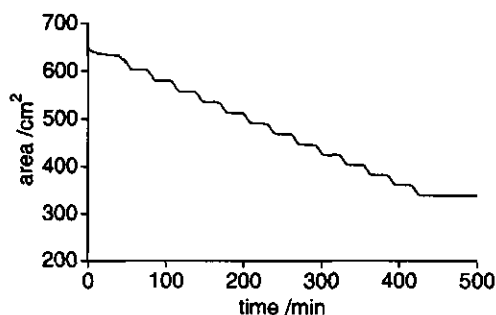***Figure 9.6.** π – A Isotherms of polymers **5-m** (——) and **6** (···).*

Figure *9.7. Isobaric measurement of a 1-9,0 monolayer at 15 mN/m and 25°C during transfer to a hydrophobic surface.*

The monolayer stability of polymers **5-m** and **6** was investigated on pure water at 25°C and a surface pressure of 25 mN/m. All polymers showed stable monolayers; the time necessary to obtain a stable monolayer was approximately 3 hours which is considerably longer than for polymers with only one mesogen per repeating unit. BAM did not reveal any crystallization during compression.

9.3.3. Langmuir-Blodgett films

Monolayers of polymer **1-9,0** could be transferred successfully at 15 and 20 mN/m from the water surface to hydrophobic and hydrophilic glass substrates, respectively, at 25°C. Figure 9.7 shows that just after the start of the experiment a spontaneous loss of the surface area of the polymer monolayer occurs. The monolayer becomes stable after 30 min. The initial area reduction can be attributed to a reorganization of the monolayer. After stabilization substrates were dipped and for both hydrophilic and hydrophobic substrates transfer was observed only during emersion of the substrate from the water subphase (Figure 9.7), which indicates Z-type transfer. For hydrophobic surfaces, the transfer ratio was 0.85 (±

Figure 9.8. *Probable arrangement of side chains in a LB monolayer of polymer 1-9,0.*

0.05) and remained constant up to 13 layers (Figure 9.7). For hydrophilic surfaces, the transfer ratio was 1.00 (± 0.05) for the first cycle and leveled off to a value of 0.80 (± 0.05) for the fifth up till the tenth dipping cycle. The barrier did not move during the waiting cycle prior to the subsequent dipping, which indicates a fast stabilization of the monolayer after the substrate has been pulled out.

Monolayers of polymer **1-9,0** have also been transferred to hydrophilic silicon wafers with a transfer ratio of 0.70. Transfer of multiple monolayers was not successful: after transfer of a monolayer, the resulting LB layer was washed off during the following immersion of the substrate. The washing off could not be prevented by changing the immersion speed. Atomic Force Microscopy revealed that the monolayer of polymer **1-9,0** was smooth and had a thickness of approximately 1.3 ± 0.2 nm, which is significantly smaller than the length of a side chain (2.7 nm).[23] The difference in experimental and theoretical thickness indicates that the side chains lie tilted on the surface, as is schematically depicted in Figure 9.8. The tilt does not have to be as regular as depicted in Figure 9.8 and does not have to be homogeneous throughout the whole sample. The tilt can probably be ascribed to the fact that the side chains are not space-filling, especially at low transfer ratios, and the relatively low transfer ratio. Other polymers that have tilted side chains in LB films are poly(maleic anhydride-*alt*-octadec-1-ene)[14] and Schiff base modified poly(maleic anhydride-*alt*-styrene).[44]

Figure 9.9 shows the X-ray reflectivity curves of a multilayer (10 layers) of polymer **1-9,0** transferred to a glass substrate by the LB technique before and after annealing in the mesophase. In general, X-ray reflectivity is a powerful method to investigate interfacial properties of layered materials. From the specular reflectivity, in which the reflected intensity depends on the wave vector transfer perpendicular to the sample surface, the density profile in the direction perpendicular to the sample surface can be obtained.

The curve marked by crosses in Figure 9.9 results from the reflectivity measurement without annealing. In the reflection pattern so-called Kiessig fringes are visible indicating a layer on top of the glass substrate with a relatively smooth surface. The Kiessig fringes originate from interference of X-ray beams reflected at the air-polymer interface and at the polymer-substrate interface. Hence, a mean total film thickness of 19.6 nm can be calculated from the period of the Kiessig fringes. In addition, a rather broad so-called multilayer Bragg peak can be observed resulting from a one-dimensional periodicity in the direction perpendicular to the substrate. The position of the Bragg peak that arises from a layered structure within the LB film corresponds to a mean *d* spacing of 3.95 nm.
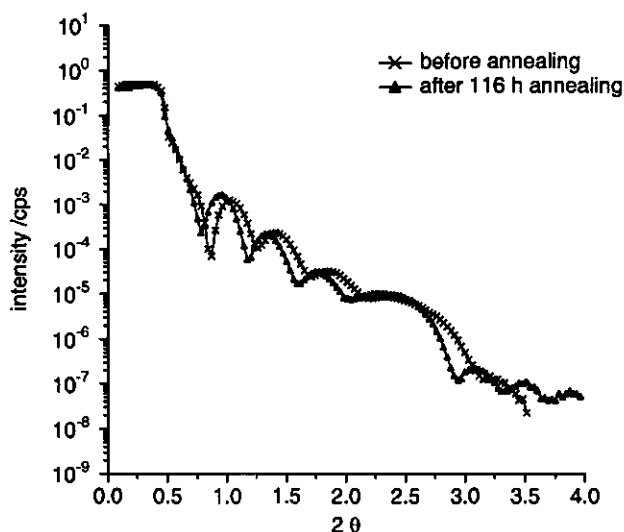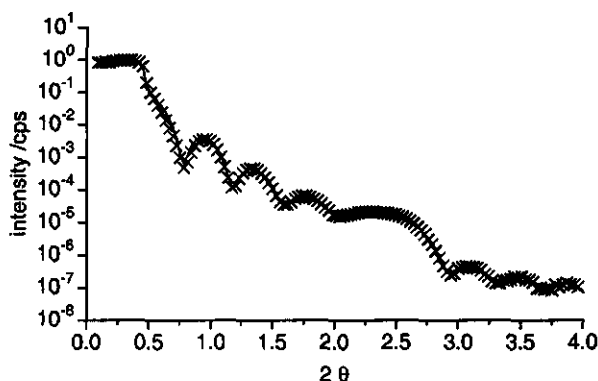
Figure 9.9. *Reflected X-ray intensity as a function of twice the angle of incidence θ for a LB film of polymer 1-9,0 on hydrophilic glass after 10 dipping cycles.*

Annealing of the sample for 116 h in the mesophase (135°C) results in a slight shift of the fringes to a smaller period in the 2θ-values, which indicates an increase of the mean total film thickness to 20.5 nm (Figure 9.9). The interface roughness seems to be unchanged, as can be concluded from the very similar slope of both curves. Furthermore, the Bragg peak sharpens, which indicates a more uniform d spacing within the film.

From the comparison of the d spacing (3.95 nm) and the film thickness (19.6 nm), it follows that the LB film consists of five layers. These five layers have been obtained by transferring ten Langmuir monolayers, which indicates that the LB film has a double layer periodicity. The side chains in this double layer will not overlap due to a lack of space, which is obvious from the results from Section 9.3.2. In this section it was shown that the minimal area to accommodate the repeating units is governed by the mesogenic side chains and not by the polymer backbone. The d spacing of the double layer structure in the LB film (3.95 nm) is significantly smaller than the calculated d spacing of a calculated smectic double layer (S_{A2}). Therefore we suggest that the side chains may be tilted, i.e. the LB film may have a smectic C2 structure. However, we have no solid evidence that certifies this assumption. Since the isobaric measurement (Figure 9.7) indicates Z-type transfer, which implicates that the LB film should have a monolayer periodicity (smectic A1 or C1), the double layer periodicity requires a reorientation of side chains during/after transfer of the Langmuir monolayer.

The preliminary fitting result for the annealed film in Figure 9.10 agrees well with the experimental results. Only in the region of small incidence angles there is some deviation, which can be explained by a lateral inhomogenity of the sample. At small angles of incidence the X-ray beam illuminates a rather large sample area (26 · 6 mm), whereas at larger incidence angles this area is much smaller (0.1 · 6 mm). Hence, the influence of

Figure 9.10. *Reflected X-ray intensity as a function of twice the angle of incidence θ for a LB film of polymer 1-9,0 on hydrophilic glass after 10 dipping cycles (crosses) and the model fits (solid line).*
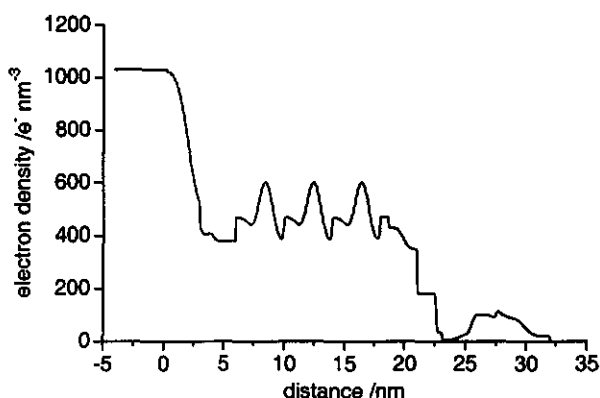
Figure 9.11. *Electron density profile of a LB film of polymer 1-9,0 as given in Figure 9.9 (after 116 h annealing) as a function of the depth.*

inhomogenities and irregularities over which the beam averages at small incidence angles is much larger and masks the signal from well-ordered regions of the sample. However, the existence of the Bragg peak is a clear indication of the presence of these well-ordered regions. The low intensity of the Bragg peak shows that these well-ordered regions are quite small. Indeed, as shown in the electron density profile resulting from the fit (Figure 9.11) the periodic layering within the LB film contains only 3 double layers with a double layer structure. The width of the Bragg peak arises from both a superposition of the Bragg peak with the Kiesig fringes at this position and a relatively high roughness.

As described by van der Wielen et al.[24] the different electron densities can be related to backbone regions, spacer regions, and mesogen regions. Although there is no hard evidence that a certain electron density corresponds to a certain region, there are indications that the assignment as described below is reasonable. However, one must bear in mind that
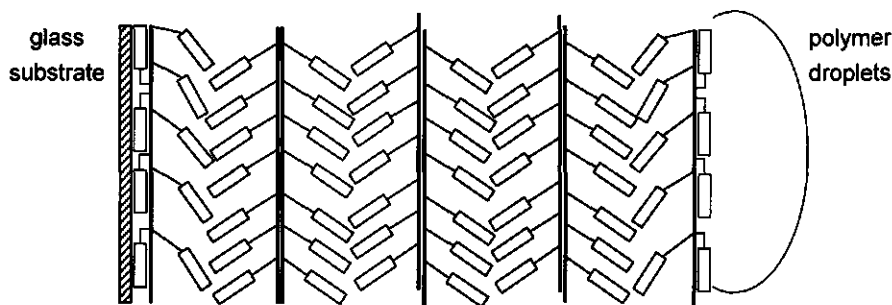
Figure 9.12. *Schematic representation of the proposed layered structure within the annealed LB film of polymer 1-9,0 after annealing at 135°C for 116 h. The tilt direction of the side chains is arbitrarily chosen and the side chains may tilt randomly.*

the electron density profile (Figure 9.11) results from preliminary fitting results and some strange phenomena in this profile have not been explained at the present time. Furthermore, only one sample has been studied.

The region close to the substrate is difficult to interpret. The Z-type transfer and the good adhesion properties would result in a situation where the polymer backbone is at the glass substrate. In comparison to the 'bulk' of the LB film, however, the electron density profile clearly shows a lower electron density at the substrate. This may result from surface roughness and/or may indicate some kind of disordered layer as depicted schematically in Figure 9.12. One must keep in mind that the picture of the first layer in figure 9.12 is rather speculative. The orientation of the mesogens at the substrate-polymer interface (Figure 9.12) is difficult to explain, since it is expected that Z-type transfer would result in orientation of the adhesive maleic acid moieties, i.e. the polymer backbone, towards the glass substrate. However, a similar orientation of mesogens was observed before in annealed spincoated films of polymer **1-9,0**.[24] Although Figure 9.12 shows a situation with only mesogens at the glass substrate, it may be possible that also some acid moieties may be in contact with the glass substrate.

The peaks in Figure 9.11 with the highest electron density in the film can be assigned to the backbone region, since it is expected that this layer has the highest density due to the oxygen atoms in the acid groups. The peaks in Figure 9.11 with a slightly lower electron density can be assigned to the mesogen layer. The electron density minima between the maxima of the mesogen and backbone regions can be ascribed to the spacer region. The electron density is low compared to the backbone and mesogen regions because the spacers form a less dense layer.

The top layer has a lower electron density than the 'bulk' of the film because it may consist of multidomain droplets, that lay on top of an ordered layer. The region of the high electron density plateau in the left of Figure 9.11 is ascribed to the glass substrate.

To get a more detailed picture of the surface of the annealed LB film AFM measurements were performed (Figure 9.13). These measurements showed clear dewetting of
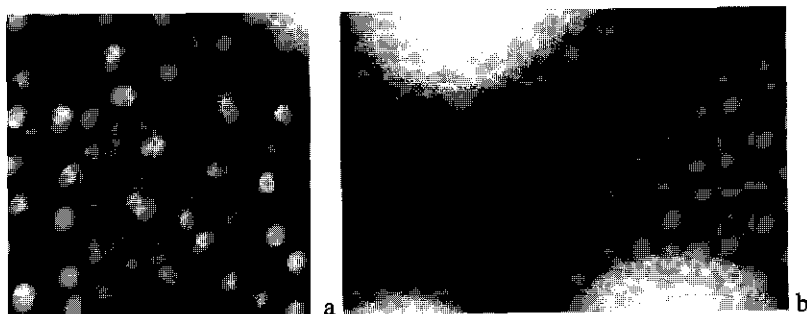
Figure 9.13. *AFM images of the Langmuir-Blodgett film of polymer **1-9,0** after annealing for 116 h in the mesophase (135°C): 1.7 · 1.7 μm (a) and 0.17 · 0.25 μm (b).*

the top layers (Figure 9.13a). The droplets are in average of a height of about 40-50 nm and of a width of between 100 and 200 nm. The presence of these droplets partially explains the disordered profile obtained with X-ray reflection. However, underneath the droplets the complete and relatively smooth polymer film was visible (Figure 9.13b). A closer look at this film between the droplets allows us to distinguish a typical terracelike surface of a smectic ordered SCLCP with step heights of about 3.7 ± 0.2 nm. This height agrees quite well with the mean d spacing determined by X-ray reflectivity.

In contrast to the dewetting of ordered spincoated films, which have an interdigitated layer periodicity,[24] the dewetting in the LB films only seems to occur in the upper layer (Figures 9.12 and 9.13). The dewetting in the upper layer arises from the orientation of hydrophilic acid groups at the polymer-air interface, which induces a relatively high surface energy. Dewetting may take place until no hydrophilic groups are present at the polymer-air interface, i.e. the surface energy has reached a minimum. The double layer periodicity probably prevents the film from an almost complete dewetting as is observed in spincoated films.[24]

9.4. Conclusions

SCLC poly(maleic acid-*alt*-1-alkene)s with methoxybiphenyl mesogens form stable well-ordered Langmuir films with high collapse pressures. The polymer backbone determines the minimal area necessary to accommodate the repeating units and the interactions between mesogens hardly influence this area. When the mesogen density is doubled, the mesogens determine the minimal area necessary to accommodate the repeating units. BAM experiments show that SCLCPs with methoxybiphenyl mesogens strongly aggregate on the water subphase and form islands. Upon compression these islands merge together.

The behavior of Langmuir films of a SCLC poly(maleic acid-*alt*-1-alkene)s with cyanobiphenyl mesogens differs strongly from that of similar polymers with methoxybiphenyl mesogens. For SCLCPs with cyanobiphenyl mesogens, BAM reveals that

the polymer spreads nicely and does not result in island formation. The lift-off areas of these polymers suggest an orientation of the cyanobiphenyl mesogens with the cyano groups in contact with the subphase. Due to the tendency of cyanobiphenyl mesogens to form antiparallel pairs, compression results in the formation of a triple layer. This was confirmed by BAM experiments. Backbones with a higher content of anhydride moieties have a more rigid backbone and therefore do not undergo triple layer formation. BAM experiments showed that these polymers form islands that merge upon compression.

Langmuir layers of SCLC poly(maleic acid-*alt*-1-alkene)s with methoxybiphenyl mesogens show Z-type transfer with high transfer ratios towards hydrophylic and hydrophobic glass substrates. On hydrophilic silicon, these polymers probably have tilted side chains in the LB monolayer. LB multilayers on hydrophilic glass may also consist of polymers with (randomly) tilted side chains, and X-ray reflectivity measurements show a *d* spacing of 3.95 nm. This may indicate that the film has a double layer periodicity, e.g. smectic C2. The double layer periodicity requires a reorientation of the side chains during or after transfer, because Z-type transfer would result in films with a monolayer periodicity. However, the results are obtained from only one sample and, consequently, a generalization of the results cannot be made.

Annealing of the LB films results in an increase of the mean film thickness and a more uniform *d* spacing within the film. Fitting of a model on the experimental X-ray reflectivity data is difficult. However, there are indications that the first layer on the glass substrate is slightly disordered. The following three double layers may be well-ordered, and on top of these three double layers droplets are present. The presence of droplets was confirmed by AFM measurements. These droplets indicate that dewetting has occurred before or after annealing. The main reason for this dewetting may be the presence of acidic groups at the polymer-air interface, which induce a relatively high surface energy. Therefore a reorientation of polymer at the polymer-air interface will occur which decreases the surface energy.

9.5. References

1   Ulman, U. *An Introduction to Ultrathin Organic Films*; Academic Press: Boston, 1991; Chapter 2.

2   Nguyen, D. M.; Mayer, T. M.; Hubbard, T. M.; Singer, D. K.; Mann, Jr. J. A.; Lando, J. B. *Macromolecules*, **1997**, *30*, 6150.

3   Ren, Y.; Tian, Y.; Sun, R.; Xi, S.; Zhao, Y.; Huang, X. *Langmuir* **1997**, *13*, 5120.

4   Geue, T.; Pietsch, U.; Stumpe, J. *Thin Solid Films* **1996**, *284-285*, 228.

5   Ou, S. H.; Percec, V.; Mann, J. A.; Lando, J. B.; Zhou, L.; Singer, K. D. *Macromolecules* **1993**, *26*, 7264.

6   Adams, J.; Rettig, W.; Duran, R. S.; Naciri, J.; Shashidar, R. *J. Phys. Chem.* **1993**, *97*, 2021.

7   Menzel, H.; Rambke, B. *Macromol. Chem. Phys.* **1997**, *198*, 2073.

8   Tsukruk, V. V.; Bliznyuk, V. N. *Prog. Polym. Sci.* **1997**, *22*, 1089.

9   Chen, X.; Yang, K.-Z.; Xue, Q.-B.; Zhang, Q.-Z. *Thin Solid Films* **1998**, *327-329*, 145.

10 Chen, X.; Xue, Q.-B.; Yang, K.-Z.; Zhang, Q.-Z. *Thin Solid Films* **1996**, *286*, 232.

11 Nieuwkerk, A. C.; van Kan, E. J. M.; Kimkes, P.; Marcelis, A. T. M.; Sudhölter, E. J. R. *Langmuir* **1998**, *14*, 6448.

12 Lee, B.-J.; Choi, G.; Kwon, Y.-S. *Thin Solid Films* **1996**, *284-285*, 564.

13 Aspin, I. P.; Barros, A. M.; Hodge, P.; Towns, C. R.; Ali-Adib, Z. *Polymer* **1995**, *36*, 1707.

14 Davis, F.; Hodge, P.; Towns, C. R.; Ali-Adib, Z. *Macromolecules* **1991**, *24*, 5695.

15 Niwa, M.; Matsuyoshi, E.; Higashi, N. *Langmuir* **1989**, *5*, 1256.

16 Ali-Adib, Z.; Tredgold, R. H.; Hodge, P.; Davis, F. *Langmuir* **1991**, *7*, 363.

17 Tredgold, R. H.; Allen, R. A.; Hodge, P.; Khosdel, E. *J. Phys. D: Appl. Phys.* **1987**, *20*, 1385.

18 Jones, R.; Tredgold, R. H.; Hoorfar, A.; Allen, R. A.; Hodge, P. *Thin Solid Films* **1985**, *134*, 57.

19 Hodge, P.; Khosdel, E.; Tredgold, R. H.; Vickers, A. J.; Winter, C. S. *British Polym. J.* **1985**, *17*, 368.

20 Tredgold, R. H.; Vickers, A. J.; Hoorfar, A.; Hodge, P.; Khosdel, E. *J. Phys. D: Appl. Phys.* **1985**, *18*, 1139.

21 Winter, C. S.; Tredgold, R. H.; Vickers, A. J.; Khosdel, E.; Hodge, P. *Thin Solid Films* **1985**, *134*, 49.

22 Tredgold, R. H.; Winter, C. S. *Thin Solid Films* **1983**, *99*, 81.

23 Nieuwhof, R. P.; Marcelis, A. T. M.; Sudhölter, E. J. R.; Picken, S. J.; de Jeu, W. H. *Macromolecules* **1999**, *32*, 1398 (Chapter 3).

24 van der Wielen, M. W. J.; Cohen Stuart, M. A.; Fleer, G. J.; de Boer, D. K. G.; Leenaers, A. J. G.; Nieuwhof, R. P.; Marcelis, A. T. M.; Sudhölter, E. J. R. *Langmuir* **1997**, *13*, 4762.

25 Nieuwhof, R. P.; Marcelis, A. T. M.; Sudhölter, E. J. R.; van der Wielen, M. W. J.; Cohen Stuart, M. A.; Fleer, G. J. *Macromol. Symp.* **127**, 115 (1998).

26 Frost, A. M.; Kolosentseva, I. A.; Razumovskii, V. V. *Zh. Prikl. Khim.* **1974**, *47*, 731.

27 Kurbanova, R. A.; Mirzaoglu, R.; Kurbanov, S.; Karatas, I.; Pamuk. V.; Ozcan, E.; Okudan, A.; Güler, E. *J. Adhesion Sci. Technol.* **1997**, *11*, 105.

28 Bistac, S.; Vallat, M.F.; Schultz, J. *J. Adhesion* **1996**, *56*, 205.

29 Thery, S.; Jacquet, D.; Mantel, M. *J. Adhesion* **1996**, *56*, 15.

30 Kolosentseva, I. A.; Frost, A. M.; Razumovskii, V. V. *Zakakras. Mater. Ikh. Primen* **1975**, *2*, 10.

31 Nieuwhof, R. P.; Marcelis, A. T. M.; Sudhölter, E. J. R. *Macromolecules* in press (Chapter 4).

32 Nieuwhof, R. P.; Marcelis, A. T. M.; Sudhölter, E. J. R.; Picken, S. J.; van Puijenbroek, R. R. *Macromol. Chem. Phys.* submitted (Chapter 5).

33 Cohen Stuart, M. A.; Wegh, R. A. J.; Kroon, J. M.; Sudhölter, E. J.R. *Langmuir* **1996**, *12*, 2863.

34 Als-Nielsen, J. *Handbook of Synchrotron Radiation*; Brown, G., Moncton, D. E., Eds.; Elsevier: Amsterdam, 1991, Vol. 3.

35 Fitting program REFGR by Ivan Samoilenko.

36 Finkelmann, H.; Ringsdorf, H.; Wendorff, J.H. *Makromol. Chem.* **1978**, *179*, 273.

37 Everaars, M. D.; Marcelis, A. T. M.; Sudhölter, E. J. R. *Thin Solid Films* **1994**, *242*, 78.

38 McFate, C.; Ward, D.; Olmsted, J., III. *Langmuir* **1993**, *9*, 1036.

39 Xue, J.; Jung, C. S.; Kim, M. W. *Phys. Rev. Lett.* **1992**, *69*, 474.

40 Biensan, C.; Desbat, B.; Turlet, J. M. *Thin Solid Films* **1996**, *284-285*, 293.

41 Craig, A. A.; Imrie, C. T. *Macromolecules* **1995**, *28*, 3617.

42   Imrie, C. T.; Schleeh, T.; Karasz, F. E.; Attard, G. S. *Macromolecules* **1993**, *26*, 539.

43   Noordegraaf, M. A.; Kuiper, G. J.; Marcelis, A. T. M.; Sudhölter, E. J. R. *Macromol. Chem. Phys.* **1997**, *198*, 3681.

44   Dhathathreyan, A.; Mary, N. L.; Radhakrishnan, G.; John Collins, S. *Macromolecules* **1996**, *29*, 1827.

Concluding remarks

A new class of liquid-crystalline materials has been developed that may be used as a splittable primer layer for coating applications. The problem of lack of adhesion of common side-chain liquid-crystalline polymers (SCLCPs) has been solved by incorporating maleic anhydride (MA) moieties in the polymer backbone. These moieties are known to promote adhesion towards metal surfaces.[1,2,3,4] Copolymerization of MA and mesogenic 1-alkenes yielded alternating SCLCPs. Copolymerization of MA with mesogenic methacrylates yielded SCLCPs with different amounts of MA, which may show different adhesive behavior. A second class of materials, the poly(ketone)s, contain polar carbonyl moieties in the backbone that also may promote adhesion towards metal surfaces.

The majority of the synthesized polymers exhibit smectic mesophases. The degree of order in these mesophases can be altered by changing the length of the spacer or mesogenic substituent, or by changing the mesogen density. The type of mesophase can be altered by small variations in the molecular structure. In general, it can be concluded that these polymers exhibit layered smectic mesophases if the mesogens are apolar or do not have strong dipoles, like methoxybiphenyl mesogens. On the other hand, the polymers exhibit nematic mesophases if the mesogens are more polar than methoxybiphenyl mesogens, like azobenzene or cyanobiphenyl mesogens.

The phase transition temperatures of the materials are important, because they are closely related to the anticipated coating removal temperature. Therefore, tuning the transition temperatures has been an important issue in the development of the novel SCLCPs. The glass transition temperature can be lowered by increasing the spacer length. The isotropization temperature can also be tuned, but the dependence of the isotropization temperature on spacer length is different for the various types of polymer backbones.

Rheological measurements have pointed out that the phase transitions of the SCLCPs are accompanied by drastic changes in mechanical properties like complex viscosity, loss modulus and storage modulus. Due to the low molecular weight of the synthesized materials, the polymers flow easily in the melt.

With respect to coating applications of the SCLCPs, the behavior of the polymers in thin films is extremely important. Significant aspects of the film are the adhesion between a polymer film and a solid substrate, the stability of the morphology of the film and the thickness of the film. Two model systems have been studied: (i) Langmuir-Blodgett films and (ii) spincoated films. The Langmuir-Blodgett films have a significantly different structure than spincoated films, which finds its origin in the different kind of film formation. In contrast to spincoated films, the dewetting in Langmuir-Blodgett films only occurs in the upper layer.

The behavior of these polymers in spincoated films on silicon oxide surfaces has been studied by van der Wielen.[5] Spincoated films of SCLC poly(maleic anhydride-*alt*-1-alkene)s having methoxybiphenyl mesogens on silicon wafers show lamellar ordering upon annealing above the glass transition temperature (T_g), whereas the unannealed films do not show any

orientation of the smectic domains.[6,7] After prolonged heating, the films break up and start to dewet.[8] In the final stage of dewetting, droplets sit on top of a rather stable interdigitated smectic layer that does not participate in the dewetting. This typical autophobic behavior indicates that the adhesive forces of the polymer to the oxidized silicon substrate are stronger than the cohesive forces between the mesogens. The autophobic behavior of the material may be beneficial for the application as a splittable primer layer, because it only occurs in the mesophase and, at a faster rate, in the isotropic melt.

In comparison to smooth silicon oxide surfaces, the behavior of spincoated films is different on silicon surfaces with a roughness dimension that is close to the size of an ordered bilayer. For these 'rough' surfaces, the development of a layered structure cannot compete with the formation of random polycrystalline domains.[9] On the other hand, the film breaks up less easily on 'rough' surfaces.

Summarizing, we gained much insight in the structure-property relations of SCLCPs with polar moieties in the backbone. These SCLCPs meet the requirements for application as a primer, i.e. they form lamellar ordered mesophases and contain adhesion-enhancing moieties. Furthermore, the phase transitions are accompanied by drastic changes in the mechanical properties. The behavior of these SCLCPs in films on rough surfaces, however, may be disadvantageous for primer applications. Furthermore, the behavior of the primer layer in the presence of an additional coating on top of it requires some attention.

Besides the potential application of these polymers in coating removal, these intriguing materials may be beneficial for other applications due to the presence of polar moieties that can be modified chemically. An interesting application may be the use of these polymers in blends of SCLCPs or liquid crystals with common thermoplastics known as polymer dispersed liquid crystals. The presence of anhydride moieties makes the SCLCPs suitable for grafting for example amine-endfunctionalized polymers. The resulting graft copolymer may act as a compatibilizer for two immiscible polymers and therefore enhance the mechanical properties of the blend.

References

1   Frost, A. M.; Kolosentseva, I. A.; Razumovskii, V. V. *Zh. Prikl. Khim.* **1974**, *47*, 731.

2   Kurbanova, R. A.; Mirzaoglu, R.; Kurbanov, S.; Karatas, I.; Pamuk, V.; Ozcan, E.; Okudan, A.; Güler, E. *J. Adhesion Sci. Technol.* **1997**, *11*, 105.

3   Bistac, S.; Vallat, M. F.; Schultz, J. *J. Adhesion* **1996**, *56*, 205.

4   Thery, S.; Jacquet, D.; Mantel, M. *J. Adhesion* **1996**, *56*, 15.

5   van der Wielen, M. W. J. Dissertation Wageningen University and Research Centre (1999).

6   van der Wielen, M. W. J.; Cohen Stuart, M. A.; Fleer, G. J.; de Boer, D. K. G.; Leenaers, A. J. G.; Nieuwhof, R. P.; Marcelis, A. T. M.; Sudhölter, E. J. R. *Langmuir* **1997**, *13*, 4762.

7   van der Wielen, M. W. J.; Cohen Stuart, M. A.; Fleer, G. J.; Schlatmann, A. R.; de Boer, D. K. G. *Phys. Rev. E* submitted.

8   van der Wielen, M. W. J.; Cohen Stuart, M. A.; Fleer, G. J. *Langmuir* **1998**, *14*, 7065.

9   van der Wielen, M. W. J.; Cohen Stuart, M. A.; Fleer, G. J. *Adv. Mater.* in press.

Summary

The combination of mesogens and adhesion-enhancing moieties in one polymer results in side-chain liquid-crystalline polymers (SCLCPs) that may exhibit adhesion towards metal surfaces. These materials may be suitable for application in splittable primers, which require a high degree of order in combination with adhesion.

SCLCPs consist of a polymer backbone with mesogenic moieties in the side chains. The mesogens are attached to the polymeric backbone via a flexible spacer, which serves to decouple the motions of the backbone and the mesogens. The properties of these materials can be tuned to a desirable level by varying the molecular architecture. The research described in this thesis was aimed to obtain SCLCPs that contain adhesion-enhancing moieties. Special attention was paid to the effect of molecular architecture of these 'adhesive' SCLCPs on their mesomorphic properties.

The first step towards SCLCPs that may show good adhesion was the alternating copolymerization of maleic anhydride (MA) and mesogenic 1-alkenes. These SCLCPs showed high glass transition temperatures and highly ordered smectic mesophases. The mesophase width increased with spacer length. The terminal alkyl group length determined the degree of order in the hexatic mesophase that was present just above the glass transition temperature. A terminal methoxy group induced a hexatic smectic B mesophase, intermediate terminal alkyl groups induced a smectic E mesophase, and long terminal alkyl groups induced a crystal smectic B mesophase. If the spacer was shorter than the terminal alkyl group, an interdigitated smectic A mesophase was found in which the terminal alkyl groups overlap. A strong correlation was found between the glass transition temperature and the temperature at which the hexagonal or orthorhombic ordered mesophase disappears. Introduction of an ester linkage between the spacer and biphenyl mesogen or replacing the terminal alkoxy group by a cyano terminal group induced a lowering of transition temperatures and a lower degree of order in the mesophase.

These polymers, however, only contain one mesogen per four atoms in the polymer backbone, whereas common SCLCPs like poly(siloxane)s, poly(methacrylate)s, and poly(vinyl ether)s contain one mesogen per two atoms in the polymer backbone. Therefore, it is interesting to study the effect of doubling the mesogen density on the mesomorphic behavior of poly(MA-*alt*-1-alkenes). Two approaches were applied to obtain a higher mesogen density. The first method consists of grafting different mesogenic alcohols onto SCLC copolymers from MA and 1-alkenes carrying biphenyl mesogens. This grafting reaction resulted in monoesters of maleic acid. FTIR and ^{1}H NMR showed high degrees of modification. Grafting methoxybiphenyl-containing alcohols having different spacer lengths onto methoxybiphenyl-containing polymers yielded polymers exhibiting smectic A mesophases with a variable degree of order and interdigitation. The best ordered materials were obtained with nearly equal spacer lengths of the parent polymer and the alcohol. The glass transition temperature decreased with spacer length, whereas the isotropization temperature remained almost constant. Grafting azobenzene-containing alcohols onto

methoxybiphenyl-containing copolymers yielded SCLCPs exhibiting only nematic mesophases. The effect of the 4'-azobenzene terminal group on the temperature window of the mesophase was CN > OMe > F > H. Grafting a cyanostilbene-containing alcohol onto a methoxybiphenyl-containing copolymer resulted in a polymer that exhibited a smectic E mesophase with complete interdigitation of side chains. Introducing methoxybiphenyl mesogens into cyanobiphenyl-containing copolymers or vice versa resulted in polymers with smectic A mesophases. Furthermore, an increase in isotropization temperatures was observed in comparison with polymers carrying only one type of mesogen. This indicates specific favorable interactions between unlike mesogens.

The second approach is the alternating copolymerization of MA with swallow-tailed 1-alkenes having two mesogens. In contrast to similar SCLCPs from 1-alkenes with one mesogen per repeating unit, these novel polymers exhibited lower isotropization temperatures and higher glass transitions. The degree of order in the mesophase strongly increased: these SCLCPs exhibit a highly ordered smectic H phase. The polymers with a hexyl spacer between the malonate junction and the mesogen exhibited a uniaxially limited-correlation-length smectic E mesophase which has, according to our knowledge, not been observed before. The highest transition temperatures and entropy changes were observed for polymers with completely interdigitated side chains.

Because MA and 1-alkenes copolymerize in an alternating fashion, the MA content of the copolymer could not be altered. For copolymers of mesogenic methacrylates and MA the mesogen density or the MA content can be tuned due to the tendency of methacrylates to homopolymerize. This approach resulted in SCLCPs with an MA content between 0 and 30%. These polymers exhibit smectic A1 and smectic E1 mesophases for copolymers with a hexyl spacer and methoxybiphenyl mesogens. Furthermore, it has been found that the isotropization temperature increases and the width of the monotropic smectic A1 mesophase decreases with increasing MA content. For a series of methoxybiphenyl-containing copolymers with about 25% MA, the glass transition temperature decreased with increasing spacer length, whereas the isotropization temperature showed little dependence on spacer length. For octyl or shorter spacers, these polymers exhibited a smectic E mesophase, whereas for longer spacers these polymers exhibited smectic B mesophases. These mesophases transformed into a smectic A1 mesophase for SCLCPs with heptyl or longer spacers. SCLCPs with cyanoazobenzene mesogens exhibited only a smectic Ad mesophase, whereas polymers with cyanobiphenyl mesogens were not liquid crystalline.

A completely new class of materials that may show adhesion are the poly(1,4-ketone)s. These polymers are obtained via the copolymerization of carbon monoxide with 1-alkenes and form a class of polymeric materials which in their spectrum of properties differ from the widespread poly(olefin) commodities like poly(ethylene), poly(propylene) and poly(styrene). This results from the presence of polar carbonyl moieties in the polymer backbone, which strictly alternate with the apolar olefin fragments. By using mesogenic 1-alkenes instead of common aliphatic 1-alkenes, a novel class of liquid-crystalline materials was obtained. For methoxybiphenyl mesogens, these copolymers exhibited highly ordered

smectic E mesophases and high glass transition temperatures. The transition temperatures of these polymers could be tuned by altering the spacer length or by dilution of mesogen-containing alkenes with 1-hexene. Polymers with cyanobiphenyl or methoxyazobenzene mesogens exhibited nematic mesophases. These polymers were the first-ever nitrogen containing copolymers of this type. Increase of the spacer length or the 1-hexene content of methoxybiphenyl-containing copolymers resulted in a decrease of the surface polarity of spincoated films. The decomposition temperature of these SCLCPs started far above the isotropization temperature of the polymers.

SCLCPs from MA and mesogenic 1-alkenes or methacrylates were studied with rheology and temperature-dependent X-ray diffraction. Rheology revealed a transition in the smectic A mesophase that can probably be ascribed to the emergence of rotational diffusion of the mesogen. The viscoelastic behavior of the materials was mainly governed by the mesogenic interactions instead of the polymeric nature of the materials. Temperature-dependent X-ray diffraction revealed drastic changes in the smectic order just below the isotropization transition. For the poly(MA-*alt*-1-alkene) based SCLCP it was found that the smectic Ad-smectic A2 transition was accompanied by a strong decrease in loss modulus, storage modulus, and the complex viscosity, whereas the smectic A2-isotropic transition was not accompanied by a significant change in these mechanical properties.

The formation and transfer of Langmuir layers of SCLC poly(maleic acid-*alt*-1-alkene)s with biphenyl mesogens on aqueous subphases was studied by the use of the Langmuir-Blodgett technique. Brewster angle microscopy showed that the SCLCPs with methoxybiphenyl mesogens strongly aggregate on the water subphase and form islands. These islands merge together upon compression. In contrast, SCLCPs with cyanobiphenyl mesogens spread nicely. Compression of these polymers resulted in the formation of triple layers. Langmuir monolayers of SCLCPs with methoxybiphenyl mesogens show Z-type transfer. AFM and X-ray reflectivity measurements of the resulting Langmuir-Blodgett mono- and/or multilayers indicate that the side chains of these polymers are possibly tilted. The multilayers have a double layer periodicity, which requires a reorientation of the side chains during or after transfer. Annealing of these Langmuir-Blodgett films resulted in an increase of the mean film thickness and a more uniform *d* spacing within the multilayer. With AFM droplets were observed on top of the multilayer indicating dewetting of the upper layer.

Samenvatting

De combinatie van mesogenen en hechtingsbevorderende groepen in een polymeer leidt tot zijketen vloeibaar-kristallijne polymeren (SCLCP) die kunnen hechten op metaaloppervlakken. Deze materialen zijn mogelijk geschikt voor toepassing in splijtbare primers, die een hoge mate van ordening in combinatie met hechting moeten vertonen.

SCLCPs bestaan uit een polymeerhoofdketen en hebben mesogene groepen in de zijketens. De mesogenen zijn gekoppeld aan de polymeerhoofdketen via een flexibele spacer, welke de bewegingen van de hoofdketen en de mesogenen ontkoppeld. De eigenschappen van deze materialen kunnen worden gestuurd door variaties in de moleculaire structuur. Het onderzoek beschreven in dit proefschrift had als doel SCLCPs te ontwikkelen met hechtingsbevorderende groepen. Speciale aandacht werd geschonken aan het effect van variaties in de moleculaire structuur van deze hechtende SCLCPs op de vloeibaar-kristallijne eigenschappen.

De eerste stap naar hechtende SCLCPs was de alternerende copolymerisatie van maleïnezuuranhydride (MA) en mesogene 1-alkenen. Deze SCLCPs hebben hoge glasovergangstemperaturen en vertonen hooggeordende mesofasen. Het temperatuurgebied van deze mesofase nam toe met de spacerlengte. De lengte van de eindstandige alkylgroep bepaalde de mate van ordening in de hexatische vloeibaar-kristallijne fase, welke net boven de glasovergangstemperatuur was te vinden. Een eindstandige methoxygroep induceerde een hexatisch smectische B mesofase, eindstandige groepen met een gemiddelde lengte induceerden een smectische E mesofase en lange eindstandige groepen induceerden een kristallijn smectische B mesofase. Wanneer de spacer korter was dan de eindstandige alkylgroep vertoonde het polymeer een geïnterdigiteerde mesofase waarin de eindstandige alkylgroepen overlappen. Verder was er een sterk verband tussen de glasovergangstemperatuur en de temperatuur waarbij de hexagonale of orthorhombische ordening verdween. Het invoegen van een estergroep tussen de spacer en het bifenylmesogeen of het vervangen van de eindstandige alkylgroep door een cyanogroep zorgde voor lagere overgangstemperaturen en een lagere ordeningsgraad in de mesofase.

De bovengenoemde polymeren bevatten echter maar één mesogen per vier atomen in de hoofdketen, terwijl standaard SCLCPs als poly(siloxanen), poly(methacrylaten) en poly(vinylethers) één mesogeen per twee atomen in de hoofdketen hebben. Het is daarom interessant om het effect van een verdubbeling van de mesogeendichtheid op de vloeibaar-kristallijne eigenschappen van poly(MA-*alt*-1-alkenen) te bestuderen. Er zijn twee methodes toegepast om een hogere mesogeendichtheid te verkrijgen. De eerste methode bestond uit het koppelen van verschillende mesogene alcoholen aan SCLC copolymeren van MA en 1-alkenen met bifenylmesogenen. Deze koppelingsreaktie leidde tot monoesters van maleïnezuur. FTIR en ^{1}H NMR duiden op hoge modificatiegraden. Het koppelen van methoxybifenylbevattende alcoholen met verschillende spacerlengtes resulteerde in polymeren die een smectische A mesofase vertoonden met verschillende gradaties in overlap van de zijketens. De glasovergangstemperatuur nam af met de spacerlengte, terwijl de

151

isotropisatietemperatuur nagenoeg constant bleef. Het koppelen van azobenzeenbevattende alcoholen resulteerde in SCLCPs die slechts een nematische mesofase vertonen. Het effect van de eindstandige groep van 4'-azobenzeen op de grootte van het temperatuursgebied van de mesofase was CN > OMe > F > H. Het koppelen van een cyanostilbeenbevattend alcohol resulteerde in een polymeer dat een smectische E mesofase vertoonde met volledige overlap van zijketens. De combinatie van methoxybifenyl- en cyanobifenylmesogenen in één polymeer resulteerde in polymeren die een smectische A mesofase vertoonden. Verder namen in vergelijking met polymeren met maar één type mesogen de isotropisatietemperaturen toe. Dit duidt op specifieke interacties tussen ongelijke mesogenen.

De tweede benadering was de alternerende copolymerisatie van MA met zwaluwstaartvormige 1-alkenen die twee mesogenen bevatten. In tegenstelling tot vergelijkbare SCLCPs van 1-alkenen met één mesogeen per repeterende eenheid hebben deze nieuwe polymeren lagere isotropisatietemperaturen en hogere glasovergangstemperaturen. De mate van ordening in de mesofase nam sterk toe: deze polymeren vertonen de hooggeordende smectische H fase. De polymeren met een hexylspacer tussen de malonaatvertakking en het mesogeen vertoonden een smectische E fase met een in één richting beperkte correlatielengte. Dit is volgens ons nog niet eerder gevonden. De hoogste overgangstemperaturen en entropieverschillen werden gevonden voor polymeren waarbij de zijketens volledig overlappen.

Omdat MA en 1-alkenen op een alternerende wijze met elkaar polymeriseren kan van copolymeren het MA gehalte niet worden veranderd. Voor copolymeren van mesogene methacrylaten en MA kan de mesogeendichtheid of het MA-gehalte wel worden aangepast, omdat methacrylaten de neiging hebben te homopolymeriseren. Op deze manier werden SCLCPs verkregen met een MA gehalte variërend tussen de 0 en 30%. Wanneer de methoxybifenylmesogenen via een hexylspacer aan de hoofdketen waren gekoppeld, vertonen de SCLCPs smectische A1 en smectische E1 fasen. Verder werd gevonden dat de isotropisatietemperatuur toenam en het temperatuurgebied van de monotrope smectische A1 fase afnam met een toename in het MA gehalte. Voor een serie methoxybifenylbevattende copolymeren met een MA-gehalte van ongeveer 25% nam de glasovergangstemperatuur af met de spacerlengte, terwijl de isotropisatietemperatuur weinig van de spacerlengte afhing. Voor octyl- en kortere spacers vertonen deze polymeren een smectische E mesofase, terwijl voor langere spacers een smectische B mesofase werd gevonden. Voor SCLCPs met heptyl- of langere spacers werden deze mesofasen gevolgd door een smectische A1 fase. SCLCPs met cyanoazobenzeenmesogenen vertonen alléén een smectische Ad mesofase, terwijl polymeren met cyanobifenylmesogenen niet vloeibaar-kristallijn waren.

Een volledig nieuwe klasse van materialen die goede hechting kunnen vertonen zijn poly(1,4-ketonen). Deze polymeren ontstaan uit de copolymerisatie van koolmonoxide met 1-alkenen en vormen een klasse van polymeren die in hun scala aan eigenschappen verschillen van poly(olefine) bulkpolymeren als poly(ethyleen), poly(propylene) en poly(styreen). Dit is het gevolg van de aanwezigheid van polaire carbonylgroepen in de polymeerhoofdketen, die perfect alterneren met de apolaire alkeenfragmenten. Door in plaats van gewone alifatische 1-

alkenen mesogene 1-alkenen te gebruiken werd een nieuwe klasse van vloeibaar-kristallijne materialen verkregen. In het geval van methoxybifenylmesogenen vertoonden deze polymeren hooggeordende smectische E mesofasen en hoge glasovergangstemperaturen. De overgangstemperaturen van deze polymeren kunnen worden gestuurd door de spacerlengte aan te passen of door de mesogene 1-alkenen te verdunnen met 1-hexeen. Polymeren met cyanobifenyl- of methoxyazobenzeenmesogenen vertoonden nematische mesofasen. Deze polymeren zijn de eerste stikstofbevattende copolymeren van dit type. Verlengen van de spacer of verhogen van het 1-hexeen gehalte resulteerde in een afname van de oppervlaktepolariteit van de films. De ontledingstemperatuur van deze SCLCPs begon ver boven de isotropisatietemperatuur van de polymeren.

SCLCPs van MA en mesogene 1-alkenen of methacrylaten zijn bestudeerd met behulp van reologie en temperatuurafhankelijke röntgendiffractie. Reologie liet een overgang binnen de smectische A mesofase zien die waarschijnlijk kan worden toegeschreven aan het opkomen van rotatie diffusie van het mesogeen. Het viscoelastisch gedrag van de materialen wordt hoofdzakelijk bepaald door de interacties tussen mesogenen, in plaats van door het polymere karakter van de materialen. Net beneden de isotropisatieovergang toonde temperatuurafhankelijke röntgendiffractie drastische veranderingen in de smectische ordening. Voor een op poly(MA-*alt*-1-alkeen) gebaseerd SCLCP werd gevonden dat de smectisch Ad-smectisch A2 overgang samenviel met een sterke afname in de verlies- en opslagmodulus en de complexe viscositeit, terwijl de smectisch A2-isotroop overgang niet samenviel met een significante verandering in deze mechanische eigenschappen.

De vorming en overdracht van Langmuir lagen van poly(maleïnezuur-*alt*-1-alkenen) met bifenyl mesogenen vanaf water is bestudeerd met behulp van de Langmuir-Blodgett techniek. Brewster hoek microscopie liet zien dat de SCLCPs met methoxybifenyl mesogenen sterk aggregeren en eilanden vormen op een water subfase. Deze eilanden groeien samen gedurende compressie. SCLCPs met cyanobiphenyl mesogenen spreiden daarentegen wel goed. Compressie van deze polymeren resulteerde in de vorming van drievoudige lagen. Langmuir monolagen van SCLCPs met methoxybifenyl mesogenen werden volgens Z-type overgebracht. AFM en röntgenreflectiemetingen van de ontstane Langmuir-Blodgett mono- en/of multilagen lieten zien dat de zijstaarten mogelijk onder een hoek staan met de richting loodrecht op het substraatoppervlak. De multilagen hadden een dubbellaag periodiciteit, die echter een heroriëntatie van de zijketens vereist tijdens of na overdracht. Temperen van deze Langmuir-Blodgett films bij 135°C zorgde voor een gemiddeld dikkere film en een uniformere smectische laagdikte binnen de multilaag. Met AFM werden druppels waargenomen bovenop deze multilaag. De aanwezigheid van druppels duidt op 'dewetting' van de toplaag.

Dankwoord

Wursche bin ich sehr dankbar für seine Hilfe mit den Polyketonpolymerizationen und einige Messungen an diesen Polymeren. Voor metingen op het gebied van de moleculaire dynamica waren de mensen van de vakgroep Polymeertechnologie van de TU Delft bijzonder behulpzaam. Ten eerste wil ik Michael Wübbenhorst bedanken. Onze plezierige samenwerking heeft een erg mooi artikel opgeleverd. Helaas ging het wat te ver om het in mijn proefschrift te zetten. Ben Norder wil ik bedanken voor het uitvoeren van de reologische metingen en Dr. K. te Nijenhuis voor de hulp bij het interpreteren van de reologie resultaten. I am very grateful to Prof. dr. G. Luckhurst (University of Southampton, UK) for his remarks concerning the SCLCPs with swallow-tailed side chains. Clemens Padberg (Universiteit Twente) wil ik bedanken het doormeten van mijn *bagger* met zijn high-tech GPC opstelling. Toch jammer dat die kolommen nog steeds niet zijn verstopt.

Verder wil ik natuurlijk de dames van het secretariaat, Ronald de Bruin, Pleun van Lelieveld en de blowers van de glasblazerij, Jurrie Menkman en Gert Nieuwboer, bedanken voor hun goede service. Harm *dit is illegale software dus ik help niet meer* Niederlander wil ik bedanken voor zijn hulp bij computerproblemen.

Een groot deel van de afgelopen vier jaar heb ik doorgebracht op de labzaal of op de *werk*kamer. Mede dankzij mijn (ex-)lab- en kamergenoten was dit een bijzonder plezierige tijd. Alle (ex-)collega AIOs, OIOs, beursalen, analisten, postdocs en andere medewerkers van het laboratorium van Organische Chemie wil ik bedanken voor de gezellige koffiepauzes, lunchpauzes, pannekoekpauzes, labuitjes en natuurlijk de borrels. Dorien Derksen wil ik in het bijzonder bedanken voor de tijd die we samen in de borrelcommissie doorbrachten.

Voordat ik het vergeet wil ik Leontine de Graaf bedankten, die mijn *taxi* was gedurende de allereerste week van Hengelo naar Wageningen. Ik vond het leuk om met je mee te rijden.

Mijn beide paranimfen Sicco de Vos en Martijn Hackmann ben ik erg dankbaar voor de opvang in Ulm. Sicco en Martijn, tijdens de beginperiode van mijn promotie bleven jullie me scherp houden met snoeiharde e-mails. Het was bijzonder om door jullie door Ulm te zijn gesleept.

Mijn ouders: jullie wil ik bedanken, omdat jullie altijd achter mij stonden tijdens mijn studie en mijn promotie. Ook al was het niet altijd even duidelijk waar ik mee bezig was, dit boekje verklaart hopelijk veel. Tenslotte wil ik Denise bedanken voor al haar steun gedurende de laatste jaren. Denise, dankzij jou was ik de frustraties van het onderzoek thuis alweer vergeten. Bedankt voor alles.

Natuurlijk zullen er mensen zijn die niet met name zijn genoemd in dit dankwoord, maar toch veel voor me betekend hebben. Natuurlijk wil ik ook jullie bedanken.

René

Curriculum Vitae

René Peter Nieuwhof kwam ter wereld op 30 augustus 1971 in het pitoreske stadje Harlingen. Bijna een jaar later verhuisde hij naar het Fries-Groningse dorpje Gerkesklooster-Stroobos, waar hij opgroeide. In 1983 begon hij met het VWO aan het Lauwers College in Buitenpost, waarvan hij in juni 1989 het diploma behaalde. Aansluitend studeerde hij Chemische Technologie aan de Friesland-vestiging van de Universiteit Twente. Na een jaar, met het propadeuse diploma op zak, verruilde hij Fryslân voor het Twentsche om daar zijn studie af te maken. Tijdens zijn studie liep hij stage bij de Zentrale Forschung van Bayer AG in Leverkusen. Na een periode van ongeveer 10 maanden te hebben gewerkt in de onderzoeksgroep Materiaalkunde en Technologie van Polymeren onder begeleiding van dr.ir. Harold Gankema en Prof.dr. Martin Möller, ronde hij zijn studie af op 30 januari 1995. De maanden erna werkte hij in dezelfde onderzoeksgroep aan cyclische siloxanen en amino-getermineerde poly(styrenen). In mei 1995 begon hij met een promotieonderzoek op het gebied van vloeibaar-kristallijne polymeren, welke zouden kunnen worden toegepast in een nieuw verfverwijderingsconcept. Dit onderzoek vond plaats onder begeleiding van Prof.dr. Ernst Sudhölter en dr. Ton Marcelis. De resultaten van het onderzoek kunt u terugvinden als u terugbladert in dit proefschrift.

Sinds 1 september 1999 is hij werkzaam bij TNO Industrie, afdeling Polymeerproducten en coatings, te Eindhoven.

List of publications

- Order in thin films of side-chain liquid-crystalline polymers - M.W.J. van der Wielen, M.A. Cohen Stuart, G.J. Fleer, D.K.G. de Boer, A.J.G. Leenaers, R.P. Nieuwhof, A.T.M. Marcelis, E.J.R. Sudhölter, *Langmuir* **13**, 4762-4766 (1997).
- Adhesive liquid-crystalline polymers - R.P. Nieuwhof, A.T.M. Marcelis, E.J.R. Sudhölter, M.W.J. van der Wielen, M.A. Cohen Stuart, G.J. Fleer, *Macromol. Symp.* **127**, 115-121 (1998).
- Specular and non-specular X-ray reflection from inorganic and organic multilayers - D.K.G. de Boer, A.J.G. Leenaers, M.W.J. van der Wielen, M.A. Cohen Stuart, G.J. Fleer, R.P. Nieuwhof, A.T.M. Marcelis, E.J.R. Sudhölter, *Physica B* **248**, 274-279 (1998).
- Side-chain liquid-crystalline polymers from the alternating copolymerization of maleic anhydride and 1-olefins carrying biphenyl mesogens - R.P. Nieuwhof, A.T.M. Marcelis, E.J.R. Sudhölter, S.J. Picken, W.H. de Jeu, *Macromolecules* **32**, 1398-1406 (1999).
- Thermotropic behavior of side-chain liquid-crystalline copolymers from maleic anhydride and mesogen-containing methacrylates - R.P. Nieuwhof, A.T.M. Marcelis, E.J.R. Sudhölter, *Macromol. Chem. Phys.* in press.
- Modification of side-chain liquid-crystalline poly(maleic anhydride-*alt*-1-alkene)s with mesogen-containing alcohols - R.P. Nieuwhof, A. Koudijs, A.T.M. Marcelis, E.J.R. Sudhölter, *Macromolecules* in press.
- Highly ordered side-chain liquid-crystalline polymers from maleic anhydride and swallow-tailed 1-alkenes having two mesogens - R.P. Nieuwhof, A.T.M. Marcelis, E.J.R. Sudhölter, R.R. van Puijenbroek, S.J. Picken, to be submitted.
- Side-chain liquid-crystalline poly(ketone)s: effect of spacer length, mesogen type and mesogen density on mesomorphic behavior - R.P. Nieuwhof, A.T.M. Marcelis, E.J.R. Sudhölter, R. Wursche, B. Rieger, to be submitted.
- Molecular and cooperative dynamics of smectic B and smectic E phases of a maleic anhydride based liquid-crystalline copolymer - a dielectric relaxation study - M. Wübbenhorst, R.P. Nieuwhof, A.T.M. Marcelis, E.J.R. Sudhölter, J. van Turnhout, to be submitted.
- Langmuir and Langmuir-Blodgett films of side-chain liquid-crystalline copolymers with maleic acid moieties in the backbone - R.P. Nieuwhof, P. Kimkes, A.T.M. Marcelis, E.J.R. Sudhölter, R. Opitz, to be submitted.
- Rheology of side-chain liquid-crystalline copolymers with maleic anhydride moieties in the backbone - R.P. Nieuwhof, A.T.M. Marcelis, E.J.R. Sudhölter, B. Norder, to be submitted.